

Dissertation zur Erlangung des Doktorgrades
der Fakultät für Chemie und Pharmazie
der Ludwig-Maximilians-Universität München

**New Aspects of Process and Formulation Development for
Freeze-Drying of Proteins**



Jacqueline Horn
aus Bottrop

2018

Erklärung

Diese Dissertation wurde im Sinne von §7 der Promotionsordnung vom 28. November 2011 von Herrn Prof. Dr. Wolfgang Frieß betreut.

Eidesstattliche Versicherung

Diese Dissertation wurde eigenständig und ohne unerlaubte Hilfe erarbeitet.

München, den 27.05.2018

Jacqueline Horn

Dissertation eingereicht am: 29.03.2018

1. Gutachter: Prof. Dr. Wolfgang Frieß

2. Gutachter: Prof. Dr. Gerhard Winter

Mündliche Prüfung: 17.05.2018

*If at first you don't succeed,
try, try, try again.*

Acknowledgements

This thesis was prepared between February 2014 and July 2017 at the Department of Pharmacy, Pharmaceutical Technology and Biopharmaceutics at the Ludwig-Maximilians Universität in Munich under the supervision of Prof. Dr. Wolfgang Frieß.

First of all, I would like to express my deepest gratitude to my supervisor, Prof. Dr. Wolfgang Frieß, for giving me the opportunity to work in this exciting and relevant research field. Being part of this enthusiastic team under your encouraging scientific guidance enabled a fantastic working atmosphere. I am also grateful that you allowed me to present my results at several scientific conferences in Garmisch-Partenkirchen, Berlin and Breckenridge and supported my research stay in Copenhagen.

Special thanks goes to Prof. Dr. Gerhard Winter for always providing sound advice and his continuous interest in my research. Your enthusiasm for new technologies was always contagious and admirable.

Sampreeti Jena and Prof. Dr. Alptekin Aksan are highly appreciated for their great efforts and all the work that was put in the cooperation with the University of Minnesota. I always enjoyed discussing our experimental plans and results of our collaborative work with both of you.

Moreover, I am very thankful for the opportunity to supervise so many students in their Master's theses. It meant learning on both sides, for me as supervisor and for you as pharmaceutical technology students on the special issue of freeze-drying techniques. Against this background, I would like to express my sincere gratitude to all of the students I worked with, in particular to Michaela, Robina, Julia and Eleonora. I know that working in the lab is not always easy but means hard work. I am hence very thankful for all of the experiments you carried out and all of the analyses you performed. In this context, I would also like to thank Prof. Davide Fissore for enabling the great exchange between the Politecnico di Torino and the LMU München. This collaboration is worth being deepened further in the future.

I further appreciate that Prof. Dr. Hanns-Christian Mahler gave Prof. Frieß and me the opportunity for a collective authorship of a book chapter of the prestigious book publisher John Wiley & Sons edited by Satoshi Ohtake, David Lechuga and Ken-ichi Izutsu.

I enjoyed my two research stays in Copenhagen which were mainly facilitated by Dr. Holger Grohgan and Dr. Korbinian Löbmann. Both of you always gave worthwhile scientific input whenever there was a question. Holger did an excellent job as supervisor during Robina's

eight weeks stay at the University of Copenhagen and I would like to address my deepest gratitude for this.

The challenging handling of the optical fibers was facilitated by Manfred Resch from Infap GmbH – more than one repair of the fibers had to be conducted. Without Manfred's help I would not have been able to perform all the OFS experiments.

I would also like to thank Coriolis Pharma enabling the measurements at the freeze-drying microscope, in particular, to Matthias Wurm, being always supportive whenever there was a need.

I could not have imagined a better lab mate for almost three years, Corinna. It was a good atmosphere in our lab, also if one or the other instrument broke yet another time. You were always supportive when anyone needed help.

Furthermore, I will not forget the regular running group of Teresa, Cihad and Laura (and of course all the other infrequently participating runners). This also includes the Thursday's Shakers training, for which I hope the sessions are still taking place.

The mutual support between the research groups of Prof. Winter and Prof. Frieß created a good scientific but also collaborative working atmosphere. In addition, diverse trips such as hiking, skiing, city trips or congresses, contributed to the pleasant environment. Good times are always coupled to good people: Ivi and Teresa, you made me sad to leave but also Ellen, Olaf, Ben and Tobi, thank you for the great time. Ivi, I will not forget about your selflessness and unlimited support. Teresa, sports bring people together and this is true.

Writing a PhD thesis and working in the lab demands for discipline, persistence and consistency. This is why I am very grateful that my family, in particular my father and my mother, enabled me to adapt these characteristics early in life and during my years of competitive sport. Getting honoured with the PhD title is my personal Olympic medal.

Steffi and Michelle, you are the best sisters I can imagine. Stay as you are.

Melli, Miri and Lukas, you always give me support without asking why. I am very lucky to call you my friends.

I still cannot believe that I found you, Philipp. You always have an open ear for my worries, you help me selflessly and you are my safe haven. Thank you.

General Table of Content

Chapter 1	
Introduction - Drying for protein stabilization/formulation	1
Chapter 2	
Objectives of the Thesis	36
Chapter 3	
Detection of Collapse and Crystallization of Saccharide, Protein and Mannitol Formulations by Optical Fibers in Lyophilization	38
Chapter 4	
Effects of Excipient Interactions on the State of the Freeze-Concentrate and Protein Stability	59
Chapter 5	
Impact of Fast and Conservative Freeze-Drying on Product Quality of Protein-Mannitol- Sucrose-Glycerol Lyophilizates	98
Chapter 6	
Crystallizing Amino Acids as Bulking Agents in Freeze-Drying	130
Chapter 7	
Final Summary	167
Chapter 8	
Appendix	170

Chapter 1

Introduction - Drying for Protein Stabilization and its Formulation Aspects

This chapter is intended to be published in the book “Drying Technologies for Biotechnology and Pharmaceutical Applications: Current Status and Future Trends”, edited by Davide Lechuga, Satoshi Ohtake, Ken-Ichi Izutsu (John Wiley & Sons, Inc.) and was prepared by Jacqueline Horn, Hanns-Christian Mahler and Wolfgang Friess.

Abstract

Drying can significantly improve the stability of protein drugs compared to liquid formulation and mostly, freeze-drying (lyophilisation) is employed for drug products for that respect. However, chemical degradation, like formation of disulfide bonds, oxidation, deamidation or glycation as well as physical instability, conformational or colloidal also occur in the dried state. Due to the complexity of the protein molecules a comprehensive analysis with a multitude of methods such as particle analysis, chromatography, circular dichroism or infrared spectroscopy are necessary. Typical excipients in drying include sugars, polyols or polymers. The two leading hypotheses for their ability to stabilize proteins in the dried state are the water replacement and the immobilization in an amorphous glass. Each step of freeze- or spray- drying process like freezing, droplet formation, water removal affects protein stability in different ways. Interfacial related stress occurs in almost all process steps whereas concentration effects are important during freeze-concentration or droplet formation.

Keywords

Protein stability, freeze-drying, spray-drying, physical instability, chemical instability, water replacement, glass dynamics, residual moisture, glass transition

Table of Content

Abstract	1
Keywords.....	1
Introduction.....	4
1. Protein Stability.....	4
1.1. Physical Instability of Proteins	4
1.2. Chemical Instability of Proteins	6
1.2.1. Disulfide Bond Formation	6
1.2.2. Deamidation	7
1.2.3. Oxidation.....	7
1.2.4. Glycation.....	7
1.3. Analysis of Protein Stability	8
1.3.1. Particle Analysis in Protein Formulations.....	8
1.3.2. Other Purity Tests for Proteins	9
1.3.3. Analysis of Higher Order Structure	9
2. Protein Stability in the Dried State	10
2.1 Theoretical Considerations.....	10
2.1.1. Water Replacement Hypothesis	10
2.1.2. Glass Dynamics Hypothesis and Vitrification [55].....	11
2.2. Analysis of the Dried State	11
2.2.1. Investigation of Endo- and Exothermic Processes: Glass transition and Crystallization.....	12
2.2.2. Sample Morphology – Crystalline or Amorphous Matrix?	12
2.2.3. Residual Moisture	13
2.3. Excipients Used to Stabilize Proteins in the Dried State	13
2.3.1. Sugars.....	14
2.3.2. Polyols	15
2.3.3. Polymers	16
2.3.4. Amino acids	16
2.3.5. Further Excipients: Metal ions/HP- β -CD/Surfactants/Buffers.....	17

3. How Does the Process Influence Protein Stability?	18
3.1. Process of Freeze-drying	18
3.1.1. Freezing	18
3.1.1.1. Annealing	20
3.1.2. Drying	20
3.1.3. Typical Defects in Lyophilized Products beyond Protein Stability	21
3.2. Process of Spray-drying	22
3.2.1. Protein Stability during Droplet Formation	22
3.2.2. Protein stability during the drying phase	22
References	23

Introduction

Between 2010 and 2014, fifty-four novel biopharmaceuticals were approved in the US or Europe, with almost one third of them being monoclonal antibodies. Amongst others, further biopharmaceuticals approved included hormones, enzymes, vaccines and fusion proteins [1]. In total, more than 200 biopharmaceuticals are currently on the market, typically for refrigerated storage (2-8°C) and either in liquid or lyophilized dosage form [2].

This chapter is intended to discuss mechanisms of protein stabilization in liquid and dried formulations as well as the corresponding analytical methods. Furthermore, the impact of the drying process itself on protein stability is summarized.

1. Protein Stability

Protein stability is related to the primary sequence and the higher order molecular structure (secondary, tertiary and quaternary structure). Protein instabilities can be categorized as physical or chemical instabilities [3]. The latter include the formation or the breakage of covalent bonds resulting in new chemical entities. Examples include deamidation, fragmentation and oxidation. Physical instabilities, in contrast, are defined as altered physical state of the protein, including unfolded state, aggregation and precipitation. In practice, both chemical and physical instability reactions occur simultaneously for proteins, and can also lead to each other. For example, attractive protein-protein interactions may become stronger as a consequence of chemical changes such as oxidation or deamidation, and hence, both oxidation or deamidation in combination with aggregation may be found.

External stresses are drivers for protein instability. In particular, these factors include interfaces (such as air/liquid and ice/liquid), temperature (heat) and light. Formulation parameters such as protein concentration, pH, ionic strength, and quality and quantity of excipients determine the stability and can – to some extent – stabilize (or destabilize) the protein against external stresses [4,5].

1.1. Physical Instability of Proteins

Physical instabilities can include changes in secondary or tertiary structure (conformational instability) or formation of multimers (aggregates, precipitation) (colloidal instability). Conformational and colloidal instability can be interconnected, as changes in higher order structural change may expose structural elements such as hydrophobic parts of the protein previously buried within the fold, which may also change aggregation propensity.

Important conformational instability pathways are thermal or chemical denaturation, and also cold denaturation has been discussed in this context [3]. Thermal denaturation is the unfolding of the protein upon increase of temperature. The melting temperature (T_m) at which half of the protein is denatured can be measured by differential scanning calorimetry (DSC). But also other methods which trace unfolding during a temperature ramp provide comparable information, such as FT-IR [6]. The T_m value of biopharmaceuticals should be well above the intended storage temperature, as well as accelerated conditions (higher temperature) that may occur temporarily during storage, processing or shipment and during formulation development and/or stability testing. Cold denaturation, i.e. denaturation at low temperatures is typically less relevant for the stability of biopharmaceuticals, but has been discussed being a concern during the freezing step in freeze-drying (3.1.1) [7]. Proteins can also be unfolded by chaotropic agents, called chemical denaturation. Guanidinium hydrochloride or urea concentration series has been used to gain information about the free energy of unfolding [8,9].

Colloidal instability reflects the association of individual protein molecules to larger species. These protein molecules can be native or conformationally altered, and thus, more prone for association. Colloidal instability is mainly driven by repulsive and attractive forces between protein molecules. The strength of these forces mainly depends on charge and charge distribution of the molecules and on surface hydrophobicity. Thus, important factors affecting the colloidal stability via the charge and charge interactions are charge and charge distribution of the protein molecules themselves as well as pH, buffer composition and ionic strength of the formulation. The net repulsion or attraction between protein molecules can be characterized by the osmotic second virial coefficient [10–12].

As a result of the interplay between conformational and colloidal instability, aggregates can form. These aggregates can be dimers, oligomers, soluble aggregates and larger subvisible and visible particles and precipitates, recently also called protein particles or proteinaceous particles (Figure 1-1) [13].

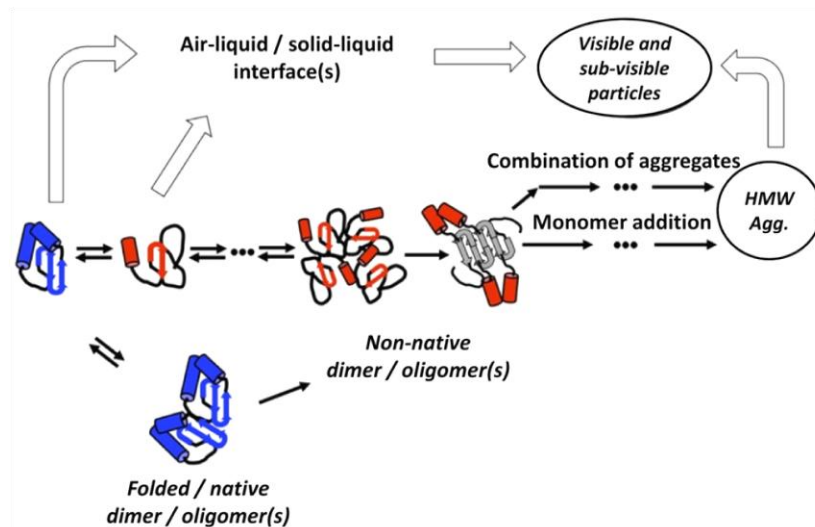


Figure 1-1. Scheme of possible aggregation mechanisms of proteins. Stress factors as temperature, pH or ionic strength may induce different aggregation pathways. Interfacial stress is mainly driven by air-liquid or solid-liquid interfaces such as the ice-liquid interface during freezing. Blue proteins represent native protein structure, whereas the red ones are partially or completely unfolded. The figure is modified from [13].

1.2. Chemical Instability of Proteins

Various chemical changes in the protein primary sequence can occur. This includes breakage or formation of disulfide bonds, deamidation, oxidation and glycation, which are described in more detail in the following and also isomerization, hydrolysis, β -elimination and racemization, for all of which the reader is referred to literature [3,14,15].

1.2.1. Disulfide Bond Formation

In case cysteine residues are present in the primary protein sequence, oxidation of two cysteine residues may result in formation of a cystin linkage or disulfide bond. This can occur 1) within one protein molecule leading to a different conformation or 2) two protein molecules inducing the formation of covalent aggregates [16,17].

In case disulfide bonds are already present in a given molecule, there is also the risk that the bond may be reduced, and disulfide bonds re-form in a different pattern. This can lead to 1) disulfide exchange in a given molecule (mispairing), leading to different conformation or 2) disulfide formation between two molecules leading to covalent aggregates or 3) a protein molecule staying in its reduced form. Latter has been a significant issue during fermentation of antibodies [18]. Copper sulfate can provide protection against this disulfide reduction by acting as oxidizing agent [19]. It was shown for β -galactosidase that the freeze-dried formulation was more susceptible to the disulfide degradation pathway than the aqueous

solution and in the freeze-dried samples covalent disulfide bonds were formed whereas in solution noncovalent soluble aggregates resulted [20].

1.2.2. Deamidation

Deamidation is another common degradation pathway. Thereby, an asparagine or glutamine amide side group is transformed into the corresponding carboxylic acid and the release of ammonium makes the reaction effectively irreversible [3]. The reaction is accelerated either at acidic (pH <4) or at basic/neutral conditions (pH >6) based on different mechanisms. The latter mechanism via an intramolecular cyclization process forming a succinimide as intermediate is more common in protein formulations. The pentacyclic intermediate of asparagine is more stable than the hexacyclic one of glutamine and therefore asparagine reacts faster than glutamine. With more than just one asparagine or glutamine in the primary sequence, different deamidated protein species can result [3,15,21,22]. Consequently, pH and acidity in the dried state are the key factors concerning this instability pathway. Deamidation leads to changes in the charge heterogeneity in a molecule affecting charge based inter- and intramolecular interactions. In case deamidation occurs in a part of the molecule that relates to potency or binding, such as the CDR region of a monoclonal antibody, partial or full loss of efficacy may result [23].

1.2.3. Oxidation

Some amino acids are sensitive to oxidation including methionine, tryptophan as well as cysteine (see 1.2.1), histidine, and tyrosine. The oxidation process is usually mediated by reactive oxygen species and influenced by various intrinsic or extrinsic factors, such as protein structure and folding, pH, metals and light. Reactive oxygen species can result from metal-induced Fenton reactions, side-chain oxidations of polymers such as excipients, contaminants e.g., peroxides in excipients, light and other sources [24].

1.2.4. Glycation

Glycation - also referred to as Browning or Maillard reaction - is the non-enzymatic reaction of a reducing sugar with a primary or secondary amine e.g. lysine residues. The amine reacts with the carbonyl group to a Schiff base, a reactive species which reacts further to more stable N-glycosylated amines of brown colour, giving the reaction its name. Sugars are frequently used as protein stabilizers in dried formulations and the Maillard reaction is the reason why non-reducing sugars like sucrose or trehalose are used instead of reducing

sugars like glucose, lactose, fructose or maltose. One also has to be aware of the fact that sucrose may invert into the reducing sugars glucose and fructose at elevated temperatures or acidic conditions [25,26].

1.3. Analysis of Protein Stability

Protein drug stability is investigated in long-term stability studies at intended and accelerated storage conditions. Due to the various potential chemical and physical changes, a broad panel of analytical methods is recommended and typically applied. Stress parameters used in development to evaluate formulation parameters such as pH, type/amount of excipients are temperature, light, mechanical stress by shaking or freeze-thaw stress [27,28]. Typical standard analytical tools for routine stability testing include turbidity, color, pH, osmolality, subvisible particles, visible particles, purity methods e.g. evaluating size, charge or hydrophobicity based separation, and measurement of content. Further methods, such as spectroscopic techniques can serve for biophysical characterization or extended characterization, and monitoring of other critical excipients may monitor related changes.

1.3.1. Particle Analysis in Protein Formulations

Particle analysis has become very important given aggregation and precipitation is a typical instability pathway for most proteins. It has been speculated that protein aggregates / particles can lead to enhanced immune response to the protein drug molecules [29,30]. Recently it has been suggested that protein aggregates / particles are only relevant for modulating the immune response if substantially chemically modified e.g. by oxidation [31,32].

The amount or size of particles has to be evaluated by several different methods (e.g. light obscuration, nanoparticle tracking analysis, dynamic light scattering). Additionally, visual inspection should be performed during formulation development, since it is mandatory as in-process testing during manufacturing (100% inspection and pulling drug product units with any visible particulate present) and quality control (release and stability). The size of particles visible for the human eye is a topic of debate. In fact, the size, type, number, color, refractive index of particulates, but also the method of detection (unaided eye vs. magnification, color/type of background, light intensity, inspection duration, capability and ability of the operator) affect the outcome of the test. This is why it is not reasonable to define a “size” of visible particles. Number and size of smaller particles in the subvisible region ($\geq 2 \mu\text{m}$) are quantified by e.g. light obscuration or microscope methods (according to USP <788> and Ph. Eur. 2.9.19). Recently, micro-flow imaging has also been suggested for quantification,

yet this method has significant shortcomings which render it currently no viable option for quality control purposes.

The determination of particles in the nanometer region may provide an additional level of characterization. For example, nanoparticle tracking analysis (NTA) and resonant mass measurement (RMM) are emerging technologies used for detection of particles in the submicron ($<1\ \mu\text{m}$) size range. High molecular weight species, i.e. soluble aggregates are detected by size exclusion chromatography (1 – 50 nm) (1.3.2).

All the technologies mentioned have their specific measurement (size) range, and advantages and disadvantages and should be used complementarily. Some methods are generally used for quality control, such as light obscuration, visible particle inspection and size-exclusion chromatography, while others serve solely for extended characterization.

1.3.2. Other Purity Tests for Proteins

Chromatographic methods are widely used to identify physical and chemical changes of proteins. Size exclusion chromatography (SEC) is the analytical workhorse for the characterization and quantification of soluble higher molecular weight species (protein aggregates) and soluble fragments. Complementary methods to SEC are asymmetrical flow field-flow fractionation (AF4) or analytical ultracentrifugation (AUC). Purity testing also includes capillary electrophoresis (CE-SDS) or related gel-based methods, such as sodium dodecyl sulfate polyacrylamide gel electrophoresis (SDS-PAGE). Chemical changes can be monitored e.g. by reversed-phase, hydrophobic interaction, hydrophilic interaction, ion exchange chromatography (IEC) or isoelectric focusing (IEF). IEC and IEF are well established methods for the characterization of charge heterogeneity, but due to the faster analysis and the less complex method development, there is a trend towards CE techniques like capillary isoelectric focusing (cIEF) and capillary zone electrophoresis (CZE) [33,34].

1.3.3. Analysis of Higher Order Structure

Circular dichroism (CD) can be used to identify changes in secondary (far-UV CD, 190 – 250 nm, peptide bond conformation) and tertiary (near-UV CD, $> 250\ \text{nm}$, absorption of aromatic amino acids and cystine) protein structure based on the difference in absorption of left- and right-handed circularly polarized light. The location and intensity of characteristic bonds (α -helices, β -sheets, unordered structures) at certain wavelengths are used for analysis. Dry powders need to be rehydrated for CD analysis ignoring the potential impact of reconstitution [35].

Fourier transform infrared spectroscopy (FTIR) enables liquid as well as solid state analysis of the secondary protein structure. It is based on the Amid I C=O stretching band at 1700 cm^{-1} to 1600 cm^{-1} . The drawback of this method is the low sensitivity not being able to detect smallest structural changes of the protein structure, in particular if only single domains of the protein are affected [36]. Fluorescence, UV and RAMAN based methods may be used orthogonally. More innovative higher order structure analysis methods include hydrogen-deuterium exchange (HDX).

2. Protein Stability in the Dried State

2.1. Theoretical Considerations

Compared to the aqueous solution the dried state is characterized by a matrix that reduces protein mobility, and less water (as residual moisture), which is mediating many chemical reactions [37,38]. The pharmaceutical industry developed various drying techniques suitable for protein stabilization, mainly adopted from food industry [39,40]. This includes vacuum-drying [41,42], fluid bed drying [43], film-drying [44], freeze-drying [45], spray-drying [46] or spray-freeze-drying [47] of which freeze-drying is clearly dominant and preferred. All drying methods have in common that stabilizers are required to ensure protein stability.

Dry products which provide good protein stability are typically based on amorphous matrices. For the classic low molecular sugar, mostly sucrose matrices, two hypotheses regarding the stabilization mechanism are discussed [48,49], which however cannot explain all cases of stabilization or destabilization. In some cases the water replacement theory helps explain the stabilization effect and in other cases the vitrification concept. The debate about the preferable hypothesis is still ongoing [49].

2.1.1. Water Replacement Hypothesis

As the name “water replacement theory” implies, the sugar molecules replace the hydrogen bonds of water at the surface of the protein. Thus, the sugar molecules stabilize the native conformation of the protein and thermodynamically stabilize against unfolding [50]. Theoretically, a sugar monolayer around the protein molecule should be adequate to retain complete protein activity replacing water at all hydrogen bonding sites. The fact that an increasing sugar to protein ratio leads to increased protein stability up to a saturation limit supports the water replacement theory. A similar molar ratio of sugar to protein of around 350 - 400 was shown to be sufficient for freeze- and spray dried monoclonal antibodies

[51,52]. Saturation was also shown for five different proteins at a similar or lower molar ratio [53]. Hydrogen bonding between sugar and protein can be assessed by FT-IR [54].

2.1.2. Glass Dynamics Hypothesis and Vitrification [55]

The second hypothesis on stabilization of proteins in the dried state is the so called “glass dynamics” or “vitrification” hypothesis, which is based on kinetic considerations. The mobility of the protein molecules is limited in the glassy matrix. As a consequence, reactions between protein molecules, but also of protein molecules with water or oxygen, are slowed down, as the time-scale of reactions is prolonged. This reduced mobility is reflected in α - and β -relaxations of the matrix [49]. It is not clear yet, which of these relaxations is more relevant for protein stability or whether it is the combination of both. The α -relaxation, also called global or slow dynamics or primary motions, reflects slow translational and rotational motions on a seconds-to-months time scale. The motions correlate with the viscosity of the entire system and are therefore related to the glass transition [56,57]. In contrast, β -relaxations, also named secondary motions or Johari-Goldsteins relaxations [57], are local dynamics in spatial proximity which influence motions at a time scale of picoseconds. Since small distances between protein molecules drive protein aggregation slowing down β -relaxations is suggested for improving protein stability [49,56]. Excipients with low molecular weight, e.g. glycerol and sorbitol, may be able to increase local β -relaxation times, but decrease global α -relaxation times, hence antiplasticizing β -motions and plasticizing α -motions at the same time [56,58,59].

2.2. Analysis of the Dried State

As described above, vitrification in an amorphous matrix with low mobility and hydrogen bonding is important to stabilize proteins in the dried state. To characterize these features, typically three basic routine tools can be utilized: differential scanning calorimetry (DSC), X-Ray powder diffraction (XRD) and residual moisture determination (Karl-Fischer or TGA). Also other more sophisticated tools have been applied and the reader is referred to the primary literature e.g. on small angle X-ray scattering (SWAXS), dielectric relaxation spectroscopy (DRS), dynamic mechanical analysis (DMA), fluorescence spectroscopy, nuclear magnetic resonance (NMR), positron annihilation lifetime spectroscopy (PALS), hydrogen/deuterium exchange mass spectroscopy (HDX MS) [60,61] or solid-state NMR [62].

2.2.1. Investigation of Endo- and Exothermic Processes: Glass transition and Crystallization

Differential scanning calorimetry (DSC) is the standard tool for the determination of the glass transition temperatures (T_g) of amorphous solids. It can also be used to characterize crystallization events, polymorph variants, relaxation behaviors, T_g of the freeze-concentrate (T_g') and melting points [63]. The DSC comparatively measures the heat capacities of a sample and a reference pan during cooling and heating cycles. Endothermic events (e.g. melting point) are characterized by a positive heat flow, hence energy input, whereas exothermic events (i.e., crystallizations, relaxations) set energy free and thus, lead to a negative signal. The T_g characterizes the temperature at which amorphous solids transform from a glassy, rubbery state into a state with viscous flow accompanied by a distinct decrease in viscosity. This event is not related to a formal phase change, but a step in the DSC baseline occurs as the heat capacity changes. Storage temperatures of amorphous solids should not exceed T_g , as in this case macroscopic collapse of the formulation would result. Furthermore, protein stability can be drastically decreased upon storage above or close to T_g as the molecular mobility jumps up [64–66]. Furthermore, it is essential to assess the storage stability of amorphous solids since the metastable amorphous form tends to transform into a stable crystalline polymorph, potentially indicated by an exothermic crystallization peak depending on kinetics.

2.2.2. Sample Morphology – Crystalline or Amorphous Matrix?

XRD is the method of choice to gain information about sample morphology. The operation principle is the reflection of X-rays in an angle dependent manner. Diffraction angles and patterns can be assigned to distinct structures based on Bragg's law. Thus the absence of peaks indicates an amorphous structure and peak patterns allows for the differentiation of crystalline polymorphs. Mannitol for example forms at least four different polymorphs in addition to the amorphous form. Both, the form itself as well as polymorphic transitions have to be considered regarding long term storage stability. The hemihydrate form is prone to transform into one of the anhydrites (α -, β - or δ -polymorph). The released crystal water is transferred into the amorphous phase acting as plasticizer. Ultimately T_g is decreased, the mobility of the system increased and instability reactions between protein molecules enhanced. The released water may also be an important reaction partner itself e.g. for hydrolytic reactions. The most stable crystalline mannitol form is the β -polymorph. It was shown that both spray- and freeze-drying rendered mainly the β -polymorph if no protein was present in the formulation. Increasing lysozyme concentrations stimulated the formation of α -

mannitol during spray-drying and of δ -mannitol upon freeze-drying [67]. Thus, not only process differences, but also formulation differences affect which polymorph forms.

2.2.3. Residual Moisture

The residual moisture content is an important quality attribute of the dried material. A higher water content may be directly related to reduced protein stability with water molecules acting as reaction partner or as plasticizer increasing molecular mobility. Thus, it is important to evaluate the impact of differently dried material on long-term stability. The duration and especially temperature of the secondary drying in freeze-drying is the most decisive step for the amount of moisture remaining. Typically, a residual moisture content below 2% is being aimed for, considering many reactions would generally be slowed down below this level [68], although this clearly depends on the specific product (protein, formulation etc.). Further drying to very low amounts of moisture may lead to so-called overdrying [69]. Karl-Fischer titration is the standard method for determination of the residual moisture. Thermogravimetric analysis (TGA) could also be used and recently spectroscopic analysis for non-destructive high throughput analysis has been introduced [70,71].

2.3. Excipients Used to Stabilize Proteins in the Dried State

Most proteins require additional stabilizers to retain their activity during drying and subsequent storage. The amount of stabilizer which can be added may be limited by physiological considerations since parenterally applied solutions, obtained after reconstitution, should preferably be isotonic. The amount of stabilizer needed may follow different rules. On the one hand, the higher the ratio of stabilizing sugar to protein molecules the better the stability and the increment of stability improvement levels off at higher ratios [51]. On the other hand, at higher protein concentration, less stabilizer may be needed due to a self-stabilization of the protein by steric repulsion of vicinal protein molecules and a reduced interface to protein molecule ratio at which denaturation could occur [72]. Although equal numbers of protein molecules are damaged, the relative fraction at higher protein concentration is lower [72,73]. In freeze-drying, one distinguishes between cryo- and lyoprotectants whereby some excipients combine both features. Cryoprotectants are known from nature as protectors against freezing induced stress [74] and lyoprotectors protect against drying induced stress. Stabilizers used for spray-dried products are comparable to the ones used in freeze-drying. More important in spray-drying is the T_g of the excipients which should be higher than the process temperature in order to prevent viscous flow. During spray-drying it also needs to be considered that the water content of the formed particles and

thus the product Tg depends on the moisture level of the drying environment and differs between the different stages of a spray-dryer, as does the temperature. Thus, the situation may be rather complex. Since freeze-drying is conducted at low temperatures, this factor is of minor importance and secondary drying temperature, especially in the temperature ramp phase going into secondary drying, and storage temperature should not exceed the formulation Tg.

2.3.1. Sugars

Disaccharides are the most commonly used protein stabilizers. Due to their small size and flexibility, they are able to cover the protein surface acting directly on the protein. During drying, they typically form amorphous matrices as a key parameter for stabilization. They combine cryo- and lyoprotectant characteristics and the mechanism of stabilization has been discussed above in more detail.

The most frequently utilized sugars in freeze- and spray-drying are sucrose and trehalose. Both of them are non-reducing sugars, hence not susceptible for Maillard reactions. Due to its less stable glycosidic bond, sucrose may invert into the reducing monosaccharides glucose and fructose, even in freeze-drying studies, more markedly at low pH (Figure 1-2) and significantly high temperatures [75–79].

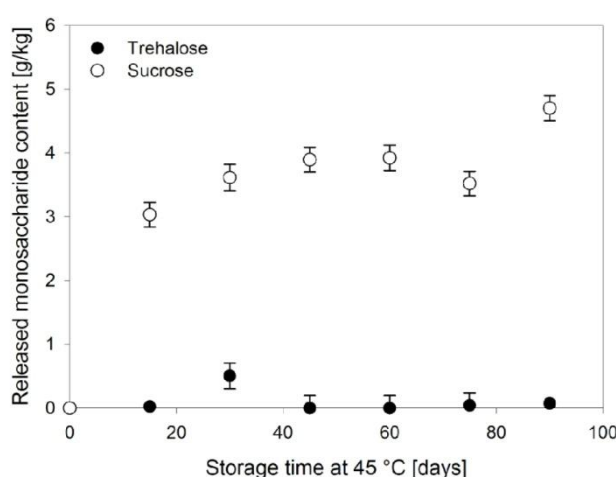


Figure 1-2. Progression of Maillard reaction in freeze-dried disaccharide matrices (2.5 % m/V) determined by the release of the monosaccharide glucose via an enzymatic reaction. Trehalose (black) and sucrose (white) were lyophilized with BSA (1 % m/m) and stored under controlled humidity conditions (22% rel. humidity) at 45 °C, reproduced with permission from [79].

Both sucrose and trehalose show relatively high Tg values with 75 °C and 118 °C, respectively, which is advantageous for spray-drying and for storage [80]. Particularly, trehalose shows one of the highest Tg values compared to the other sugars and also the

relaxation time and the concluding fragility of the glass are important factors for its usage as stabilizing excipient [81,82]. On the other hand, trehalose solutions showed a higher viscosity compared to sucrose solutions [83].

Trehalose is more prone to crystallization during freeze-concentration [84] which could lead to a loss of cryoprotective function and protein stability problems. The crystalline modification may transform into the amorphous state in the course of the freeze-drying process and thus may not be obvious when only testing the final product [76,85]. Upon spray-drying of protein solutions containing sugars as stabilizers, the plasticizing effect of moisture and thus stickiness of the resulting particles needs to be carefully considered (see also 2.2.3) [86,87]. Specifically for spray-drying of proteins for inhalative use other sugars can be considered as the drying behavior may be different rendering aerodynamically more favorable particles and lactose and glucose are preferred and approved for use in dry powder inhalers.

2.3.2. Polyols

The group of polyols which are frequently used for drying of proteins includes e.g. glycerol, sorbitol and mannitol, showing different characteristics. The first two are plasticizing agents but may also improve protein stability in the dried state [58,59,88]. Due to their low T_g (glycerol $-93\text{ }^\circ\text{C}$ [89] and sorbitol $0\text{ }^\circ\text{C}$ [90]), they are not suitable as the only stabilizer for dried protein formulations as they do not render a solid material at room temperature. Thus, they need to be used in combination with other excipients having higher T_g [56]. Glycerol at low concentrations exhibits an antiplasticizing effect to the local motions of a protein formulation. The temperature needs to be below a critical antiplasticization temperature, which interestingly increases with lower glycerol concentrations [91]. Various studies explain an improved protein stability in presence of glycerol by the increased relaxation time of local fast dynamics (β -relaxation) while the timescales for global relaxations is lowered [56,58,88,92]. The improved protein stability may also be explained differently by an increased density of the packing reducing the free volume. Small voids left by larger glass forming molecules such as sucrose are filled by the plasticizer [56,93]. The smaller glycerol molecules are additionally sterically more suitable at gaining access to the surface of the protein molecules compared to larger excipients. Once the free volume is saturated by glycerol, the plasticizing characteristics dominate and glycerol acts as lubricant, accelerating the dynamics on all timescales [56].

Adding sorbitol to sucrose or trehalose-based antibody formulations led to a decrease of the global relaxation time τ and, in some cases, improved stability. Sorbitol did not affect the native structure stability in combination with trehalose, but with sucrose. Thus, the global

relaxation time τ could not predict stability adequately [59]. The combination of sucrose and sorbitol was beneficial also for other proteins and the effect may not be polyol specific but also small amino acids were suitable [94]. Upon spray-drying, the stabilizing effect of sorbitol on an IgG antibody was comparable to the effect of trehalose [86].

Polyols like mannitol do not have plasticizer properties, but are used as bulking agents in freeze-drying. Bulking agents crystallize during the process and do not stabilize protein molecules but render robust scaffolds for good cake appearance (see also 2.2.2). It is important to achieve complete mannitol crystallization in order to prevent subsequent crystallization during storage. Spray-dried mannitol remains amorphous and is hence able to stabilize the protein in an amorphous matrix.

2.3.3. Polymers

Polymers can also stabilize proteins in the dried state. Usually, polymers show high T_g which makes them suitable stabilizers by increasing the T_g of the whole formulation. The macromolecules differ in their stabilization mechanism from small molecules like sugars. Polymers hinder the protein interactions sterically, they increase the viscosity of the solution and hence slowing down the mobility, or they react via preferential exclusion [38]. Furthermore, they prevent pH drops of phosphate buffers during freezing or the crystallization of excipients. Commonly used polymers include serum albumins, polyvinylpyrrolidone, dextran, polyethylenglycole or hydroxyethylcellulose of different molecular weight [38].

Polymers may not only be beneficial, but can also negatively affect protein stability. Phase separation triggered by the polymer can be detrimental for proteins [95]. As a high T_g is not the only factor for a stable dried protein formulation, hydroxyethylstarch did not improve the protein stability compared to sucrose and trehalose [82]. One reason is the less efficiency in forming hydrogen bonds with proteins as for example demonstrated for freeze-dried formulations of LDH containing dextran or trehalose [96]. Human serum albumin contains free sulfhydryl groups, and thus, may lead to covalent aggregation (heteroaggregation) with cysteine-containing proteins. Also, the regulatory and safety status of the choice of excipients may in some cases be unfavorable for the choice of polymers for some parenteral products.

2.3.4. Amino acids

A stabilizing effect of amino acids on proteins is still unclear. Forney-Stevens et al. screened 15 amino acids regarding the stabilization of two model proteins, rHSA and ACT, in the

freeze-dried state [94]. It seems as if the positive amino acids, which are also larger in size than the other amino acids, have an advantageous stabilization effect. Added in small amount to sucrose, they formed amorphous lyophilizates. In contrast, glycine is a crystalline bulking agent and also phenylalanine crystallizes during freeze-drying, if the ratio of amino acid to sugar exceeds a certain limit [97]. Arginine also exhibited beneficial effects as amorphous stabilizer on freeze-dried protein formulations [98]. The arginine counter-ion plays an important role and chloride performed best regarding stabilization [98]. Concerning spray-drying isoleucine was reported to improve flowability of the powder and protein stability of an IgG1 antibody [99].

2.3.5. Further Excipients: Metal ions / HP- β -CD / Surfactants / Buffers

Surfactants adsorb to interfaces with a higher tendency than proteins. Thereby, they keep protein molecules off the interface where proteins may unfold. The most critical interfaces are the ice/freeze-concentrate interface formed during the freezing step in freeze-drying and the air-liquid interface generated upon droplet formation during spray-drying [100]. Stabilization of protein molecules by direct binding has been shown for albumin fusion proteins and albumin with a lipophilic binding pocket [101], whereas binding to other proteins is still up to debate. Typical surfactants used are the non-ionic polysorbate 20 and 80.

Cyclodextrins (CDs) are ring-shape molecules consisting of at least six glucose molecules. They are amphiphilic with a hydrophilic outer surface and a rather hydrophobic interior. The CDs limited solubility can be improved by substitution e.g. with hydroxypropyl- or sulfobutyl-groups. By incorporating hydrophobic moieties of a distinct size in their interior, CDs can improve solubility or reduce hydrophobic interactions. It was also shown that the CD derivatives have surfactant similar characteristics which make them suitable stabilizers against interface induced stresses [102], however, probably acting via different mechanism than non-ionic surfactants [103]. Concentrations higher than 1 % leads to a lyoprotectant behavior and also a good stability of spray-dried trypsin has been shown by CDs due to their glass forming characteristics [104].

Buffers are added to protein formulations to keep the pH consistent. The pH is one of the most important parameters in protein formulations as it affects all instability pathways, chemical reactions, colloidal interactions, as well as conformational stability (see also 1.1 and 1.2). Additionally the counter-ion effect has to be considered when comparing the typically negatively charged buffer salts phosphate or citrate to histidine or Tris. Concerning the dried state, histidine has been shown to be beneficial for protein stability [105] (see also 2.3.4). On

the other hand, crystallization of buffer salts may have a detrimental effect on protein stability (see also 3.1.1).

Metal ions, specifically divalent cations like zinc, copper or calcium can bind to specific protein binding sites and may in some cases stabilize (but also destabilize) the native protein conformation. It was reported that phosphofructokinase stability was substantially improved if the divalent metal ions were added to a sucrose based formulation [106]. Spray-dried formulations of recombinant human growth hormone were stabilized by zinc in combination with polysorbate 20 without any sugar stabilizer by formation of a dimer complex [107].

3. How Does the Process Influence Protein Stability?

3.1. Process of Freeze-drying

The freeze-drying process can be separated into the steps freezing including annealing, primary drying at low product temperature under reduced pressure in order to remove ice from the frozen system by sublimation and secondary drying at higher product temperature and reduced pressure to desorb water from the product. Each step requires special consideration in the context of drying protein products.

3.1.1. Freezing

Freezing is the first step after dispersing the liquid solution into the product containers and can already be detrimental for proteins. Several factors of influence are discussed. Cold denaturation describes the unfolding of proteins at low temperature due to a lower barrier in Gibbs free energy of unfolding [108]. It is difficult to determine the impact of cold denaturation on protein stability because ice formation and freeze concentration are two phenomena which influence protein stability and occur in parallel during freezing. Cold denaturation is assumed to be of minor relevance since the freezing step is rather short and often occurs at temperatures below the product temperature in freeze-drying [7].

Another major critical effect during freezing is the formation of a freeze-concentrated liquid as a very densely structured hexagonal crystal lattice [109–111]. Both the protein concentration and the excipient concentrations increase. Especially for proteins sensitive to native-like aggregation, highly concentrated areas could promote particle formation during freezing [111].

Another phenomenon occurring during freeze-concentration is the crystallization of buffer components due to their limitation in solubility. In some cases, a pH shift of more than three pH units is the result. A famous example is sodium phosphate buffer in which the basic disodium salt is the less soluble component and precipitates during freezing. This shifts the acid-base balance towards the base since the base is removed from the equilibrium. Protons are set free and decrease the pH [108] which lead to denaturation of sensitive proteins, e.g. LDH [112]. Potassium phosphate in contrast leads to a pH increase since the monobasic salt precipitates during freezing [113,114]. Further pH shift inducing buffers are succinate or tartrate. To prevent this phenomenon low buffer concentrations or high protein concentrations can be used or buffers may be selected which are not prone to pH-shift like histidine, glycine, citrate or Tris. Addition of 0.25 M sucrose already prevented the pH shift to a large extent for both sodium and potassium phosphate buffer [114]. Thus the whole formulation composition influences the freezing behavior and hence the impact on protein stability. A recent article proposed the use of counter ions which balance the pH shift of the buffer salt [115]. They investigated tetramethylammonium chloride (TMACl) whose anion is incorporated into the ice crystal structure during freezing leading to a concentration dependent basification. When used together with sodium phosphate buffer, the concluding acidification by the phosphate is diminished by the TMACl.

Freeze concentration concerns all excipients. For example a 0.9 % sodium chloride solution concentrates 24-fold [89]. This enormous increase in ionic strength may influence the protein stability by reducing repulsive charge interactions. On the other hand it was shown that sodium chloride could prevent aggregation of rHA upon lyophilization which was correlated to a water uptake in short spatial proximity to rHA facilitating refolding into the native rHA [116]. The freeze concentration of sugars is one important factor for the cryopreservation of proteins. High sugar concentrations result in high viscosities which slow down the molecular mobility of the system and hence prolong unfolding kinetics of the proteins [117].

In addition, the ice-liquid interface itself can be detrimental for the protein. Proteins adsorb to the ice surface which promotes unfolding. The extent of unfolding at the ice-liquid interface is protein dependent. Infrared spectroscopy could show that the IgG and LDH structure changed at the ice-liquid interface leading to a higher β -sheet content, whereas the structure was unchanged in the freeze concentrated liquid [118]. Regarding rhIFN- γ , aggregate formation could not be linked to the adsorption at the ice-liquid interface but most likely occurred at the air-liquid interface during reconstitution [100]. The ice-liquid interface may make the protein more susceptible for unfolding or structural perturbation. By addition of surfactants like polysorbates, interface related damages are usually prevented.

The amount of interfacial area and the ice crystal size respectively depend on the chosen ice nucleation technique. The typical so called uncontrolled nucleation technique is the shelf-ramped freezing which leads to a high number of small ice crystals formed from bottom to the top due to a high degree of supercooling. Overall the surface area may be rather heterogeneous as the degree of supercooling varies within a batch as crystallization occurs at random. Recently several different techniques to induce controlled ice nucleation were established [119]. Controlled nucleation techniques lead to nucleation at defined product temperature for the entire batch. Comparative studies of controlled nucleated and randomly nucleated protein formulations could show changed physical characteristics, for example faster reconstitution times for highly concentrated mAb formulations, however, did not improve the protein stability [120,121].

3.1.1.1. Annealing

Annealing, also called thermal treatment, is the increase in temperature during the freezing step after the initial freezing prior to primary drying. Thereby, bulking agents like mannitol or glycine should crystallize completely and the ice crystal size should be increased providing larger pores and lower cake resistance to vapor flow. The increase in temperature is recommended to be close to the T_g' of the solute in order to increase the mobility of the system [122]. Crystalline bulking agents should be fully crystalline after the freeze-drying process, since they are responsible for the formation of a mechanically stable cake structure. Furthermore, bulking agents usually exhibit a low T_g' (mannitol $-35\text{ }^\circ\text{C}$ [123]) causing difficulties in drying and storage stability. Additionally, during the annealing step, undesired crystallization of amorphous stabilizers like trehalose can occur. This crystallization resulted in a unfolding of BSA measured in freeze/thaw studies performed at typical mannitol annealing temperatures of $-20\text{ }^\circ\text{C}$ [124].

3.1.2. Drying

After freezing the chamber pressure is reduced to initiate the drying process. Primary drying removes mainly the ice formed during freezing (80-90% of water) and during secondary drying at higher shelf temperature the water kept in the freeze-concentrate evaporates.

As the main part of the protein is phase-separated from the ice and located in the cryo-concentrated region, one could assume that the primary drying is not the main stress on the protein. Nevertheless, if primary drying is carried out above T_g' , the mobility of the amorphous phase is increased which could enhance interactions between the protein molecules or protein molecules and reaction partners. Furthermore, product temperatures

above T_g' e.g. induced by too high chamber pressure or too high shelf temperature could induce macroscopic collapse. It was shown that collapse is not necessarily detrimental to protein stability [125], but other quality attributes like macroscopic appearance or reconstitution times may be affected.

The subsequent secondary drying to remove water which is bound stronger to the solids is commonly performed at 20 °C or higher. By desorption of water molecules parts of the protein's hydration shell are removed. Many proteins require water in their active sites for their biologic function, hence removal of this water may induce loss of activity [126].

Regarding the macroscopic appearance, the product temperature should stay below T_g during secondary drying in order to prevent macroscopic collapse. However, collapse does not need to be a drawback concerning protein stability [97,125].

Currently many development projects focus on highly concentrated protein formulations mainly of monoclonal antibodies. The solutions may exhibit high viscosity and consequently a higher concentration of excipients like salts is required to reduce the viscosity. The formulations may also show a higher cake resistance to vapor flow and can exhibit very long reconstitution times. Additionally, the ratio of stabilizing excipient molecules to protein molecules may be lower compared to low protein concentration formulation as isotonicity limits the excipient concentrations. Colandene et al. demonstrated a marked increase in T_g' and T_c with increasing mAb concentration which was much more pronounced for T_c [127]. Thus, drying above T_g' , but below T_c was easily possible preserving cake structure as well as protein stability.

3.1.3. Typical Defects in Lyophilized Products beyond Protein Stability

For marketed lyophilized drug products appealing cake appearance is a critical factor. Defects like loose cake, larger cracks, shrinkage, vial fogging, melt down or collapse may be give rise to complaints or rejects although not related to protein stability [128]. Melt down and collapse are both related to high product temperatures commonly at the end of primary drying [129]. Cracks on top of the cake or shrinkage usually occur when amorphous matrices are used as main excipient. This is due to tension within the cake, when the desorbing water forces its way through the cake. As a result, the cake either cracks or shrinks by detaching from the vial wall, which both leads to relaxation [130–132]. Formulation creeping upwards at the vial surface after filling and subsequent drying in this position is called vial fogging. Abdul-Fattah et al. showed that it can be reduced by several factors of formulation or process design. However, most effective was the use of hydrophobic vials [133].

3.2. Process of Spray-drying

In contrast to freeze-drying, spray-drying is a one stage process. Two major stresses occur. Firstly, upon atomization an enormous air-liquid interface is generated which triggers protein adsorption and aggregation. Secondly, drying at higher temperature is performed which can be critical for the conformational stability of the protein and may lead to oxidation [129].

3.2.1. Protein Stability during Droplet Formation

First, the solution is atomized into a spray. In this step, the main stress results from the newly generated enormous air-liquid interface. Protein molecules adsorb to the air-liquid interface. This results in high local protein concentration fostering intermolecular interactions and potentially partial unfolding [134]. Ultimately soluble or insoluble aggregates can be formed. Addition of surfactants is the method of choice to protect the protein by preventing its adsorption. The addition of polysorbate was confirmed to reduce the extent of protein surface aggregation and increase protein stability e.g. for BSA, rHGH, LDH and recombinant IL-11 by ESCA and stability assays [107,135–137]. Different nozzle types are available and the stress induced by the shear or temperature effect of the nozzle itself needs to be considered [138,139].

3.2.2. Protein stability during the drying phase

During the drying phase, as the water evaporates, the temperature is a highly critical factor [135]. It requires a careful balance. The droplet temperature must not exceed the protein melting temperature as long as the protein is still in solution. At the same time, the temperature has to be high enough to ensure drying results in a non-sticking powder with adequate residual moisture [140]. The temperature setting have to be decided against the background of the ongoing endothermal drying process which keeps the droplet temperature low as long as substantial evaporation proceeds close to inlet air temperature conditions for a short time. The dried particles ultimately face the outlet temperature conditions for longer time. The residual moisture typically is higher as compared to freeze-dried products and may be reduced in an additional drying step at higher temperature and vacuum similar to secondary drying in freeze drying [99,141]. This may also help to reduce the risk of recrystallization of amorphous excipients. Amorphous excipients like sucrose, trehalose or cyclodextrins have been demonstrated to be essential for protein stabilization during the drying phase [86,142–144]. During spray-drying also oxidation can occur as air is used as the typical drying gas. Addition of methionine has been shown to prevent rhIL-11 from oxidation and formation of related species [137].

References

- [1] G. Walsh, Biopharmaceuticals benchmarks, *Nat. Biotechnol.* 32 (2014) 992–1000.
- [2] <https://www.pharmacircle.com>, accessed in 03/2016, (2016).
- [3] M. C. Manning, D. Chou, B. Murphy, R. Payne, D. Katayama, Stability of protein pharmaceuticals: An update, *Pharm. Res.* 27 (2010) 544–575.
- [4] H. C. Mahler, W. Friess, U. Grauschopf, S. Kiese, Protein Aggregation: Pathways, Induction Factors and Analysis, *J. Pharm. Sci.* 98 (2009) 2909–2934.
- [5] W. Wang, Protein aggregation and its inhibition in biopharmaceutics, *Int. J. Pharm.* 289 (2005) 1–30.
- [6] S. Matheus, W. Friess, H. C. Mahler, FTIR and nDSC as analytical tools for high-concentration protein formulations., *Pharm. Res.* 23 (2006) 1350–63.
- [7] J. Kasper, W. Friess, The freezing step in lyophilization: Physico-chemical fundamentals, freezing methods and consequences on process performance and quality attributes of biopharmaceuticals, *Eur. J. Pharm. Biopharm.* 78 (2011) 248–263.
- [8] A. Schön, E. Freire, Three easy pieces, *Biochim. Biophys. Acta - Gen. Subj.* 1860 (2016) 975–980.
- [9] B. Clarkson, A. Schön, E. Freire, Conformational stability and self-association equilibrium in biologics, *Drug Discov. Today.* 21 (2016) 342–347.
- [10] J. Rubin, L. Linden, W. Coco, A. Bommarius, S. Behrens, Salt-Induced Aggregation of a Monoclonal Human Immunoglobulin G1, *J. Pharm. Sci.* 102 (2013) 377–386.
- [11] E. Chi, S. Krishnan, T. W. Randolph, J. F. Carpenter, Physical stability of proteins in aqueous solution: Mechanism and driving forces in nonnative protein aggregation, *Pharm. Res.* 20 (2003) 1325–1336.
- [12] B. Frka-Petesic, D. Zanchi, N. Martin, S. Carayon, S. Huille, C. Tribet, Aggregation of antibody drug conjugates at room temperature: SAXS and light scattering evidence for colloidal instability of a specific subpopulation, *Langmuir.* 32 (2016) 4848-4861.
- [13] S. Amin, G. V. Barnett, J. Pathak, C. Roberts, P. Sarangapani, Protein aggregation, particle formation, characterization & rheology, *Curr. Opin. Colloid Interface Sci.* 19 (2014) 438–449.

- [14] W. Wang, S. Singh, D.L. Zeng, K. King, S. Nema, Antibody Structure, Instability, and Formulation, *J. Pharm. Sci.* 96 (2009) 1–26.
- [15] M. Lai, E. M. Topp, Solid-state chemical stability of proteins and peptides, *J. Pharm. Sci.* 88 (1999) 489–500.
- [16] T. Dillon, M. Ricci, C. Vezina, G. Flynn, Y. Liu, D. Rehder, M. Plant, B. Henkle, Y. Li, S. Deechongkit, B. Varnum, J. Wypych, A. Balland, P. Bondarenko, Structural and functional characterization of disulfide isoforms of the human IgG2 subclass, *J. Biol. Chem.* 283 (2008) 16206–16215.
- [17] J. Wypych, M. Li, A. Guo, Z. Zhang, T. Martinez, M. Allen, S. Fodor, D. Kelner, G. Flynn, Y. Liu, P. Bondarenko, M. Ricci, T. Dillon, A. Balland, Human IgG2 antibodies display disulfide-mediated structural isoforms, *J. Biol. Chem.* 283 (2008) 16194-16205.
- [18] K. Hutterer, R. Hong, J. Lull, X. Zhao, T. Wang, R. Pei, M. Le, O. Borisov, R. Piper, Y. Liu, K. Petty, I. Apostol, G. Flynn, Monoclonal antibody disulfide reduction during manufacturing Untangling process effects from product effects, *MAbs.* 5 (2013) 608-613.
- [19] W. Chaderjian, E. Chin, R. Harris, T. Etcheverry, Effect of Copper Sulfate on Performance of a Serum-Free CHO Cell Culture Process and the Level of Free Thiol in the Recombinant Antibody Expressed, *Biotechnol. Prog.* 21 (2008) 550–553.
- [20] S. Yoshioka, Y. Aso, K. Izutsu, T. Terao, Aggregates Formed During Storage of β -Galactosidase in Solution and in the Freeze-Dried State, *Pharm. Res.* 10 (1993) 687-691.
- [21] B. Li, R. Schowen, E. M. Topp, R. Borchardt, Effect of N-1 and N-2 residues on peptide deamidation rate in solution and solid state., *AAPS J.* 8 (2006) 166-73.
- [22] M. C. Manning, K. Patel, R. Borchardt, Stability of Protein Pharmaceuticals, *Pharm. Dev. Technol.* 6 (1989) 903–918.
- [23] R. Harris, B. Kabakoff, F. Macchi, F. Shen, M. Kwong, J. Andya, S. Shire, N. Bjork, K. Totpal, A. Chen, Identification of multiple sources of charge heterogeneity in a recombinant antibody, *J. Chromatogr. B. Biomed. Sci. Appl.* 752 (2001) 233–245.
- [24] S. Hovorka, C. Schoenneich, Oxidative degradation of pharmaceuticals: Theory, mechanisms and inhibition, *J. Pharm. Sci.* 90 (2001) 253–269.

- [25] S. Fischer, J. Hoernschemeyer, H. C. Mahler, Glycation during storage and administration of monoclonal antibody formulations, *Eur. J. Pharm. Biopharm.* 70 (2008) 42–50.
- [26] A. Hawe, W. Friess, Development of HSA-free formulations for a hydrophobic cytokine with improved stability, *Eur. J. Pharm. Biopharm.* 68 (2008) 169–182.
- [27] A. Hawe, M. Wiggernhorn, M. van de Weert, J. Garbe, H. C. Mahler, W. Jiskoot, Forced degradation of therapeutic proteins, *J. Pharm. Sci.* 101 (2012) 895–913.
- [28] E. Tamizi, A. Jouyban, Forced degradation studies of biopharmaceuticals: Selection of stress conditions, *Eur. J. Pharm. Biopharm.* 98 (2015) 26–46.
- [29] J. F. Carpenter, T. W. Randolph, W. Jiskoot, D. Crommelin, C. Middaugh, G. Winter, Y. Fan, S. Kirshner, D. Verthelyi, S. Kozlowski, K. Clouse, P. Swann, A. Rosenberg, B. Cherney, Overlooking Subvisible Particles in Therapeutic Protein Products: Gaps That May Compromise Product Quality, *J. Pharm. Sci.* 98 (2009) 1201–1205.
- [30] E. M. Moussa, J. Panchal, B. Moorthy, J. Blum, M. Joubert, L. Narhi, E. M. Topp, Immunogenicity of Therapeutic Protein Aggregates, *J. Pharm. Sci.* 105 (2016) 417-430.
- [31] J. Bessa, S. Boeckle, H. Beck, T. Buckel, S. Schlicht, M. Ebeling, A. Kiialainen, A. Koulov, B. Boll, T. Weiser, T. Singer, A. Rolink, A. Iglesias, The immunogenicity of antibody aggregates in a novel transgenic mouse model, *Pharm. Res.* 32 (2015) 2344–2359.
- [32] B. Boll, J. Bessa, E. Folzer, A. Ríos Quiroz, R. Schmidt, P. Bulau, C. Finkler, H. C. Mahler, J. Huwyler, A. Iglesias, A. V. Koulov, Extensive chemical modifications in the primary protein structure of IgG1 subvisible particles are necessary for breaking immune tolerance, *Mol. Pharm.* 14 (2017) 1292-1299.
- [33] E. Tamizi, A. Jouyban, The potential of the capillary electrophoresis techniques for quality control of biopharmaceuticals-A review, *Electrophoresis.* 36 (2015) 831–858.
- [34] Z. Sobic, D. Houde, A. Blum, T. Carlage, Y. Lyubarskaya, Application of imaging capillary IEF for characterization and quantitative analysis of recombinant protein charge heterogeneity, *Electrophoresis.* 29 (2008) 4368–4376.
- [35] M. Bloemendal, W. Jiskoot, Circular Dichroism Spectroscopy, in: W. Jiskoot, D.J.A. Crommelin (Eds.), *Methods Struct. Anal. Protein Pharm.*, (2005) 83–130.

- [36] M. Van der Weert, J. Hering, P. Haris, Fourier Transform Infrared Spectroscopy, in: W. Jiskoot, D. Crommelin (Eds.), *Methods Struct. Anal. Protein Pharm.*, (2005) 131–166.
- [37] W. Wang, Instability, stabilization, and formulation of liquid protein pharmaceuticals, *Int. J. Pharm.* 185 (1999) 129–188.
- [38] W. Wang, Lyophilization and development of solid protein pharmaceuticals, *Int. J. Pharm.* 203 (2000) 1–60.
- [39] B. Roser, Trehalose, a new approach to premium dried foods, *Trends Food Sci. Technol.* 2 (1991) 166–169.
- [40] X. Chen, A. Mujumdar, *Drying Technologies in Food Processing*, John Wiley & Sons, (2009).
- [41] M. Mattern, G. Winter, U. Kohnert, G. Lee, Formulation of proteins in vacuum-dried glasses. II. Process and storage stability in sugar-free amino acid systems., *Pharm. Dev. Technol.* 4 (1999) 199–208.
- [42] V. Kumar, V. Sharma, D. Kalonia, In situ precipitation and vacuum drying of interferon alpha-2a: Development of a single-step process for obtaining dry, stable protein formulation, *Int. J. Pharm.* 366 (2009) 88–98.
- [43] P. Wildfong, A. Samy, J. Corfa, G. Peck, K. Morris, Accelerated fluid bed drying using NIR monitoring and phenomenological modeling: Method assessment and formulation suitability, *J. Pharm. Sci.* 91 (2002) 631–639.
- [44] A. M. Abdul-Fattah, D. Lechuga-Ballesteros, D. Kalonia, M. J. Pikal, The impact of drying method and formulation on the physical properties and stability of methionyl human growth hormone in the amorphous solid state, *J. Pharm. Sci.* 97 (2008) 163-184.
- [45] L. Rey, J. May, *Freeze Drying / Lyophilization of Pharmaceutical and Biological Products*, (2010).
- [46] M. Bowen, R. Turok, Y. Maa, Spray Drying of Monoclonal Antibodies: Investigating Powder-Based Biologic Drug Substance Bulk Storage, *Dry. Technol.* 31 (2013) 1441-1450.
- [47] S. Wanning, R. Süverkrüp, A. Lamprecht, Pharmaceutical spray freeze drying, *Int. J. Pharm.* 488 (2015) 136–153.

- [48] L. Chang, D. Shepherd, J. Sun, D. Ouellette, K. Grant, X. Tang, M. J. Pikal, Mechanism of protein stabilization by sugars during freeze-drying and storage: native structure preservation, specific interaction, and/or immobilization in a glassy matrix?, *J. Pharm. Sci.* 94 (2005) 1427–1444.
- [49] M. T. Cicerone, M. J. Pikal, K. Qian, Stabilization of proteins in solid form, *Adv. Drug Deliv. Rev.* 93 (2015) 14–24.
- [50] S. Prestrelski, N. Tedeschi, T. Arakawa, J. F. Carpenter, Dehydration-induced conformational transitions in proteins and their inhibition by stabilizers, *Biophys. J.* 65 (1993) 661–71.
- [51] J. Cleland, X. Lam, B. Kendrick, J. Yang, T. Yang, D. Overcashier, D. Brooks, C. Hsu, J. F. Carpenter, A specific molar ratio of stabilizer to protein is required for storage stability of a lyophilized monoclonal antibody, *J. Pharm. Sci.* 90 (2001) 310–321.
- [52] J. Andya, Y. Maa, H. Costantino, P. Nguyen, N. Dasovich, T. Sweeney, C. Hsu, S. Shire, The effect of formulation excipients on protein stability and aerosol performance of spray-dried powders of a recombinant humanized anti- IgE monoclonal antibody., *Pharm Res.* 16 (1999) 350–358.
- [53] B. Wang, S. Tchessalov, N. Warne, M. J. Pikal, Impact of sucrose level on storage stability of proteins in freeze-dried solids: I. Correlation of protein-sugar interaction with native structure preservation, *J. Pharm. Sci.* 98 (2009) 3131–3144.
- [54] S. Allison, B. Chang, T. W. Randolph, J. F. Carpenter, Hydrogen bonding between sugar and protein is responsible for inhibition of dehydration-induced protein unfolding, *Arch. Biochem. Biophys.* 365 (1999) 289–298.
- [55] S. Yoshioka, Y. Aso, Correlations between Molecular Mobility and Chemical Stability During Storage of Amorphous Pharmaceuticals, *J. Pharm. Sci.* 96 (2007) 960–981.
- [56] M. T. Cicerone, A. Tellington, L. Trost, A. Sokolov, Substantially Improved Stability of Biological Agents in Dried Form - The Role of Glassy Dynamics in Preservation of Biopharmaceuticals, *Bioprocess Int.* 1 (2003) 36–47.
- [57] G. Zografi, A. Newman, Interrelationships Between Structure and the Properties of Amorphous Solids of Pharmaceutical Interest, *J. Pharm. Sci.* 106 (2016) 5-27.
- [58] M. T. Cicerone, C. Soles, Fast dynamics and stabilization of proteins: binary glasses of trehalose and glycerol, *Biophys. J.* 86 (2004) 3836–3845.

- [59] L. Chang, D. Shepherd, J. Sun, X. Tang, M. J. Pikal, Effect of sorbitol and residual moisture on the stability of lyophilized antibodies: Implications for the mechanism of protein stabilization in the solid state, *J. Pharm. Sci.* 94 (2005) 1445–1455.
- [60] V. Wahl, J. Khinast, A. Paudel, Lyophilized protein powders: A review of analytical tools for root cause analysis of lot-to-lot variability, *TrAC - Trends Anal. Chem.* 82 (2016) 468-491.
- [61] V. Wahl, O. Scheibelhofer, U. Roessler, S. Leitgeb, T. De Beer, J. Khinast, The influence of residual water on the secondary structure and crystallinity of freeze-dried fibrinogen, *Int. J. Pharm.* 484 (2015) 95–102.
- [62] E. Suihko, R. Forbes, D. Apperley, A solid-state NMR study of molecular mobility and phase separation in co-spray-dried protein–sugar particles, *Eur. J. Pharm. Sci.* 25 (2005) 105–112.
- [63] S. Clas, C. Dalton, B. Hancock, Differential scanning calorimetry: applications in drug development, *Pharm. Sci. Technol. Today.* 2 (1999) 311–320.
- [64] S. Duddu, P. Dal Monte, Effect of glass transition temperature on the stability of lyophilized formulations containing a chimeric therapeutic monoclonal antibody., *Pharm. Res.* 14 (1997) 591–595.
- [65] J.F. Carpenter, B. Chang, W. Garzon-Rodriguez, T. W. Randolph, Rational Design of Stable Lyophilized Protein Formulations: Theory and Practice, in: Springer US, (2002) 109–133.
- [66] R. Fang, P. Grobelny, R. Bogner, M. J. Pikal, Protein Internal Dynamics Associated With Pre–System Glass Transition Temperature Endothermic Events: Investigation of Insulin and Human Growth Hormone by Solid State Hydrogen/Deuterium Exchange, *J. Pharm. Sci.* 105 (2016) 3290-3295.
- [67] H. Grohganz, Y. Lee, J. Rantanen, M. Yang, The influence of lysozyme on mannitol polymorphism in freeze-dried and spray-dried formulations depends on the selection of the drying process, *Int. J. Pharm.* 447 (2013) 224–230.
- [68] M. J. Pikal, Freeze-Drying of Proteins. Part I: Process Design, *Biopharm.* 3 (1990) 18-23.
- [69] M. J. Pikal, S. Shah, Intravial distribution of moisture during the secondary drying stage of freeze drying, *PDA J. Pharm. Sci. Technol.* 51 (1997) 17–24.

- [70] T. Lin, C. Hsu, Determination of residual moisture in lyophilized protein pharmaceuticals using a rapid and non-invasive method: near infrared spectroscopy., *PDA J. Pharm. Sci. Technol.* 56 (2002) 196–205.
- [71] D. Duncan, J. Veale, I. Cook, K. Ward, Using Laser-Based Headspace Moisture Analysis for Rapid Nondestructive Moisture Determination of Sterile Freeze-Dried Product, 1–12.
- [72] V. Mozhaev, K. Martinek, Structure-stability relationships in proteins: new approaches to stabilizing enzymes, *Enzyme Microb. Technol.* 6 (1984) 50–59.
- [73] S. Allison, A. Dong, J. F. Carpenter, Counteracting effects of thiocyanate and sucrose on chymotrypsinogen secondary structure and aggregation during freezing, drying, and rehydration, *Biophys. J.* 71 (1996) 2022–2032.
- [74] J. H. Crowe, J. F. Carpenter, L. Crowe, The role of vitrification in anhydrobiosis, *Annu. Rev. Physiol.* 60 (1998) 73–103.
- [75] J. O'Brian, Stability of Trehalose, Sucrose and Glucose to Nonenzymatic Browning in Model Systems, *J. Food Sci.* 61 (1996) 679–682.
- [76] P. Sundaramurthi, R. Suryanarayanan, Trehalose Crystallization During Freeze-Drying: Implications On Lyoprotection, *J. Phys. Chem. Lett.* 1 (2010) 510–514.
- [77] S. Ohtake, Y. Wang, Trehalose: Current Use and Future Applications, *J. Pharm. Sci.* 100 (2011) 2020–2053.
- [78] C. Colaço, B. Roser, Trehalose-a multifunctional additive for food preservation, in: *Food Packag. Preserv.*, Springer US, Boston, MA, (1994) 123–140.
- [79] C. Schebor, L. Burin, M. Buera, J. Chirife, Stability to Hydrolysis and Browning of Trehalose, Sucrose and Raffinose in Low-moisture Systems in Relation to Their Use as Protectants of Dry Biomaterials, *LWT - Food Sci. Technol.* 32 (1999) 481–485.
- [80] L. Taylor, G. Zografi, Sugar-polymer hydrogen bond interactions in lyophilized amorphous mixtures., *J. Pharm. Sci.* 87 (1998) 1615–21.
- [81] N. Chieng, M. T. Cicerone, Q. Zhong, M. Liu, M. J. Pikal, Characterization of dynamics in complex lyophilized formulations: II. Analysis of density variations in terms of glass dynamics and comparisons with global mobility, fast dynamics, and Positron Annihilation Lifetime Spectroscopy (PALS), *Eur. J. Pharm. Biopharm.* 85 (2013) 197-206.

- [82] Y. Xu, J. F. Carpenter, M. T. Cicerone, T. W. Randolph, Contributions of local mobility and degree of retention of native secondary structure to the stability of recombinant human growth hormone (rhGH) in glassy lyophilized formulations, *Soft Matter*. 9 (2013) 7855.
- [83] M. Sola-Penna, J. Meyer-Fernandes, Stabilization against thermal inactivation promoted by sugars on enzyme structure and function: why is trehalose more effective than other sugars?, *Arch. Biochem. Biophys.* 360 (1998) 10–14.
- [84] S. Jena, R. Suryanarayanan, A. Aksan, Mutual Influence of Mannitol and Trehalose on Crystallization Behavior in Frozen Solutions., *Pharm. Res.* 33 (2016) 1413–25.
- [85] P. Sundaramurthi, T. W. Patapoff, R. Suryanarayanan, Crystallization of Trehalose in Frozen Solutions and its Phase Behavior during Drying, *Pharm. Res.* 27 (2010) 2374-2383.
- [86] M. Maury, K. Murphy, S. Kumar, A. Mauerer, G. Lee, Spray-drying of proteins: effects of sorbitol and trehalose on aggregation and FT-IR amide I spectrum of an immunoglobulin G., *Eur. J. Pharm. Biopharm.* 59 (2005) 251–261.
- [87] B. Gikanga, R. Turok, A. Hui, M. Bowen, O. Stauch, Y. Maa, Manufacturing of High-Concentration Monoclonal Antibody Formulations via Spray Drying-the Road to Manufacturing Scale., *PDA J. Pharm. Sci. Technol.* 69 (2015) 59–73.
- [88] M. T. Cicerone, J. Douglas, β -Relaxation governs protein stability in sugar-glass matrices, *Soft Matter*. 8 (2012) 2983.
- [89] F. Franks, Freeze-drying: From empiricism to predictability, *Cryo Letters*. 11 (1990) 93–110.
- [90] L. Yu, D. Mishra, D. Rigsbee, Determination of the Glass Properties of D-Mannitol Using Sorbitol as an Impurity, *J. Pharm. Sci.* 87 (1998) 774–777.
- [91] J. Obrzut, A. Anopchenko, J. Douglas, B. Rust, Relaxation and antiplasticization measurements in trehalose–glycerol mixtures – A model formulation for protein preservation, *J. Non. Cryst. Solids*. 356 (2010) 777–781.
- [92] S. Bhattacharya, R. Suryanarayanan, Local mobility in amorphous pharmaceuticals - Characterization and implications on stability, *J. Pharm. Sci.* 98 (2009) 2935–2953.
- [93] M. Roussanova, J. Andrieux, M. Alam, J. Ubbink, Hydrogen bonding in maltooligomer-glycerol-water matrices: Relation to physical state and molecular free volume., *Carbohydr. Polym.* 102 (2014) 566–75.

- [94] K. Forney-Stevens, R. Bogner, M. J. Pikal, Addition of Amino Acids to Further Stabilize Lyophilized Sucrose-Based Protein Formulations: I. Screening of 15 Amino Acids in Two Model Proteins., *J. Pharm. Sci.* 105 (2016) 697–704.
- [95] M. Heller, J. F. Carpenter, T. W. Randolph, Effects of phase separating systems on lyophilized hemoglobin, *J. Pharm. Sci.* 85 (1996) 1358–1362.
- [96] M. Mensink, P. Van Bockstal, S. Pieters, L. de Meyer, H. Frijlink, K. van der Voort Maarschalk, W. Hinrichs, T. De Beer, In-line near infrared spectroscopy during freeze-drying as a tool to measure efficiency of hydrogen bond formation between protein and sugar, predictive of protein storage stability., *Int. J. Pharm.* 496 (2015) 792–800.
- [97] T. Bosch, Aggressive Freeze-Drying – a fast and suitable method to stabilize biopharmaceuticals, Ludwig-Maximilians Universität München, (2014).
- [98] P. Stärtzel, H. Gieseler, M. Gieseler, A. M. Abdul-Fattah, M. Adler, H. C. Mahler, P. Goldbach, Freeze Drying of L-Arginine/Sucrose-Based Protein Formulations, Part I: Influence of Formulation and Arginine Counter Ion on the Critical Formulation Temperature, Product Performance and Protein Stability, *J. Pharm. Sci.* 104 (2015) 2345–2358.
- [99] S. Schüle, T. Schulz-Fademrecht, P. Garidel, K. Bechtold-Peters, W. Frieß, Stabilization of IgG1 in spray-dried powders for inhalation, *Eur. J. Pharm. Biopharm.* 69 (2008) 793–807.
- [100] S. Webb, S. Golledge, J. Cleland, J. F. Carpenter, T. W. Randolph, Surface adsorption of recombinant human interferon- γ in lyophilized and spray-lyophilized formulations, *J. Pharm. Sci.* 91 (2002) 1474–1487.
- [101] N. Bam, T. W. Randolph, J. Cleland, Stability of protein formulations: investigation of surfactant effects by a novel EPR spectroscopic technique, *Pharm. Res.* 12 (1995) 2-11.
- [102] T. Serno, R. Geidobler, G. Winter, Protein stabilization by cyclodextrins in the liquid and dried state, *Adv. Drug Deliv. Rev.* 63 (2011) 1086–106.
- [103] T. Serno, E. Härtl, A. Besheer, R. Miller, G. Winter, The Role of Polysorbate 80 and HP β CD at the Air-Water Interface of IgG Solutions, *Pharm. Res.* 30 (2013) 117–130.
- [104] A. Millqvist-Fureby, M. Malmsten, B. Bergenståhl, Spray-drying of trypsin - Surface characterisation and activity preservation, *Int. J. Pharm.* 188 (1999) 243–253.

- [105] B. Chen, R. Bautista, K. Yu, G. Zapata, M. Mulkerrin, S. Chamow, Influence of histidine on the stability and physical properties of a fully human antibody in aqueous and solid forms., *Pharm. Res.* 20 (2003) 1952–60.
- [106] J. F. Carpenter, L. Crowe, J. Crowe, Stabilization of phosphofructokinase with sugars during freeze-drying: characterization of enhanced protection in the presence of divalent cations, *Biochim. Biophys. Acta - Gen. Subj.* 923 (1987) 109–115.
- [107] Y. Maa, P. Nguyen, S. Hsu, Spray-Drying of Air–Liquid Interface Sensitive Recombinant Human Growth Hormone, *J. Pharm. Sci.* 87 (1998) 152–159.
- [108] B. Bhatnagar, R. Bogner, M. J. Pikal, Protein Stability During Freezing: Separation of Stresses and Mechanisms of Protein Stabilization, *Pharm. Dev. Technol.* 12 (2007) 505–523.
- [109] T. Jennings, The importance of process water, in: *Lyophilization Introd. Basic Princ.*, Interpharm Press, Englewood, USA, (1999).
- [110] A. Twomey, K. Kurata, Y. Nagare, H. Takamatsu, A. Aksan, Microheterogeneity in frozen protein solutions, *Int. J. Pharm.* 487 (2015) 91–100.
- [111] U. Roessl, S. Leitgeb, B. Nidetzky, Protein freeze concentration and micro-segregation analysed in a temperature-controlled freeze container, *Biotechnol. Reports.* 6 (2015) 108–111.
- [112] T. Anchordoquy, J. F. Carpenter, Polymers Protect Lactate Dehydrogenase during Freeze-Drying by Inhibiting Dissociation in the Frozen State, *Arch. Biochem. Biophys.* 332 (1996) 231–238.
- [113] B. Bhatnagar, M. J. Pikal, R. Bogner, Study of the Individual Contributions of Ice Formation and Freeze-Concentration on Isothermal Stability of Lactate Dehydrogenase during Freezing, *J. Pharm. Sci.* 97 (2008) 798–814.
- [114] B. Szkudlarek, Selective crystallization of phosphate buffer components and pH changes during freezing: Implications to protein stability, in: *University of Michigan, Ann Arbor, MI, USA, (1997).*
- [115] Ľ. Krausková, J. Procházková, M. Klačková, L. Filipová, R. Chaloupková, S. Malý, J. Damborský, D. Heger, Suppression of protein inactivation during freezing by minimizing pH changes using ionic cryoprotectants, *Int. J. Pharm.* 509 (2016) 41–49.

- [116] H. Costantino, K. Griebenow, P. Mishra, R. Langer, A. Klivanov, Fourier-transform infrared spectroscopic investigation of protein stability in the lyophilized form, *Biochim. Biophys. Acta - Protein Struct. Mol. Enzymol.* 1253 (1995) 69–74.
- [117] X. Tang, M. J. Pikal, Measurement of the Kinetics of Protein Unfolding in Viscous Systems and Implications for Protein Stability in Freeze-Drying, *Pharm. Res.* 22 (2005) 1176–1185.
- [118] J. Schwegman, J. F. Carpenter, S. L. Nail, Evidence of partial unfolding of proteins at the ice/freeze-concentrate interface by infrared microscopy, *J. Pharm. Sci.* 98 (2009) 3239–3246.
- [119] R. Geidobler, G. Winter, Controlled ice nucleation in the field of freeze-drying: Fundamentals and technology review, *Eur. J. Pharm. Biopharm.* 85 (2013) 214–222.
- [120] R. Geidobler, I. Konrad, G. Winter, Can Controlled Ice Nucleation Improve Freeze-Drying of Highly-Concentrated Protein Formulations?, *J. Pharm. Sci.* 102 (2013) 3915–3919.
- [121] G. Winter, I. Vollrath, A. Hawe, R. Geidobler, I. Presser, W. Frieß, Controlled ice nucleation in freeze-drying, in: *Free. Pharm. Biol.*, Breckenridge, USA, (2016).
- [122] R. Esfandiary, S. Gattu, J. Stewart, S. M. Patel, Effect of Freezing on Lyophilization Process Performance and Drug Product Cake Appearance, *J. Pharm. Sci.* 105 (2016) 1427–1433.
- [123] B. Chang, C. Randall, Use of subambient thermal analysis to optimize protein lyophilization, *Cryobiology.* 29 (1992) 632–656.
- [124] S. Jena, J. Horn, R. Suryanarayanan, W. Friess, A. Aksan, Effects of Excipient Interactions on the State of the Freeze-Concentrate and Protein Stability, *Pharm. Res.* 34 (2017) 462–478.
- [125] K. Schersch, O. Betz, P. Garidel, S. Muehlau, S. Bassarab, G. Winter, Systematic investigation of the effect of lyophilization collapse on pharmaceutically relevant proteins, Part 2: Stability During Storage at Elevated Temperatures, *Eur. J. Pharm. Biopharm.* 85 (2013) 240–252.
- [126] A. Barman, C. Smitherman, M. Souffrant, G. Gadda, D. Hamelberg, Conserved Hydration Sites in Pin1 Reveal a Distinctive Water Recognition Motif in Proteins, *J. Chem. Inf. Model.* 56 (2016) 139–147.

- [127] J. Colandene, L. Maldonado, A. Creagh, J. Vrettos, K. Goad, T. Spitznagel, Lyophilization Cycle Development for a High-Concentration Monoclonal Antibody Formulation Lacking a Crystalline Bulking Agent, *J. Pharm. Sci.* 96 (2007) 1598–1608.
- [128] R. Depaz, S. Pansare, S. M. Patel, Freeze-Drying Above the Glass Transition Temperature in Amorphous Protein Formulations While Maintaining Product Quality and Improving Process Efficiency, *J. Pharm. Sci.* 105 (2016) 40–49.
- [129] X. Tang, M. J. Pikal, Design of Freeze-Drying Processes for Pharmaceuticals: Practical Advice, *Pharm. Res.* 21 (2004) 191–200.
- [130] S. Ullrich, S. Seyferth, G. Lee, Measurement of Shrinkage and Cracking in Lyophilized Amorphous Cakes Part 3: Hydrophobic Vials and the Question of Adhesion, *J. Pharm. Sci.* 104 (2015) 2040–2046.
- [131] S. Ullrich, S. Seyferth, G. Lee, Measurement of Shrinkage and Cracking in Lyophilized Amorphous Cakes Part 4: Effects of Freezing Protocol, *Int. J. Pharm.* 495 (2015) 52-57.
- [132] S. Rambhatla, J.P. Obert, S. Luthra, C. Bhugra, M. J. Pikal, Cake shrinkage during freeze drying: a combined experimental and theoretical study., *Pharm. Dev. Technol.* 10 (2005) 33–40.
- [133] A. M. Abdul-Fattah, R. Oeschger, H. Roehl, I. Bauer Dauphin, M. Worgull, G. Kallmeyer, H. C. Mahler, Investigating factors leading to fogging of glass vials in lyophilized drug products, *Eur. J. Pharm. Biopharm.* 85 (2013) 314–326.
- [134] E. Koepf, G. Brezesinski, W. Friess, The Film Tells The Story: Physicochemical Characteristics of IgG at the Liquid-Air Interface, *Eur. J. Pharm. Biopharm.* 119 (2017) 396-407.
- [135] M. Adler, G. Lee, Stability and surface activity of lactate dehydrogenase in spray-dried trehalose, *J. Pharm. Sci.* 88 (1999) 199–208.
- [136] M. Adler, M. Unger, G. Lee, Surface composition of spray-dried particles of bovine serum albumin/trehalose/surfactant, *Pharm. Res.* 17 (2000) 863–70.
- [137] M. Fitzner, Chemical and physicochemical stability of spray dried rhIL-11 formulations, Friedrich-Alexander Universität Erlangen-Nürnberg, (2003).
- [138] K. Schmid, C. Arpagaus, W. Friess, Evaluation of the Nano Spray Dryer B-90 for pharmaceutical applications., *Pharm. Dev. Technol.* 16 (2011) 287–94.

- [139] J. Schaefer, G. Lee, Arrhenius activation energy of damage to catalase during spray-drying, *Int. J. Pharm.* 489 (2015) 124–130.
- [140] M. Maury, K. Murphy, S. Kumar, L. Shi, G. Lee, Effects of process variables on the powder yield of spray-dried trehalose on a laboratory spray-dryer, *Eur. J. Pharm. Biopharm.* 59 (2005) 565–573.
- [141] Y. Maa, P. Nguyen, J. Andya, N. Dasovich, T. Sweeney, S. Shire, C. Hsu, Effect of spray drying and subsequent processing conditions on residual moisture content and physical/biochemical stability of protein inhalation powders, *Pharm. Res.* 15 (1998) 768–775.
- [142] P. Lassner, M. Adler, G. Lee, Formation of Insoluble Particulates in a Spray-Dried F(ab')₂ Fragment, *J. Pharm. Sci.* 103 (2014) 1021–1031.
- [143] J. Broadhead, S. Rouan, I. Hau, C. Rhodes, The effect of process and formulation variables on the properties of spray-dried beta-galactosidase, *J. Pharm. Pharmacol.* 46 (1994) 458–67.
- [144] S. Branchu, R. Forbes, P. York, S. Petrán, H. Nyqvist, O. Camber, Hydroxypropyl- β -cyclodextrin inhibits spray-drying-induced inactivation of β -galactosidase, *J. Pharm. Sci.* 88 (1999) 905–911.

Chapter 2

Objectives of the Thesis

Analytical tools that are capable to monitor the freeze-drying process are increasingly required for improved process understanding [1]. The optical fiber system (OFS) was already shown to measure temperature during the freeze-drying process and, moreover, to be potentially able to detect glass transition or crystallization events directly in the freeze-dryer [2]. This potential was investigated in freeze/thaw and freeze-drying experiments and compared to the standard DSC and FDM measurements (**Chapter 3**). The impact of different saccharides and proteins, excipient concentration and heating rate was comprehensively studied. Mannitol (Man) crystallization was characterized by OFS and DSC. The potential of the OFS as analytical tool in lyophilisation processes was investigated with collapse and non-collapse lyophilisation cycles of different sugar solutions.

The first step in freeze-drying, the freezing step, already determines many of the final product characteristics as pore size or excipient crystallinity and affects protein stability. Therefore, the impact of the freeze-concentrate composition consisting of the bulking agent Man, the protein stabilizer trehalose (Tre) and the protein BSA was characterized upon freezing, annealing at -20 °C and after thawing (**Chapter 4**). DSC, IR and XRD were used to characterize the frozen solutions while IR, CD, turbidity, LO and HP-SEC facilitated the determination of the BSA structure and the formation of aggregates in liquid samples before and after freeze-thawing. Crystallization of the excipients was correlated to protein unfolding and aggregate formation in different Man/Tre/BSA ratios. This study was performed in cooperation with Prof. Alptekin Aksan and Sampreeti Jena from the University of Minnesota.

Freeze-drying is time- and cost-intensive due to its low process temperatures and the hence long drying times [3]. Fast freeze-drying at higher product temperatures (T_p) would hence enable shorter process times at reduced production costs. Typically, amorphous sugar formulations would collapse if dried at high T_p . Therefore, the crystalline bulking agent Man was added to sucrose (Suc) to freeze-dry at high T_p s without defects in cake appearance despite collapse of the Suc matrix (**Chapter 5**). The aim was to minimize process time without harming cake structure and protein process stability. The freeze-dried cakes were comprehensively studied regarding their physical characteristics (residual moisture (RM),

glass transition temperatures (T_g), Man crystallinity and reconstitution times) and regarding protein process stability (particle and aggregate formation). The results were compared to conservative freeze-drying at low T_p and hence long drying time.

A 4/1 Man/Suc ratio was required for complete Man crystallization. This high proportion of crystallizing bulking agent prevented a higher stabilizer content that may be necessary for adequate protein stabilization. Therefore, alternative bulking agents were to be identified which: (1) crystallize at lower bulking agent to Suc ratio compared to Man and (2) have no negative impact on cake characteristics and protein stability. Crystallizing amino acids (AA) (phenylalanine, leucine, isoleucine, methionine, glycine) were identified as potential bulking agents and were thoroughly investigated in different AA/Suc ratios (**Chapter 6**). XRPD was a key method to detect AA crystallization. Suitable cake appearance was a prerequisite for further selection. The AA/Suc lyophilizates had to withstand macrocollapse despite fast freeze-drying at high T_p . Residual moisture, T_g values as well as reconstitution times complemented the analyses of the freeze-dried AA/Suc samples. Protein process stability (turbidity, sub-visible particles and aggregate formation) was tested with the three most promising bulking agents (phenylalanine, isoleucine and leucine).

References

- [1] S. Nail, S. Tchessalov, E. Shalaev, A. Ganguly, E. Renzi, F. Dimarco, L. Wegiel, S. Ferris, W. Kessler, M. J. Pikal, G. Sacha, A. Alexeenko, T.N. Thompson, C. Reiter, J. Searles, P. Coiteux, Recommended Best Practices for Process Monitoring Instrumentation in Pharmaceutical Freeze Drying—2017, AAPS PharmSciTech. (2017).
- [2] J. Kasper, M. Wiggerhorn, M. Resch, W. Friess, Implementation and evaluation of an optical fiber system as novel process monitoring tool during lyophilization., *Eur. J. Pharm. Biopharm.* 83 (2013) 449–59.
- [3] X. Tang, M. J. Pikal, Design of Freeze-Drying Processes for Pharmaceuticals: Practical Advice, *Pharm. Res.* 21 (2004) 191–200.

Chapter 3

Detection of Collapse and Crystallization of Saccharide, Protein and Mannitol Formulations by Optical Fibers in Lyophilization

The following chapter has been published as research article in the *Frontiers in Chemistry* journal and appears in this thesis with the journal's permission:

Jacqueline Horn and Wolfgang Friess

Detection of Collapse and Crystallization of Saccharide, Protein, and Mannitol Formulations by Optical Fibers in Lyophilization

Frontiers in Chemistry 6 (2018), 1–9

doi:10.3389/fchem.2018.00004.

Abstract

The collapse temperature (T_c) and the glass transition temperature of freeze-concentrated solutions (T_g') as well as the crystallization behavior of excipients are important physicochemical characteristics which guide the cycle development in freeze-drying. The most frequently used methods to determine these values are differential scanning calorimetry (DSC) and freeze-drying microscopy (FDM). The objective of this study was to evaluate the optical fiber system (OFS) unit as alternative tool for the analysis of T_c , T_g' and crystallization events. The OFS unit was also tested as a potential online monitoring tool during freeze-drying. Freeze/thawing and freeze-drying experiments of sucrose, trehalose, stachyose, mannitol and highly concentrated IgG1 and lysozyme solutions were carried out and monitored by the OFS. Comparative analyses were performed by DSC and FDM. OFS and FDM results correlated well. The crystallization behavior of mannitol could be monitored by the OFS during freeze/thawing as it can be done by DSC. Online monitoring of freeze-drying runs detected collapse of amorphous saccharide matrices. The OFS unit enabled the

analysis of both T_c and crystallization processes, which is usually carried out by FDM and DSC. The OFS can hence be used as novel measuring device. Additionally, detection of these events during lyophilization facilitate online-monitoring. Thus the OFS is a new beneficial tool for the development and monitoring of freeze-drying processes.

Keywords

Freeze-drying, lyophilization, optical fiber system, glass transition, collapse, crystallization, monitoring

Abbreviations

DSC	Differential scanning calorimetry
FBG	Fiber bragg grating
FDM	Freeze-drying microscopy
OFS	Optical fiber system
PAT	Process analytical technology
T_c	Collapse temperature
T_{cry}	Crystallization temperature
T_g'	Glass transition temperature of the freeze-concentrated solution
T_{OFS}	Temperature of OFS peak during heating

Table of Content

Abstract	38
Keywords.....	39
Abbreviations	39
1. Introduction	41
2. Materials and Methods.....	43
2.1. Materials	43
2.2. The optical fiber system (OFS).....	43
2.2.1. OFS unit.....	43
2.2.2. OFS – Determination of the T_c and T_{cry} during freeze/thawing	44
2.2.3. OFS – Use in freeze-drying cycles	44
2.3. Differential scanning calorimetry (DSC).....	45
2.4. Freeze-drying microscopy (FDM)	45
2.5. Statistical analysis.....	45
3. Results and Discussion	46
3.1. OFS thermograms.....	46
3.2. Detailed investigation of the T_{OFS} peak.....	46
3.2.1. Impact of heating rate on peak location of T_{OFS}	47
3.2.2. Impact of solute concentration on peak location of T_{OFS}	47
3.2.3. Comparison of OFS with DSC and FDM	48
3.3. OFS Application to detect crystallization events	49
3.4. OFS Application during lyophilization	51
4. Conclusion.....	53
Acknowledgements.....	54
Author Contributions	54
References	55

1. Introduction

Freeze-drying is commonly used for the long-term stabilization of biopharmaceuticals which cannot be stabilized adequately in the liquid state. Efficient development of freeze-drying cycles is of utmost importance as the process is time and cost consuming. Short process times without putting the protein stability at risk are desired [1–3]. It is essential to analyze the formulation to be freeze-dried regarding critical parameters for the freeze-drying process.

Typical parameters of amorphous matrices, as formed by the most frequently used saccharides for stabilization of proteins, sucrose and trehalose, are the collapse temperature (T_c) and the glass transition temperature (T_g') of the freeze-concentrated solution [4,5]. They characterize temperatures at which the mobility of the system greatly increases, either at the drying front (T_c) or in the frozen state (T_g'). T_c is typically determined by freeze-drying microscopy (FDM) whereas the standard method for T_g' is differential scanning calorimetry (DSC). FDM mimics the freeze-drying process in miniature by freezing and drying small volumes of formulation under the microscope. T_c can be defined as either the onset of visible collapse or full collapse [5,6]. T_g' as analyzed by DSC reflects the temperature at which the heat capacity of the freeze-concentrated formulation markedly changes [4]. Both values help to define the upper limit of the product temperature (T_p) during the primary drying step. In lab scale, T_p is typically measured by thermocouples that can only represent the temperature of the surrounding environment although the local temperature of the sublimation front might be more critical for the occurrence of collapse. T_c values are usually 1 to 3 °C higher than T_g' values and drying above T_c may result in macrocollapse of the lyophilizate. Drying above T_g' but below T_c can be utilized e.g. for highly concentrated protein formulations [7]. It enables higher product temperatures, faster drying and thus shorter process times without loss of cake structure if protein stability is preserved [7]. Nanoparticle suspensions were also shown to increase collapse temperatures [8]. Macrocollapse is not only a question of elegant cake appearance, but it can, but not necessarily has to be correlated to higher residual moisture levels after the process, destabilization of the API, longer reconstitution time or prolonged secondary drying [6,9,10]. Nevertheless, since it is known that an 1 °C increase in T_p can shorten primary drying times by about 13%, the interest is to dry at the highest possible T_p [11]. Crystalline bulking agents like mannitol not necessarily stabilize proteins but form crystalline scaffolds that provide robust and elegant cake structures [12–15]. Their controlled and complete crystallization during the freeze-drying process is of interest since partial crystallization might induce subsequent crystallization of the amorphous fraction during storage leading to potential loss of drug stability [16]. Crystallization occurs mainly during thermal treatment before drying starts [17]. In order to force crystallization, an annealing step

is usually conducted at temperatures above T_g' [18]. The temperature at which crystallization (T_{cry}) occurs can be determined by DSC measurements [13].

Thus, the correct characterization of the system is of utmost importance. FDM and DSC both provide good approximations but are based on low sample volume which is dried in a thin film by FDM or freeze/thawed in small aluminum crucibles by DSC not necessarily reflecting the several milliliters in a vial during freeze-drying. Furthermore, the high heating rates of 5 to 20 °C/min in DSC analysis do not correspond to the typical 0.5 to 1 °C/min during lyophilization but facilitates the T_g' analysis due to a more distinct baseline shift [19]. The heating rates applied in FDM analysis are lower, however, may still not represent the heating rate within the vial [5]. The distance from heating source (shelf) to the product combined with the larger sample volume does not lead to a direct transfer of the applied heating rate to the whole product container which slows down the real heating rate in contrast to FDM. The operator itself affects also FDM results as the analysis is performed visually.

Higher T_c values compared to FDM were measured by optical coherence tomography based freeze-drying microscopy (OCT-FDM) indicating that much higher product temperatures can potentially be targeted upon freeze-drying [20]. In OCT-FDM a single vial freeze-dryer connected to an OCT based camera enables to measure T_c values directly in the product container with the correct filling volume. However, this setup does not represent the conditions of a regular freeze-dryer, e.g. shielding effects of surrounding vials. Crystallization of mannitol and the impact of sucrose could be shown by through-vial impedance spectroscopy (TVIS) [21]. This method enables the monitoring of several vials non-invasively and is based on interfacial polarization of glass vials filled with liquid and/or solid. Dielectric analysis (DEA) could also analyze eutectic temperatures of mannitol-water and sodium chloride water system besides the crystallization of mannitol [22]. There are only few approaches for the determination of the aforementioned characteristics directly in the freeze-dryer [20,21,23]. Apart from TVIS, De Beer et al. implemented an in-line RAMAN system to detect mannitol crystallization and to differentiate between different mannitol polymorphs [23]. The reader is additionally referred to an excellent recent review on the process monitoring devices currently on the market [24].

Kasper et al. introduced the optical fiber system (OFS) as potential novel tool to monitor freeze-drying processes [25]. The OFS consists of a glass fiber with embedded wavelength dependent reflectors, so called fiber bragg gratings (FBGs). FBGs reflect a certain wavelength of incoming laser light which is detected by an interrogation unit that at the same time acts as light source. The OFS could be established as temperature measuring device by shielding the sensors through embedding in stainless steel tubes. This shielding protects the sensor from forces which occur e.g. during crystallization to which the OFS is sensitive as

well besides temperature. However, unshielded OFS sensors may enable the detection of T_g' , T_c or T_{cry} . Therefore, in this study, temperature and force effects were to be studied by shielded and unshielded OFS sensors. Ultimately, the purpose of this work was to evaluate the possible application of the OFS to analyze collapse, glass transition and crystallization in the product vial in a freeze dryer as well as the potential of the OFS as monitoring device during a lyophilization process.

2. Materials and Methods

2.1. Materials

Sucrose (Sigma-Aldrich Chemie GmbH, Steinheim, Germany), trehalose (Hayashibara, Okayama, Japan), stachyose (A & Z Food Additives, HangZhou, China) and D(-)-mannitol (VWR International, Ismaning, Germany) were used in different concentrations (5 %, 10 % or 20 % [m/V]) as excipient formulations. The excipients were dissolved in purified water (ELGA LabWater, Celle, Germany). A monoclonal IgG₁ antibody (mAb) and lysozyme were used as model proteins. 150 mg/mL mAb with 10 % (m/V) sucrose in 10 mM sodium phosphate buffer pH 7.0 and 100 mg/mL lysozyme with 10 % (m/V) trehalose in purified water served as protein formulations. All formulations were filtered with 0.2 μ m polyethersulfone membrane syringe filters (VWR International GmbH, Ismaning, Germany) prior to use.

2.2. The optical fiber system (OFS)

2.2.1. OFS unit

The working principle and the design of the used OFS is described elsewhere [25]. An OFS unit of two individual OFS sensors was developed (Figure 3-1 A). The temperature was measured by a calibrated, metal-shielded OFS sensor (type: os4210, Micron Optics, Atlanta, GA, USA; T range: -40 °C - 120 °C, short term accuracy \pm 0.2 °C, response time 0.3 s). Strain induced events were detected by an unshielded OFS sensor (type: fs-FBG, SM1500SC P, polyimide coating removed; INFAP GmbH, München, Germany). OFS data were recorded every 10 seconds for the complete run time (ENLIGHT 1.0 Sensing Analysis Software by Micron Optics).

6R or 10R glass vials (FiolaxTM clear, MGLas AG, Műnnerstadt, Germany) filled with either 4 or 6 mL were stoppered for freeze/thawing experiments or semi-stoppered for lyophilization runs with corresponding lyophilization stoppers (type: Westar[®], West Pharmaceutical

Services, Eschweiler, Germany). The OFS unit was mounted through the center of the stoppers so that the sensor unit was placed centrally in the solution (Figure 3-1 B). Experiments were performed in triplicates at least if not stated otherwise. Two sensor units were used.

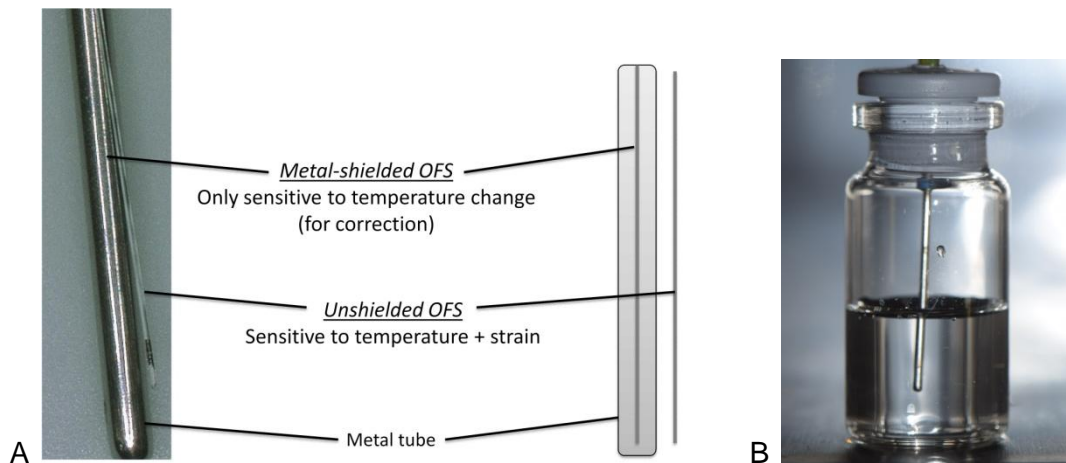


Figure 3-1. A - Scheme of the OFS unit consisting of shielded and unshielded sensor. B – Placement of OFS unit in a filled glass vial.

2.2.2. OFS – Determination of the T_c and T_{cry} during freeze/thawing

Freeze/thaw cycles between +20 °C and -50 °C at 2.5, 1.0, or 0.5 °C/min with 90 min hold times were carried out using an FTS LyoStar™ 3 (SP Scientific, Stone Ridge, NY, USA) freeze-dryer. The wavelength numbers of the unshielded sensor were plotted against the temperature data of the shielded sensor. Wavelength peaks were determined as OFS peak T_{OFS} .

2.2.3. OFS – Use in freeze-drying cycles

Freeze-drying was performed with the FTS LyoStar™. Non-collapse lyophilization cycles were intended to produce lyophilizates with an elegant cake appearance whereas collapse lyophilization cycles should induce a collapse of the lyophilizates (Table 3-1). The endpoint of primary drying was controlled by comparative pressure measurement (difference ≤ 5 mTorr) between capacitance manometer and Pirani gauge sensor.

Table 3-1. Collapse and non-collapse freeze-drying cycles of sucrose (20 % / 10 %) and stachyose (20%) solutions.

Freeze-drying cycle	Collapse (1)	Non-collapse (1)	Collapse (2)	Non-collapse (2)
Freezing			-50 °C 1 °C/min 1.5 h	
Primary Drying	0 °C 65 mTorr 0.1 °C/min	-25 °C 30 mTorr 0.1 °C/min	10 °C 750 mTorr 1 °C/min	-15 °C 120 mTorr 0.6 °C/min
Secondary Drying	20 °C 65 mTorr 0.1 °C/min 4 h	20 °C 30 mTorr 0.1 °C/min 4 h	20 °C 750 mTorr 0.05 °C/min 4 h	20 °C 120 mTorr 1 °C/min 4 h

2.3. Differential scanning calorimetry (DSC)

Tg' and Tcry were analyzed with a Mettler Toledo DSC 821e (Gießen, Germany). 30 µL sample in 40 µL aluminum crucibles were cooled down to -60 °C and heated to +20 °C at 10, 2.5, 1.0 or 0.5 °C/min. The heating curves were analyzed for Tg' - as the midpoint of the transition - and Tcry peaks.

2.4. Freeze-drying microscopy (FDM)

Collapse temperatures Tc were determined by FDM (Linkam FDSC 196 freeze-drying stage with LinkSys32 software, Linkam Scientific Instruments, Tadworth, United Kingdom) equipped with a Duo 2.5 vacuum pump (Pfeiffer Vakuum GmbH, Asslar, Germany) and an Axiolmager A1 microscope used with a 200-fold magnification (Carl Zeiss AG, Oberkochen, Germany). 2 µL of sample was placed on the sample holder together with a spacer and covered by a glass slide. Samples were cooled down to -50 °C with 1 °C/min. A pressure of 0.1 mbar was applied and the samples were heated to -40 °C or -30 °C with 5 °C/min. The sample was held at these conditions to achieve a sufficient thickness of the sublimation front. Tc was detected as onset of collapse in the following drying step at 1 °C/min to 0 °C. Pictures were taken every two seconds.

2.5. Statistical analysis

Statistical analysis was carried out using SigmaPlot 12.5 (Systat Software GmbH, Erkrath, Germany). One-way ANOVA tests were performed followed by pairwise multiple comparison procedures (Holm-Sidak method).

3. Results and Discussion

3.1. OFS thermograms

Typically, the unshielded OFS sensor detected several events during freezing and thawing of a sugar solution (Figure 3-2). Cooling down the solution led to supercooling below the freezing point. As ice nucleation started, many small crystals grew, which did not seem to expose strain on the sensor. The combination of ice crystal growth, solidification of the product and increasing viscosity due to cryoconcentration led to a shift to lower wavelengths with decreasing the T_p to $-50\text{ }^\circ\text{C}$. During thawing the unshielded OFS sensors showed a pronounced peak close to $-30\text{ }^\circ\text{C}$, which could be explained by the rapid change in viscosity of the amorphous freeze-concentrate and thus release of mechanical strain [25,26]. This event occurred at a high rate leading to an overshooting peak after which, with rising temperature, the thawing curve approaches the freezing curve. This peak correlated either to T_g' or to T_c . Ice melting led to only a marginal signal and the already reached viscous flow around the sensor might cover up the effect of the event. The OFS shielded by a stainless steel tube did not exhibit this peak but only a temperature profile which corresponded to thermocouple data.

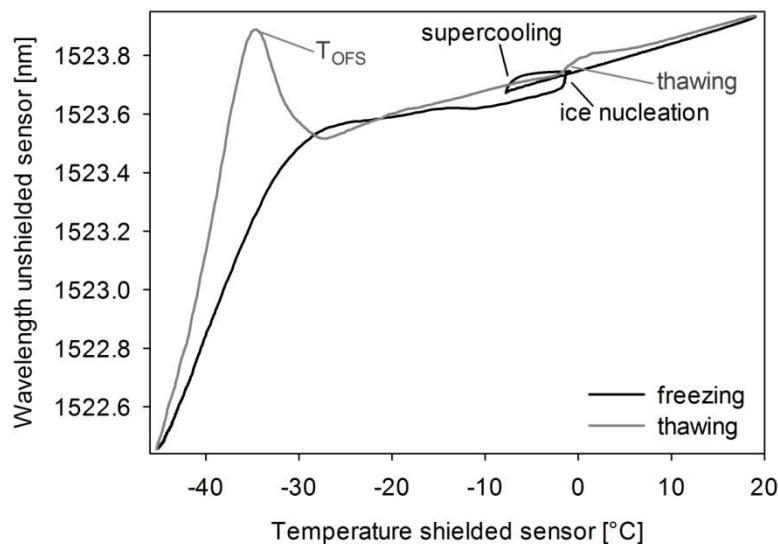


Figure 3-2. OFS thermogram of sucrose 20% (m/V). Cooling/heating rate $1\text{ }^\circ\text{C}/\text{min}$. Black line: freezing scan, gray line: thawing scan.

3.2. Detailed investigation of the T_{OFS} peak

First, it was to be proven whether the T_{OFS} peak at around $-30\text{ }^\circ\text{C}$ resulted from the glass transition and was not an artifact. Therefore, several excipients with different T_g' values were

investigated. The two commonly used disaccharides sucrose and trehalose both showed T_g' and T_{OFS} values of around -32 °C to -28 °C (Figure 3-4). Stachyose, a rarely used tetrasaccharid, showed a T_g' value of -23.8 ± 0.2 °C and a T_{OFS} peak at -23.8 ± 0.4 °C. Due to the shift of both, the T_g' value and the T_{OFS} peak, to higher temperatures as compared to the discaccharides, the T_{OFS} peak can be attributed to the glass transition of the maximally freeze-concentrated solution or to the collapse. This differentiation was carried out in subsequent experiments (see 3.2.3).

3.2.1. Impact of heating rate on peak location of T_{OFS}

T_g' value obtained in DSC analyses shift to higher values with increasing the heating rate [4,19]. Typically, in literature heating at 5 to 20 °C/min is performed as the T_g can be detected with higher sensitivity and sharpness of the transition as compared to analyzing at lower rates [4,27]. Nevertheless it would be beneficial to measure a more realistic T_g' value at slower heating rates e.g. at 1 °C/min. For both sucrose and trehalose solutions, the T_g' shifted to higher values with increasing heating rates in DSC. In contrast, the T_{OFS} peak did not shift between 0.5 and 2.5 °C/min (Table 3-2). The highest DSC heating rate of 10 °C/min could not be applied in the OFS setup in the freeze-dryer. In subsequent experiments, 1 °C/min was used as default.

Table 3-2. T_{OFS} peaks and T_g' values of sucrose (20 %) and trehalose (20 %, 10 %) solutions at different heating rates. Cooling to -50 °C was performed with the same rate as heating. Mean values for n=2, mean ± SD for n≥3.

Heating rate [°C/min]	Sucrose 20 %		Trehalose 20 %		Trehalose 10 %	
	T _{OFS} [°C]	T _g ' [°C]	T _{OFS} [°C]	T _g ' [°C]	T _{OFS} [°C]	T _g ' [°C]
10	-	-30.6 ± 0.04	-	-26.4 ± 0.9	-	-27.2 ± 0.3
2.5	-33.8 ± 0.3	-32.3 ± 0.02	-31.3 ± 0.8	-28.5 ± 0.6	-29.1	-29.0 ± 0.2
1	-34.1 ± 0.7	-33.1 ± 0.1	-31.2	-29.4 ± 0.6	-28.8 ± 0.5	-29.9 ± 0.3
0.5	-34.3 ± 0.6	-34.0 ± 0.4	-	-30.3 ± 0.9	-30.5	-30.5 ± 0.4

3.2.2. Impact of solute concentration on peak location of T_{OFS}

Cryoconcentration during freezing should end up at the same solute concentration range of the solute in the freeze concentrate, independent of the starting concentration. Nevertheless, higher starting concentrations lead to a more pronounced capacity change at T_g' in DSC measurements (Figure 3-3 A, Table 3- 3) which can be explained by the decreasing freeze-concentrate to ice ratio with decreased solute concentration [19]. The T_g' value itself was independent of the sugar concentration. Also the sensitivity of the OFS was affected by the disaccharide concentration. The most pronounced peaks resulted at the highest

concentration of 20 % whereas at the pharmaceutically more relevant solid content of 10 % and 5 % the peak was flattened and shifted to higher temperature (Figure 3-3 B). The T_{OFS} results for 10 % and 20% sugar solutions were similar and close to the T_g' values. The substantially different T_{OFS} for 5 % trehalose (-21.1 ± 2.0 °C) and 5 % sucrose (-24.3 ± 1.4 °C) are due to the limited sensitivity of the OFS. In comparison to Kasper et al., the sensitivity of the OFS was improved by to the removal of the polyimide coating [25]. But with a lower amorphous phase content the change in force on the sensor is less pronounced and the sensor more in contact with ice. Since the OFS thermograms of 10 % sugar solutions showed distinct peaks this pharmaceutically relevant concentration was used for subsequent experiments.

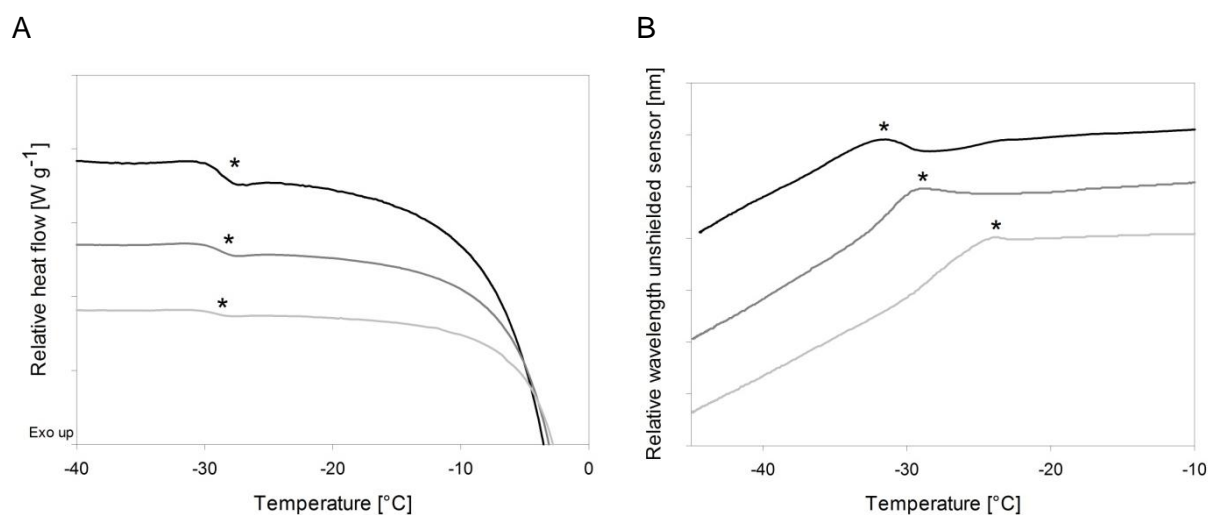


Figure 3-3. The effect of total solid content of trehalose solutions on **A.** T_g' in DSC and **B.** T_{OFS} peaks during heating. Cooling/heating rates were 1 °C/min; black line: 20 %, dark grey line: 10 %, gray line: 5 %; * T_g' and T_{OFS} peak resp.

Table 3- 3. T_{OFS} peaks and T_g' values of sucrose and trehalose solutions at different concentrations (20 %, 10 %, 5 %). Cooling/heating rates were 1 °C/min. Mean values for $n=2$, mean \pm SD for $n \geq 3$.

Concentration [% (m/V)]	Sucrose		Trehalose	
	T_{OFS} [°C]	T_g' [°C]	T_{OFS} [°C]	T_g' [°C]
20	-34.1 ± 0.7	-33.1 ± 0.1	-31.2	-29.4 ± 0.6
10	-29.9 ± 1.0	-33.3 ± 0.2	-28.8 ± 0.5	-29.9 ± 0.3
5	-24.3 ± 1.4	-33.7 ± 0.2	-21.1 ± 2.0	-30.5 ± 0.1

3.2.3. Comparison of OFS with DSC and FDM

In order to assign the T_{OFS} peak results to either T_g' or T_c , additionally FDM was performed. Sucrose, trehalose and stachyose solutions did not allow to tell since their T_g' and T_c values differed only slightly (Figure 3-4) [19,28]. The T_c and T_g' values of stachyose solutions were

within 1.3 °C and T_{OFS} was only 1.3 °C lower than T_c . T_c and T_g' values of sugar solutions are usually close together [5]. Therefore protein solutions were used to tell whether T_{OFS} reflects T_c or T_g' . The presence of protein at higher concentration in disaccharide solutions was shown to lead to a much more pronounced increase in T_c as compared to T_g' [7,29]. Consequently, lysozyme 100 mg/mL / 10 % trehalose and mAb 150 mg/mL / 10 % sucrose were analyzed with OFS, DSC and FDM. Whereas T_{OFS} and T_c did not show a significant difference, T_g' differed statistically significant ($p < 0.05$). Thus, T_{OFS} corresponds to T_c . FDM is based on a subjective evaluation of the onset of collapse. In contrast, the OFS peak is simple to evaluate which helps to avoid differences between various operators, reduces the standard deviation and the OFS unit can easily be placed in the vial filled with formulation.

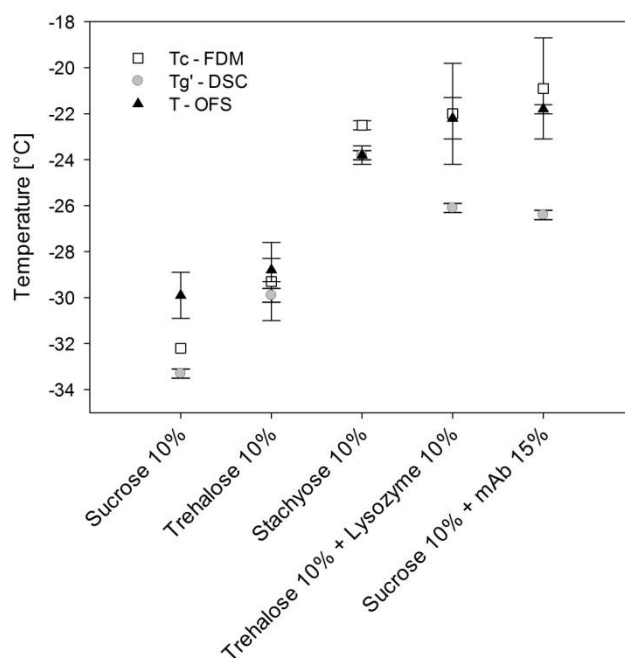


Figure 3-4. Comparison of T_g' , T_c and T_{OFS} values of different sugar and protein formulations. Heating/cooling at 1 °C/min.

3.3. OFS Application to detect crystallization events

Crystallizing excipients are used in freeze-drying as bulking agents for improved cake appearance since they form robust cake structures. Mannitol is the most preferred excipient for this purpose [30,31]. Complete crystallization of the bulking agent after lyophilization is a prerequisite. Partial crystallization during freezing can cause vial breakage during heating due to a secondary crystallization of the non-crystalline fraction and its associated volume expansion [32]. Later crystallization upon storage might cause stability problems of the drug [33]. Therefore, it is important to monitor the crystallization process during lyophilization. Typically, crystallinity is analyzed in the lyophilized product by X-ray powder diffraction, DSC

measurements, NIR - or Raman spectroscopy [34]. Mannitol crystallization upon freeze-drying was thoroughly investigated with these methods [12–14,17,18,23,35–38]. Kasper et al. already observed a small peak in OFS thermograms of 5% mannitol solutions during freezing and assigned it as mannitol crystallization [25]. However, that OFS was less sensitive due to its coating and a more comprehensive investigation of crystallization events was targeted in the study at hand.

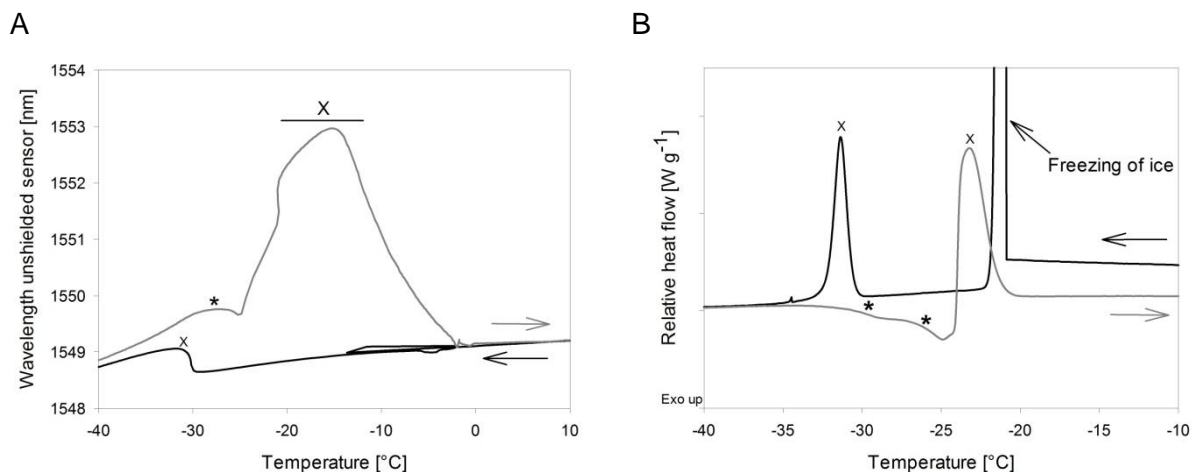


Figure 3-5. A. OFS and B. DSC freezing and thawing scans of mannitol 10 % (m/V). Cooling/heating rate at 1 °C/min; black line: freezing curve, grey line: heating curve. *: T_{OFS} peaks / Tg'; X: crystallization.

The OFS freezing scan of mannitol solutions showed a broad peak at -32.8 ± 0.8 °C, which started to arise at -30 °C already and could therefore be attributed to mannitol crystallization according to the DSC results (-30.5 ± 0.9 °C) (Figure 3-5). The T_{OFS} peak in the thawing scan at -28.1 ± 0.8 °C correlates to T_c of the non-crystalline mannitol fraction. The height of this peak was similar to the T_{OFS} peaks obtained for the amorphous sugar systems (Figure 3-5 A). DSC scans of the mannitol solution rendered two Tg' values in the same temperature range with Tg'¹: -29.5 ± 0.2 °C and Tg'²: -24.1 ± 0.9 °C (Figure 3-5 B) which corresponded to literature [13,14,39]. Thus, the OFS peak can be assigned to an increased viscous flow of the amorphous mannitol fraction.

A pronounced and broad OFS peak starting at -25 °C and with a maximum at -16.5 ± 0.9 °C was observed during thawing. DSC revealed a second exothermic event at -22.6 ± 0.9 °C which was in good agreement with literature values for mannitol crystallization (-19.3 °C [13], -22.4 °C [14], onset at -22 °C [40]). Accordingly, the OFS peak can be attributed to the mannitol crystallization. The height and width of the peak emphasized (1) that the major fraction of mannitol only crystallized in the thawing phase and (2) that mannitol crystallization exerts substantial force onto the OFS sensor. The high forces of mannitol crystallization are

known to lead to vial breakage during freeze-drying [32,41]. Thermal mechanical analysis and strain gage techniques demonstrated that volume expansion due to initial crystallization and subsequent crystallization during thawing were the trigger for the vial breakage [32]. In our studies with 10 % mannitol solutions some experiments ended up in vial breakage, too. Vial breakage corresponded to the highest measured OFS peaks. In DSC measurements a 2-fold higher mannitol crystallization peak area was found during thawing as compared to freezing indicating that upon thawing double the amount of mannitol crystallized. Whereas 1 % mannitol solutions did not show crystallization in DSC thawing curves and were fully crystalline already after freezing [14], the amount of non-crystalline mannitol increases with higher mannitol concentration (10 %). Annealing, a typically used hold step above T_g' for complete crystallization of bulking agents, led to disappearance of the mannitol crystallization peak in the OFS thawing curves. This demonstrated again that the peak can be assigned to mannitol crystallization.

Hence the OFS was able to determine phase transitions from solid to viscous flow as well as crystallization of amorphous excipients during freezing and thawing. Thus it can be used as alternative analysis tool to FDM and DSC analysis. The OFS might be more representative for the reality in freeze-drying, since drying rates, freeze-dryer environment, filling volume, and type and size of container correspond to the freeze-drying process.

3.4. OFS Application during lyophilization

The ultimate goal was to develop the OFS unit into a process monitoring tool for the freeze-drying process. Kasper already showed that the shielded OFS could be used as a temperature monitoring tool complementary to the usual thermocouples [25]. The unshielded sensor may offer additional options. Therefore, two types of uncommon lyophilization cycles were carried out and monitored with the OFS unit. A slow ramp of 0.1 °C/min was applied during the start of primary drying to reach a shelf temperature of 0 °C in order to induce collapse during this ramp phase (collapse cycle (1)). For comparison, the same ramp rate but to a lower shelf temperature and at lower chamber pressure was carried out in the non-collapse cycle (1). Faster rates and higher pressure values were necessary to force the occurrence of collapse in stachyose samples due to the higher T_c value (collapse cycle (2)).

The collapse lyophilization cycles demonstrated that collapse can be detected by the unshielded OFS. Both tested saccharides, sucrose 20 % and stachyose 20 %, showed a peak in the unshielded OFS signal during the primary drying heating ramp (Figure 3-6). After lyophilization, collapse could be confirmed visually. The location of the peak was associated with the temperature measured by the shielded OFS. Both values were close to the T_{OFS}

peaks previously determined in the freezing and thawing experiments. The peak of sucrose was broader and less sharp compared to stachyose which was attributed to the slower heating ramp. Sucrose 20% did not show any OFS peaks or visual signs of collapse when dried utilizing the corresponding non-collapse cycles. For Stachyose 20% a broader transition was noted, which depended on the ramp rate, but no marked peak.

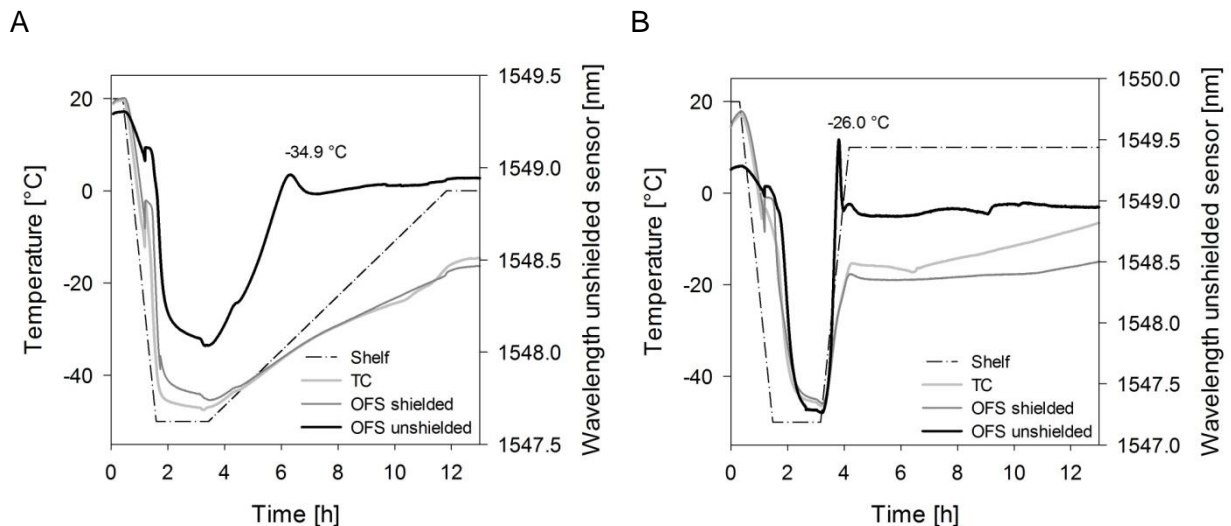


Figure 3-6. Temperature profiles of A. sucrose 20 % samples (collapse cycle (1)) and B. stachyose 20 % samples (collapse cycle (2)) obtained with a conventional thermocouple (TC) or an OFS embedded into a stainless steel tube (OFS shielded) in correlation to the unshielded OFS signal. For a better overview, only the first 13 hours of the process are shown and pressure values are not included.

Furthermore, the impact of the solute concentration was investigated. For 10 % sucrose samples dried with collapse cycle (2) a smaller peak shifted to higher temperatures resulted with the unshielded OFS (Figure 3-7). As T_c and T_{OFS} in freezing and thawing cycles were not shifted in DSC at this concentration, the sensitivity of the OFS system may be too low to detect collapse at this concentration at the correct temperature during primary drying. Thus detection of collapse during a freeze-drying run is in general possible, but limited to higher solute concentrations and potential broader transitions may make the evaluation more complex.

In order to further develop the OFS as a process monitoring tool, future studies have to focus on an algorithm for detection of peaks and transitions based on the readouts. Formulations with different excipients and concentrations have to be analyzed. This needs to include studies with crystalline bulking agent in combination with an amorphous matrix to learn whether also microcollapse can be detected.

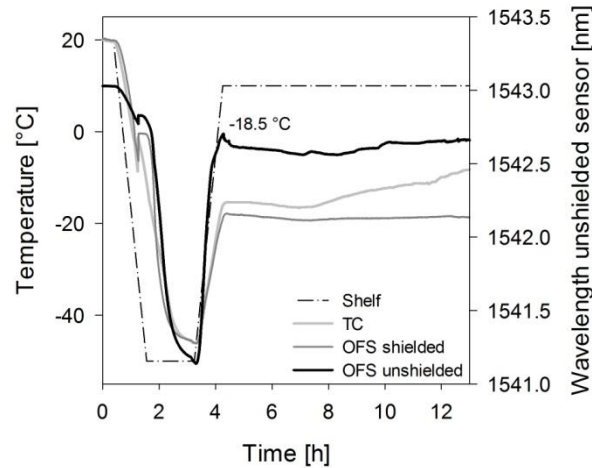


Figure 3-7. Temperature profiles of sucrose 10 % samples (collapse cycle (2)) obtained with a conventional thermocouple (TC) or an OFS embedded into a stainless steel tube (OFS shielded) in correlation to the unshielded OFS signal.

4. Conclusion

In this study, the OFS unit could be successfully established as alternative tool for determination of T_c of amorphous systems as well as of T_{cry} of crystalline phases. The OFS unit combines temperature measurement with the ability to detect force or strain in one device. We could show that the T_{OFS} peak was in good correlation with FDM results. Since the OFS tracks processes that take place in the original sample vial in the freeze-dryer itself the data may be more representative for the product and process development than the data obtained with other instruments like FDM and DSC on manipulated samples. The results furthermore indicate that T_{OFS}/T_c values should be set as the upper limit of the product temperature during primary drying rather than T_g' [7,29]. The OFS unit is a promising tool that could potentially be developed into a monitoring tool for the entire freeze-drying process. Up to now collapse occurring in the primary drying phase could be detected at high concentrations whereas the desired non-collapse is more difficult to define in terms of the OFS signal. In order to develop the OFS into a process monitoring tool the sensitivity has to be further improved to enable determination of T_c values at lower amorphous excipient concentrations, below <10 %. The OFS may also provide further insights into the properties of the freeze-concentrate.

Acknowledgements

The authors gratefully thank Manfred Resch from INFAP GmbH for supporting this study with his knowledge, expertise and sensor assembly. We also acknowledge Coriolis Pharma for providing the freeze-drying microscope for this study.

Author Contributions

JH and WF created study design and interpreted the obtained data. JH performed the experiments and the corresponding analysis. The work was drafted by JH and critically reviewed by WF. JH and WF did the final proof of the version to be published and agreed to be accountable for all aspects of the work in ensuring that questions related to the accuracy or integrity of any part of the work are appropriately investigated and resolved.

References

- [1] R. Pisano, D. Fissore, A. Barresi, P. Brayard, P. Chouvenc, B. Woinet, Quality by design: optimization of a freeze-drying cycle via design space in case of heterogeneous drying behavior and influence of the freezing protocol, *Pharm. Dev. Technol.* 18 (2013) 280–295.
- [2] S. Bosca, A. Barresi, D. Fissore, Fast freeze-drying cycle design and optimization using a PAT based on the measurement of product temperature, *Eur. J. Pharm. Biopharm.* 85 (2013) 253–262.
- [3] G. Oetjen, P. Haseley, *Freeze-Drying*, Wiley-VHC, Weinheim, (2004).
- [4] S.K Pansare, S. M. Patel, Practical Considerations for Determination of Glass Transition Temperature of a Maximally Freeze Concentrated Solution, *AAPS PharmSciTech.* 17 (2016) 1–15.
- [5] E. Meister, H. Gieseler, Freeze-dry microscopy of protein/sugar mixtures: Drying behavior, interpretation of collapse temperatures and a comparison to corresponding glass transition data, *J. Pharm. Sci.* 98 (2009) 3072–3087.
- [6] T. Bosch, *Aggressive Freeze-Drying – a fast and suitable method to stabilize biopharmaceuticals*, Ludwig-Maximilians Universität München, (2014).
- [7] J. Colandene, L. Maldonado, A. Creagh, J. Vrettos, K. Goad, T. Spitznagel, Lyophilization Cycle Development for a High-Concentration Monoclonal Antibody Formulation Lacking a Crystalline Bulking Agent, *J. Pharm. Sci.* 96 (2007) 1598–1608.
- [8] J. Beirowski, S. Inghelbrecht, A. Arien, H. Gieseler, Freeze drying of nanosuspensions, 2: the role of the critical formulation temperature on stability of drug nanosuspensions and its practical implication on process design, *J. Pharm. Sci.* 100 (2017) 4471–4481.
- [9] K. Chatterjee, E. Shalaev, R. Suryanarayanan, Partially Crystalline Systems in Lyophilization: II. Withstanding Collapse at High Primary Drying Temperatures and Impact on Protein Activity Recovery, *J. Pharm. Sci.* 94 (2005) 809–820.
- [10] S. Passot, F. Fonseca, N. Barbouche, M. Marin, M. Alarcon-Lorca, D. Rolland, M. Rapaud, Effect of Product Temperature During Primary Drying on the Long-Term Stability of Lyophilized Proteins, *Pharm. Dev. Technol.* 12 (2007) 543–553.
- [11] M. J. Pikal, *Freeze-Drying of Proteins. Part I: Process Design*, *Biopharm.* 3 (1990) 18-23.

- [12] R. Johnson, C. Kirchhoff, H. Gaud, Mannitol-sucrose mixtures--versatile formulations for protein lyophilization., *J. Pharm. Sci.* 91 (2002) 914–922.
- [13] A. Hawe, W. Frieß, Impact of freezing procedure and annealing on the physico-chemical properties and the formation of mannitol hydrate in mannitol-sucrose-NaCl formulations, *Eur. J. Pharm. Biopharm.* 64 (2006) 316–325.
- [14] B. Peters, L. Staels, J. Rantanen, F. Molnár, T. De Beer, V. Lehto, J. Ketolainen, Effects of cooling rate in microscale and pilot scale freeze-drying – Variations in excipient polymorphs and protein secondary structure, *Eur. J. Pharm. Sci.* 95 (2016) 72–81.
- [15] D. Varshney, S. Kumar, E. Shalaev, P. Sundaramurthi, S. Kang, L. Gatlin, R. Suryanarayanan, Glycine Crystallization in Frozen and Freeze-dried Systems: Effect of pH and Buffer Concentration, *Pharm. Res.* 24 (2007) 593–604.
- [16] K. Izutsu, S. Kojima, Excipient crystallinity and its protein-structure-stabilizing effect during freeze-drying, *J. Pharm. Pharmacol.* 54 (2002) 1033–1039.
- [17] S. Jena, J. Horn, R. Suryanarayanan, W. Friess, A. Aksan, Effects of Excipient Interactions on the State of the Freeze-Concentrate and Protein Stability, *Pharm. Res.* 34 (2017) 462–478.
- [18] X. Liao, R. Krishnamurthy, R. Suryanarayanan, Influence of processing conditions on the physical state of mannitol--implications in freeze-drying., *Pharm. Res.* 24 (2007) 370–376.
- [19] L. Her, S. L. Nail, Measurement of Glass Transition Temperatures of Freeze-Concentrated Solutes by Differential Scanning Calorimetry, *Pharm. Res.* 11 (1994) 54–59.
- [20] K. Greco, M. Mujat, K. Galbally-kinney, D. Hammer, R. Ferguson, N. Iftimia, P. Mulhall, P. Sharma, W. Kessler, M. J. Pikal, Accurate prediction of collapse temperature using optical coherence tomography-based freeze-drying microscopy, *J. Pharm. Sci.* 102 (2013) 1773–1785.
- [21] M. Arshad, G. Smith, E. Polygalov, I. Ermolina, Through-vial impedance spectroscopy of critical events during the freezing stage of the lyophilization cycle: The example of the impact of sucrose on the crystallization of mannitol, *Eur. J. Pharm. Biopharm.* 87 (2014) 598–605.

- [22] S. Evans, K. Morris, A. Mackenzie, N. Lordi, Dielectric characterization of thermodynamic first order events in model frozen systems intended for lyophilization, *PDA J. Pharm. Sci. Technol.* 49 (1995) 2–8.
- [23] T. De Beer, M. Alleso, F. Goethals, A. Coppens, Y. Vander Heyden, H. Lopez De Diego, J. Rantanen, F. Verpoort, C. Vervaet, J. Remon, W. Baeyens, Implementation of a process analytical technology system in a freeze-drying process using Raman spectroscopy for in-line process monitoring, *Anal. Chem.* 79 (2007) 7992–8003.
- [24] S. L. Nail, S. Tchessalov, E. Shalaev, A. Ganguly, E. Renzi, F. Dimarco, L. Wegiel, S. Ferris, W. Kessler, M. J. Pikal, G. Sacha, A. Alexeenko, T. Thompson, C. Reiter, J. Searles, P. Coiteux, Recommended Best Practices for Process Monitoring Instrumentation in Pharmaceutical Freeze Drying—2017, *AAPS PharmSciTech.* (2017).
- [25] J. Kasper, M. Wiggenghorn, M. Resch, W. Friess, Implementation and evaluation of an optical fiber system as novel process monitoring tool during lyophilization., *Eur. J. Pharm. Biopharm.* 83 (2013) 449–59.
- [26] M. Akyurt, G. Zaki, B. Habeebullah, Freezing phenomena in ice-water systems, *Energy Convers. Manag.* 43 (2002) 1773–1789.
- [27] N. Coleman, D. Craig, Modulated temperature differential scanning calorimetry: A novel approach to pharmaceutical thermal analysis, *Int. J. Pharm.* 135 (1996) 13–29.
- [28] G. Adams, J. Ramsay, Optimizing the lyophilization cycle and the consequences of collapse on the pharmaceutical acceptability of *Erwinia L-asparaginase*, *J. Pharm. Sci.* 85 (1996) 1301–1305.
- [29] R. Depaz, S. Pansare, S. M. Patel, Freeze-Drying Above the Glass Transition Temperature in Amorphous Protein Formulations While Maintaining Product Quality and Improving Process Efficiency, *J. Pharm. Sci.* 105 (2016) 40–49.
- [30] K. Patel, B. Munjal, A. Bansal, Effect of cyclophosphamide on the solid form of mannitol during lyophilization, *Eur. J. Pharm. Sci.* 101 (2017) 251–257.
- [31] W. Kaiyaly, U. Khan, S. Mawlud, Influence of mannitol concentration on the physicochemical, mechanical and pharmaceutical properties of lyophilised mannitol, *Int. J. Pharm.* 510 (2016) 73–85.

- [32] G. Jiang, M. Akers, M. Jain, J. Guo, A. Distler, R. Swift, M. Wadhwa, F. Jameel, S. Patro, E. Freund, Mechanistic studies of glass vial breakage for frozen formulations. I. Vial breakage caused by crystallizable excipient mannitol., *PDA J. Pharm. Sci. Technol.* 61 (2007) 441–451
- [33] T. W. Randolph, Phase Separation of Excipients during Lyophilization: Effects on Protein Stability, *J. Pharm. Sci.* 86 (1997) 1198–1203.
- [34] B. Shah, V. Kakumanu, A. Bansal, Analytical techniques for quantification of amorphous/crystalline phases in pharmaceutical solids, *J. Pharm. Sci.* 95 (2006) 1641–1665.
- [35] T. De Beer, P. Vercruyssen, A. Burggraeve, T. Quinten, J. Ouyang, X. Zhang, C. Vervaet, J. Remon, W. Baeyens, In-line and real-time process monitoring of a freeze drying process using Raman and NIR spectroscopy as complementary process analytical technology (PAT) tools, *J. Pharm. Sci.* 98 (2009) 3430–3446.
- [36] S. Jena, R. Suryanarayanan, A. Aksan, Mutual Influence of Mannitol and Trehalose on Crystallization Behavior in Frozen Solutions., *Pharm. Res.* 33 (2016) 1413–1425.
- [37] X. Liao, R. Krishnamurthy, R. Suryanarayanan, Influence of the active pharmaceutical ingredient concentration on the physical state of mannitol-implications in freeze-drying, *Pharm. Res.* 22 (2005) 1978–1985.
- [38] X. Liao, R. Krishnamurthy, R. Suryanarayanan, Influence of Processing Conditions on the Physical State of Mannitol—Implications in Freeze-Drying, *Pharm. Res.* 24 (2007) 370–376.
- [39] R. Cavatur, N. Vemuri, A. Pyne, Z. Chrzan, D. Toledo-Velasquez, R. Suryanarayanan, Crystallization behavior of mannitol in frozen aqueous solutions, *Pharm. Res.* 19 (2002) 894–900.
- [40] A. Pyne, R. Surana, R. Suryanarayanan, Crystallization of Mannitol below T_g' during Freeze-Drying in Binary and Ternary Aqueous Systems, *Pharm. Res.* 19 (2002) 901-908.
- [41] N. Williams, T. Dean, Vial breakage by frozen mannitol solutions: correlation with thermal characteristics and effect of stereoisomerism, additives, and vial configuration., *J. Parenter. Sci. Technol.* 45 (1991) 94–100.

Chapter 4

Effects of Excipient Interactions on the State of the Freeze-Concentrate and Protein Stability

The following chapter has been published as research article in the Pharmaceutical Research journal and appears in this thesis with the journal's permission:

Sampreeti Jena, Jacqueline Horn, Raj Suryanarayanan, Wolfgang Friess and Alptekin Aksan
Effects of excipient interactions on the state of the freeze-concentrate and protein stability
Pharmaceutical Research 34 (2017), 462-478
doi: 10.1007/s11095-016-2078-y

The supplementary data was inserted into this chapter.

Additional data was appended at the end of this chapter.

Abstract

The thermodynamic state of the final lyophile in freeze-dried formulations directly affects the stability of the active pharmaceutical ingredient (API). Crystallization of trehalose and mannitol in frozen solutions has been shown to be a function of their initial composition. However, to date a detailed study of the effect of concentrations of the API and other excipients on the crystallinity of mannitol and trehalose in frozen solutions has not been reported. The physical form as well as the crystallinity of mannitol and trehalose during freeze-drying can have major effects not only on the morphology of the final lyophile but also on the long term stability of the API. The effect of different concentrations of bovine serum albumin (BSA), polysorbate 20, and deuterium oxide (D₂O) on the crystallinity of mannitol and trehalose in frozen solutions was evaluated by differential scanning calorimetry, X-ray diffractometry, and FTIR spectroscopy during freezing and annealing. The secondary structure of BSA was probed by IR spectroscopy in frozen solutions and by circular dichroism

spectroscopy in thawed solutions. Trehalose crystallization was accompanied by unfolding of BSA. The addition of BSA delayed and reduced the extent of mannitol and trehalose crystallization. Similar effects were observed upon adding D₂O (> 5% w/w) and low concentrations of polysorbate 20 (< 0.2% w/w) with retention of BSA in its native conformation in both frozen and thawed solutions. At high BSA to trehalose mass ratio, the protein was able to stabilize itself in the frozen state, but unfolded upon thawing. The API and other excipients, in a concentration-dependent manner, influenced the physical state of the freeze concentrate as well as the stability of the API during freezing and thawing.

Keywords

Crystallization, freeze-drying, glass transition, mannitol, trehalose

Abbreviations

API	Active Pharmaceutical Ingredient
AUC	Area under curve
BSA	Bovine Serum Albumin
CD	Circular Dichroism
DSC	Differential Scanning Calorimetry
FCL	Freeze-concentrated liquid
FTIR	Fourier Transform Infrared Spectroscopy
HPSEC	High Performance Size Exclusion Chromatography
IR	Infrared
LO	Light Obscuration
XRD	Powder X-ray Diffractometry

Table of Content

Abstract	59
Keywords.....	60
Abbreviations	60
1. Introduction	62
2. Materials and Methods	64
2.1. Materials	64
2.2. Differential Scanning Calorimetry (DSC)	64
2.3. Powder X-ray Diffractometry (XRD).....	64
2.4. IR Spectroscopy.....	65
2.5. UV Circular Dichroism	65
2.6. High Performance Size Exclusion Chromatography	65
2.7. Light Obscuration (LO)	66
2.8. Turbidity (A350 nm).....	66
3 Results	67
3.1. Glass transition	67
3.2. Infrared Spectroscopy	71
3.3. X-Ray Diffractometry (XRD)	76
3.4. Circular Dichroism (CD) Analysis of the Thawed Samples	77
3.5. Characterization of Aggregates	79
4. Discussion	81
5. Conclusions	86
Acknowledgements and Disclosures.....	86
6. Additional Data	87
Additional Material and Methods	87
Lyophilization	87
Freeze-Thawing	87
Results and Discussion.....	87
References	89

1. Introduction

Freeze-dried protein formulations generally contain several different excipients that serve specific functions. This investigation focuses on quantification of the physical and thermodynamics states of the bulking agent, and the lyoprotectant (the two main excipients in a formulation) in the frozen state, as this directly relates to the stability of the active pharmaceutical Ingredient (API) to be stabilized. The bulking agent is desired to be crystalline in order to provide structure to the cake in the lyophilized form [1,2]. On the other hand, the lyoprotectant must remain amorphous during freeze-drying and the subsequent storage period in order to stabilize the API. Crystallization or phase separation of the lyoprotectant can impair its ability to protect the API against the stresses experienced during freezing and drying [3,4]. Mannitol has a strong tendency to crystallize during freezing and therefore, is widely used as a bulking agent [5,6]. Trehalose, a non-reducing glass-forming sugar with a high glass transition temperature ($\sim 117^\circ\text{C}$), is a popular lyoprotectant [7–10].

In the absence of prolonged annealing or external seeding, trehalose could be retained in the amorphous state, both during freezing and drying [11,12]. But recently it was shown that in the presence of crystallizing co-solutes such as succinic acid and mannitol, trehalose could be crystallized from the frozen solution by annealing above the glass transition temperature of the amorphous freeze-concentrate (T_g') [11–13]. Trehalose crystallization can compromise the stability of the API in the final product, leading to unfolding and aggregation of the protein [1,3,14–16] and thus, loss of biological activity. Additionally, non-crystallizing co-solutes such as sucrose and proteins, at high concentrations, could inhibit mannitol crystallization [13,17], compromising the structural integrity of the product. We have previously demonstrated that crystallization of frozen mannitol-trehalose solutions during annealing above T_g' was exclusively dictated by the mass ratio of mannitol to trehalose (R) in the solution [18]. When $R < 1$, both of the excipients remained amorphous, while both mannitol and trehalose crystallized when $R \geq 1$. In the past, the effect of both crystallizing and non-crystallizing solutes such as NaCl and proteins including lysozyme, human serum albumin and human monoclonal antibodies on the extent of mannitol crystallization and in some cases, the physical form of the crystalline mannitol has been studied [19–23]. But till date, no report exists on the effects of varying concentrations protein and other excipients such as surfactant and deuterium oxide on the physical states of both mannitol and trehalose in frozen mannitol-trehalose solutions and their repercussions on the stability of the protein.

Presence of proteins can alter the glass transition temperature of the freeze concentrate as well as its mobility at the annealing temperature [13,24], consequently influencing the nucleation and growth of crystallizing phases. Surfactants, depending on their concentration and chemical structure, inhibit or promote the growth of the crystalline phases [25,26]. They

are also known to either prevent or promote protein unfolding, and precipitation in the frozen state through ice interface coverage, and specific binding to the protein surface [27,28]. Polysorbate 20 (hereafter referred to by its popular trade name, Tween 20) is a common non-ionic polysorbate surfactant used for stabilization of emulsions and suspensions. Deuterium oxide, used frequently as a solvent in spectroscopic studies, has been known to effect specific interaction between macro-molecules by changing their surface charge density (by H/D exchange) [29,30]. Moreover, D₂O has been shown to protect cells and proteins against thermal denaturation [31,32].

In this study, changes in the secondary and tertiary structures of bovine serum albumin in the frozen state caused by crystallization of the lyoprotectant (trehalose) and the bulking agent (mannitol) were investigated. We have previously demonstrated that in the absence of an API, crystallization of mannitol and trehalose is governed by the mass ratio of mannitol to trehalose in the initial solution [18]. We hypothesize here that the addition of the API (albumin, in this case) will affect the state (propensity for, and the extent of crystallization as well as the physical form of crystallizing phases) of mannitol and trehalose in the frozen solution, which will in turn directly affect the stability of the API. We further test this hypothesis when certain other excipients (specifically, Tween 20 and D₂O) are included in the formulation.

For a comprehensive analysis, a multitude of analytical techniques was employed. Differential Scanning Calorimetry (DSC) was used to characterize the physical state of the amorphous freeze concentrate before and after annealing. Infrared (IR) spectroscopy enabled us to detect solute crystallization in the freeze-concentrated liquid (FCL), and low temperature powder X-ray Diffractometry (XRD) was used to identify the crystalline phases. IR spectroscopy also provided information on protein hydration level and protein secondary structure in the frozen state. Circular dichroism (CD) spectroscopy enabled characterization of the secondary structure of the protein in thawed solutions, where the low protein concentration rendered IR spectroscopy unreliable. Turbidity analysis was conducted to detect the formation of insoluble aggregates, and high performance size exclusion chromatography (HPSEC) was used to detect and characterize both soluble and insoluble aggregates.

2. Materials and Methods

2.1. Materials

D-(+)- trehalose dihydrate (MW 378.33 kDa, 99.9% purity, Sigma-Aldrich, St. Louis, MO), Bovine Serum Albumin (MW 66.5 Da, \geq 99% purity, Sigma-Aldrich), deuterium oxide (MW 20.03 Da, 99.9% purity, Cambridge Isotope Laboratories, Andover, MA), Tween 20 (MW 1227.54 Da, $>$ 98.0% purity, Biorad Laboratories, Hercules, CA), and D-mannitol (MW 182.17 Da, \geq 98% purity, Sigma-Aldrich) were used as received. Aqueous solutions were prepared gravimetrically in ultrapure water.

2.2. Differential Scanning Calorimetry (DSC)

A differential scanning calorimeter (Q2000, TA Instruments, New Castle, DE) equipped with a refrigerated cooling accessory was used. The instrument was calibrated using tin. About 50 mg of the sample solution was weighed in an aluminium pan, which was hermetically sealed (Tzero pan and lid with a pin-hole). Dry nitrogen was used as the purge gas at a flow rate of 50 ml/min. The solution was initially cooled from room temperature down to -50 °C at 20 °C/min, held for 2 minutes and then heated at 1 °C/min back to room temperature. When there was an annealing step included in the experiment, the solution cooled down to -50 °C was heated at 1 °C/min to -18 °C where it was held for 20 hours. The eutectic melting temperature (T_e) of trehalose-water binary system is -2.5 °C [33–35] and the glass transition temperature of trehalose freeze-concentrate is reported to be in the range of -32 to -40 °C [36]. Annealing was conducted at -18 °C. After the annealing period, the experimental solution was again cooled rapidly (20 °C/min) to -50 °C and then heated at 1 °C/min back to room temperature. The DSC data were analyzed using TA Universal Analysis software.

2.3. Powder X-ray Diffractometry (XRD)

A powder X-ray diffractometer (D8 ADVANCE; Bruker AXS, Madison, WI) equipped with a variable temperature stage (TTK 450; Anton Paar, Graz-Straßgang, Austria) and a Si strip one-dimensional detector (LynxEye; Bruker AXS, Madison, WI) was used. In experiments including an annealing step, the experimental solution was cooled from RT to -50 °C at 20 °C/min, held for 2 min and then heated at 1 °C/min back to -18 °C where it was held for 20 hours. After the annealing period, the solution was heated at 1 °C/min back to room temperature. During annealing at -18 °C, XRD patterns were collected continuously with a dwell time of 900 s. Solutions were exposed to Cu K α radiation (40 kV \times 40 mA) over an

angular range of 5–27° 2 θ with a step size of 0.05°. The XRD patterns were analyzed using commercially available software (JADE 2010).

2.4. IR Spectroscopy

The experimental solution (~100 nL) was sandwiched between two CaF₂ windows, sealed with vacuum grease to generate a thin film, ~ 1 μm thick. The assembly was then transferred to the infrared microscope attached to the FTIR spectrometer, (Thermo-Nicolet Continuum with a mercury cadmium telluride detector, Thermo Electron, Waltham, MA) equipped with a freeze-drying cryostage (FDCS 196, Linkam Scientific Instruments Ltd., UK). Solutions were cooled from RT at 10 °C/min and as soon as ice crystallization was microscopically observed, the temperature was rapidly brought (at 30 °C/min) back up to -18 °C, where the sample was held for 20 hours. IR spectra were acquired at a resolution of 4 cm⁻¹ and a total of 128 scans were averaged in the 4000–930 cm⁻¹ wavenumber range. The data was collected continuously from a fixed region (25 μm x 25 μm) in the FCL region both during equilibrium freezing, and annealing and analyzed using OMNIC (Thermo-Nicolet) software.

2.5. UV Circular Dichroism

Spectra were recorded using a J-815 circular dichroism spectropolarimeter (JASCO) using a 1 cm path length quartz cuvette over the range of 190–260 nm at ambient temperature. Data were collected every 0.2 nm with a bandwidth of 1 nm, averaged over 8 scans. An integration time of 8 seconds at 50 nm/min and a 2 nm slit width were used. The solutions were diluted with ultrapure water to reach a protein concentration of 0.2 mg/mL. The background spectra of the solvent medium (identical dilution) were subtracted from the final spectra and data were obtained as mean residue ellipticity (Θ). To estimate protein secondary structure content, analysis of the relevant CD spectra was carried out using the CDPro software. The basis set 7 of the CDPro software was used. Analysis was performed using the SELCON 3 method [37].

2.6. High Performance Size Exclusion Chromatography

Size exclusion chromatography was performed using an Agilent 1100 series HPLC system equipped with an UV/Vis detector for detection at 280 nm (Agilent Technologies, Santa Clara, California, USA). A TSKgel® G3000 SWXL column (dimension: 300 x 7.8 mm, TOSOH Bioscience, Stuttgart) and 100 mM sodium phosphate / 150 mM sodium chloride buffer at pH 7.4 mobile phase with a flow rate of 0.4 mL/min was used. Samples were

annealed in stoppered 2 R vials at -20 °C for 20 hours (heating/cooling rate: 1 °C/min) using a FTS Lyostar 3 freeze-drier (SP Scientific, Stone Ridge, USA). Prior to analysis, samples were diluted to 1 mg/mL and centrifuged. The integrated peak intensity was determined before and after freeze-thawing after blank subtraction. Monomer recovery (in percent) was determined by comparing the integrated intensity of the monomers before and after freeze-thawing.

2.7. Light Obscuration (LO)

A PAMAS SVSS-35 particle counter with a HCB-LD-25/25 sensor (PAMAS – Partikelmess- und Analysesysteme GmbH, Rutesheim, Germany) was used to determine subvisible particles. The system was rinsed with highly purified water before each analysis. The rinsing volume was 0.2 ml, followed by four measurements of 0.2 ml according to USP 787. PAMAS PMA software was used to determine particles $\geq 1 \mu\text{m}$, $\geq 10 \mu\text{m}$ and $\geq 25 \mu\text{m}$. The results are given in cumulative particles per milliliter.

2.8. Turbidity (A350 nm)

Turbidity of the freeze-thawed samples was measured by UV/VIS-spectroscopy at 350 nm. A NanoDrop 2000 spectrophotometer (PEQLab Biotechnology GmbH, Erlangen, Germany) was used. Each formulation was measured as triplicate with its corresponding formulation without protein as blank solution.

3. Results

3.1. Glass transition

We first explored the effect of BSA concentration in solution on the crystallinity (propensity and extent) of mannitol in the frozen state. Glass transition temperatures (T_g') of frozen solutions containing mannitol (10% w/w), trehalose (5%) and increasing concentrations of BSA were measured using DSC (Table 4-1, Figure 4-1 A). A single glass transition event was identified in all unannealed solutions containing BSA. In these samples, immediately following glass transition, an exothermic peak attributable to mannitol crystallization was also observed. In the absence of BSA, the DSC scan revealed two distinct glass transitions, one before and the other after the crystallization exotherm. Mannitol-trehalose systems were investigated in detail earlier [18]. Multiple glass transitions suggest heterogeneity in the FCL and arise due to partial mannitol crystallization [18]. BSA, in a concentration dependent manner, gradually increased the T_g' of the amorphous FCL. The crystallization onset temperature, an indicator of crystallization propensity, increased as a function of BSA concentration while the enthalpy of crystallization decreased. Upon further heating, a very prominent endotherm attributed to the melting of the ice-mannitol eutectic was observed. With increasing BSA concentration, the endotherm shifted to higher temperatures (Figure 4-1 B).

Table 4-1. Glass transition temperature(s), T_g' ; onset of crystallization, area under exotherms and eutectic-ice melting temperatures during heating of unannealed samples.

Composition	Glass Transition Temperature(s) (°C)*	Crystallization onset temperature (°C)*	Enthalpy of crystallization (J/g)*	Mannitol-ice eutectic melting temperature (°C) [#]
10%M+5%T (control)	-42.5 ± 0.1 (T_g') -34.2 ± 0.3 (T_g'')	-38.1 ± 0.8	20.8 ± 0.4	-1.6 ± 0.0
10%M+5%T+2%BSA	-36.3 ± 0.4	-33.8 ± 1.2	19.5 ± 0.4	-1.6 ± 0.1
10%M+5%T+4%BSA	-34.3 ± 1.6	-28.7 ± 0.6	16.1 ± 0.6	-1.1 ± 0.2
10%M+5%T+6%BSA	-33.5 ± 1.8	-28.1 ± 0.8	15.4 ± 0.6	-0.8 ± 0.1
10%M+5%T+8%BSA	-33.3 ± 0.3	-26.1 ± 0.9	15.1 ± 0.5	-0.7 ± 0.0

M mannitol, T trehalose, BSA bovine serum albumin. Samples were cooled from RT to -50 °C at 20 °C/min, held for 2 min and warmed back up to RT at 1 °C/min. * Samples analyzed in quadruplicate; [#] samples analyzed in duplicate.

The effect of annealing the frozen solution at -18 °C was examined and the results are presented in Table 4-2. Comparing T_g 's and the associated heat capacity change (ΔC_p) before and after annealing enabled us to determine the change in the composition and size

of the FCL due to solute crystallization during annealing. In the DSC scans collected after annealing, no crystallization exotherm was observed, suggesting complete mannitol crystallization during annealing (Figure 4-2). Additionally, annealing caused a pronounced increase in the T_g' . With increasing BSA concentration, there was a progressive increase in T_g' after annealing (Figure 4-2), while the mass fraction of solute crystallized during annealing (change in ΔC_p before and after annealing; $\Delta\Delta C_p$) was inversely proportional to the BSA concentration. These observations suggest that BSA was predominantly retained in the FCL.

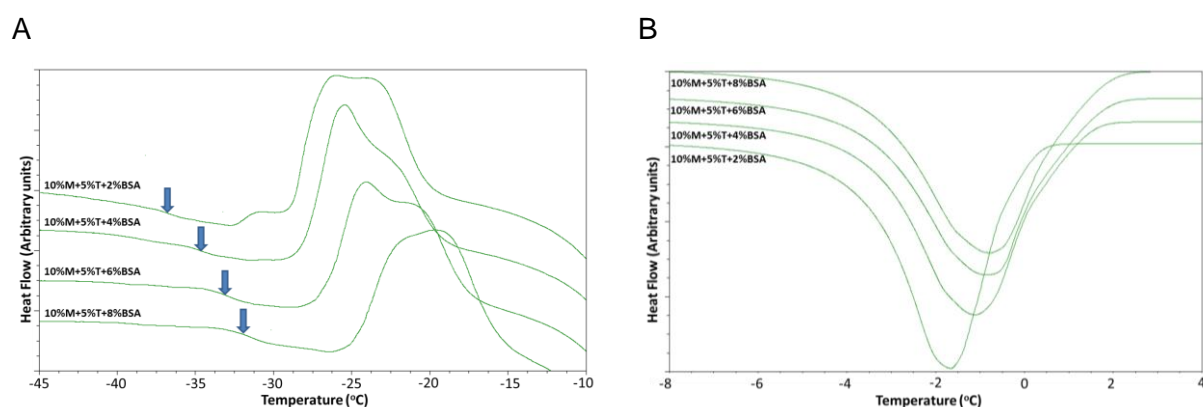


Figure 4-1. DSC heating curves of frozen solutions containing mannitol, trehalose and BSA. While the mannitol (10% w/w) and trehalose (5% w/w) concentrations were fixed, that of BSA was progressively increased. A - Glass transitions of the freeze concentrate (blue arrows); B - Mannitol-ice eutectic melting temperature. Solutions were cooled from room temperature to $-50\text{ }^{\circ}\text{C}$ at $20\text{ }^{\circ}\text{C}/\text{min}$, held for 2 minutes and then heated at $1\text{ }^{\circ}\text{C}/\text{min}$ back to room temperature. The heat flow was recorded during the final heating. Data only up to $-10\text{ }^{\circ}\text{C}$ (A) / $4\text{ }^{\circ}\text{C}$ (B) is shown.

Table 4-2. Glass transition temperature(s), T_g' ; and the corresponding heat capacity change, ΔC_p , before and after annealing at $-18\text{ }^{\circ}\text{C}$ for 20 h.

Composition	T_g' before annealing ($^{\circ}\text{C}$)*	T_g' after annealing ($^{\circ}\text{C}$) [#]	% change in ΔC_p [#]
10%M+5%T (control)	-42.5 ± 0.1 (T_g') -34.2 ± 0.3 (T_g'')	-32.6 ± 0.3	60.2 ± 1.1
10%M+5%T+2%BSA	-36.3 ± 0.4	-29.6 ± 0.5	51.3 ± 1.2
10%M+5%T+4%BSA	-34.3 ± 1.6	-25.8 ± 0.6	49.2 ± 2.1
10%M+5%T+6%BSA	-33.5 ± 1.8	-23.0 ± 0.6	47.6 ± 1.3
10%M+5%T+8%BSA	-33.3 ± 0.3	-22.4 ± 0.7	45.2 ± 1.8

M mannitol, T trehalose, BSA bovine serum albumin. Samples were cooled at $20\text{ }^{\circ}\text{C}/\text{min}$ to $-60\text{ }^{\circ}\text{C}$, held for 2 min and warmed to $-18\text{ }^{\circ}\text{C}$ at $1\text{ }^{\circ}\text{C}/\text{min}$. Samples were annealed for 20 h at $-18\text{ }^{\circ}\text{C}$, cooled back to $-60\text{ }^{\circ}\text{C}$ at $20\text{ }^{\circ}\text{C}/\text{min}$ and then warmed back up to room temperature at $1\text{ }^{\circ}\text{C}/\text{min}$. *Samples analyzed in quadruplicate; [#] samples analyzed in duplicate.

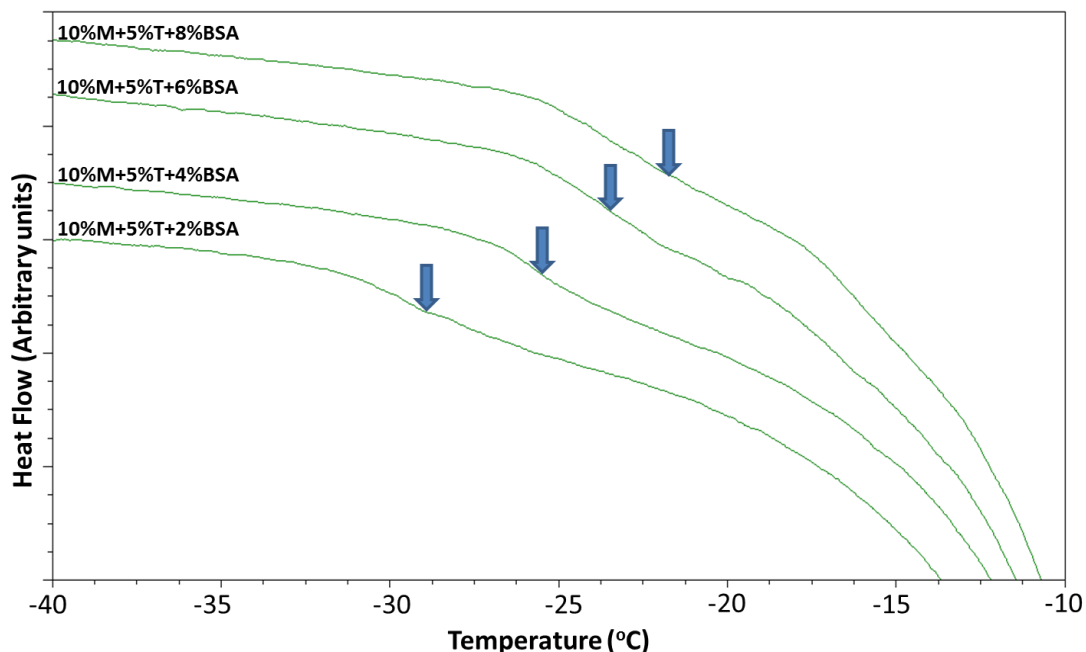


Figure 4-2. DSC heating curves of frozen annealed solutions containing mannitol, trehalose and BSA. While the mannitol (10% w/w) and trehalose (5% w/w) concentrations were fixed, that of BSA was progressively increased. Glass transitions of the freeze concentrate have been denoted by blue arrows. Effect of increasing BSA concentration on the thermal behavior of frozen annealed mannitol-trehalose-BSA solutions during warming. Glass transitions of the freeze concentrate have been denoted by blue arrows. Solutions were cooled from room temperature to $-50\text{ }^{\circ}\text{C}$ at $20\text{ }^{\circ}\text{C}/\text{min}$, held for 2 min, heated up to $-18\text{ }^{\circ}\text{C}$, and annealed isothermally for 20 hours. After annealing, the solutions were cooled back down to $-50\text{ }^{\circ}\text{C}$ at $20\text{ }^{\circ}\text{C}/\text{min}$, and reheated at $1\text{ }^{\circ}\text{C}/\text{min}$ back to room temperature. The heat flow was recorded during the final heating. Data only up to $-10\text{ }^{\circ}\text{C}$ is shown.

In Table 4-3, the effect of two additives, Tween 20 and deuterium oxide, on the thermal behavior of the frozen annealed solutions is summarized. In our earlier investigation, when the trehalose and mannitol concentrations were 8 and 10% (w/w) respectively, both the solutes crystallized when annealed [18]. However, the solute crystallization was incomplete since a T_g' was observed even in the annealed solutions (Table 4-3). In the presence of BSA, both before and after annealing, a single glass transition was observed (Figure 4-3 A). The one exception was the sample containing Tween 20 (1% w/w) in which two glass transition events were observed (Figure 4-3 A). In the presence of D_2O (5% w/w) and low concentrations of Tween 20 (up to 0.2% w/w), no exotherms were observed while heating the frozen solutions to the annealing temperature ($-18\text{ }^{\circ}\text{C}$). On the other hand, a higher concentration of Tween 20 (1% w/w) induced crystallization at a much lower temperature during heating and also increased the extent of crystallization (enthalpy of crystallization) before annealing more than in solutions without D_2O or Tween 20. In samples containing no additive, there was a pronounced decrease in ΔC_p associated with glass transition post annealing ($\sim 49\%$) and in samples containing 1% w/w Tween 20, no glass transition could not be detected after annealing (Figure 4-3 B). The change in ΔC_p was considerably reduced ($\sim 27\text{-}39\%$) in solutions containing D_2O and Tween 20 (up to 0.2% w/w). When frozen

solutions containing D₂O (>4% w/w) and low concentrations of Tween 20 (up to 0.2% w/w) were heated to RT after annealing, the glass transition was followed by a weak crystallization exotherm (~ 5 J/g; Figure 4-3 B). This could be attributed to residual mannitol crystallization. Crystallization exotherms were absent in all other samples, suggesting complete mannitol crystallization during annealing.

Table 4-3. Glass transition temperature(s), T_g'; and the corresponding heat capacity change, ΔC_p, before and after annealing at -18 °C for 20 h.

Composition	T _g ' before annealing (°C)	T _g ' after annealing (°C)	ΔC _p before annealing (kJ/kg K)	ΔC _p after annealing (kJ/kg K)	Enthalpy of crystallization (J/g)
10%M+8%T	-40.2 ± 0.3	-32.1 ± 0.1	0.048 ± 0.003	0.023 ± 0.001	11.2 ± 0.2
10%M+8%T+4%BSA	-39.9 ± 0.3	-27.8 ± 0.2	0.054 ± 0.002	0.026 ± 0.004	9.9 ± 0.4
10%M+8%T+4%BSA +0.1% Tween 20	-37.6 ± 0.3	-35.0 ± 0.3	0.053 ± 0.002	0.038 ± 0.001	-
10%M+8%T+4%BSA +0.2% Tween 20	-41.4 ± 0.2	-34.7 ± 0.2	0.052 ± 0.003	0.037 ± 0.001	-
10%M+8%T+4%BSA +1.0% Tween 20	-45.8 ± 0.2 -36.4 ± 0.1	-	0.055 ± 0.001 0.062 ± 0.002	-	14.8 ± 0.3
10%M+8%T+4%BSA +5% D ₂ O	-35.8 ± 0.4	-33.7 ± 0.3	0.051 ± 0.002	0.031 ± 0.003	-

M mannitol, T trehalose, BSA bovine serum albumin. Note: Blank spaces indicate that either glass transition or crystallization exothermic peak was not detected during heating. Samples were cooled at 20 °C/min to -60 °C, held for 2 min and warmed to -18 °C at 1 °C/min. Samples were annealed for 20 h at -18 °C, cooled back to -60 °C at 20 °C/min and then warmed back up to room temperature at 1 °C/min. All samples were analyzed in duplicate.

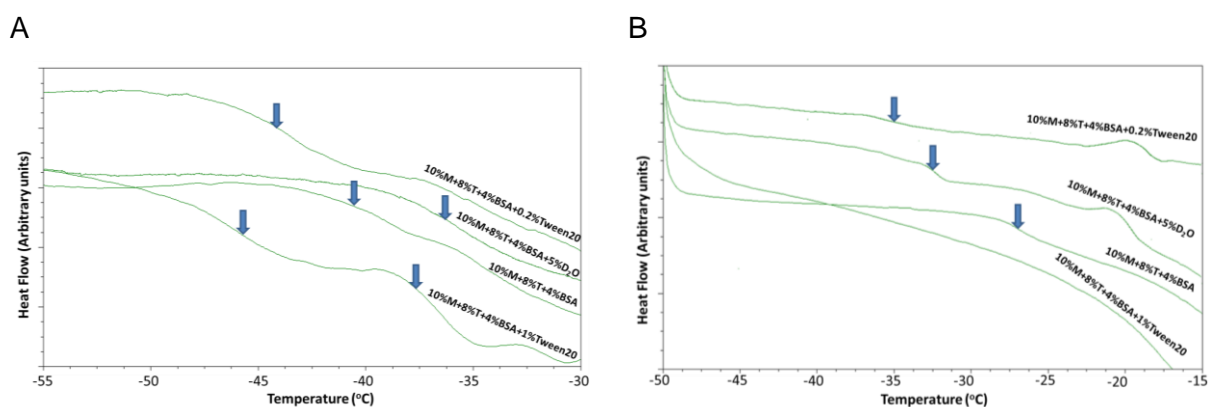


Figure 4-3. DSC heating curves of frozen solutions containing mannitol, trehalose and BSA. The effect of excipients (Tween 20 and D₂O) on the thermal behavior of the A - frozen, unannealed solutions and B - frozen, annealed solutions was determined. Glass transitions of the freeze concentrate have been denoted by blue arrows. Solutions were cooled from room temperature down to -50 °C at 20 °C/min, held for 2 minutes and then heated at 1 °C/min back to room temperature. The heat flow was recorded during the final heating. Data only up to -30 °C is shown.

3.2. Infrared Spectroscopy

In Figure 4-4, transmitted light microscopy images and the fingerprint regions of the respective IR spectra of frozen 10%M+8%T+4%BSA (left), and 10%M+8%T+15%BSA (right) solutions after 15 hours of annealing are shown. The physical form of mannitol crystallizing from both solutions was different, based on both XRD and IR spectroscopy. The thin, long, dark brown strands, arranged radially in the 10%M+8%T+4%BSA solution, are mannitol hemihydrate crystals. On the other hand, the flat, longitudinal almost translucent structures on the ice surface in the 10%M+8%T+15%BSA solution are anhydrous mannitol crystals. The bifurcation of the C-H stretching peak ($2970\text{--}2910\text{ cm}^{-1}$) in the IR spectra indicated solute crystallization [38–42]. Specifically, crystallization of mannitol was detected from bifurcation of the C-H in-plane bending peak ($1400\text{--}1280\text{ cm}^{-1}$) [38,41]. Likewise, crystallinity of trehalose was monitored from bifurcation of its C-O-C stretching peak ($1010\text{--}975\text{ cm}^{-1}$) [39,40,42] and the shift in its glycosidic peak [18].

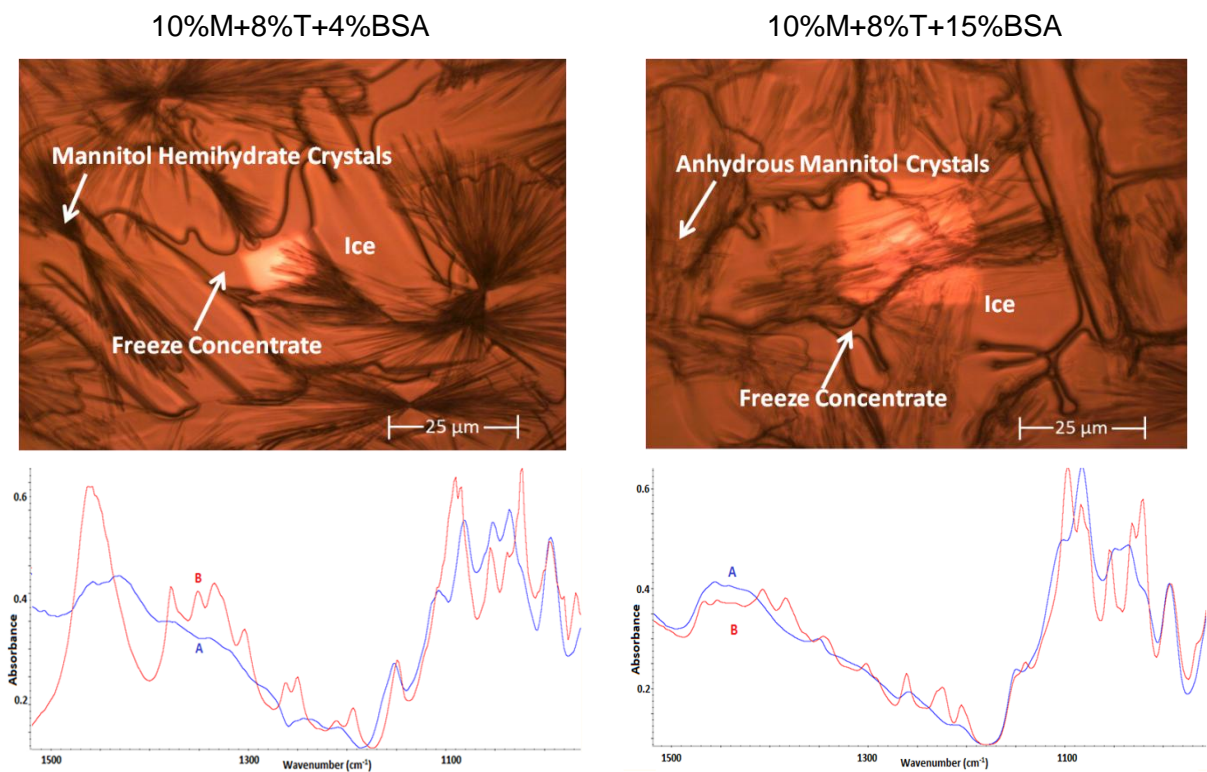


Figure 4-4. Transmitted light microscopy images (Row 1) and the corresponding FTIR spectra (Row 2) of A - 10%M+8%T+4%BSA, and B - 10%M+8%T+15%BSA solutions at $-18\text{ }^{\circ}\text{C}$ after 15 hours of annealing. Curves “A” and “B” are the IR spectra taken from a fixed region of the sample at the beginning and the end of annealing, respectively.

The peak position of the Amide II band ($1570\text{--}1530\text{ cm}^{-1}$) is sensitive to the extent of hydrogen bonding of the protein with the polar groups and molecules in its microenvironment and thus has been used to determine the hydration level of proteins [43,44]. With enhanced

hydration, Amide II shifted to higher wavenumbers. The Amide I ($1700\text{-}1600\text{ cm}^{-1}$) band is more sensitive to protein secondary structure than Amide II and has traditionally been deconvoluted by peak fitting or by secondary derivative analysis in order to yield information on the secondary structure content of proteins [45–48]. Second derivative analysis of the amide I after subtraction of an ice background, revealed 3 distinct peaks attributed to β -sheets ($1640\text{-}1620\text{ cm}^{-1}$), α -helices ($1670\text{-}1640\text{ cm}^{-1}$), and random coils ($1695\text{-}1670\text{ cm}^{-1}$). The relative fraction of each structure was calculated using their integrated peak areas. Addition of D_2O into the solution results in splitting of Amide II into the Amide II' ($1520\text{-}1420\text{ cm}^{-1}$) and Amide II ($1570\text{-}1520\text{ cm}^{-1}$) [49,50]. The extent of deuteration of the protein backbone chains can be determined by comparing the peak areas or the intensities of these bands. In FTIR analysis, all solutions were rapidly cooled at $10\text{ }^\circ\text{C}/\text{min}$, and then immediately warmed up to the annealing temperature ($-18\text{ }^\circ\text{C}$) as soon as homogenous ice crystallization was visually detected through the microscope. The samples were held at $-18\text{ }^\circ\text{C}$ for 15 hours and IR spectra were collected.

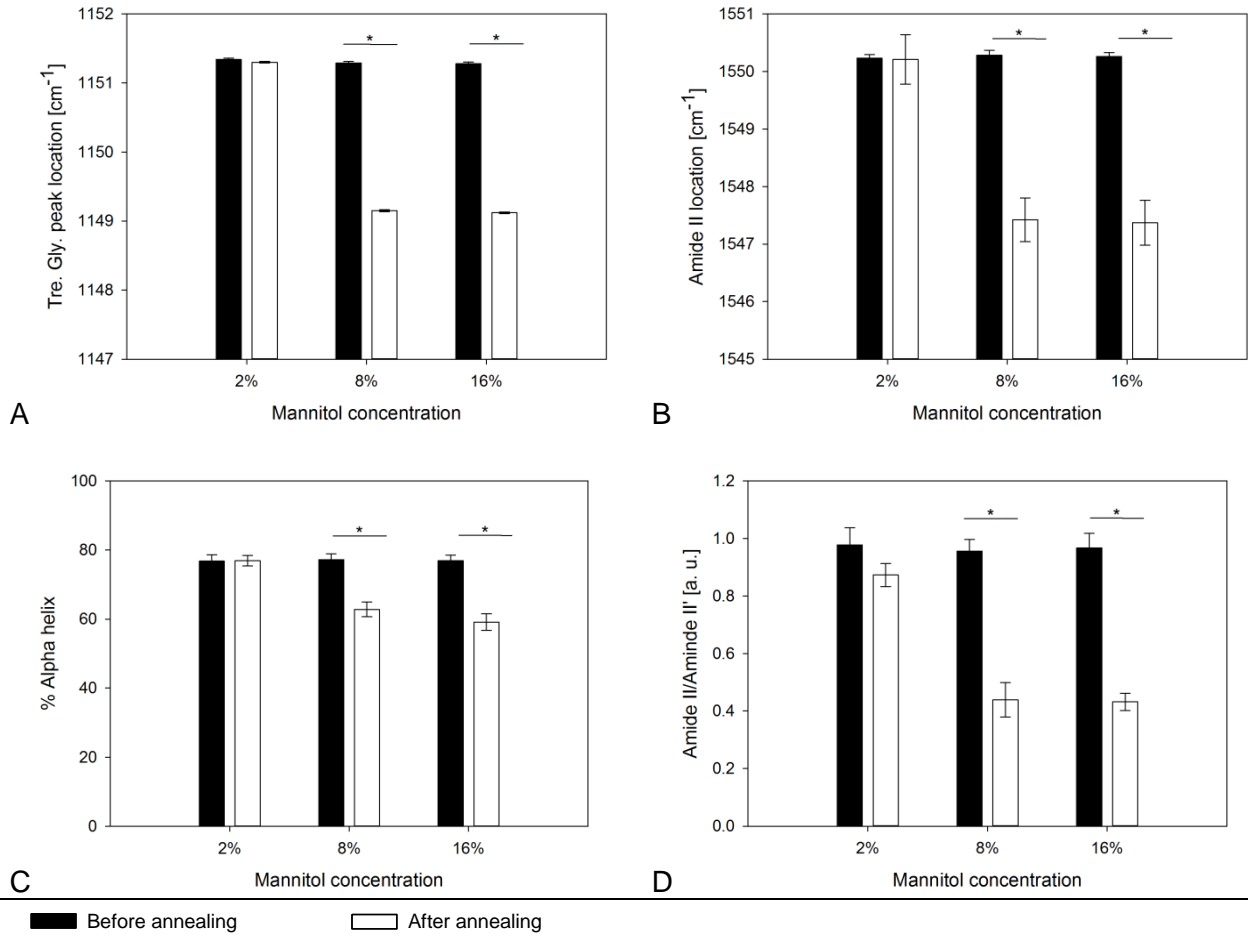


Figure 4-5. Comparison of trehalose crystallinity, protein hydration, and structure before (black) and after (white) annealing (at -18 °C for 15 hours) in frozen aqueous solutions containing X%M+8%T+4%BSA; X = 2, 8 or 16%. A - Trehalose glycosidic peak location; B – Amide II peak location; C - Percent alpha helix in secondary structure; D - Area ratio of Amide II' and Amide II peaks in the presence of 1% D₂O (w/w). Compositions that undergo change up on annealing have been marked with *.

In Figure 4-5, the effects of mannitol concentration on the crystallinity of trehalose and stability of BSA during annealing are presented. In agreement with our previous studies, at $R < 1$ both mannitol and trehalose remained amorphous until the end of the annealing period. The native secondary conformation and the degree of hydration of BSA were preserved during annealing. When $R > 1$, mannitol crystallized as a hemihydrate as soon as the annealing temperature was reached and 2 hours later, trehalose crystallized as the dihydrate (confirmed by XRD). This was followed (after 2 hours of trehalose crystallization) by a decrease in hydration and change in the secondary structure of BSA, which were evidenced by the shift in Amide II location (by 2.5 cm⁻¹) and reduced α -helix content (by 14%). An identical behavior was observed in samples containing equal concentrations of mannitol and trehalose ($R = 1$) with the only difference being that mannitol crystallization started 30 minutes into the annealing process. D₂O (1% v/v) was added to parallel sample solutions of identical composition to obtain information on the tertiary structure of BSA from the relative

intensities of the Amide II and Amide II' bands. When $R \geq 1$, unfolding of secondary structure was preceded by that of the tertiary structure, which occurred a few minutes before trehalose crystallization was detected.

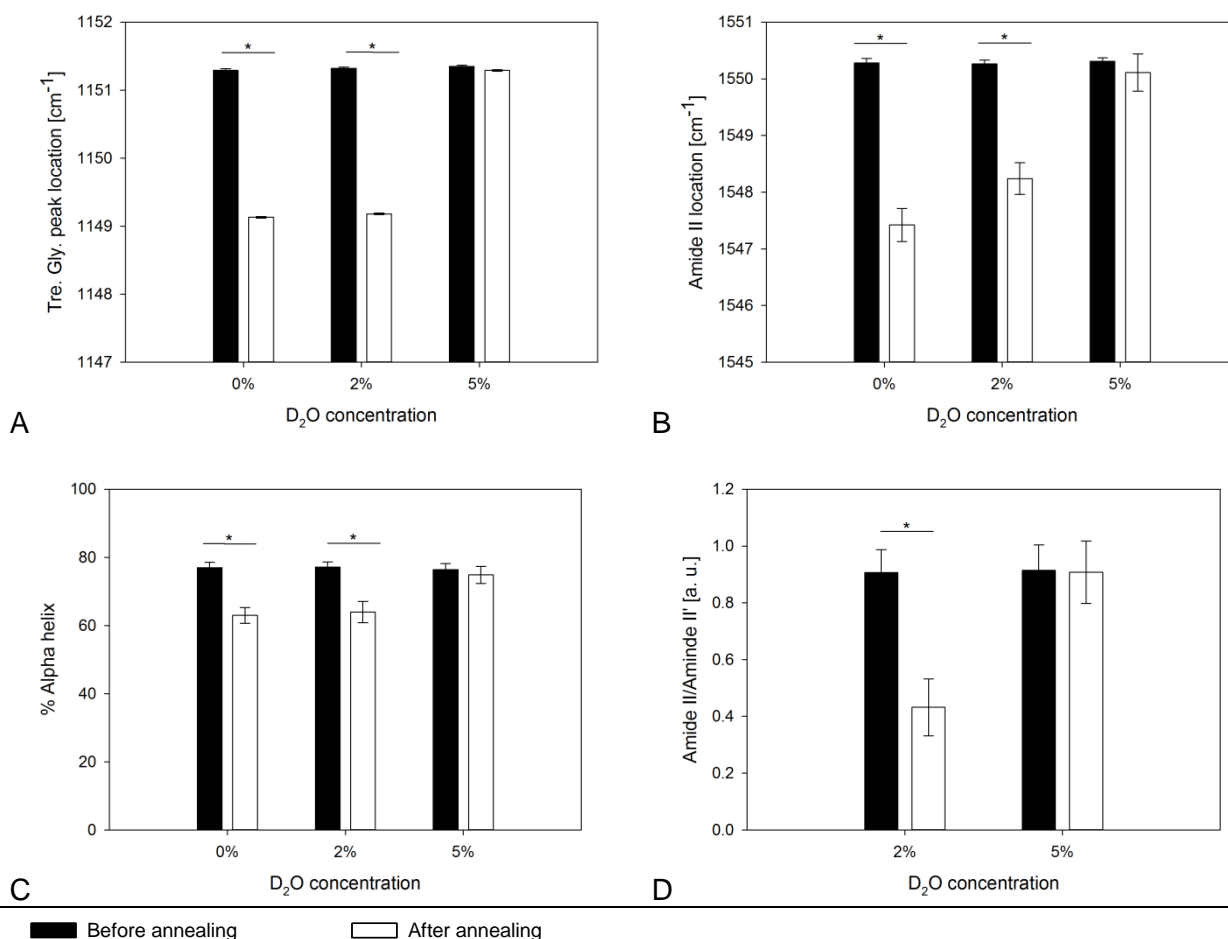


Figure 4-6. Comparison of trehalose crystallinity, protein hydration, and structure before (black) and after (white) annealing (at -18 °C for 15 hours) in frozen solutions containing 10%M+8%T+4%BSA+X%D₂O samples; X = 0, 2 and 5%. A fixed region of the frozen solution was analyzed. A - Trehalose glycosidic peak location; B – Amide II peak location; C - Percent alpha helix in secondary structure; D - Area ratio of Amide II' and Amide II peaks in the presence of 1% D₂O (w/w). Compositions that undergo change up on annealing have been marked with *.

In the absence of BSA, irrespective of trehalose concentration, mannitol crystallized as the hemihydrate, as soon as the annealing temperature was reached. On the other hand, when BSA was included in the formulations (Figure 4-7), both anhydrous and hemihydrate forms crystallized (observed both visually and spectroscopically). There was also a delay in the onset of mannitol crystallization (2 - 6 hours) upon holding at -18 °C. The delay time and the fraction of anhydrous mannitol formed were directly proportional to the initial BSA concentration in the solution. When the BSA concentration was raised to 16% w/w, mannitol crystallized entirely in the anhydrous form and trehalose was retained amorphous even after

15 hours of annealing (determined from the location of the C-O-C glycosidic peak in the IR spectra). There was also negligible change in the hydration level and secondary structure (α -helix content) of BSA at the end of annealing.

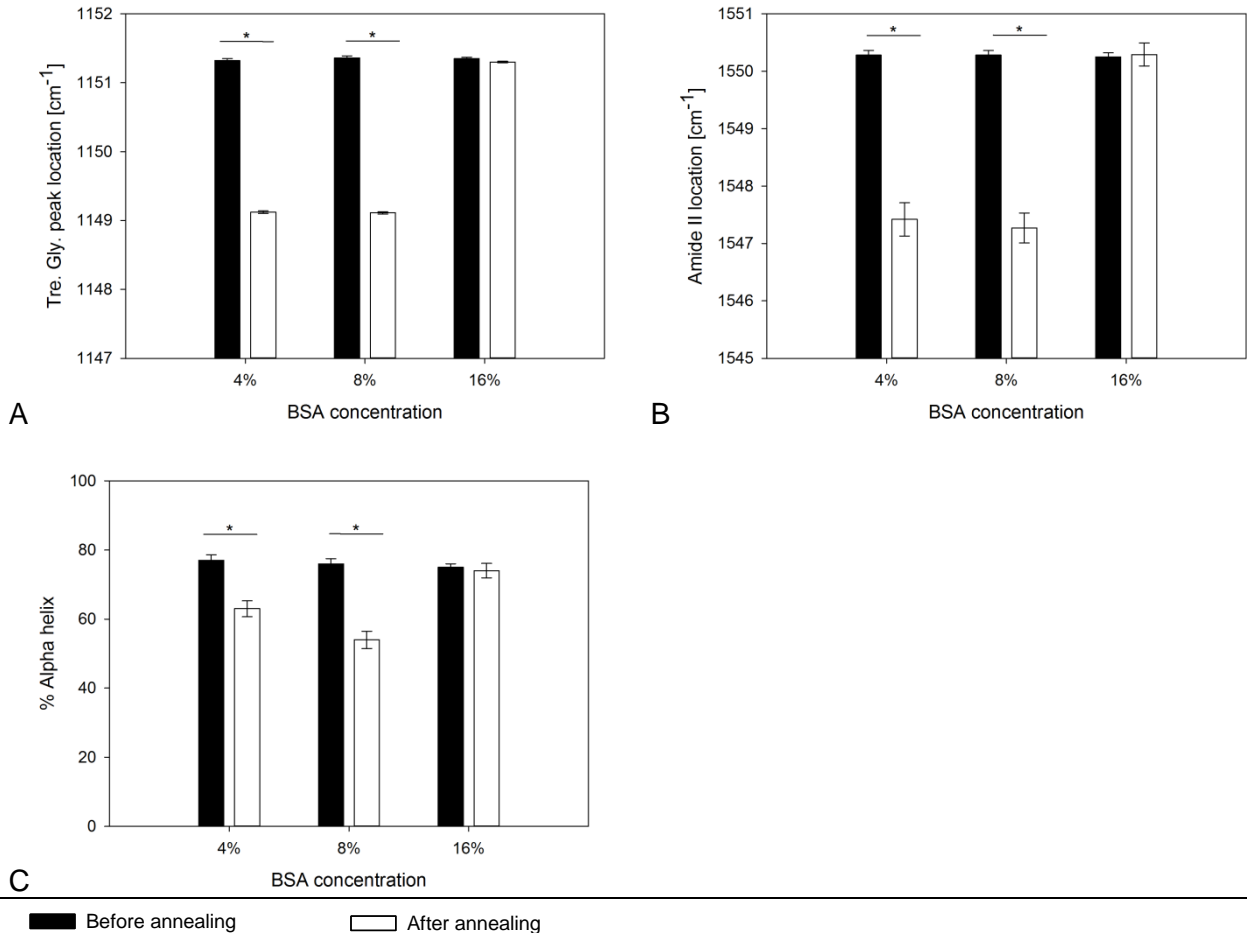


Figure 4-7. Comparison of trehalose crystallinity, protein hydration, and structure before (black) and after (white) annealing of frozen 10%M+8%T+X%BSA samples at $-18\text{ }^{\circ}\text{C}$ for 15 hours; X = 4, 8 and 16. A - Trehalose glycosidic peak location; B - Amide II peak location; C - Percent alpha helix in secondary structure. Compositions that undergo change up on annealing have been marked with *.

Addition of D₂O and Tween 20, in a concentration dependent manner, significantly affected the crystallinity of both the sugars as well as BSA stability. Upon addition of up to 4% (w/w) of D₂O (Figure 4-6), no difference in observations was noted from the sample with no additives (4%BSA+8%T+10%M). However, an initial D₂O concentration of 5% (w/w) and higher delayed the onset of mannitol crystallization (as hemihydrate) by about 5 hours, and completely suppressed trehalose crystallization throughout annealing. Congruously, the IR spectra revealed enhanced stability of BSA in terms of both hydration and secondary structure. Very similar results were seen on using Tween 20 as an excipient (Figure 4-8). At low concentrations (up to 0.2% w/w), Tween 20 delayed mannitol crystallization (as

hemihydrate) by at least 6 hours and entirely suppressed trehalose crystallization. On the other hand, at high concentrations of Tween 20 (> 1% w/w), mannitol started to crystallize in the anhydrous form as soon as the temperature was held at -18 °C. One hour into annealing, crystallization of trehalose was detected. In the presence of both high and low concentrations of the surfactant, BSA appeared to be adequately hydrated throughout annealing despite trehalose crystallization. Although hydration of protein was retained, at high concentrations of Tween 20 (> 1% w/w), a significant decrease in α helix and increase in β sheet content was observed 3 hours into the annealing.

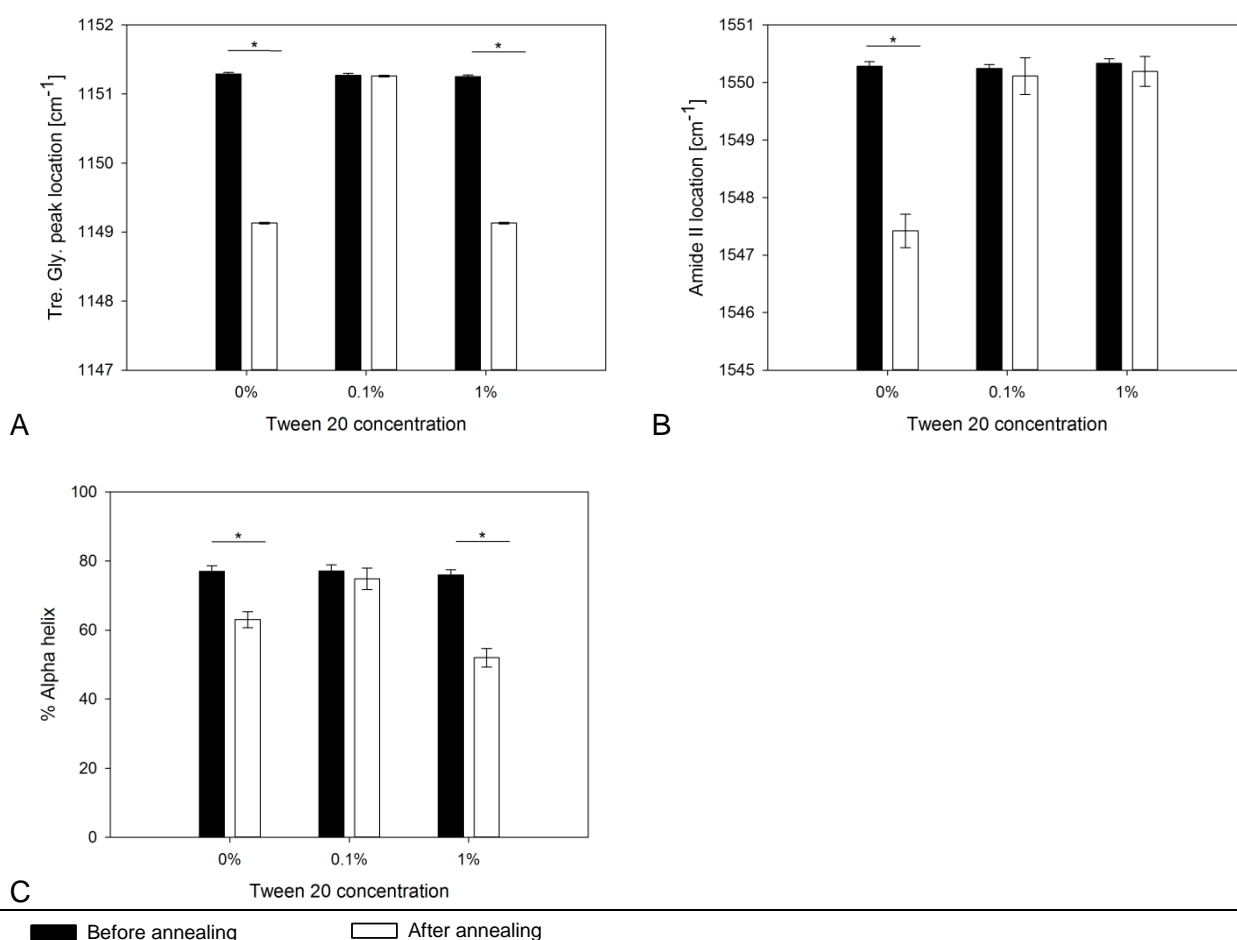


Figure 4-8. Comparison of trehalose crystallinity, protein hydration, and structure before (black) and after (white) annealing of frozen 10%M+8%T+4%BSA+X%Tween 20 samples at -18 °C for 15 hours; X = 0.1 and 1. A - Trehalose glycosidic peak location; B - Amide II peak location; C - Percent alpha helix in secondary structure. Compositions that undergo change up on annealing have been marked with *.

3.3. X-Ray Diffractometry (XRD)

XRD enabled characterization of the phases crystallizing from the frozen solutions. Trehalose dihydrate was characterized by peaks (Cu K α radiation; $\lambda=1.5407$ Å) at 8.8° (10.10 Å), 12.6° (7.00 Å), 13.7° (6.45 Å), and 16.5° 2 θ (5.36 Å) while α -anhydrous trehalose

was identified by peaks at 16.8° (5.26 \AA) and 17.8° 2θ (4.98 \AA). Mannitol hemihydrate was identified by peaks at 9.6° (4.95 \AA) and 20.5° 2θ (4.33 \AA) while δ -anhydrous form of mannitol was characterized by peaks at 9.7° (9.11 \AA) and 24.6° 2θ (3.62 \AA). Peaks at 22.7° (3.93 \AA), 24.4° (3.65 \AA), 25.8° (3.46 \AA), and 33.5° 2θ (2.68 \AA) were assigned to hexagonal ice [51]. The XRD patterns obtained at the end of annealing period for the 10%M+8%T+15%BSA and 10%M+8%T+4%BSA solutions are presented in Figure 4-9.

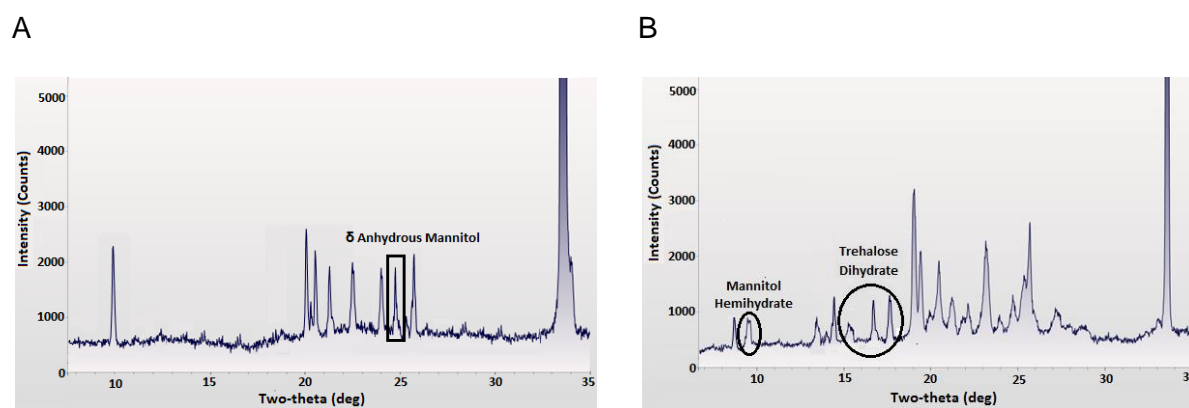


Figure 4-9. XRD patterns of A - 10%M+8%T+15%BSA, and B - 10%M+8%T+4%BSA solutions after 20 hours of annealing at -18°C .

The conclusions drawn from IR analysis were supported by the XRD data. In the presence of high concentrations of BSA (15% w/w), the δ anhydrous form of mannitol was detected 6 hours into annealing. No peaks attributable to crystalline trehalose could be detected throughout annealing. On the other hand, in the frozen solution without additives (10%M+8%T+4%BSA), in addition to ice crystallization, mannitol hemihydrate peaks appeared after 1 hour of annealing. Two hours following the onset of mannitol crystallization, peaks attributable to trehalose dihydrate were detected.

3.4. Circular Dichroism (CD) Analysis of the Thawed Samples

Structural stability of BSA in aqueous state was studied by CD. Sample solutions of composition identical to those used in IR spectroscopy and XRD experiments, were refrigerated at -20°C for a prolonged duration (20 hours). Far-UV circular dichroism is sensitive to the backbone conformation of proteins. CD was used for structural characterization of BSA in both freshly prepared solutions and in thawed solutions after annealing. Differences in secondary structure of BSA due to annealing and thawing, estimated from CD spectra, are shown in Table 4-4. CD analysis also helped determine if

refolding of BSA occurred upon thawing the samples (reversibility of freezing induced denaturation). Turbidity in some of the solutions, immediately following ice melting, indicated solute crystallization. These crystals usually dissolved within 5 minutes of thawing.

Table 4-4. Change in the secondary structure of BSA due to freezing and annealing = (% in fresh solution) - (% in thawed solution).

Composition	H (r)	H (d)	S (r)	S (d)	Turns	Unordered
4%BSA+8%T	1 ± 0.1	1 ± 0.0	-1 ± 0.1	0 ± 0.1	-1 ± 0.0	-3 ± 0.0
4%BSA+8%T+2%M	2 ± 0.1	0 ± 0.1	-1 ± 0.2	0 ± 0.1	-2 ± 0.1	-1 ± 0.1
4%BSA+8%T+10%M	15 ± 0.3	4 ± 0.1	-8 ± 0.3	-4 ± 0.1	-5 ± 0.2	-3 ± 0.1
8%BSA+8%T+10%M	17 ± 0.2	5 ± 0.1	-11 ± 0.4	-4 ± 0.1	-5 ± 0.2	-1 ± 0.1
8%BSA+4%T+10%M	24 ± 0.3	8 ± 0.0	-17 ± 0.3	-6 ± 0.1	-5 ± 0.3	-4 ± 0.0
4%BSA+8%T+10%M+ 1.0%Tween 20	16 ± 0.3	8 ± 0.2	-6 ± 0.4	-4 ± 0.1	-4 ± 0.3	-10 ± 0.1
4%BSA+8%T+10%M+ 0.2%Tween 20	4 ± 0.2	2 ± 0.1	-4 ± 0.2	-5 ± 0.2	-1 ± 0.2	-1 ± 0.2
4%BSA+8%T+10%M+ 0.1%Tween 20	4 ± 0.2	1 ± 0.1	-1 ± 0.2	0 ± 0.1	-1 ± 0.2	-3 ± 0.1
4%BSA+8%T+10%M+5%D ₂ O	4 ± 0.3	0 ± 0.2	-1 ± 0.3	1 ± 0.2	0 ± 0.2	6 ± 0.2

H(r) → Regular Helix, H(d) → Distorted helix, S(r) → Regular Sheet, S(d) → Distorted Sheet. Solutions were frozen and annealed at -18 °C for 20 hours. All samples were analyzed in duplicate.

Firstly, mannitol concentration was increased, keeping BSA and trehalose concentrations fixed at 4% and 8% w/w, respectively. When $R < 1$, solutions appeared completely transparent as soon as they were thawed, suggesting that solute crystallization had not occurred during freezing. Simultaneously, no significant change in the secondary structure of BSA was observed upon thawing. When mannitol concentration was increased to 8% w/w, the thawed solutions, even those containing additives (Tween 20 or D₂O), displayed temporary increase in turbidity. This was also the case when the BSA concentration was raised to 10% w/w. CD analysis revealed a significant decrease in α -helix (20%) content and a concomitant increase in β -sheet content (12%). A slight increase in the fractions of unordered structures and turns was noted for most of these solutions. An interesting

observation from the CD data is that the decrease in regular α -helix content and increase in the regular β -sheet content were more pronounced than the changes in the distorted fractions of both structures. The unfolding was exacerbated on increasing the mass ratio of protein to trehalose from 0.5 to 1 and 2. With the addition of D₂O or low concentrations of Tween 20 (up to 0.2% w/w), unfolding of BSA was sufficiently inhibited. When surfactant concentration was increased to 1% w/w and above, unfolding of BSA was worsened.

3.5. Characterization of Aggregates

Samples with different trehalose to BSA mass ratios at a constant mannitol concentration of 10% were analyzed post freezing and thawing. After annealing at -20 °C for 20 hours, the formation of both soluble and insoluble aggregates was investigated. Since the freezing step, depending on the formulation, facilitates the unfolding of BSA in the freeze-concentrate, subsequent aggregation represents a critical parameter for formulation development. Macroscopic appearance, turbidity and the number of subvisible particles were investigated as indication for protein precipitation.

The macroscopic appearance was unchanged after annealing of all the tested formulations. The solutions were clear without signs of aggregate formation. Since the insoluble particles scatter the light at 350 nm, the solution turbidity was measured. An increased absorbance would hence indicate insoluble particles in the sample. There was no difference between unstressed and annealed samples. An increasing BSA concentration resulted in increasing absorbance values both at 280 and 350 nm whereby the turbidity values of all formulations investigated were below 0.06 absorbance units indicating the absence of aggregates larger than approx. 35 nm (1/10 of the wavelength of 350 nm) [52].

Light obscuration was used to characterize the subvisible particles. Particles $\geq 1 \mu\text{m}$, $\geq 10 \mu\text{m}$ and $\geq 25 \mu\text{m}$ did not show a significant change between stressed and unstressed samples. For particles $\geq 1, 10$ and $25 \mu\text{m}$, the number of particles per mL was below 30,000, 200 and 110, respectively. Overall, light obscuration did not indicate that annealing at -20°C for 20 h induced subvisible particle formation.

Subsequently, two factors were evaluated with HP-SEC analysis: (1) formation of soluble higher molecular weight species and (2) monomer recovery. The analysis did not indicate the formation of soluble higher molecular weight aggregates. Since these are soluble and can be separated by HP-SEC they usually consist only of a few aggregated protein molecules [53]. Concerning monomer recovery, three compositions had a significant lower recovery after annealing (Figure 4-10). These were the two formulations with the highest BSA to trehalose ratio with and without mannitol (10%BSA+2%T and 10%BSA+2%T+10%M), as well as the

composition with 2% Tween 20 (4%BSA+8%T+10%M+2%Tween 20). Adding 10% mannitol led to even lower monomer recovery (15.1% monomer loss with mannitol vs. 11.4% without mannitol).

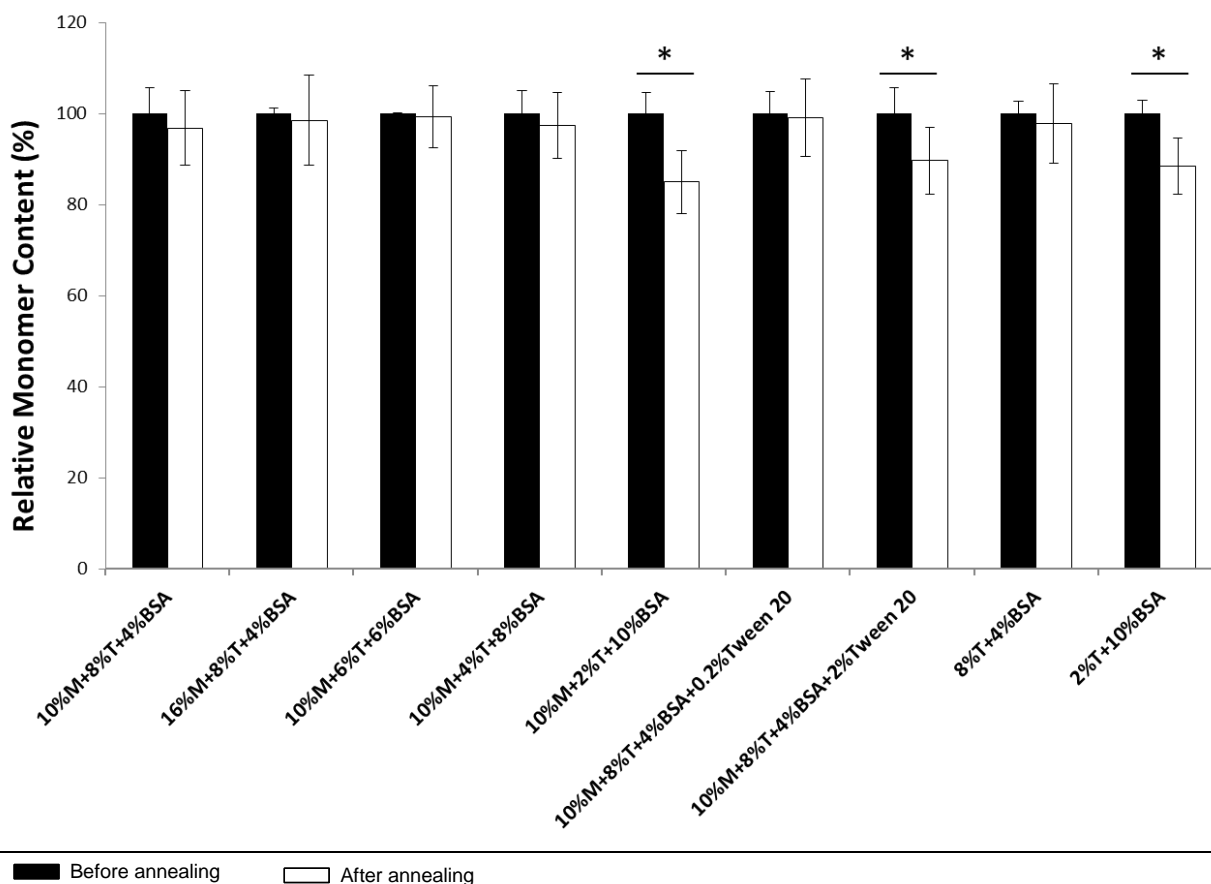


Figure 4-10. Monomer recovery from fresh samples (white bars) and samples annealed at -20 °C for 20 hours (grey bars) determined by HP-SEC at 280 nm (n=3). Mean ± SD. * P < 0.05.

As already shown with CD, high Tween 20 concentrations are detrimental to BSA structure. This could be confirmed by HP-SEC analysis. 2% Tween 20 showed a monomer recovery of 89.6% whereas the recovery of the surfactant free formulation (4%BSA+8%T+10%M) and the formulation only containing 0.2% Tween 20 was almost complete (99.8% and 99.0%, respectively). Formulations with lower BSA to trehalose ratios also showed a comparable protein recovery before and after annealing.

The HP-SEC results, in agreement with IR analysis, indicated changes in the secondary structure of BSA in these formulations after annealing. As described above, three formulations showed a monomer loss > 10% determined by HP-SEC, but no increase in soluble higher molecular weight aggregates was detected. Thus, one could assume a higher aggregate size and hence an increase in insoluble particles. However, macroscopic appearance and the turbidity and light obscuration results ruled this out. We consequently assume that the unfolded BSA molecules are still soluble. However, their increased

hydrophobicity leads to retention on the HPLC column preventing elution and hence detection.

4. Discussion

Upon adding BSA to mannitol-trehalose systems, the protein in a concentration dependent manner, delayed the onset, as well as the kinetics of mannitol crystallization. The relative extent of mannitol crystallization in various compositions can be determined from the temperature at which the melting endotherm is detected in the DSC scans while heating the frozen samples. The mannitol-ice eutectic melting usually occurs at $-2.2\text{ }^{\circ}\text{C}$ [54,55] while ice melts at a higher temperature ($0\text{ }^{\circ}\text{C}$). The measured shift in the melting endotherm to higher temperatures, with increasing BSA concentration (Figure 4-1 B), was due to increasing contribution of ice melting to the endotherm which indicated reduced extent of mannitol crystallization.

It has been previously reported that freezing and lyophilization of solutions containing mannitol in the presence of proteins such as monoclonal antibodies, lysozyme and human serum albumin, substantially reduced the extent of mannitol crystallization in a concentration dependent manner [19–22]. Pharmaceutical proteins such as monoclonal antibodies have also been shown to inhibit mannitol crystallization during spray drying [56,57]. Inhibition of crystallization by BSA could be due to its surface activity similar to that of a surfactant by virtue of its affinity for interfaces [58]. Moreover, DSC scans showed that glass transition of the freeze concentrate broadened in solutions containing BSA. This could be due to increased entropy of the solution in the presence of BSA, and/or some specific interaction between mannitol and BSA.

At low surfactant concentrations, mannitol crystallization was delayed and trehalose crystallization was inhibited in spite of a relatively mobile FCL phase at $-18\text{ }^{\circ}\text{C}$ (i.e., lower T_g') [59–61]. This could be attributed to adsorption of surfactant molecules to crystal surfaces, which impeded further propagation [26], and the reduced interactive forces between the solute molecules [62–64]. At high concentrations, Tween 20 appeared to not only facilitate crystallization of mannitol but also increased the extent of trehalose crystallization (for example, after annealing, no glass transition could be detected). Critical micelle concentration (CMC) of Tween 20 is 0.008% w/w at $25\text{ }^{\circ}\text{C}$ [65]. At lower temperatures, CMC is known to increase [66]. Thus, at an initial solution concentration of 1% w/w, a very large number of micelles can be expected to form in the FCL. Micelles have been associated with increased supersaturation of the crystallizing solute and reduced interfacial tension, both of

which accelerate the rate of nucleation [25,67–69]. Surfactant assemblies can also promote crystallization by acting as templates for nucleation and growth of crystals [70,71]. Besides, a very low T_g' indicates a comparatively mobile (less viscous) FCL at the annealing temperature, ideal for crystal growth [59–61]. Mobility of the FCL (diffusivity of any species) is directly proportional to the magnitude of the difference between the annealing and glass transition temperatures ($T_a - T_g'$) [59–61,72]. An important observation from the thermal behavior of frozen solutions before and after annealing is that in the presence of low concentrations of Tween 20 and D_2O , mannitol crystallization was incomplete. This was obvious from the % change in ΔC_p (Table 4-2) due to annealing as well as from the appearance of exotherms after annealing during warming (Figure 4-3 B). Retention of amorphous mannitol in the freeze-dried cake could have repercussions such as the formation of a mechanically fragile final product with low collapse temperature [14], and release of the sorbed water during storage [21], which can increase the mobility in the FCL and result in API instability.

At high concentrations, Tween 20 and BSA induced the formation of δ -anhydrous mannitol form instead of the hemihydrate. Presence of additives including surfactants has been known to affect the physical form of the crystallizing phases [73,74]. Additives either promote or inhibit propagation of the crystals along certain directions by engaging in specific interactions (e.g. hydrogen bonding) with functional groups along crystal faces. In the presence of solutes such NaCl and proteins such as HSA, mannitol has been found to crystallize as the δ -anhydrous form. High concentrations of BSA (15% w/w), and D_2O (5% w/w) effectively prevented crystallization of trehalose. A possible explanation for this is that both BSA and D_2O increased T_g' values, reducing ($T_a - T_g'$) and hence the mobility of the FCL at the annealing temperature. Surface coverage action of BSA could also be a factor, as explained before. This also explains the observed delay in mannitol crystallization.

Post-thaw analysis by CD mostly concurred with the changes in protein conformation measured by IR spectroscopy in the frozen state. It has been reported previously that while cold denaturation and chemical denaturation of proteins in tumour cells and monoclonal antibodies is reversible [75,76], cold denaturation of ovalbumin is irreversible [77]. It was comprehensively proven that crystallization of trehalose destabilizes protein in the frozen state and the subsequent protein unfolding was not reversed upon thawing. Crystallization of trehalose signified that the lyoprotectant could no longer interact with and stabilize the API in accordance with the water replacement theory [78,79]. Besides, proteins have been known to be susceptible to aggregation at interfaces [80,81], and crystal formation gives rise to higher interface area. At high BSA and D_2O concentrations, the protein was found to retain its hydration and native conformation in the frozen state. One reason could be that

crystallization of trehalose was avoided in these formulations. Besides, there is evidence that D₂O protects cells and proteins against thermal denaturation and heat shock [31,32].

Table 4-5. Effect of thawing rate of 10%M+4%T+8%BSA sample on the secondary structure of BSA. = (% in fresh solution) - (% in thawed solution).

Heating rate	H (r)	H (d)	S (r)	S (d)	Turns	Unordered
Fast thaw	9 ± 0.6	2 ± 0.3	-6 ± 0.8	-2 ± 0.4	-1 ± 0.3	-2 ± 0.7
Ambient	24 ± 0.3	8 ± 0.1	-17 ± 0.3	-6 ± 0.1	-5 ± 0.3	-4 ± 0.0
Slow thaw	21 ± 0.4	5 ± 0.6	-14 ± 0.3	-5 ± 0.5	-4 ± 0.6	-3 ± 0.5

H(r) > Regular Helix, H(d) > Distorted helix, S(r) > Regular Sheet, S(d) > Distorted Sheet. Solutions were frozen and annealed at -18 °C for 20 hours and thawed at different rates. The sample was immersed in a water bath at 60 °C for fast thaw, kept at room temperature for ambient thaw and immersed in a water bath with melting ice (0 °C) for slow thaw. All solutions were analyzed in duplicate.

An argument in case of samples with high protein to trehalose mass ratios is that there are very few trehalose molecules per protein molecule in the FCL for the lyoprotectant to be effective, in spite of being amorphous. BSA has been shown previously to protect itself (as well as other more labile proteins) against freezing induced stresses by acting as a molecular chaperon [82,83] and by accumulating at crystalline surfaces (forming almost a sacrificial layer) due to its strong affinity for interfaces [58,84]. CD and HPSEC results revealed protein unfolding in the thawed solutions at high BSA to trehalose mass ratios. This implied that self-stabilization of BSA, which was effective in the frozen state, lost its effectiveness during thawing. During thawing, recrystallization occurs, especially at slower thawing rates (< 20 °C/min), perturbing the stability of the proteins at the rapidly changing ice–solution interface [85,86]. All frozen solutions analyzed by CD were thawed slowly by leaving them exposed to ambient temperatures. This hypothesis was later verified when 3 samples of the composition (10%M+4%T+8%BSA) were thawed at different rates, after freezing and annealing (Table 4-5). The first frozen sample was rapidly thawed by immersing it in a water bath maintained at 60 °C, the second was thawed by leaving it exposed to room temperature, while the third was thawed very slowly by immersing it in water in equilibrium with ice (0 °C). While no difference was observed in the protein structure between the samples thawed at RT and at 0 °C, structural changes of protein in the rapidly thawed sample were significantly reduced.

In previous studies of Zakharov et al. on ice recrystallization in the presence of BSA, it has been claimed that BSA inhibits ice recrystallization at warmer temperatures [87]. But the thermal protocols used for both studies are very different. In the work of Zakharov et al.,

frozen BSA samples were very rapidly warmed (at 6 °C/min) to the temperature of interest and held. On the other hand, in the current study, frozen samples were thawed very slowly to room temperature under ambient conditions before CD analysis. This should cause an increased extent of ice recrystallization and thus account for its effect on the structure of BSA during thawing, as observed in this study. As discussed previously, samples that were thawed rapidly showed significantly reduced effects of recrystallization, in agreement with the findings of Zarkharov et al. Reports have shown that although a higher concentration of protein increases the glass transition temperature of the freeze concentrate (and thus the collapse temperature during drying), the protein concentration in the freeze-drying formulation is usually limited in order to ensure a higher weight ratio of stabilizer (> 1) to protein for its stability during storage [14]. A molar disaccharide to protein ratio of 350-400 has been reported to be sufficient to ensure protein stabilization during freeze- and spray-drying [88,89]. This should not be a limitation for a self-stabilizing API such as BSA.

At low concentrations of Tween 20, no signs of unfolding and aggregation of BSA could be detected. The possible mechanisms of protein stabilization by surfactants are ice interface coverage (protects against aggregation at crystalline interfaces [27]), screening of the hydrophobic attractive forces between proteins, and enhancement of hydration and electrostatic repulsive forces between the proteins [90]. On the other hand, at an initial concentration of 1% w/w, Tween 20 proved to be even more detrimental to protein structure. Free surfactant micelles promote protein aggregation and precipitation due to the attractive depletion force between the protein and micelle complexes [90–92]. Aggregates composed of non-native β -sheet structures have been identified while freezing globular proteins with non-ionic surfactants due to direct unfavourable binding of surfactant with protein surface and interaction with micelles [28].

Distortion in the geometry of α -helices and β -sheets arise when a few residues (about 3-4) at the end of each coil/sheet exposed to the solvent are twisted away from the solvent region to maximize their H-bonding capacity. These few residues do not conform to the regular helical geometry of the coil or the planar geometry of the sheets. A very interesting observation from secondary structure characterization was that in some thawed solutions (where BSA was denatured) there was an increase in the relative fraction of distorted α -helix content (vs. regular). This led us to believe that not only did the α -helices reduce in quantity but they were also structurally reorganized (distorted) into shorter coils. Shortening in length of α -helix coils has been identified as a consequence of denaturation [93,94]. Simultaneously, the relative fraction of regular β -sheets (vs distorted) was found to increase in the same thawed solutions implying that the β -sheets got reorganized into more robust non-native β aggregates [37,95,96].

Deuterium oxide has been used to quantify tertiary structure unfolding by monitoring the H/D exchange [45,97,98]. When a folded protein with a well-defined 3 dimensional structure is exposed to D₂O environment, the hydrophobic polypeptide chains buried in the interior of the protein remain essentially unchanged and the outer hydrophilic chains get preferentially deuterated, which is reflected in the Amide II' peak. When the 3-D tertiary structure starts to unfold, the inner hydrophobic chains get exposed to the solvent causing more H/D exchange to occur. The increased extent of deuteration is manifested as an increase in peak intensity (and area) of the Amide II' at the expense of the Amide II. Comparing integrated peak area of the Amide II' and Amide II bands, it was shown that tertiary unfolding was a precursor to secondary structure unfolding in BSA. This was in agreement with the mechanism and pathways of unfolding of membrane proteins, and RNA reported previously [98–100].

Formation of aggregates is often a consequence of protein association due to irreversible denaturation. Turbidity analysis conducted after 30 minutes (ensuring dissolution of excipient crystals) of thawing did not reveal presence of any insoluble aggregates of BSA. This is not unlikely since BSA is known to mostly form water soluble aggregates, which cannot be detected via turbidity studies [101]. A significant decrease in the monomer content was obtained in thawed solutions, especially the ones with high BSA to trehalose mass ratio (5:1) and those with high initial Tween 20 concentrations (2% w/w). These observations concurred with the post thaw CD analysis. However, no large aggregates could be detected in spite of a decrease in the monomer content. Furthermore, SEC analysis demonstrated that higher molecular weight BSA oligomers did not form upon freezing and annealing (no higher molecular species peak or significant void peak formation). Thus, the unfolded protein must have interacted with the column and retained in it on account of enhanced hydrophobicity.

5. Conclusions

Addition of surfactant (at low concentrations), protein and D₂O delayed crystallization of mannitol and inhibited crystallization of trehalose in a concentration dependent manner. On the other hand, adding high concentrations of surfactant increased the extent of crystallization of both sugars. It was established that unfolding of BSA occurred when trehalose crystallized. When solutions with high protein to trehalose mass ratio (> 1) were frozen, BSA retained its native structure due to self-stabilization. But during thawing, the self-stabilization effect of BSA diminished and BSA unfolded in the thawed solutions. In the presence of D₂O and low concentrations of Tween 20, BSA did not undergo structural changes either in frozen state or in thawed solutions. When Tween 20 concentration was increased to 1% w/w, denaturation of BSA was worsened due to micelle formation.

Acknowledgements and Disclosures

This research was funded by an NSF grant (CBET-1335936) to A.A. Parts of this work were carried out in the Characterization Facility, University of Minnesota, which receives partial support from NSF through the MRSEC program.

6. Additional Data

To gain more insight into possible stress mechanisms that lead to unfolding of BSA, formulations of mannitol with either trehalose or sucrose were stressed by freezing and thawing or by lyophilization. These data were generated post publication.

Additional Material and Methods

Lyophilization

1.2 mL of each formulation was freeze-dried in 2 R vials (Fiolax®, Schott AG, Mainz, Germany), semi-stoppered with lyophilization stoppers (B2-TR coating, West Pharmaceutical Services Deutschland GmbH & Co. KG, Eschweiler, Germany). A FTS Lyostar 3 (SP Scientific, Stone Ridge, USA) was used. Samples were first annealed at -20 °C shelf temperature set point for 20 hours (cooling rate 1 °C/min) to expose the samples to the same procedure as in the freeze-thaw study. Freezing was performed at -50 °C for 1 hour and a cooling rate of 1 °C/min. Duration of primary drying (-30 °C, 0.5 °C/min) was controlled by comparative pressure measurement between Pirani and MKS sensor (difference <5 mTorr). Secondary drying was conducted at +20 °C for 8 hours (heating rate 0.2 °C/min). Drying was performed at 60 mTorr.

Freeze-Thawing

2.0 mL of each formulation were frozen and annealed for 20 hours at -20 °C in a lab scale freeze-dryer (FTS Lyostar 3, SP Scientific, Stone Ridge, USA) in 2 R vials (Fiolax®, Schott AG, Mainz, Germany), closed with lyophilization stoppers (B2-TR coating, West Pharmaceutical Services Deutschland GmbH & Co. KG, Eschweiler, Germany). Heating and cooling rate was 1 °C/min. One or five freeze-thaw cycles were conducted.

Results and Discussion

The macroscopic appearance of the freeze-dried Man/Tre/BSA samples (compositions as shown in Figure 4-10) was homogenous within the different formulations and no cake defects could be detected. The liquid formulations before freeze-drying and reconstitution of the lyophilizates were clear, did not show formation of visible particles, sub-visible particles or increase in turbidity as did freeze-thawing (see 3.5). Freeze-drying did not lead to a decrease in monomer content in low trehalose or high Tween 20 samples (10%BSA+2%T, 10%BSA+2%T+10%M and 4%BSA+8%T+10%M+2%Tween 20 as freeze-thawing. CD

analysis also revealed that BSA suffered less structural changes by freeze-drying than by freezing, annealing and thawing.

In contrast to trehalose formulations, unfolding of BSA was not found in formulations that contained sucrose and were annealed at -20 °C and thawed except of the formulation that included 2% Tween 20. This high surfactant formulation resulted in decreased α -helix content after one annealing cycle. Macroscopic appearance, turbidity, sub-visible particle numbers and soluble aggregate content was unchanged, also after five freeze-thaw cycles.

20 hours of annealing at -20 °C followed by thawing to ambient temperature was compared to the same process but followed by drying and rehydration instead of thawing. Differences were detected in HP-SEC and CD analysis only for the freeze-thawed low trehalose or high Tween 20 samples and not in freeze-dried samples. Thus, BSA degradation cannot only be attributed to the annealing step above T_g' and the crystallization of mannitol and trehalose, but thawing induced stress played a major role. Not only ice formation and its corresponding interfaces led to unfolding as described in literature [27,80,102] but also the composition of the freeze-concentrate. Crystallization of the usually amorphous stabilizer trehalose affected the stability of BSA during the thawing process. The dilution of the freeze-concentrated solution upon thawing led to slow dissolution of the ice-freeze-concentrate interface including the trehalose and mannitol crystals. The stabilization by sucrose could be attributed to its less pronounced crystallization tendency [12,16].

References

- [1] K. Chatterjee, E. Shalaev, R. Suryanarayanan, Partially Crystalline Systems in Lyophilization: II. Withstanding Collapse at High Primary Drying Temperatures and Impact on Protein Activity Recovery, *J. Pharm. Sci.* 94 (2005) 809–820.
- [2] K. Chatterjee, E. Shalaev, R. Suryanarayanan, Partially crystalline systems in lyophilization: I. Use of ternary state diagrams to determine extent of crystallization of bulking agent, *J. Pharm. Sci.* 94 (2005) 798–808.
- [3] K. Izutsu, S. Yoshioka, T. Terao, Decreased Protein-Stabilizing Effects of Cryoprotectants Due to Crystallization, *Pharm. Res. An. Off. J. Am. Assoc. Pharm. Sci.* 10 (1993) 1232–1237.
- [4] K. Izutsu, Y. Sumie, T. Yasushi, The effects of additives on the stability of freeze-dried β -galactosidase stored at elevated temperature, *Int. J. Pharm.* 71 (1991) 137–146.
- [5] R. Johnson, C. Kirchhoff, H. Gaud, Mannitol-sucrose mixtures--versatile formulations for protein lyophilization., *J. Pharm. Sci.* 91 (2002) 914–922.
- [6] D. Wang, J. Hey, S. L. Nail, Effect of Collapse on the Stability of Freeze-Dried Recombinant Factor VIII and alpha-Amylase, *J. Pharm. Sci.* 93 (2004) 1253–1263.
- [7] J. Crowe, J. F. Carpenter, L. Crowe, The role of vitrification in anhydrobiosis, *Annu. Rev. Physiol.* 60 (1998) 73–103.
- [8] J. Crowe, L. Crowe, A. Oliver, N. Tsvetkova, W. Wolkers, F. Tablin, The Trehalose Myth Revisited: Introduction to a Symposium on Stabilization of Cells in the Dry State, *Cryobiology.* 43 (2001) 89–105.
- [9] M. Mensink, J. Šibík, H. Frijlink, K. van der Voort Maarschalk, W. Hinrichs, J. Zeitler, Thermal Gradient Mid and Far Infrared Spectroscopy As Tools for Characterization of Protein Sugar Lyophilizates, *Mol. Pharm.* 14 (2017) 3550–3557.
- [10] R. Surana, A. Pyne, R. Suryanarayanan, Effect of preparation method on physical properties of amorphous trehalose, *Pharm. Res.* 21 (2004) 1167–1176.
- [11] P. Sundaramurthi, T. Patapoff, R. Suryanarayanan, Crystallization of Trehalose in Frozen Solutions and its Phase Behavior during Drying, *Pharm. Res.* 27 (2010) 2374–2383.
- [12] P. Sundaramurthi, R. Suryanarayanan, Trehalose Crystallization During Freeze-Drying: Implications On Lyoprotection, *J. Phys. Chem. Lett.* 1 (2010) 510–514.

- [13] P. Sundaramurthi, R. Suryanarayanan, Influence of crystallizing and non-crystallizing cosolutes on trehalose crystallization during freeze-drying, *Pharm. Res.* 27 (2010) 2384–2393.
- [14] J. F. Carpenter, M. J. Pikal, B. Chang, T. W. Randolph, Rational design of stable lyophilized protein formulations: Some practical advice, *Pharm. Res.* 14 (1997) 969-975.
- [15] T. W. Randolph, Phase Separation of Excipients during Lyophilization: Effects on Protein Stability, *J. Pharm. Sci.* 86 (1997) 1198–1203.
- [16] B. Connolly, L. Le, T. Patapoff, M. Cromwell, J. Moore, P. Lam, Protein Aggregation in Frozen Trehalose Formulations: Effects of Composition, Cooling Rate, and Storage Temperature, *J. Pharm. Sci.* 104 (2015) 4170–4184.
- [17] G. Gómez, M. J. Pikal, N. Rodríguez-Hornedo, Effect of initial buffer composition on pH changes during far-from-equilibrium freezing of sodium phosphate buffer solutions, *Pharm. Res.* 18 (2001) 90–97.
- [18] S. Jena, R. Suryanarayanan, A. Aksan, Mutual Influence of Mannitol and Trehalose on Crystallization Behavior in Frozen Solutions., *Pharm. Res.* 33 (2016) 1413–1425.
- [19] A. Hawe, W. Friess, Physicochemical Characterization of the Freezing Behavior of Mannitol – Human Serum Albumin Formulations, *AAPS PharmSciTech.* 7 (2006) 1–9.
- [20] A. Kim, M. Akers, S. L. Nail, The physical state of mannitol after freeze-drying: Effects of mannitol concentration, freezing rate, and a noncrystallizing cosolute, *J. Pharm. Sci.* 87 (1998) 931–935.
- [21] X. Liao, R. Krishnamurthy, R. Suryanarayanan, Influence of the active pharmaceutical ingredient concentration on the physical state of mannitol-implications in freeze-drying, *Pharm. Res.* 22 (2005) 1978–1985.
- [22] X. Liao, R. Krishnamurthy, R. Suryanarayanan, Influence of Processing Conditions on the Physical State of Mannitol—Implications in Freeze-Drying, *Pharm. Res.* 24 (2007) 370–376.
- [23] C. Telang, L. Yu, R. Suryanarayanan, Effective inhibition of mannitol crystallization in frozen solutions by sodium chloride, *Pharm. Res.* 20 (2003) 660–667.
- [24] K. Collins, Ions from the Hofmeister series and osmolytes: effects on proteins in solution and in the crystallization process, *Methods.* 34 (2004) 300–311.

- [25] N. Rodríguez-Hornedo, D. Murphy, Surfactant-Facilitated Crystallization of Dihydrate Carbamazepine during Dissolution of Anhydrous Polymorph, *J. Pharm. Sci.* 93 (2004) 449–460.
- [26] T. Helgason, T. Awad, K. Kristbergsson, D. McClements, J. Weiss, Effect of surfactant surface coverage on formation of solid lipid nanoparticles (SLN), *J. Colloid Interface Sci.* 334 (2009) 75–81.
- [27] B. Chang, B. Kendrick, J. F. Carpenter, Surface-induced denaturation of proteins during freezing and its inhibition by surfactants, *J. Pharm. Sci.* 85 (1996) 1325–1330.
- [28] L. Kreilgaard, S. Frokjaer, J. Flink, T. W. Randolph, J. F. Carpenter, Effects of additives on the stability of Humicola lanuginosa lipase during freeze-drying and storage in the dried solid, *J. Pharm. Sci.* 88 (1999) 281–290.
- [29] X. Liu, Y. Sano, Effect of Na⁺ and K⁺ ions on the initial crystallization process of lysozyme in the presence of D₂O and H₂O, *J. Protein Chem.* 17 (1998) 479–484.
- [30] B. Liu, J. Garnett, W. Lee, J. Lin, P. Salgado, J. Taylor, Y. Xu, S. Lambert, E. Cota, S. Matthews, Promoting crystallisation of the Salmonella enteritidis fimbriae 14 pilin SefD using deuterium oxide, *Biochem. Biophys. Res. Commun.* 421 (2012) 208–213.
- [31] Y. Komatsu, K. Obuchi, H. Iwahashi, S. Kaul, M. Ishimura, G. Fahy, W. Rall, Deuterium oxide, dimethylsulfoxide and heat shock confer protection against hydrostatic pressure damage in yeast, *Biochem. Biophys. Res. Commun.* 174 (1991) 1141–1147.
- [32] B. Edington, S. Whelan, L. Hightower, Inhibition of heat shock (stress) protein induction by deuterium oxide and glycerol: additional support for the abnormal protein hypothesis of induction, *J. Cell. Physiol.* 139 (1989) 219–228.
- [33] H. Nicolajsen, A. Hvidt, Phase behavior of the system trehalose-NaCl-water, *Cryobiology.* 31 (1994) 199–205.
- [34] J. Green, C. Angell, Phase Relations and Vitrification in Saccharide-Water Solutions and the Trehalose Anomaly, *J. Physical Chem.* 93 (1989) 2880–2882.
- [35] D. Miller, J. De Pablo, H. Corti, Thermophysical Properties of Trehalose and Its Concentrated Aqueous Solutions, *Pharm. Res.* 14 (1997) 578–590.
- [36] L. Her, S. L. Nail, Measurement of Glass Transition Temperatures of Freeze-Concentrated Solutes by Differential Scanning Calorimetry, *Pharm. Res.* 11 (1994) 54–59.

- [37] N. Sreerama, S.Y.U. Venyaminov, R. Woody, Estimation of the number of α -helical and β -strand segments in proteins using circular dichroism spectroscopy, *Protein Sci.* 8 (1999) 370–380.
- [38] P. Toffel-Nadolny, Infrared spectroscopic determinations of mannitol, *Arch. Kriminol.* 168 (1980) 133–138.
- [39] J. F. Carpenter, J. Crowe, An infrared spectroscopic study of the interactions of carbohydrates with dried proteins., *Biochemistry.* 28 (1989) 3916–3922.
- [40] P. Belton, A. Gil, IR and Raman spectroscopic studies of the interaction of trehalose with hen egg white lysozyme, *Biopolymers.* 34 (1994) 957–961.
- [41] A. Burger, J. Henck, S. Hetz, J. Rollinger, A. Weissnicht, Energy / Temperature Diagram and Compression Behavior of the Polymorphs of D -Mannitol, *J. Pharm. Sci.* 89 (2000) 457–468.
- [42] S. Lin, J. Chien, In vitro simulation of solid-solid dehydration, rehydration, and solidification of trehalose dihydrate using thermal and vibrational spectroscopic techniques, *Pharm. Res.* 20 (2003) 1926–1931.
- [43] A. Pevsner, M. Diem, Infrared spectroscopic studies of major cellular components. Part I: the effect of hydration on the spectra of proteins, *Appl. Spectrosc.* 55 (2001) 788–793.
- [44] N. Wellner, P. Belton, A. Tatham, Fourier transform IR spectroscopic study of hydration-induced structure changes in the solid state of w-gliadins, *Biochem J.* 319 (1996) 741–747.
- [45] W. Gallagher, FTIR Analysis of Protein Structure, *Biochemistry.* 455 (1997) 662–666.
- [46] J. Arrondo, F. Goñi, Structure and dynamics of membrane proteins as studied by infrared spectroscopy, *Prog. Biophys. Mol. Biol.* 72 (1999) 367–405.
- [47] A. Jabs, Determination of secondary structure in proteins by fourier transform infrared spectroscopy (FTIR), *Imb Jena Image Libr. Biol. Macromol.* (2000).
- [48] H. Fabian, W. Mäntele, Infrared Spectroscopy of Proteins - Handbook of Vibrational Spectroscopy, *Handb. Vib. Spectrosc.* 1767 (2002) 1–27.
- [49] H. Vogel, Calcium-binding protein protocols, Springer Science & Business Media, (2004).

- [50] V. Uversky, S. Longhi, Instrumental analysis of intrinsically disordered proteins: assessing structure and conformation, John Wiley & Sons, (2010).
- [51] Powder Diffraction File. Hexagonal ice, card # 00-042-1142; D-trehalose dihydrate, card # 00-029-1955; trehalose anhydrate, card # 00-003-0312; β -D-mannitol, card #00-022-1797; δ -D-mannitol, card #00-022-1794, Powder Diffr. File. PA (2004).
- [52] H. C. Mahler, W. Friess, U. Grauschopf, S. Kiese, Protein Aggregation: Pathways, Induction Factors and Analysis, *J. Pharm. Sci.* 98 (2009) 2909–2934.
- [53] L. Narhi, J. Schmit, K. Bechtold-Peters, D. Sharma, Classification of Protein Aggregates, *J. Pharm. Sci.* 101 (2012) 493–498.
- [54] P. Deluca, L. Lachman, Lyophilization of pharmaceuticals I. Effect of certain physical-chemical properties, *J. Pharm. Sci.* 54 (1965) 617–624.
- [55] N. Williams, T. Dean, Vial breakage by frozen mannitol solutions: correlation with thermal characteristics and effect of stereoisomerism, additives, and vial configuration, *J. Parenter. Sci. Technol.* 45 (1991) 94–100.
- [56] Y. Maa, H. Costantino, P. Nguyen, C. Hsu, The effect of operating and formulation variables on the morphology of spray-dried protein particles, *Pharm. Dev. Technol.* 2 (1997) 213–223.
- [57] H. Costantino, J. Andya, P. Nguyen, N. Dasovich, T. Sweeney, S. Shire, C. Hsu, Y. Maa, Effect of Mannitol Crystallization on the Stability and Aerosol Performance of a Spray-Dried Pharmaceutical Protein, Recombinant Humanized Anti-IgE Monoclonal Antibody, *J Pharm Sci.* 87 (1998) 1406–1411.
- [58] A. Twomey, R. Less, K. Kurata, H. Takamatsu, A. Aksan, In Situ Spectroscopic Quantification of Protein–Ice Interactions, *J. Phys. Chem. B.* 117 (2013) 7889–7897.
- [59] T. Miyazaki, S. Yoshioka, Y. Aso, S. Kojima, Ability of polyvinylpyrrolidone and polyacrylic acid to inhibit the crystallization of amorphous acetaminophen, *J. Pharm. Sci.* 93 (2004) 2710–2717.
- [60] G. Johari, Intrinsic mobility of molecular glasses, *J. Chem. Phys.* 58 (1973) 1766.
- [61] G. Roudaut, D. Simatos, D. Champion, E. Contreras-Lopez, M. Le Meste, Molecular mobility around the glass transition temperature: a mini review, *Innov. Food Sci. Emerg. Technol.* 5 (2004) 127–134.

- [62] J. Dugua, B. Simon, Crystallization of sodium perborate from aqueous solutions. I. Nucleation rates in pure solution and in presence of a surfactant, *J. Cryst. Growth*. 44 (1978) 265–279.
- [63] N. Garti, H. Zour, The effect of surfactants on the crystallization and polymorphic transformation of glutamic acid, *J. Cryst. Growth*. 172 (1997) 486–498.
- [64] H. Ffiredi-Milhoferl'zr, L. Tuniki, N. Filipovic-VincekovicZ, D. Skrticz, V. Babic-Ivancic, N. Ganil, Induction of crystallization of calcium oxalate dihydrate in micellar solutions of anionic surfactants, *Scanning Microsc.* 9 (1995) 1061–1070.
- [65] A. Patist, S. Bhagwat, K. Penfield, P. Aikens, D. Shah, On the measurement of critical micelle concentrations of pure and technical-grade nonionic surfactants, *J. Surfactants Deterg.* 3 (2000) 53–58.
- [66] E. Mohajeri, G. Noudeh, Effect of temperature on the critical micelle concentration and micellization thermodynamic of nonionic surfactants: Polyoxyethylene sorbitan fatty acid esters, *E-Journal Chem.* 9 (2012) 2268–2274.
- [67] N. Rodríguez-Hornedo, D. Murphy, Significance of controlling crystallization mechanisms and kinetics in pharmaceutical systems, *J. Pharm. Sci.* 88 (1999) 651-660.
- [68] K. Reddy, L. Salvati, P. Dutta, P. Abel, K. Suh, R. Ansari, Reverse micelle based growth of zincophosphate sodalite: Examination of crystal growth, *J. Phys. Chem.* 100 (1996) 9870–9880.
- [69] S. Luhtala, Effect of sodium lauryl sulphate and polysorbate 80 on crystal growth and aqueous solubility of carbamazepine, *Acta Pharm. Nord.* 4 (1992) 85–90.
- [70] I. Weissbuch, L. Addadi, L. Leiserowitz, M. Lahav, Total asymmetric transformations at interfaces with centrosymmetric crystals: role of hydrophobic and kinetic effects in the crystallization of the system glycine/. alpha.-amino acids, *J. Am. Chem. Soc.* 110 (1988) 561–567.
- [71] M. Bujan, M. Sikiric, N. Filipovic-Vincekovic, N. Vdovic, N. Garti, H. Füredi-Milhofer, Effect of anionic surfactants on crystal growth of calcium hydrogen phosphate dihydrate, *Langmuir.* 17 (2001) 6461–6470.
- [72] V. Andronis, M. Yoshioka, G. Zografi, Effects of sorbed water on the crystallization of indomethacin from the amorphous state, *J. Pharm. Sci.* 86 (1997) 346–357.

- [73] R. Zhou, R. Schlam, S. Yin, R. Gandhi, M. Adams, Scale considerations for selection of saccharide excipients for liquid formulations, *J. Pharm. Sci.* 100 (2011) 1605–1606.
- [74] G. Zipp, N. Rodríguez-Hornedo, Growth mechanism and morphology of phenytoin and their relationship with crystallographic structure, *J. Phys. D Appl. Phys.* 26 (1993) B48–B55.
- [75] P. Taylor, K. Lazar, T. Patapoff, V. Sharma, K. Lazar, T. Patapoff, V. Sharma, Cold denaturation of monoclonal antibodies Cold denaturation of monoclonal antibodies, in: *MABs*, Taylor & Francis, (2010) 42–52.
- [76] W. Wolkers, S. Balasubramanian, E. Ongstad, H. Zec, J.C. Bischof, Effects of freezing on membranes and proteins in LNCaP prostate tumor cells, *Biochim. Biophys. Acta (BBA)-Biomembranes.* 1768 (2007) 728–736.
- [77] T. Koseki, N. Kitabatake, E. Doi, Freezing denaturation of ovalbumin at acid pH, *J. Biochem.* 107 (1990) 389–94.
- [78] L. Chang, M. J. Pikal, Mechanisms of protein stabilization in the solid state, *J. Pharm. Sci.* 98 (2009) 2886–2908.
- [79] L. Chang, D. Shepherd, J. Sun, D. Ouellette, K. Grant, X. Tang, M. J. Pikal, Mechanism of protein stabilization by sugars during freeze-drying and storage: native structure preservation, specific interaction, and/or immobilization in a glassy matrix?, *J. Pharm. Sci.* 94 (2005) 1427–1444.
- [80] B. Bhatnagar, R. Bogner, M. J. Pikal, Protein Stability During Freezing: Separation of Stresses and Mechanisms of Protein Stabilization, *Pharm. Dev. Technol.* 12 (2007) 505–523.
- [81] J. Dong, A. Hubel, J. Bischof, A. Aksan, Freezing-induced phase separation and spatial microheterogeneity in protein solutions, *J. Phys. Chem. B.* 113 (2009) 10081-10087.
- [82] I. Marini, R. Moschini, A. Del Corso, U. Mura, Chaperone-like features of bovine serum albumin: A comparison with alpha-crystallin, *Cell. Mol. Life Sci.* 62 (2005) 3092–3099.
- [83] J. Ellis, Proteins as molecular chaperones, *Nature.* 328 (1987) 378-379.
- [84] T. Arakawa, S. Prestrelski, W. Kenney, J. F. Carpenter, Factors affecting short-term and long-term stabilities of proteins, *Adv. Drug Deliv. Rev.* 46 (2001) 307–326.

- [85] E. Cao, Y. Chen, Z. Cui, P. Foster, Effect of freezing and thawing rates on denaturation of proteins in aqueous solutions, *Biotechnol. Bioeng.* 82 (2003) 684–690.
- [86] K. Pikal-Cleland, N. Rodríguez-Hornedo, G. Amidon, J. F. Carpenter, Protein denaturation during freezing and thawing in phosphate buffer systems: monomeric and tetrameric beta-galactosidase., *Arch. Biochem. Biophys.* 384 (2000) 398–406.
- [87] B. Zakharov, A. Fisyuk, A. Fitch, Y. Watier, A. Kostyuchenko, D. Varshney, M. Sztucki, E. Boldyreva, E. Shalaev, Ice Recrystallization in a Solution of a Cryoprotector and Its Inhibition by a Protein: Synchrotron X-Ray Diffraction Study, *J. Pharm. Sci.* 105 (2016) 2129–2138.
- [88] J. Cleland, X. Lam, B. Kendrick, J. Yang, T. Yang, D. Overcashier, D. Brooks, C. Hsu, J. F. Carpenter, A specific molar ratio of stabilizer to protein is required for storage stability of a lyophilized monoclonal antibody, *J. Pharm. Sci.* 90 (2001) 310-321.
- [89] J. Andya, Y. Maa, H. Costantino, P. Nguyen, N. Dasovich, T. Sweeney, C. Hsu, S. Shire, The effect of formulation excipients on protein stability and aerosol performance of spray-dried powders of a recombinant humanized anti- IgE monoclonal antibody., *Pharm Res.* 16 (1999) 350–358.
- [90] Y. Jia, J. Narayanan, X. Liu, Y. Liu, Investigation on the Mechanism of Crystallization of Soluble Protein in the Presence of Nonionic Surfactant, *Biophys. J.* 89 (2005) 4245-4251.
- [91] O. Velev, Y. Pan, E. Kaler, A. Lenhoff, Molecular effects of anionic surfactants on lysozyme precipitation and crystallization, *Cryst. Growth Des.* 5 (2005) 351–359.
- [92] B. Berger, C. Gendron, A. Lenhoff, E. Kaler, Effects of additives on surfactant phase behavior relevant to bacteriorhodopsin crystallization., *Protein Sci.* 15 (2006) 2682-2696.
- [93] K. Matsuo, Y. Sakurada, R. Yonehara, M. Kataoka, K. Gekko, Secondary-Structure Analysis of Denatured Proteins by Vacuum-Ultraviolet Circular Dichroism Spectroscopy, *Biophys. J.* 92 (2007) 4088–4096.
- [94] M. C. Manning, M. Illangasekare, R. Woody, Circular dichroism studies of distorted α -helices, twisted β -sheets, and β -turns, *Biophys. Chem.* 31 (1988) 77–86.
- [95] S. Kelly, N. Price, The use of circular dichroism in the investigation of protein structure and function, *Curr. Protein Pept. Sci.* 1 (2000) 349–384.

- [96] N. Greenfield, Using circular dichroism spectra to estimate protein secondary structure, *Nat Protoc.* 1 (2006) 2876–2890.
- [97] J. Kong, S. Yu, Fourier transform infrared spectroscopic analysis of protein secondary structures, *Acta Biochim. Biophys. Sin. (Shanghai)*. 39 (2007) 549–559.
- [98] C. Vigano, L. Manciu, F. Buyse, E. Goormaghtigh, J. Ruyschaert, Attenuated total reflection IR spectroscopy as a tool to investigate the structure, orientation and tertiary structure changes in peptides and membrane proteins, *Pept. Sci.* 55 (2000) 373–380.
- [99] E. Maglott, J. Goodwin, G. Glick, Probing the structure of an RNA tertiary unfolding transition state, *J. Am. Chem. Soc.* 121 (1999) 7461–7462.
- [100] J. Galka, S. Baturin, D. Manley, A. Kehler, J. O'Neil, Stability of the Glycerol Facilitator in Detergent Solutions†, *Biochemistry.* 47 (2008) 3513–3524.
- [101] G. Jordan, S. Yoshioka, T. Terao, The aggregation of bovine serum albumin in solution and in the solid state, *J. Pharm. Pharmacol.* 46 (1994) 182–185.
- [102] A. Hillgren, J. Lindgren, M. Aldén, Protection mechanism of Tween 80 during freeze – thawing of a model protein , LDH, *Int. J. Pharm.* 237 (2002) 57–69.

Chapter 5

Impact of Fast and Conservative Freeze-Drying on Product Quality of Protein-Mannitol-Sucrose-Glycerol Lyophilizates

The following chapter has been published as research article in the special issue “ISLFD - 2017” of the European Journal of Pharmaceutics and Biopharmaceutics journal and appears in this thesis with the journal’s permission:

Jacqueline Horn, Julia Schanda and Wolfgang Friess

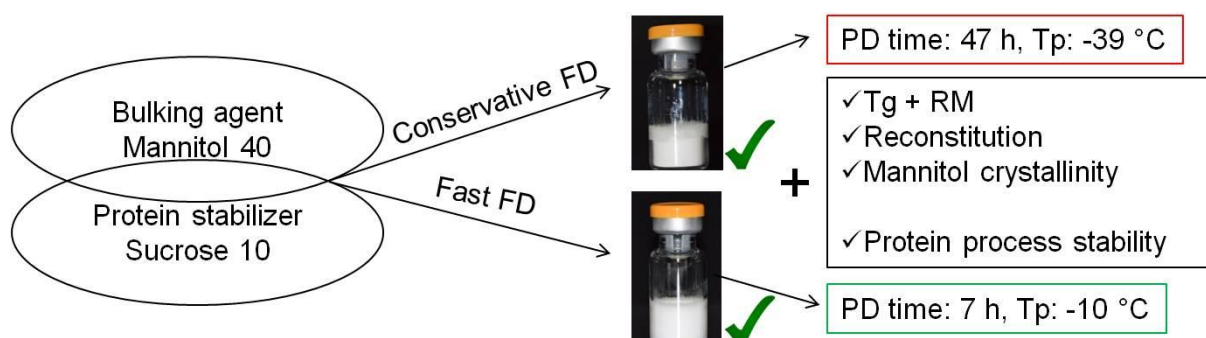
Impact of Fast and Conservative Freeze-Drying on Product Quality of Protein-Mannitol-Sucrose-Glycerol Lyophilizates

European Journal of Pharmaceutics and Biopharmaceutics 127 (2018), 342-354.

doi:10.1016/j.ejpb.2018.03.003.

The supplementary data is attached to the appendix (Chapter 8).

Graphical Abstract



Abstract

Mannitol/sucrose formulations are employed to generate lyophilizates for biopharmaceuticals with an elegant cake appearance. The aim of this study was to dry protein/mannitol/sucrose formulations as fast as possible without loss of cake appearance and protein stability. Glycerol was included as potential additional protein stabilizer. Three proteins (lysozyme and two monoclonal antibodies) at low and high concentration were analyzed comparing fast with conservative freeze-drying. Freeze-drying cycle development was carried out with mannitol/sucrose formulations. A product temperature (T_p) close to the T_e of mannitol and clearly above the T_g' of sucrose was targeted. Protein formulations were exposed to the final fast lyophilisation process and to a conservative freeze-drying cycle. Lyophilizates were characterized by differential scanning calorimetry, Karl-Fischer titration and X-ray diffractometry. Additionally, macroscopic cake appearance and reconstitution times were evaluated. Protein stability was characterized by UV/Vis spectroscopy, light obscuration and size exclusion chromatography. The fast freeze-drying cycle resulted in a primary drying time of 7 hours (T_p : $-10\text{ }^\circ\text{C}$) and a secondary drying time of 2 hours in contrast to 47 hours (T_p : $-39\text{ }^\circ\text{C}$) and 12 hours for the conservative cycle. Lyophilizates showed T_g values above $60\text{ }^\circ\text{C}$, a residual moisture level of 1%, reconstitution times of less than 35 seconds, δ -mannitol and elegant cake appearance. Mannitol/sucrose ratios below 4/1 did not lead to complete mannitol crystallization and were therefore not suitable for the selected process conditions. Characterisation of protein stability rendered low aggregation and particle levels for both, fast and conservative freeze-drying conditions. It was shown that fast freeze-drying of mannitol/sucrose formulations above T_g' at a T_p of $-10\text{ }^\circ\text{C}$ resulted in good protein process stability and appropriate cake characteristics at maximum time reduction.

Keywords

Freeze-drying, cycle development, bulking agent, mannitol, sucrose, glycerol, protein stability, glass transition, collapse, crystallization

Abbreviations

A	Annealing step
aFD	After freeze-drying
API	Active pharmaceutical ingredient
AUC	Area under the curve
bFD	Before freeze-drying
CN	Controlled nucleation
F	Freezing step
FD	Freeze-drying
Gly	Glycerol
hh	hemihydrate
HP-SEC	High performance size exclusion chromatography
HPW	Highly purified water
LO	Light obscuration
Lyso	Lysozyme
mAb	Monoclonal antibody
Man	Mannitol
mDSC	Modulated differential scanning calorimetry
PD	Primary drying step
RM	Residual moisture
SD	Standard deviation / secondary drying step
Suc	Sucrose
T _c	Collapse temperature
T _e	Eutectic temperature
T _g	Glass transition temperature of the freeze-dried cake
T _g '	Glass transition temperature of the freeze-concentrated solution
T _p	Product temperature
XRPD	X-Ray powder diffraction

Table of Content

Graphical Abstract	98
Abstract	99
Keywords.....	99
Abbreviations	100
1. Introduction	102
2. Materials and Methods	104
2.1 Materials	104
2.2 Methods	105
2.2.1 Lyophilization	105
2.2.2 Macroscopic Appearance.....	105
2.2.3 Modulated Differential Scanning Calorimetry (mDSC)	105
2.2.4 Karl-Fischer Titration	106
2.2.5 X-Ray Powder Diffraction (XRPD).....	106
2.2.6 Reconstitution Time.....	106
2.2.7 Turbidity	107
2.2.8 Light Obscuration (LO).....	107
2.2.9 High Performance Size Exclusion Chromatography (HP-SEC)	107
3 Results and Discussion	108
3.1 Development of a Fast Freeze-Drying Cycle	108
3.2 Investigation of Different Mannitol/Sucrose Ratios	112
3.3 Comparison Study of Fast and Conservative Freeze-Drying Cycle	116
3.3.1 Physical Characterization of the Lyophilizates.....	116
3.3.2 Protein Process Stability	120
3.4 Impact of Glycerol on Protein/Man/Suc/Glycerol formulations	122
4 Conclusion	122
References	123

1. Introduction

Freeze-drying is frequently used to achieve long-term storage stability of sensitive biopharmaceuticals. More than 40% of the marketed biologicals are currently freeze-dried, a number which is expected to even increase in the future [1,2]. The manufacturing process is time- and cost-intensive with regular process times of several days or even weeks [3]. Especially for drugs in high demand and full capacity utilization, faster drying would enable higher throughput at preferably reduced production costs. Several approaches were already investigated with respect to process optimization at high sublimation rates and product temperatures. Amorphous formulations were dried above the glass transition temperature of the freeze concentrate (T_g') but below the collapse temperature (T_c) [2,4]. Highly concentrated protein formulations benefitted more since T_c was raised more than T_g' with increasing protein concentration. That enabled drying at higher product temperature (T_p) of up to $-10\text{ }^\circ\text{C}$ at 100 mg/mL mAb with a T_c of $-8\text{ }^\circ\text{C}$. A 5 mg/mL protein formulation could only be dried at a T_p below $-30\text{ }^\circ\text{C}$ [2]. Another approach was to combine mannitol (Man) with sucrose (Suc) and dry at high T_p so that the amorphous matrix of Suc and protein collapsed while Man formed a crystalline scaffold without macroscopic visible defects such as e.g. eutectic melting [5]. Man and Suc are regularly combined due to their complementary characteristics. Suc probably the most frequently utilized protein stabilizer replaces water binding sites of proteins and decreases protein mobility in the dried state by vitrification [6–8]. Upon freeze-drying Suc remains amorphous which is a prerequisite for protein stabilization [8]. In contrast, the bulking agent mannitol crystallizes during the process while losing its stabilization properties [9]. The crystalline scaffold leads to an elegant cake without shrinkage or cracks [10] and helps to increase the mass of the cake or to achieve the desired tonicity of the rehydrated formulation [11,12]. Typically, Man and Suc have to be combined at a Man/Suc ratio of at least 4/1 due to inhibition of Man crystallization by Suc at lower Man/Suc ratios [5,13]. Moreover, proteins also suppress bulking agent crystallization [14].

At high ratios of Man to Suc, the crystallization of mannitol minimizes the potential collapse of amorphous sucrose, eliminates the need to conduct primary drying below the T_g' or T_c , and thereby, provides the option to perform drying at higher temperatures and enables shorter processing times. Drying of crystalline excipients to products of appropriate macroscopic appearance is limited by their eutectic temperature (T_e), in case of Man $-1.5\text{ }^\circ\text{C}$ [5]. It has already been demonstrated that collapse of the stabilizers is not necessarily coupled with protein destabilization [15–21]. To which extent macroscopic appearance should be accepted given that the protein stability is not affected is an ongoing discussion but complete collapse is not acceptable if not induced intentionally [22]. Thus, freeze-drying cycle development should aim at adequate cake appearance, unless protein stability is superior in collapsed cake structure.

The small molecular weight plasticizing agents glycerol and sorbitol were found to be beneficial for protein stability in the dried state [23–25]. Their potential lies in the prolongation of β -relaxation times or local motions [23,25–27]. Due to their small size they might be able to reduce free volumes and increase the packing density better than larger stabilizers [26,28]. Because of their low T_g values (glycerol: $-93\text{ }^\circ\text{C}$ and sorbitol: $0\text{ }^\circ\text{C}$ [29,30]) they would lead to macroscopic collapse if used as single component in a formulation. They would also lower T_g' values of Suc formulations to a considerable extent. As a consequence, fast drying at high product temperatures would be difficult in Suc/Glycerol formulations without macroscopic collapse. The appearance of crystalline mannitol reduces the potential for gross collapse, and provides the additional advantage of faster drying. In this study, glycerol was included as an additional stabilizer in a matrix comprising of amorphous sucrose and crystalline mannitol. Glycerol replaced 5% / 10% of the amorphous Suc as these low concentrations showed antiplasticizing effects in previous studies [31].

All process steps were accelerated (that is, faster cooling or heating rates) to minimize the cycle duration. The freezing step plays an important role for the whole process because it determines ice crystal growth, size and distribution, as well as the crystallization behavior of the excipients [13,32,33]. Annealing above T_g' is commonly performed to ensure complete mannitol crystallization or to force the formation of a certain Man polymorph [13,34,35]. Moreover, it can be effectively utilized to minimize the effects of the inter-vial variability in the ice nucleation temperature, which causes differences in the ice structures (size of the crystals) across a batch of vials [33]. Annealing results in a more homogeneous (or uniform) ice structure and reduces the inter-vial heterogeneity. Hence the freezing step already determines characteristics of the dried matrix. Primary drying (PD) is the step with the highest optimization potential due to its long duration [2]. The last step, secondary drying, takes only a few hours [3]. Nevertheless, the final residual moisture (RM) content and the conversion of potentially formed Man hemihydrate into the anhydrous form depends on selection of sufficiently high secondary drying temperature and duration [5]. Thus, the characteristics of freeze-dried products are mainly influenced by the FD cycle conditions and the formulation composition, but are also affected by further parameters such as container, stoppers or filling volume which are not discussed here [36].

This study aimed at a cycle development of a fast freeze-drying cycle with Man/Suc formulations that were indistinguishable from conservative dried formulations regarding their physical characteristics. Protein formulations were investigated to show that a high T_p during PD, likely coupled to higher protein mobility, does not negatively impact protein process stability. For a comprehensive analysis, freeze-dried protein formulations were characterized by DSC, Karl-Fischer titration and XRD, checked for macroscopic appearance and

reconstitution time, and protein stability was tested by LO, turbidity and HP-SEC. After development of the fast cycle with Man/Suc/Glycerol formulations, the results were compared to conservative freeze-drying conditions that provided non-collapsed amorphous matrices. Lysozyme and two monoclonal antibodies in different concentrations enabled a detailed study on impact of formulation and process. Lower Man/Suc ratios were tested with focus on complete Man crystallization and the impact of different freezing protocols.

2. Materials and Methods

2.1. Materials

Stock solutions of mannitol (Man) (VWR International, Ismaning, Germany), sucrose (Suc) (Sigma-Aldrich Chemie GmbH, Steinheim, Germany) and glycerol (AppliChem GmbH, Darmstadt, Germany) were prepared in 10 mM L-histidine (Sigma-Aldrich Chemie GmbH, Steinheim, Germany) pH 7.0 formulation buffer. Different mannitol/sucrose/glycerol (Man/Suc/Gly) weight ratios were investigated: 40/10/0, 40/9.5/0.5, 40/9/1, and 40/0/0 [mg/mL]. Protein formulations contained protein, mannitol, sucrose and glycerol. For the second study, different Man/Suc ratios dissolved in highly purified water (HPW) were examined without protein: 20/30, 25/25, 30/20, 40/10 [mg/mL]. All formulations were filtered with 0.2 μm polyethersulfone (PES) membrane syringe filters (VWR International GmbH, Ismaning, Germany) prior to use.

Hen egg white lysozyme (MW 14.3 kDa, $\epsilon = 38.94 \text{ mL mg}^{-1} \text{ cm}^{-1}$, Dalian Greensnow Egg Products Development Co., Ltd., Dalian, China) and two different monoclonal IgG₁ antibodies (MW ~ 150 kDa, $\epsilon = 1.49 \text{ mL mg}^{-1} \text{ cm}^{-1}$, referred to as mAb1 and mAb2) served as model proteins within the Man/Suc/Glycerol formulations. mAb 1 was used at lower concentration as it results in viscous formulations at high concentration. Lysozyme was dissolved in formulation buffer whereas the stock solutions of the mAbs were prepared by tangential flow filtration in Minimate™ capsules (30 kDa Omega membrane, PALL Life Science, Port Washington, NY, USA) out of lower concentrated bulk solutions. Each protein was formulated at 2 mg/mL and, additionally, lysozyme at 100 mg/mL, mAb1 at 7.5 mg/mL and mAb2 at 80 mg/mL.

2.2. Methods

2.2.1. Lyophilization

Lyophilization stoppers (B2-TR coating, West Pharmaceutical Services Deutschland GmbH & Co. KG, Eschweiler, Germany) and DIN 2R Vials (Fiolax®, Schott AG, Mainz, Germany) were cleaned with highly purified water and dried for 8 hours at 100 °C and 60 °C, respectively. A filling volume of 1.2 mL was dispensed into the vials which were semi-stoppered subsequently. The two outer rows of vials were not used for subsequent analysis. Thermocouples in different vial positions on the shelf recorded temperature values during freeze-drying.

The protein formulations were freeze-dried according to the given freeze-drying protocols (Table 5-1, Process 1 and Process 8). Controlled nucleation (CN) according to Geidobler et al. was conducted [37]. The vials were equilibrated at -5 °C for 1.5 h. At a T_p of -4 °C to -4.5 °C, the chamber pressure was reduced to 4 mbar. CN was induced by ventilation via the condenser chamber. The method was selected to enable potential scale up to larger freeze-dryers avoiding potential adjustments to the individual formulations. The different Man/Suc ratios were investigated with the fast freeze-drying cycle conditions (Process 8) and two variations of the freezing step: (1) equilibration at -5 °C, but without CN or (2) including an annealing step at -20 °C for 2 hours. Process variations performed with Man/Suc/Glycerol formulations are summarized in Table 5-1. A FTS Lyostar 3 (SP Scientific, Stone Ridge, NY, USA) and an Epsilon 2D-6 LSCplus (Martin Christ Gefriertrocknungsanlagen GmbH, Osterode am Harz, Germany) were used. The FTS freeze-dryer was used for chamber pressure values of up to 1.1 mbar while the Christ freeze-dryer was utilized at 1.1 mbar higher chamber pressure or above. The end of primary drying was controlled by comparative pressure measurement between Pirani and MKS sensor (FTS) or set manually (Christ). Vials were stoppered after secondary drying under nitrogen atmosphere at 800 mbar, crimped with flip off seals and stored at 4-8 °C.

2.2.2. Macroscopic Appearance

Images of the lyophilizates were taken with a Nikon D5300 camera (Nikon GmbH, Düsseldorf, Germany) in a black photobox.

2.2.3. Modulated Differential Scanning Calorimetry (mDSC)

The glass transition temperature (T_g) of the lyophilizates and of the freeze-concentrate (T_g') were determined with a Mettler Toledo DSC 821e (Mettler-Toledo GmbH, Giessen,

Germany) using aluminum 40 μL crucibles which were sealed hermetically. For T_g' measurement, 30 μL liquid formulation were cooled down to $-60\text{ }^\circ\text{C}$ and heated to $+20\text{ }^\circ\text{C}$ at $10\text{ }^\circ\text{C}/\text{min}$ without modulation. Regarding T_g determination, samples were prepared under controlled humidity conditions, $< 10\%$ rel. humidity. 5 to 15 mg of crushed cake were weighted into aluminum crucibles and sealed hermetically. The DSC scan was conducted from $25\text{ }^\circ\text{C}$ to $100\text{ }^\circ\text{C}$ or $140\text{ }^\circ\text{C}$ at $2\text{ }^\circ\text{C}/\text{min}$ and modulation with an amplitude of $\pm 1\text{ }^\circ\text{C}$ every 120 s. T_g and T_g' were determined as the midpoint of the transition using the Mettler StarE Software.

2.2.4. Karl-Fischer Titration

Karl Fischer titration was used to determine the residual moisture (RM) of the lyophilizates. It was performed with an Aqua 40.00 titrator (Analytik Jena AG, Halle, Germany) using a headspace oven set at $100\text{ }^\circ\text{C}$. Samples were prepared under controlled humidity conditions, $< 10\%$ rel. humidity. 10 to 20 mg of crushed cake were analyzed in 2 R vials.

2.2.5. X-Ray Powder Diffraction (XRPD)

The phase behavior of freeze-dried cakes was determined using X-ray powder diffractometry (XRPD). An XRD 3000 TT diffractometer (Rich. Seifert & Co. GmbH & Co. KG, Ahrensburg, Germany) was used equipped with a copper anode (40 kV, 30 mA, $\lambda = 0.154178\text{ nm}$) and a scintillation detector at 1000 V. The freeze-dried samples were crushed and smoothed homogeneously on copper sample holders at 0.2 mm height. Samples were analyzed in steps of 0.05° using 2 seconds per step from $5\text{-}45^\circ 2\text{-}\Theta$. The three polymorphic forms of Man (α , β , δ) and Man-hemihydrate were analyzed according to their main reference peaks: α - (9.3° , 13.7° , 17.2° , 18.7°), β - (10.4° , 14.6° , 16.8° , 18.8° , 20.3° , 23.4°), δ -mannitol (9.7° , 20.4° , 22.0° , 24.6° , 25.3°) and mannitol hemihydrate (9.6° , 17.9° , 23.1° , 25.7°) [13,38,39]. Peaks used for identification are underlined.

2.2.6. Reconstitution Time

Reconstitution time was determined by dissolving the lyophilizates with the required volume of HPW. The required reconstitution volume was calculated based on the formulation density and solid content. The time from adding HPW to complete dissolution of the cake was considered as reconstitution time. Complete dissolution was determined visually. During reconstitution, the vials were gently rolled by hand to ensure wetting of the complete lyophilizate.

2.2.7. Turbidity

Turbidity of the samples before freeze-drying and after reconstitution was measured by UV/Vis-spectroscopy at 350 nm. A NanoDrop 2000 spectrophotometer (Thermo Fisher Scientific, Waltham, MA, USA) was used. Each formulation was measured as triplicate with its corresponding formulation without protein as blank solution.

2.2.8. Light Obscuration (LO)

A PAMAS SVSS-35 particle counter with a HCB-LD-25/25 sensor (PAMAS - Partikelmess- und Analysesysteme GmbH, Rutesheim, Germany) was used to determine the number of subvisible particles before freeze-drying and after reconstitution of the lyophilizates. The system was cleaned with HPW between the analyses. The rinse volume was 0.2 ml, followed by four measurements of 0.2 ml according to USP 788 [40]. PAMAS PMA software was used to determine particles $\geq 1 \mu\text{m}$, $\geq 10 \mu\text{m}$ and $\geq 25 \mu\text{m}$.

2.2.9. High Performance Size Exclusion Chromatography (HP-SEC)

Size exclusion chromatography was performed with an Agilent 1100 series HPLC system equipped with an UV/Vis detector for detection at 280 nm (Agilent Technologies, Santa Clara, CA, USA). A TSKgel® G3000 SWXL column (dimension: 300 x 7.8 mm, TOSOH Bioscience GmbH, Stuttgart) and 100 mM sodium phosphate / 100 mM sodium sulfate buffer at pH 6.8 mobile phase with a flow rate of 0.5 mL/min was used. Prior to analysis, samples were diluted to 1 mg/mL (lysozyme) or 2 mg/mL (mAb1 and mAb2) and centrifuged (5 min, 4000 rpm, Sigma 1-15 microfuge, Sigma Laborzentrifugen GmbH, Osterode am Harz, Germany). The integrated peak intensity was determined before and after freeze-drying after blank subtraction using the ChemStation Software (Agilent Technologies, Santa Clara, CA, USA) and relative monomer recovery was determined. Soluble aggregates and fragments were referred to the AUC of monomer before freeze-drying.

3. Results and Discussion

3.1. Development of a Fast Freeze-Drying Cycle

The first aim of this study was to find optimized freeze-drying cycle conditions for a fast freeze-drying cycle that results in lyophilizates with an elegant cake appearance and the desired physico-chemical characteristics, crystallinity of the bulking agent, adequately high T_g approximately 40 °C above intended storage temperature of 2-8 °C and low RM close to 1% [3]. Man as crystalline bulking agent was combined with the amorphous stabilizer Suc at 40/10, as this weight ratio is known to lead to fully crystalline Man after freeze-drying [5,13]. Furthermore, glycerol was included as a secondary stabilizer in addition to Suc (primary stabilizer), at 5% or 10% of the Suc concentration employed in the formulations. [26]. As pure crystalline bulking agent reference, also Man as single component was investigated.

Table 5-1 gives a comprehensive overview of all process variations performed combined with the corresponding results. A target T_p of -10 °C was identified such that the T_p was much higher than the T_g' (or T_c) of Suc (T_g' : -32 °C [41], T_c : -31 °C [42]), but was still below the T_e of Man (-1.5 °C [5]). T_p values during drying are strongly affected by the applied chamber pressure. This was achieved with the chamber pressure increased to 2.2 mbar and the shelf temperature set to +20 °C. Further increase in chamber pressure to 4.3 mbar led to meltback at the bottom of the vials while 10 mbar induced “blow out” of the formulations out of the vial due to exceeding T_e (T_p during PD: 7.3 °C) and thus melting.

As the selected formulations were to be dried at T_p values clearly above the T_g' value of Suc, complete crystallization of the bulking agent was important to generate a scaffold which does not show gross collapse despite the collapse of the amorphous Suc phase. The β -polymorph of Man is considered thermodynamically more stable while α -, δ -, as well as the hemihydrate form are the metastable [43]. The transformation of Man-hemihydrate into anhydrous α , β or δ -Man during storage bears the risk of increased protein instability as more water molecules are available as potential reaction partners and the T_g of the amorphous phase decreases [44].

Impact of Fast and Conservative Freeze-Drying on Product Quality of Protein-Mannitol-Sucrose-Glycerol Lyophilizates

Table 5-1. Process variations and the corresponding results of macroscopic appearance, RM, crystallinity of Man, reconstitution times and Tg. Results are given as mean ± SD for n=3. For n=2, mean values are given. Process changes compared to the previous run are written in bold. V = elegant cake appearance. CN was performed at -4.0 °C.

Run No.	Process Variations	Freeze-drying cycle conditions	Run Time [h]	Tp in PD [°C]	Man/Suc/Gly weight ratio [mg/mL]	Macroscopic appearance	RM [%]	Mannitol polymorphism	Reconstitution time [s]	Tg [°C]
1	Starting point (conservative)	CN, F1 -50 °C, 1 °C/min, 1 h	100	-39	40/10/0	V	0.8 ± 0.1	δ, hemihydrate	19 ± 5	71.3 ± 2.1
		A -20 °C, 1 °C/min, 2 h			40/9.5/0.5		0.9 ± 0.2	δ, hemihydrate	21 ± 4	66.8 ± 4.2
		F2 -50 °C, 1 °C/min, 2 h			40/9/1		0.6 ± 0.2	δ, hemihydrate	25 ± 3	61.9 ± 0.4
		PD -35 °C, 0.5 °C/min, 0.05 mbar, 47 h			40/0/0		0.4 ± 0.1	β	12 ± 1	-
		SD 25 °C, 0.1 °C/min to 5 °C, 0.2 °C/min to 25 °C, 0.05 mbar, 12 h								
2	increased chamber pressure, increased PD shelf temp, reduced drying time	CN, F1 -50 °C, 1 °C/min, 1 h	29	-20	40/10/0	V	1.3 ± 0.1	δ, hemihydrate	68 ± 3	52.6 ± 4.1
		A -20 °C, 1 °C/min, 2 h			40/9.5/0.5		1.2 ± 0.1	δ, hemihydrate	68 ± 6	44.2 ± 1.9
		F2 -50 °C, 1 °C/min, 2 h			40/9/1		1.0 ± 0.1	δ, hemihydrate	79 ± 12	44.5 ± 7.3
		PD 0 °C , 0.5 °C/min, 0.53 mbar, 12.5 h			40/0/0		-	-	-	-
		SD 25 °C, 0.1 °C/min to 5 °C, 0.2 °C/min to 25 °C, 0.53 mbar, 4 h								
3a	increased chamber pressure, increased PD shelf temp, reduced drying time 3 different SD shelf temps (3a-3c)	CN, F1 -50 °C, 1 °C/min, 1 h	29	-15.4	40/10/0	V	1.7	δ, hemihydrate	39 ± 3	50.1 ± 0.4
		A -20 °C, 1 °C/min, 2 h			40/9.5/0.5		1.5	δ, hemihydrate	64 ± 10	45.9 ± 0.4
		F2 -50 °C, 1 °C/min, 2 h			40/9/1		1.5	δ, hemihydrate	38 ± 15	41.5 ± 0.4
		PD 10 °C , 0.5 °C/min, 1.1 mbar, 9.5 h			40/0/0		1.0	β	21 ± 4	-
		SD 25 °C, 0.2 °C/min, 1.1 mbar, 4 h								
3b	as 3a, but prolongation of SD at 40 °C for 4 h		35	-15.4	40/10/0	V	1.1	δ, less hemihydrate	28 ± 13	57.2 ± 1.1
					40/9.5/0.5		0.9	δ, less hemihydrate	47 ± 22	65.9 ± 3.6
					40/9/1		0.5	δ	42 ± 13	62.9 ± 0.7
					40/0/0		0.8	β	28 ± 6	-
3c	as 3b, but prolongation of SD at 60 °C for 4 h		41	-15.4	40/10/0	V	0.2	δ	22 ± 5	66.0 ± 5.4
					40/9.5/0.5		0.4	δ	25 ± 3	58.4 ± 1.2
					40/9/1		0.3	δ	37 ± 25	52.4 ± 2.3

Run No.	Process Variations	Freeze-drying cycle conditions	Run Time [h]	Tp in PD [°C]	Man/Suc/Gly weight ratio [mg/mL]	Macroscopic appearance	RM [%]	Mannitol polymorphism	Reconstitution time [s]	Tg [°C]
3c					40/0/0		0.2	β	18 ± 3	-
4	increased chamber pressure	CN, F1 -50 °C, 1 °C/min, 1 h A -20 °C, 1 °C/min, 2 h F2 -50 °C, 1 °C/min, 2 h PD 10 °C, 0.5 °C/min, 2.2 mbar, 6.3 h SD 57 °C , 0.2 °C/min, 2.2 mbar , 4 h	28	-14	40/10/0 40/9.5/0.5 40/9/1 40/0/0	V	0.3 ± 0.1 0.3 ± 0.1 0.3 ± 0.1 0.3 ± 0.1	δ δ δ β	40 ± 28 34 ± 5 33 ± 14 23 ± 5	64.8 ± 2.1 56.4 ± 2.1 48.9 ± 1.0 -
5	annealing step skipped, accelerated freezing	CN, F1 -50 °C, 1 °C/min, 2 h PD 10 °C, 0.5 °C/min, 2.2 mbar, 6.3 h SD 57 °C, 0.2 °C/min, 2.2 mbar, 4 h	24	-12.5	40/10/0 40/9.5/0.5 40/9/1 40/0/0	V	0.1 ± 0.1 0.1 ± 0.1 0.1 ± 0.1 0.3 ± 0.1	δ δ δ β	36 ± 8 21 ± 6 29 ± 8 17 ± 4	68.7 ± 4.6 52.1 ± 2.1 46.2 -
6	accelerated drying ramps	CN, F1 -50 °C, 1 °C/min, 2 h PD 10 °C, 1 °C/min , 2.2 mbar, 6.3 h SD 57 °C, 0.5 °C/min, 2.2 mbar, 4 h	20	-13	40/10/0 40/9.5/0.5 40/9/1 40/0/0	V	0.1 ± 0.1 0.1 ± 0.1 0.1 ± 0.1 0.2 ± 0.1	δ δ δ β	29 ± 2 26 ± 3 17 ± 3 18 ± 3	62.4 ± 1.4 53.0 42.4 -
7	accelerated drying ramps, increased PD shelf temp, decreased SD shelf temp, prolongation of PD time	CN, F1 -50 °C, 1 °C/min, 2 h PD 20 °C , 1 °C/min, 2.2 mbar, 7 h SD 40 °C , 1 °C/min , 2.2 mbar, 4 h	18	-10	40/10/0 40/9.5/0.5 40/9/1 40/0/0	V	0.9 ± 0.1 0.6 ± 0.1 0.5 ± 0.1 1.0 ± 0.1	δ δ δ β	36 ± 8 21 ± 6 29 ± 8 17 ± 4	66.0 ± 1.4 57.5 57.9 -
8	reduced SD drying time, fast freeze-drying cycle	CN, F1 -50 °C, 1 °C/min, 2 h PD 20 °C, 1 °C/min, 2.2 mbar, 7 h SD 40 °C, 1 °C/min, 2.2 mbar, 2 h	15.7	-10	40/10/0 40/9.5/0.5 40/9/1 40/0/0	V	1.1 ± 0.1 0.9 ± 0.1 0.8 ± 0.1 0.9 ± 0.1	δ δ δ β	17 ± 5 34 ± 4 17 ± 6 17 ± 3	73.8 ± 0.6 66.0 ± 0.1 63.5 ± 2.3 -

CN – controlled nucleation step performed according to Geidobler et al. [37], F – freezing step, A – annealing step, PD – primary drying step, SD – secondary drying step, Tp - product temperature in the steady state of PD.

The addition of amorphous excipients led to modified crystallization behaviour of Man. In all formulations including an amorphous phase, Man crystallized mainly as δ -Man as it was shown by Johnson et al. for the Man/Suc 40/10 ratio [5]. The small amount of glycerol had no measurable effect on Man crystallization. In contrast, pure Man resulted in the β -form with the applied cooling rate of 1 °C/min. Kim et al. reported that slow freezing (0.2 °C/min) of 10% Man led to a mixture of α - and β -Man, fast freezing in liquid nitrogen to mainly δ -Man whereas a 5% solution formed to β -Man confirming our results [45]. Which Man modification forms thus depends on freezing protocol, process conditions, Man concentration and additional excipients [5,13,45,46].

The secondary drying temperature apparently affected the amount of hemihydrate left in the lyophilizate after drying. Secondary drying temperatures above or equal to 40 °C forced most likely the transformation of the hemihydrate into anhydrous Man forms as no hemihydrate could be detected by XRD. High annealing temperatures during freezing were also shown to impact the formation of Man-hemihydrate more than the secondary drying temperature [13]. This emphasizes the complexity of factors that determine the formation of hemihydrate in the final lyophile.

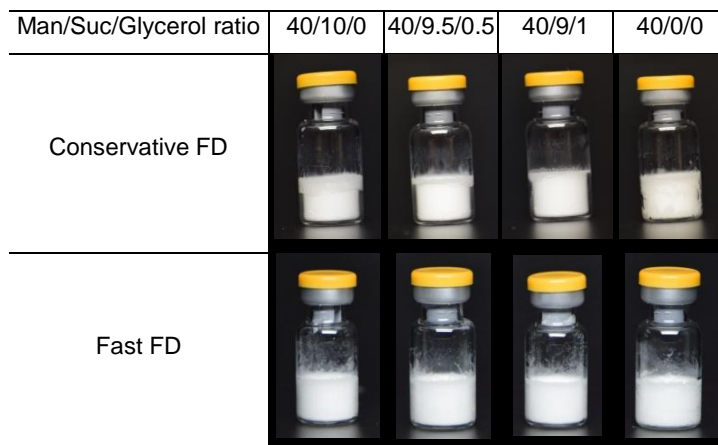


Figure 5-1. Macroscopic appearance of Man/Suc/Glycerol lyophilizates that differ in Man/Suc/Glycerol ratio and freeze-drying cycle (Table 1, Process 1 / Process 8).

All lyophilizates exhibited an elegant macroscopic appearance without defects due to the crystalline Man scaffold. Collapse of the amorphous fraction was not visible (Figure 5-1). RM could be set into the required target value of about 1%. Tg values were in the expected range of Suc above 50 °C with the given RM. As expected Tg decreased with addition of the plasticizing agent glycerol. Reconstitution was fast and did not change throughout the process development. Annealing could be skipped without any change in the product characteristics. As controlled nucleation (CN) was performed, we assume that the

equilibration time in the supercooled state and the ice nucleation itself play a major role in facilitating Man crystallization making the annealing step redundant. Additionally, increased heating or cooling rates of 1 °C/min were not detrimental for product quality. Consequently, this cycle fulfilled all the requirements for a fast cycle without loss in product quality. The total run time in the final fast freeze-drying process was 15.7 hours.

3.2. Investigation of Different Mannitol/Sucrose Ratios

40/10 ratio of mannitol to sucrose was used for cycle development as this is known to be beneficial for complete mannitol crystallization [5,13]. However, a higher percentage of the amorphous stabilizer sucrose would be advantageous in order to achieve a high stabilizer to protein ratio, in particular for high concentrated protein formulations. A molar ratio of protein to sucrose of 3600:1 has been shown to be necessary for lyophilized mAb formulations [47]. In our accelerated cycle conditions the T_p of -10 °C was 25 °C, hence clearly, above the T_g' value of mannitol [10]. Therefore, the crystallization tendency of mannitol might be favored. Previous studies on different Man/Suc ratios were performed at a T_p below the T_g' of mannitol [13,48,49]. Therefore, lower Man/Suc ratios were first tested in the fast freeze-drying cycle regarding their potential for complete mannitol crystallization.

Both the freezing step, in particular the nucleation technique or an annealing step, affect the crystallization of mannitol [33,35,50–53]. Therefore, three different freezing techniques were also tested: (i) isothermal hold at -5°C for 1 h (no CN), (ii) shelf ramp cooling followed by annealing at -20 °C for 2 h, and (iii) isothermal hold at -5 °C for 1 h followed by CN. [37].

Macroscopic Appearance

Figure 5-2 shows representative images of the lyophilized samples obtained from different freezing protocols and different Man/Suc ratios. Samples subjected to CN exhibited better cake appearance, in particular at the low Man/Suc ratios (20/30, 25/25). Once the Man/Suc ratio was sufficiently high an appropriate (30/20) or good (40/10) cake appearance was found. CN samples did not show macroscopic collapse at all Man/Suc ratios although large pores and skin formation pointed at incomplete Man crystallization upon freezing at the low Man/Suc ratios (20/30, 25/25).

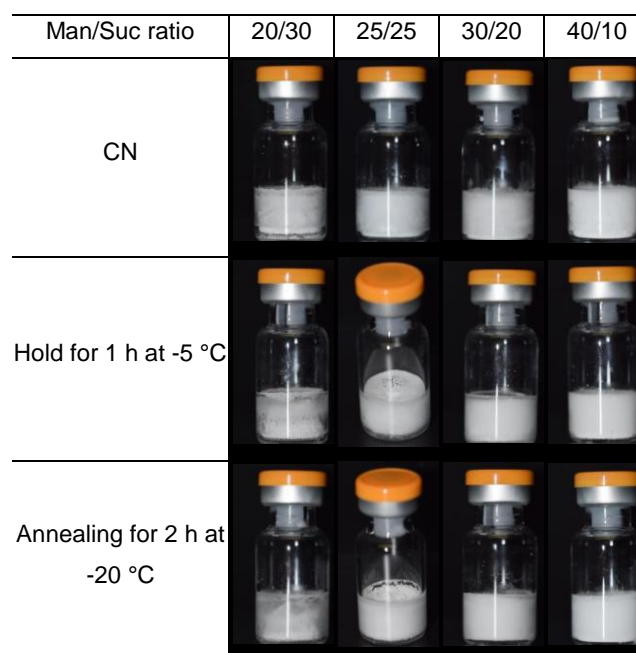


Figure 5-2. Macroscopic appearance of Man/Suc lyophilizates that differ in Man/Suc ratio and freezing protocol. The fast freeze-drying cycle (Table 5-1, Process 8) was performed with adjusted freezing protocols.

Phase behavior of mannitol XRD diffractograms demonstrated that Man crystallization occurred at all Man/Suc ratios with all three freezing protocols (Figure 5-3). Within one freezing procedure, the crystallization behavior of the four different Man/Suc ratios was similar. CN led to a mixture of β -Man, δ -Man and Man-hemihydrate, whereas samples that were held at -5 °C for one hour were dominated by the β -polymorphs and less δ -Man and Man-hemihydrate, with annealing at -20 °C β -Man resulted. Thus, the freezing protocol has a major impact on the product characteristics of the lyophilizate which is in accordance with literature [43] whereas the Man to sucrose ratio had less effect. Crystalline Man was found in all lyophilizates although the macroscopic appearance indicated collapse at all Man/Suc ratios of 25/25 and lower. This indicates delayed Man crystallization in the PD and not during freezing. Incomplete scaffold formation by the crystalline Man would be another explanation.

Differential Scanning Calorimetry

In DSC only Man/Suc 40/10 samples did not show an exotherm during the first heating scan indicating complete mannitol crystallization (Figure 5-3). At lower Man/Suc ratio recrystallization peaks occurred, demonstrating crystallization of amorphous mannitol while they were less pronounced at Man/Suc 30/20 compared to the lower ratios of 25/25 and 20/30. We speculate that small amounts of amorphous ManI remained at the 30/20 Man/Suc ratio. The second DSC scan did not show an exothermic peak in all formulations indicating complete mannitol crystallization after the first heating scan. Correspondingly, with increasing

mannitol content and thus higher mannitol crystallinity, T_g values increased. Samples of the lowest Man/Suc ratio of 20/30 showed a T_g value of 27.9 °C after different freezing protocols whereas at Man/Suc 40/10 ratio and holding for one hour at -5 °C resulted in a T_g of 55.2 °C. A T_g value of 12 °C is reported for dry amorphous mannitol and of 75 °C for amorphous sucrose [13,54]. Thus, the T_g value of the 20/30 ratio was probably decreased by amorphous mannitol while the T_g value of Man/Suc 40/10 was dominated by only sucrose due to complete mannitol crystallization.

Resulting from this study, Man/Suc 40/10 was used for subsequent experiments since complete mannitol crystallization is a prerequisite which can be further diminished by proteins and should be avoided.

Impact of Fast and Conservative Freeze-Drying on Product Quality of Protein-Mannitol-Sucrose-Glycerol Lyophilizates

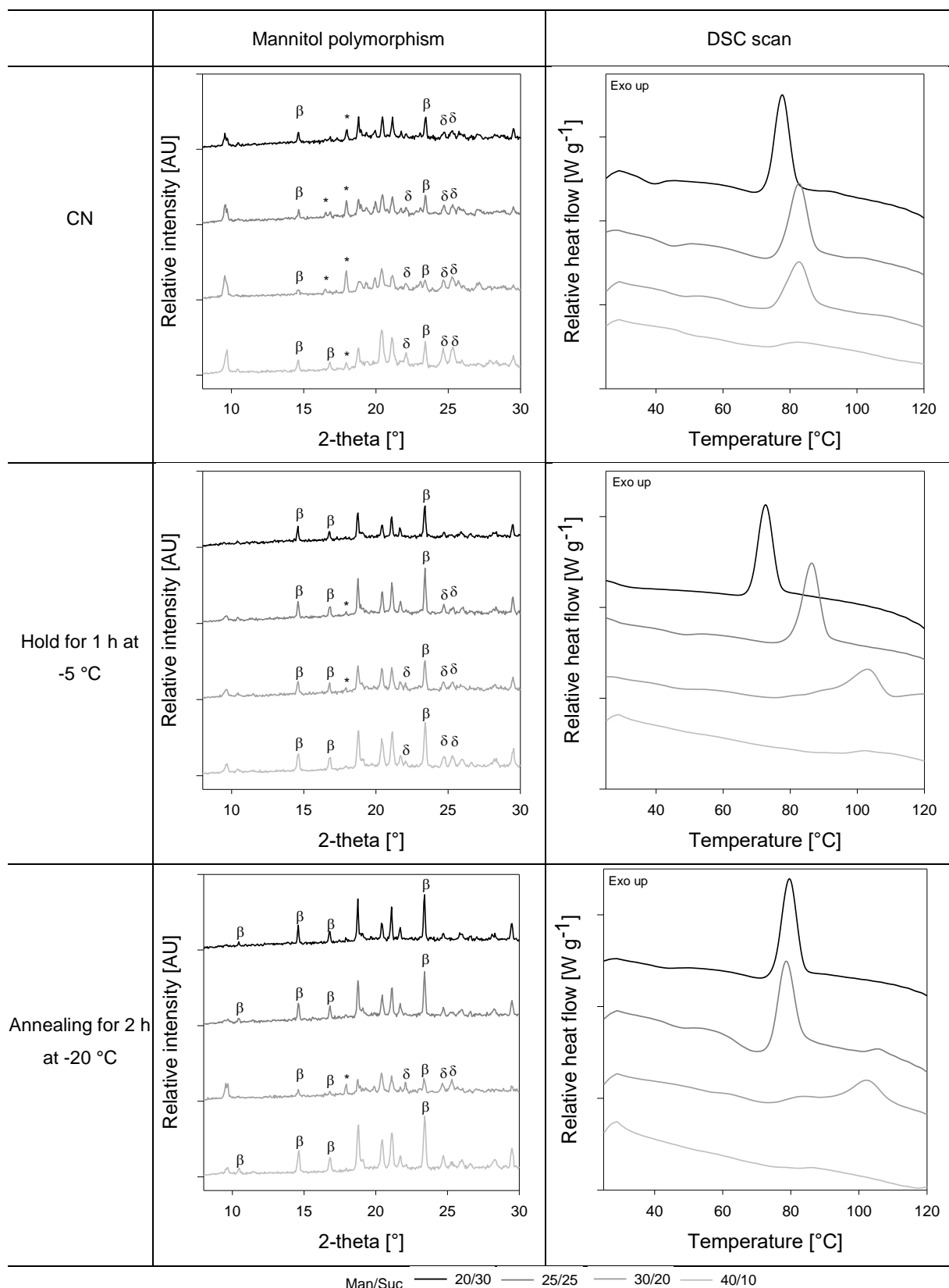


Figure 5-3. XRPD and DSC of Man/Suc lyophilizates that differ in Man/Suc ratio and freezing protocol. The fast freeze-drying cycle was performed with adjusted freezing protocols (Table 5-1, Process 8). Mannitol polymorphs are marked, * refers to mannitol-hemihydrate.

3.3. Comparison Study of Fast and Conservative Freeze-Drying Cycle















The fast freeze-drying cycle with T_p during PD above T_g' of the amorphous phase was compared to a conservative cycle with T_p below T_g' (see Table 5-1, processes 8 and 1). With T_g' values of $-33.7\text{ }^\circ\text{C}$, $-37.2\text{ }^\circ\text{C}$ and $-38.2\text{ }^\circ\text{C}$ of Man/Suc/Glycerol 40/10/0, 40/9.5/0.5, and 40/9/1, respectively, threshold T_p of $-39\text{ }^\circ\text{C}$ was chosen for PD below T_g' for all formulations. Three different proteins were investigated at two concentrations and four different Man/Suc/Glycerol ratios.

3.3.1. Physical Characterization of the Lyophilizates

Macroscopic Appearance

The macroscopic appearance of lyophilizates is an important characteristic although it does not determine protein stability [16,17,55,56]. Furthermore, it is up to discussion which appearance is acceptable [22].

Figure 5-4. Macroscopic appearance of Protein/Man/Suc (x/40/10) formulations after conservative (Table 5-1, Process 1) and fast (Table 5-1, Process 8) freeze-drying.

	Placebo	mAb1		mAb2		Lysozyme	
		2 mg/mL	7.5 mg/mL	2 mg/mL	80 mg/mL	2 mg/mL	100 mg/mL
Conservative FD							
Fast FD							

Vials containing Protein/Man/Suc x/40/10 formulations are shown in Figure 5-4. Independent of the freeze-drying cycle, the protein type and content, the protein formulations at different Man/Suc/Glycerol ratios showed similar adequate cake appearance (see supplementary material). At higher protein concentration, especially in products dried with the fast cycle, fogging was observed. This creeping of product at the inner vial surface is related to the presence of surface active ingredients (surfactants or a surface active API). At higher protein

content the surface pressure may be higher [57] and change in surface pressure could foster fogging. Regularly, fogging is caused by marangoni flow in the liquid state and could not be caused by the drying process. It occurs on the hydrophilic vial surface and could be avoided by using hydrophobic vials [36]. We used regular type I borosilicate glass after cleaning with HPW. Long time periods between liquid filling and the start of freeze-drying are critical enabling creeping at the inner vial surface.

Sample morphology (XRPD)

Additionally, the lyophilizates were characterized regarding the Man polymorphs (Table 5-2). Proteins as well as other formulation components are able to suppress or modify the crystallization behavior of Man [13,14,34,49,58]. Pure Man exhibited the β -Man after both freeze-drying processes while the addition of protein induced the formation of mainly δ -Man. Grohganz et al. demonstrated the same behavior for lysozyme [49]. Our results also showed that the mAbs and Suc \pm Glycerol as excipients without protein induced the same shift to δ -Man. Typically, the formulation with the highest protein content showed lower peak heights corresponding to crystalline Man (see supplementary material, Figure 8-4).

Table 5-2. Mannitol modifications in Protein/Man/Suc/Glycerol lyophilizates. Formulations were freeze-dried with conservative (Table 5-1, Process 1) or fast (Table 5-1, Process 8) process conditions.

Formulation	Man/Suc 40/10		Man/Suc/Glycerol 40/9.5/0.5		Man/Suc/Glycerol 40/9/1		Man 40	
	Cons FD	Fast FD	Cons FD	Fast FD	Cons FD	Fast FD	Cons FD	Fast FD
Placebo	δ , hh	δ , β^1 , hh ¹	δ , hh	δ , β	δ , hh	δ , β^1	β	β
mAb1	2 mg/mL	δ	δ , hh	δ	δ	δ	δ	δ
	7.5 mg/mL	δ , hh	δ , hh	δ	δ , hh	δ	δ	δ
mAb2	2 mg/mL	δ , hh	δ , hh	δ	δ	δ	δ	δ
	80 mg/mL	δ^1	δ^1	δ^1	δ^1	δ^1	δ^1	δ^1
Lyso	2 mg/mL	δ , hh	δ , hh	δ	δ , hh	δ	δ	δ , β
	100 mg/mL	δ^1	δ^1	δ^1	δ^1	δ^1	δ^1	δ^1

hh refers to mannitol-hemihydrate, ¹ only weak signal.

Almost all samples prepared with the conservative freeze-drying cycle also showed the hemihydrate peak at 17.9°. This was probably due to the lower secondary drying temperature (20 °C) as compared to the fast freeze-drying cycle (40 °C). During development of the fast freeze-drying cycle (Table 5-1, Process 3) the hemihydrate content decreased with increasing secondary drying temperature.

Tg and RM

Figure 5-5 shows that the RM values of the formulations processed with the fast freeze-drying cycle lay within the targeted range of 1%. The conservative freeze-drying cycle showed consistent results. Thus, the samples produced by the fast freeze-drying cycle rendered the same Tg and RM as samples dried by the conservative process. The Tg of a multi component system depends on the ratio of the individual components and their specific Tg [59]. Both water (Tg: -108 °C / -137 °C [60,61]) and glycerol (Tg: -93 °C [29]) act as plasticizing agents and decrease the Tg but were present at only low concentrations in the samples. The measured Tg values are characterized by the main amorphous compound Suc (Tg: 75 °C [54], Figure 5-5) due to the low RM values.

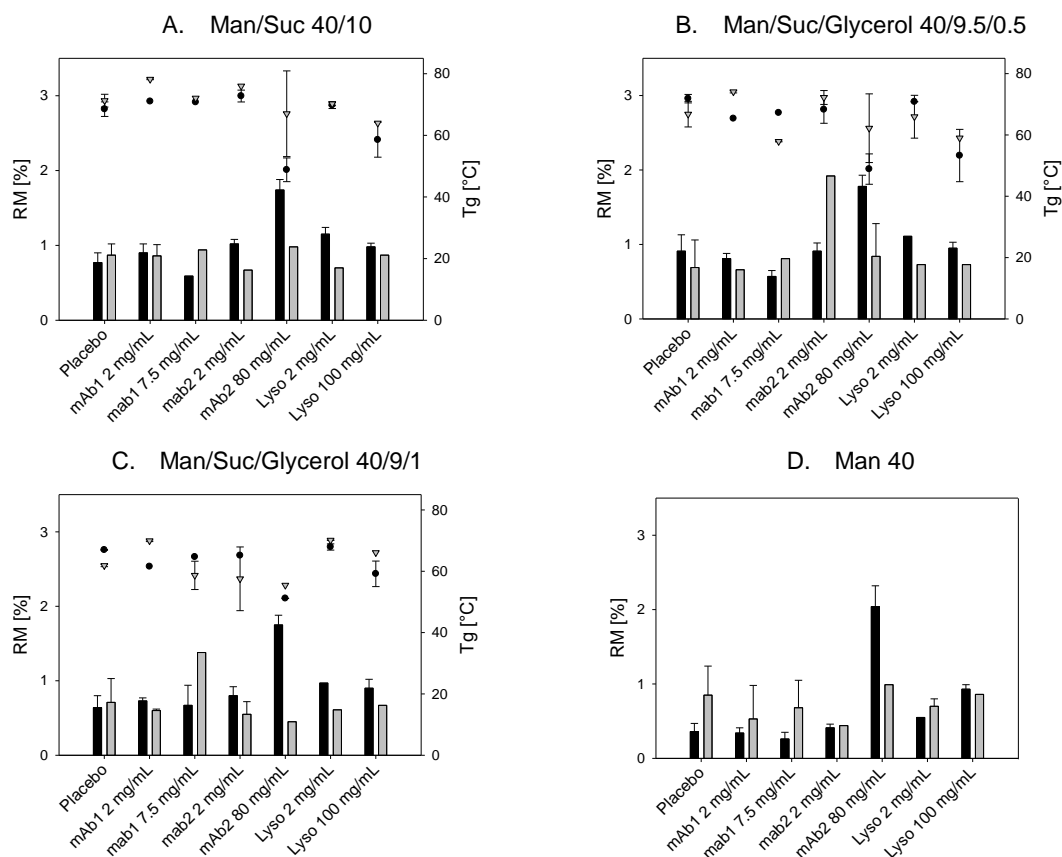


Figure 5-5. Tg (symbols) and RM (bars) of Protein/Man/Suc/Glycerol lyophilizates. A-D shows the different Man/Suc/Glycerol ratios. Formulations were freeze-dried with conservative (black, Table 5-1, Process 1) or fast (grey, Table 5-1, Process 8) process conditions. $n \geq 3$: mean \pm SD; $n = 2$: mean.

Reconstitution Time

Reconstitution time is an important quality attribute and depends on protein concentration, crystallinity and wettability of the excipients, chosen reconstitution method or storage

conditions, for example [62–65]. The process itself has little influence unless the process influenced the crystallinity of the excipients. It was described that fast freezing in liquid nitrogen enabled faster reconstitution than slow freezing with a 0.2 °C/min ramp [45]. This was explained by the different distribution of Man polymorphs on the one hand, and on the other hand by the number and size of the ice crystals that lead to different specific surface area. Annealing can both improve [35] or prolong [66] reconstitution. Recent studies indicate that not annealing but the cooling rate during freezing affects the reconstitution time by changing the pore size of the dried matrix [67]. Thus, not the surface area but the ability to penetrate into pores explains the reconstitution behaviour. Improved reconstitution times by CN were also explained by the changed cake morphology and hence better wettability and penetration of the liquid into the pores [68].

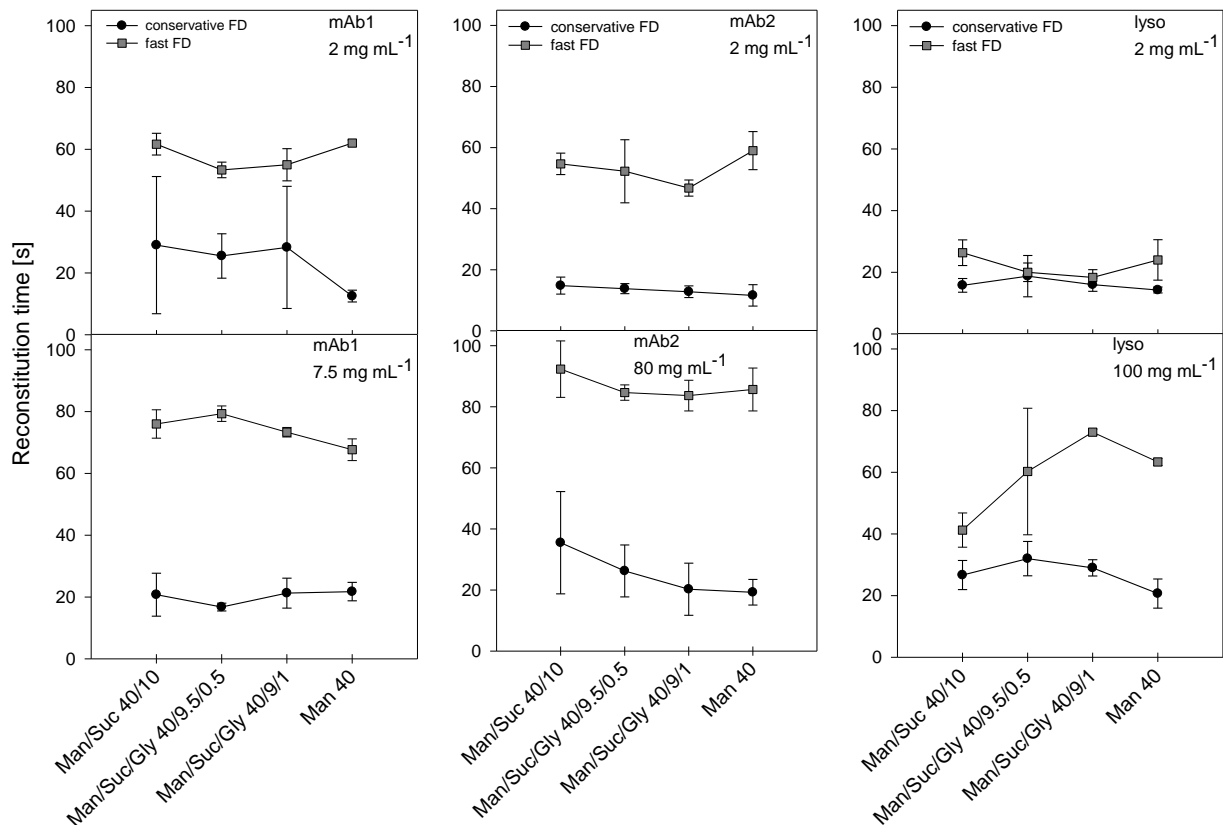


Figure 5-6. Reconstitution times of Protein/Man/Suc/Glycerol lyophilizates. Formulations were freeze-dried with conservative (black circles, Table 5-1, Process 1) or fast (grey squares, Table 5-1, Process 8) process conditions. n≥3: mean ± SD. Data of placebo formulations can be found in Table 5-1, Process 8; Process 1.

All samples showed fast reconstitution within less than 100 seconds (Figure 5-6). A clear difference of the freeze-drying cycles could be detected. Placebo and low concentrated lysozyme (2 mg/mL) formulations reconstituted within 30 s. All other formulations reconstituted within the same time when dried with the conservative cycle but significantly

slower when dried with the fast freeze-drying cycle. It appears that the collapsed amorphous phase consisting of Suc, protein and glycerol hinders the access of water to non-dissolved matrix. However, the prolonged reconstitution was not observed for placebo formulations and for low concentrated lysozyme formulations. Thus, the incorporation of protein into the amorphous matrix seems to play a role. The total mass of collapsed amorphous matrix was increased in the high concentrated protein formulations. Since the low concentration mAb formulations differed from the lysozyme formulations also the protein characteristics are important. Bosch measured also different reconstitution times of lyophilizates that were dried at different chamber pressures [17]. Increased chamber pressure during drying prolonged reconstitution times to a small degree in phenylalanine - trehalose lyophilizates. Others described that reconstitution times did not differ between collapsed and non-collapsed lyophilizates [15,18].

3.3.2. Protein Process Stability

The formulations were characterized regarding their protein stability after freeze-drying in terms of insoluble and soluble aggregates.

Turbidity – A350 nm

Absorbance at 350 nm was measured before freeze-drying and after reconstitution since insoluble aggregates larger than 35 nm scatter the light at this wavelength [69]. All formulations were clear upon visual inspection of any sign that large aggregates formed upon freeze-drying. This was confirmed by the low turbidity values below 0.06 AU except for the highly concentrated protein formulations (mAb2 80 mg/mL, lysozyme 100 mg/mL) which resulted in higher absorbance. There was no difference between samples dried with fast or conservative cycle.

Sub-Visible Particle Analysis

Sub-visible particles were characterized by light obscuration. Placebo formulations did not show an increase in particle numbers after freeze-drying and reconstitution. In contrast, particles $\geq 1 \mu\text{m}$ increased to 30.000 - 40.000 particles per mL in the mAb formulations and to approximately 10.000 particles per mL in the lysozyme formulations. Concentration of the protein, formulation composition or freeze-drying cycle conditions showed no significant impact on the number of particles. This increase and the number of particles after freeze-drying is commonly observed if no surfactant is included in the formulation [70]. All

formulations showed 50 – 200 particles per mL $\geq 10 \mu\text{m}$ and thus numbers below the specification given in the pharmacopoeias (<6000 per mL [40,71]). Only the 80 mg/mL mAb2 formulations showed a pronounced increase to approximately 1000-2000 particles per mL for all formulations regardless of the applied freeze-drying cycle. Similarly, the formulations exhibited less than 50 particles per mL, but 100-150 particles per mL for mAb2 80 mg/mL for particles $\geq 25 \mu\text{m}$ without impact of the lyophilisation cycle.

Soluble Aggregates

HP-SEC indicated no loss in monomer recovery after freeze-drying for both freeze-drying protocols. Probably due to the total absence of surfactants, the formulations exhibited a slight increase in higher molecular weight species to less than 1% aggregates and less than 1.5% in Man 40 formulations without amorphous phase (Figure 5-7).

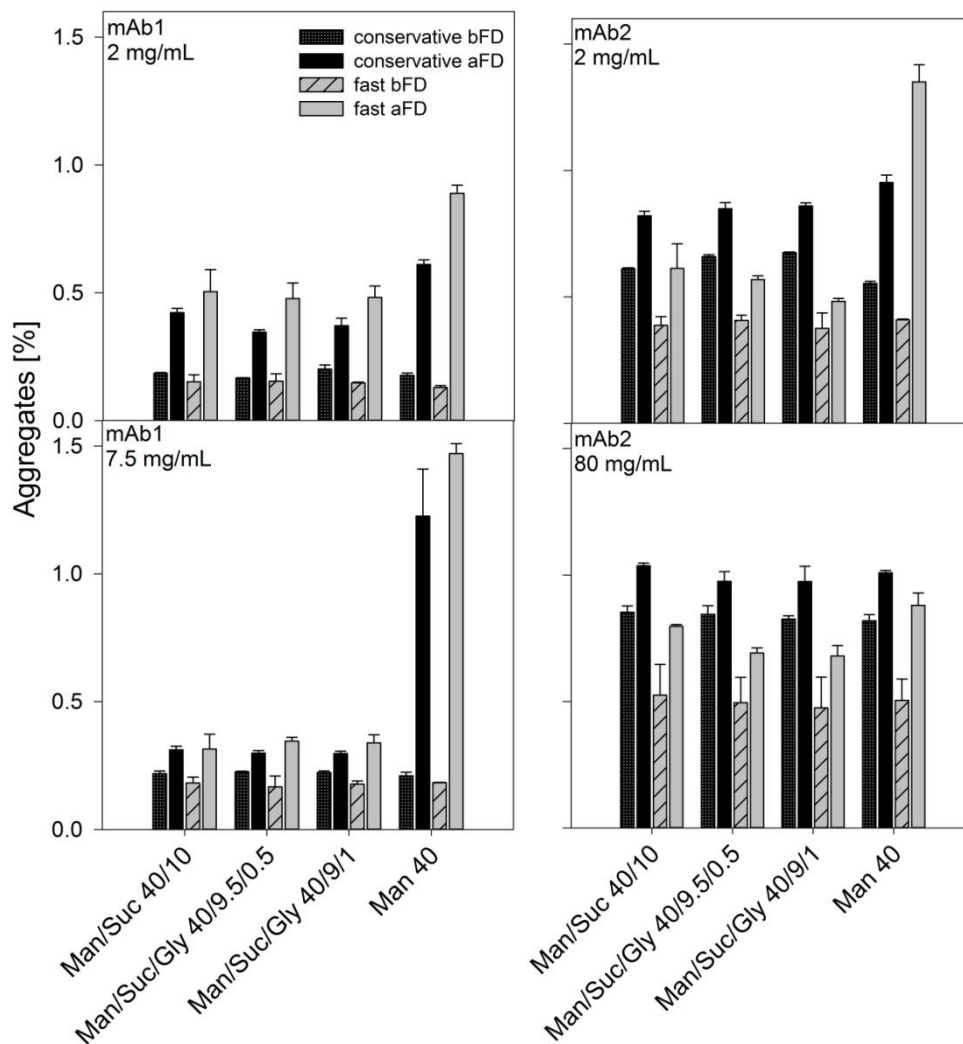


Figure 5-7. Soluble aggregates of mAb/Man/Suc/Gly formulations determined by HP-SEC. Formulations of conservative (black bars, Table 5-1, Process 1) and fast (grey bars, Table 5-1, Process 8) freeze-drying cycles are shown. n=3: mean \pm SD.

3.4. Impact of Glycerol on Protein/Man/Suc/Glycerol formulations

Glycerol was chosen as formulation component as it was previously shown that there might be additional protein stabilizing effects due to prolonged β -relaxation times [25,26,72]. Macroscopic appearance, reconstitution times, mannitol crystallinity and also protein process stability did not change significantly with addition of glycerol. Only a decrease of Tg values was determined as expected. Still, long time stability improvement of the proteins cannot be excluded, however, could not be confirmed in this study.

4. Conclusion

This study focused on maximum time reduction of the conservative freeze-drying process without losing protein process stability. The crystalline Man scaffold was used to gain elegant cake appearance while Suc acted as amorphous protein stabilizer. High Tp during PD led to collapse of the amorphous phase which was already shown not to be detrimental for protein stability [15–21]. The freeze-drying process could be shortened tremendously, e.g. PD time from 47 hours at -39 °C Tp to 7 hours at -10 °C Tp. Man crystallization was mainly affected by different Man/Suc ratios. Only a Man/Suc 40/10 ratio rendered complete Man crystallization. RM, Tg values, Man crystallinity, macroscopic appearance and also reconstitution times showed good results. The comparison of conservative and fast freeze-drying with different protein formulations showed that collapse of the amorphous phase did not lead to instabilization of the proteins during the process. Thus the fast freeze-drying process enabled fast process times without defects of cake appearance and protein process stability.

References

- [1] M. J. Pikal, H. Constantino, Excipients for use in lyophilized pharmaceutical peptide, protein, and other bioproducts, in: M. Constantino, M.J. Pikal (Eds.), *Lyophilization Biopharm.*, AAPS Press, Arlington, Virginia, (2004) 139–228.
- [2] R. Depaz, S. Pansare, S. M. Patel, Freeze-Drying Above the Glass Transition Temperature in Amorphous Protein Formulations While Maintaining Product Quality and Improving Process Efficiency, *J. Pharm. Sci.* 105 (2016) 40–49.
- [3] X. Tang, M. J. Pikal, Design of Freeze-Drying Processes for Pharmaceuticals: Practical Advice, *Pharm. Res.* 21 (2004) 191–200.
- [4] J. Colandene, L. Maldonado, A. Creagh, J. Vrettos, K. Goad, T. Spitznagel, Lyophilization Cycle Development for a High-Concentration Monoclonal Antibody Formulation Lacking a Crystalline Bulking Agent, *J. Pharm. Sci.* 96 (2007) 1598–1608.
- [5] R. Johnson, C. Kirchhoff, H. Gaud, Mannitol-sucrose mixtures--versatile formulations for protein lyophilization., *J. Pharm. Sci.* 91 (2002) 914–922.
- [6] S. Prestrelski, N. Tedeschi, T. Arakawa, J. F. Carpenter, Dehydration-induced conformational transitions in proteins and their inhibition by stabilizers, *Biophys. J.* 65 (1993) 661–71.
- [7] S. Yoshioka, Y. Aso, Correlations between Molecular Mobility and Chemical Stability During Storage of Amorphous Pharmaceuticals, *J. Pharm. Sci.* 96 (2007) 960–981.
- [8] M. T. Cicerone, M. J. Pikal, K. Qian, Stabilization of proteins in solid form, *Adv. Drug Deliv. Rev.* 93 (2015) 14–24.
- [9] K. Izutsu, S. Yoshioka, T. Terao, Effect of Mannitol Crystallinity in the Stabilization of Enzymes during Freeze-Drying, *Chem. Pharm. Bull.* 42 (1994) 5–8.
- [10] J. Liu, Physical characterization of pharmaceutical formulations in frozen and freeze-dried solid states: techniques and applications in freeze-drying development., *Pharm. Dev. Technol.* 11 (2006) 3-28.
- [11] D. Dixon, S. Tchessalov, A. Barry, N. Warne, The impact of protein concentration on mannitol and sodium chloride crystallinity and polymorphism upon lyophilization, *J. Pharm. Sci.* 98 (2009) 3419–3429.
- [12] J. F. Carpenter, B.. Chang, W. Garzon-Rodriguez, T. W. Randolph, Rational Design of Stable Lyophilized Protein Formulations: Theory and Practice, in: Springer US, (2002) 109–133.

- [13] A. Hawe, W. Frieß, Impact of freezing procedure and annealing on the physico-chemical properties and the formation of mannitol hydrate in mannitol-sucrose-NaCl formulations, *Eur. J. Pharm. Biopharm.* 64 (2006) 316–325.
- [14] S. Jena, J. Horn, R. Suryanarayanan, W. Friess, A. Aksan, Effects of Excipient Interactions on the State of the Freeze-Concentrate and Protein Stability, *Pharm. Res.* 34 (2017) 462–478.
- [15] K. Schersch, O. Betz, P. Garidel, S. Muehlau, S. Bassarab, G. Winter, Systematic investigation of the effect of lyophilizate collapse on pharmaceutically relevant proteins I: Stability after freeze-drying, *J. Pharm. Sci.* 99 (2010) 2256–2278.
- [16] K. Schersch, O. Betz, P. Garidel, S. Muehlau, S. Bassarab, G. Winter, Systematic Investigation of the Effect of Lyophilizate Collapse on Pharmaceutically Relevant Proteins, Part 2: Stability During Storage at Elevated Temperatures, *J. Pharm. Sci.* 101 (2012) 2288–2306.
- [17] T. Bosch, Aggressive Freeze-Drying – a fast and suitable method to stabilize biopharmaceuticals, Ludwig-Maximilians Universität München, (2014).
- [18] S. Tchessalov, D. Dixon, N. Warne, Lyophilization above collapse, U.S. Patent Application No. 12/536,321., (2009).
- [19] D. Wang, J. Hey, S. L. Nail, Effect of Collapse on the Stability of Freeze-Dried Recombinant Factor VIII and alpha-Amylase, *J. Pharm. Sci.* 93 (2004) 1253–1263.
- [20] K. Chatterjee, E. Shalaev, R. Suryanarayanan, Partially Crystalline Systems in Lyophilization: II. Withstanding Collapse at High Primary Drying Temperatures and Impact on Protein Activity Recovery, *J. Pharm. Sci.* 94 (2005) 809–820.
- [21] S. Passot, F. Fonseca, N. Barbouche, M. Marin, M. Alarcon-Lorca, D. Rolland, M. Rapaud, Effect of Product Temperature During Primary Drying on the Long-Term Stability of Lyophilized Proteins, *Pharm. Dev. Technol.* 12 (2007) 543–553.
- [22] S. M. Patel, S. L. Nail, M. J. Pikal, R. Geidobler, G. Winter, A. Hawe, J. Davagnino, S. Rambhatla Gupta, Lyophilized Drug Product Cake Appearance: What Is Acceptable?, *J. Pharm. Sci.* 106 (2017) 1706–1721.
- [23] M. T. Cicerone, C. Soles, Fast dynamics and stabilization of proteins: binary glasses of trehalose and glycerol, *Biophys. J.* 86 (2004) 3836–3845.

- [24] L. Chang, D. Shepherd, J. Sun, X. Tang, M. J. Pikal, Effect of sorbitol and residual moisture on the stability of lyophilized antibodies: Implications for the mechanism of protein stabilization in the solid state, *J. Pharm. Sci.* 94 (2005) 1445-1455.
- [25] M. T. Cicerone, J.. Douglas, β -Relaxation governs protein stability in sugar-glass matrices, *Soft Matter.* 8 (2012) 2983.
- [26] M. T. Cicerone, A. Tellington, L. Trost, A. Sokolov, Substantially Improved Stability of Biological Agents in Dried Form - The Role of Glassy Dynamics in Preservation of Biopharmaceuticals, *Bioprocess Int.* 1 (2003) 36–47.
- [27] S. Bhattacharya, R. Suryanarayanan, Local mobility in amorphous pharmaceuticals - Characterization and implications on stability, *J. Pharm. Sci.* 98 (2009) 2935–2953.
- [28] M. Roussenova, J. Andrieux, M. Alam, J. Ubbink, Hydrogen bonding in maltooligomer-glycerol-water matrices: Relation to physical state and molecular free volume., *Carbohydr. Polym.* 102 (2014) 566–75.
- [29] F. Franks, Freeze-drying: From empiricism to predictability, *Cryo Letters.* 11 (1990) 93–110.
- [30] L. Yu, D. Mishra, D. Rigsbee, Determination of the Glass Properties of D-Mannitol Using Sorbitol as an Impurity, *J. Pharm. Sci.* 87 (1998) 774–777.
- [31] J. Obrzut, A. Anopchenko, J. F. Douglas, B. Rust, Relaxation and antiplasticization measurements in trehalose–glycerol mixtures – A model formulation for protein preservation, *J. Non. Cryst. Solids.* 356 (2010) 777–781.
- [32] S. Passot, I. Trélea, M. Marin, M. Galan, G. Morris, F. Fonseca, Effect of Controlled Ice Nucleation on Primary Drying Stage and Protein Recovery in Vials Cooled in a Modified Freeze-Dryer, *J. Biomech. Eng.* 131 (2009).
- [33] J. Kasper, W. Friess, The freezing step in lyophilization: Physico-chemical fundamentals, freezing methods and consequences on process performance and quality attributes of biopharmaceuticals, *Eur. J. Pharm. Biopharm.* 78 (2011) 248–263.
- [34] X. Liao, R. Krishnamurthy, R. Suryanarayanan, Influence of the active pharmaceutical ingredient concentration on the physical state of mannitol-implications in freeze-drying, *Pharm. Res.* 22 (2005) 1978–1985.
- [35] J. Searles, J. F. Carpenter, T. W. Randolph, Annealing to optimize the primary drying rate, reduce freezing-induced drying rate heterogeneity, and determine T'g pharmaceutical lyophilization, *J. Pharm. Sci.* 90 (2001) 872–887.

- [36] A. M. Abdul-Fattah, R. Oeschger, H. Roehl, I. Bauer Dauphin, M. Worgull, G. Kallmeyer, H.-C. Mahler, Investigating factors leading to fogging of glass vials in lyophilized drug products, *Eur. J. Pharm. Biopharm.* 85 (2013) 314–326.
- [37] R. Geidobler, S. Mannschedel, G. Winter, A new approach to achieve controlled ice nucleation of supercooled solutions during the freezing step in freeze-drying, *J. Pharm. Sci.* 101 (2012) 4409–4413.
- [38] B. Peters, L. Staels, J. Rantanen, F. Molnár, T. De Beer, V.P. Lehto, J. Ketolainen, Effects of cooling rate in microscale and pilot scale freeze-drying – Variations in excipient polymorphs and protein secondary structure, *Eur. J. Pharm. Sci.* 95 (2016) 72–81.
- [39] Y. Xie, W. Cao, S. Krishnan, H. Lin, N. Cauchon, Characterization of mannitol polymorphic forms in lyophilized protein formulations using a multivariate curve resolution (MCR)-based Raman spectroscopic method, *Pharm. Res.* 25 (2008) 2292-2301.
- [40] USP <788>, USP/NF general chapter <788> particulate matter in injections, Ed. Rockville, MD United States Pharmacopoeial Conv. (2008).
- [41] B. Chang, C. Randall, Use of subambient thermal analysis to optimize protein lyophilization, *Cryobiology.* 29 (1992) 632–656.
- [42] G. Adams, J. Ramsay, Optimizing the lyophilization cycle and the consequences of collapse on the pharmaceutical acceptability of *Erwinia L-asparaginase*, *J. Pharm. Sci.* 85 (1996) 1301–1305.
- [43] I. Oddone, P. Van Bockstal, T. De Beer, R. Pisano, Impact of vacuum-induced surface freezing on inter- and intra-vial heterogeneity, *Eur. J. Pharm. Biopharm.* 103 (2016) 167–178.
- [44] B. Hancock, G. Zografi, The relationship between the glass transition temperature and the water content of amorphous pharmaceutical solids, *Pharm. Res.* 11 (1994) 471-477.
- [45] A. Kim, M.. Akers, S. L. Nail, The physical state of mannitol after freeze-drying: Effects of mannitol concentration, freezing rate, and a noncrystallizing cosolute, *J. Pharm. Sci.* 87 (1998) 931–935.
- [46] A. Hawe, W. Friess, Physicochemical Characterization of the Freezing Behavior of Mannitol – Human Serum Albumin Formulations, *AAPS PharmSciTech.* 7 (2006) 1–9.

- [47] J. Cleland, X. Lam, B. Kendrick, J. Yang, T. Yang, D. Overcashier, D. Brooks, C. Hsu, J. F. Carpenter, A specific molar ratio of stabilizer to protein is required for storage stability of a lyophilized monoclonal antibody, *J. Pharm. Sci.* 90 (2001) 310-321.
- [48] S. Passot, F. Fonseca, M. Alarcon-Lorca, D. Rolland, M. Marin, Physical characterisation of formulations for the development of two stable freeze-dried proteins during both dried and liquid storage, *Eur. J. Pharm. Biopharm.* 60 (2005) 335–348.
- [49] H. Grohganz, Y. Lee, J. Rantanen, M. Yang, The influence of lysozyme on mannitol polymorphism in freeze-dried and spray-dried formulations depends on the selection of the drying process, *Int. J. Pharm.* 447 (2013) 224–230.
- [50] R. Esfandiary, S. Gattu, J. Stewart, S. M. Patel, Effect of Freezing on Lyophilization Process Performance and Drug Product Cake Appearance, *J. Pharm. Sci.* 105 (2016) 1427–1433.
- [51] X. Li, S. L. Nail, Kinetics of glycine crystallization during freezing of sucrose/glycine excipient systems, *J. Pharm. Sci.* 94 (2005) 625–631.
- [52] J. Searles, J. F. Carpenter, T. W. Randolph, The ice nucleation temperature determines the primary drying rate of lyophilization for samples frozen on a temperature-controlled shelf, *J. Pharm. Sci.* 90 (2001) 860–871.
- [53] S. M. Patel, C. Bhugra, M. J. Pikal, Reduced pressure ice fog technique for controlled ice nucleation during freeze-drying., *AAPS PharmSciTech.* 10 (2009) 1406–1411.
- [54] L. Taylor, G. Zografi, Sugar-polymer hydrogen bond interactions in lyophilized amorphous mixtures., *J. Pharm. Sci.* 87 (1998) 1615–1621.
- [55] M. Taylor, S. Tanna, T. Sahota, Systematic investigation of the effect of lyophilizate collapse on pharmaceutically relevant proteins I: Stability after freeze-drying, *J. Pharm. Sci.* 99 (2010) 4215–4227.
- [56] K. Schersch, O. Betz, P. Garidel, S. Muehlau, S. Bassarab, G. Winter, Systematic investigation of the effect of lyophilizate collapse on pharmaceutically relevant proteins III: Collapse during storage at elevated temperatures, *Eur. J. Pharm. Biopharm.* 85 (2013) 240–252.
- [57] E. Koepf, G. Brezesinski, W. Friess, The Film Tells The Story: Physicochemical Characteristics of IgG at the Liquid-Air Interface, *Eur. J. Pharm. Biopharm.* 119 (2017) 396-407.

- [58] W. Cao, Y. Xie, S. Krishnan, H. Lin, M. Ricci, Influence of Process Conditions on the Crystallization and Transition of Metastable Mannitol Forms in Protein Formulations During Lyophilization, *Pharm. Res.* 30 (2013) 131–139.
- [59] W. Brostow, R. Chiu, I. Kalogeras, A. Vassilikou-Dova, Prediction of glass transition temperatures: Binary blends and copolymers, *Mater. Lett.* 62 (2008) 3152–3155.
- [60] N. Giovambattista, C. Angell, F. Sciortino, H. Stanley, Glass-transition temperature of water: A simulation study, *Phys. Rev. Lett.* 93 (2004) 47801–47804.
- [61] G. Johari, Water's Tg-endothrm, sub-Tg peak of glasses and Tg of water, *J. Chem. Phys.* 119 (2003) 2935–2937.
- [62] T. Werk, J. Huwyler, M. Hafner, J. Luemkemann, H. C. Mahler, An Impedance-Based Method to Determine Reconstitution Time for Freeze-Dried Pharmaceuticals, *J. Pharm. Sci.* 104 (2015) 2948–2955.
- [63] P. Hiwale, A. Amin, L. Kumar, A. Bansal, Variables Affecting Reconstitution Time of Dry Powder for Injection, *Pharm. Technol.* 37 (2008) 1–8.
- [64] W. Cao, S. Krishnan, M. Ricci, L. Shih, D. Liu, J. Gu, F. Jameel, Rational design of lyophilized high concentration protein formulations-mitigating the challenge of slow reconstitution with multidisciplinary strategies, *Eur. J. Pharm. Biopharm.* 85 (2013) 287–293.
- [65] B. Bhatnagar, Reconstitution of Highly Concentrated Lyophilized Proteins, in: *Int. Soc. Lyophilization Free.*, Havana, Cuba, (2017).
- [66] S. Webb, J. Cleland, J. F. Carpenter, T. W. Randolph, Effects of annealing lyophilized and spray-lyophilized formulations of recombinant human interferon- γ , *J. Pharm. Sci.* 92 (2003) 715–729.
- [67] K. Beech, J. Biddlecombe, C. van der Walle, L. Stevens, S. Rigby, J. Burley, S. Allen, Insights into the influence of the cooling profile on the reconstitution times of amorphous lyophilized protein formulations, *Eur. J. Pharm. Biopharm.* 96 (2015) 247-254.
- [68] D. Awotwe-Otoo, C. Agarabi, E. Read, S. Lute, K. Brorson, M. Khan, R. Shah, Impact of controlled ice nucleation on process performance and quality attributes of a lyophilized monoclonal antibody, *Int. J. Pharm.* 450 (2013) 70–78.
- [69] H. C. Mahler, W. Friess, U. Grauschopf, S. Kiese, Protein Aggregation: Pathways, Induction Factors and Analysis, *J. Pharm. Sci.* 98 (2009) 2909–2934.

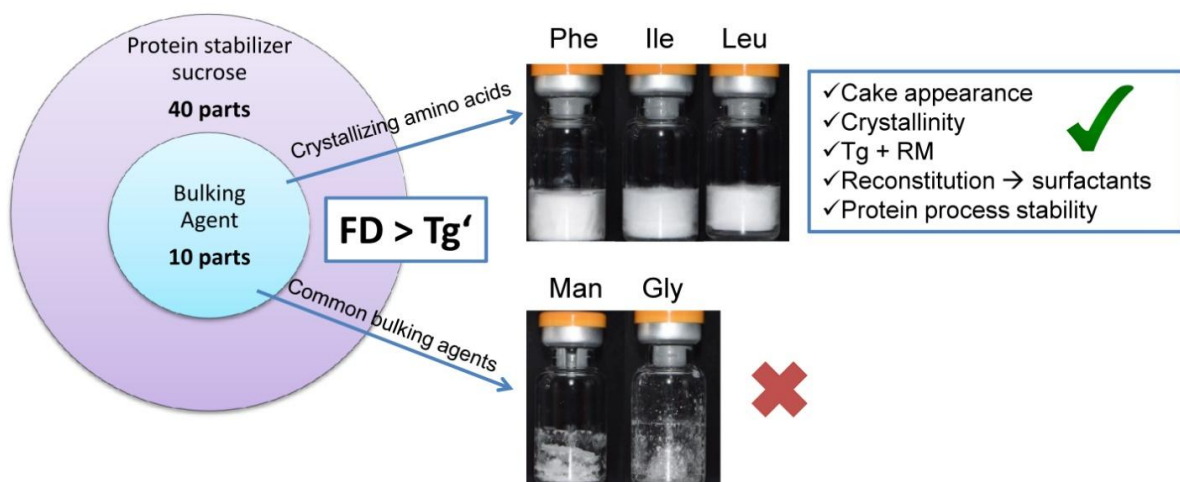
- [70] K. Schersch, Effect of Collapse on Pharmaceutical Protein Lyophilizates, Ludwig-Maximilians-Universität München, (2009).
- [71] Ph.Eur., 2.9.19 Particulate contamination: Sub-visible Particles, Eur. Dir. Qual. Med. 8 (2014) 438–441.
- [72] D. Averett, M. T. Cicerone, J. Douglas, J. de Pablo, Fast relaxation and elasticity-related properties of trehalose-glycerol mixtures, *Soft Matter*. 8 (2012) 4936.

Chapter 6

Crystallizing Amino Acids as Bulking Agents in Freeze-Drying

The following chapter has been submitted as research article to the European Journal of Pharmaceutics and Biopharmaceutics journal in March 2018. It was prepared by Jacqueline Horn, Eleonora Tolardo, Davide Fissore and Wolfgang Friess.

Graphical Abstract



Abstract

Bulking agents as mannitol (Man) and glycine (Gly) require high bulking agent to stabilizer ratios to ensure their crystallization during the freeze-drying process. The aim of this study was to investigate several amino acids (AA) as potential alternative bulking agents in low AA to sucrose (Suc) ratios. A fast freeze-drying process was performed above the collapse temperature (T_c) of the amorphous phase challenging the crystalline AA scaffold. Lyophilizates and liquid formulations were characterized by differential scanning calorimetry, Karl-Fischer titration and X-ray powder diffraction as well as macroscopic cake appearance and reconstitution times were evaluated. Stability of a monoclonal antibody was investigated by UV-Vis spectroscopy, light obscuration and size exclusion chromatography. Phenylalanine (Phe), leucine (Leu) and isoleucine (Ile) crystallized upon freeze-drying at 5/45 and 10/40 AA/Suc ratios. 2.5/47.5 AA/Suc ratio showed less pronounced crystallization. Crystallization peaks were not suppressed by 2 or 50 mg/mL antibody in Leu and Ile lyophilizates. Reconstitution times could be improved by addition of surfactant. No signs of protein aggregation were detected after freeze-drying. Man and Gly yielded unacceptable cake appearance when dried with the fast freeze-drying cycle in such low bulking agent to Suc ratios. Leu, Ile and Phe can be used as alternate bulking agents at lower bulking agent to Suc ratios compared to Man or Gly. The selected AAs provided promising cake characteristics and good protein process stability.

Keywords

Freeze-drying, lyophilization, amino acid, leucine, isoleucine, phenylalanine, mannitol, bulking agent, crystallization, sucrose, protein stability, glass transition, collapse

Abbreviations

AA	Amino acid
AU	Absorbance unit
aFD	After freeze-drying
API	Active pharmaceutical ingredient
AUC	Area under the curve
bFD	Before freeze-drying
FD	Freeze-drying
Gly	Glycine
His	Histidine
HP-SEC	High performance size exclusion chromatography
HPW	Highly purified water
Ile	Isoleucine
Leu	Leucine
LO	Light obscuration
mAb	Monoclonal antibody
Man	Mannitol
DSC	Differential scanning calorimetry
Met	Methionine
Phe	Phenylalanine
PS 20 / 80	Polysorbate 20 / 80
RM	Residual Moisture
SD	Standard deviation
Suc	Sucrose
T _c	Collapse temperature
T _e	Eutectic temperature
T _g	Glass transition temperature of the freeze-dried cake
T _g '	Glass transition temperature of the maximally freeze-concentrated solution
T _p	Product temperature
XRPD	X-Ray powder diffraction

Table of Content

Graphical Abstract	130
Abstract	131
Keywords.....	131
Abbreviations.....	132
1. Introduction	135
2. Materials and Methods.....	137
2.1 Materials	137
2.2 Methods	138
2.2.1 Lyophilization	138
2.2.2 Macroscopic Appearance.....	139
2.2.3 Digital Microscopy	139
2.2.4 Differential Scanning Calorimetry (DSC)	139
2.2.5 Karl-Fischer Titration	140
2.2.6 X-Ray Powder Diffraction (XRPD).....	140
2.2.7 Reconstitution Time.....	141
2.2.8 Turbidity	141
2.2.9 Light Obscuration (LO)	141
2.2.10 High Performance Size Exclusion Chromatography (HP-SEC)	142
3. Results and Discussion	143
3.1 Characterization of AA - Suc Formulations.....	143
3.1.1 DSC of Freeze-Concentrated AA/Suc Formulations.....	143
3.1.2 Screening of AAs and the Impact of Annealing on the Lyophilizates	144
3.1.3 Impact of pH on Physical Characteristics of AA/Suc Lyophilizates	150
3.1.4 Impact of Lower T_p on the Quality of AA:Suc Lyophilizates.....	151
3.2 Freeze-Drying of the Model mAb in AA/Suc Formulations.....	153
3.2.1 Physical characterization.....	154
3.2.2 Protein stability.....	156
4. Conclusions.....	157

References 159

1. Introduction

Freeze-drying of biopharmaceuticals is one approach to prolong their shelf life [1]. In order to achieve acceptable cake appearance drying below the glass transition temperature of the freeze-concentrate (T_g') or at least below the collapse temperature (T_c) is recommended [2,3]. Operating at product temperatures (T_p) below T_g' and T_c may correspond to long drying times depending on the choice of excipients and the protein concentration [2–4]. In fact, high protein concentrations were reported to increase both, T_g' and specifically T_c , enabling faster drying at higher T_p [3]. Drying at even higher T_p would be favourable, especially at low protein concentration, but the resulting macrocollapse would result in rejected batches [5]. Collapse of freeze-dried matrices was already reported not to be detrimental for protein stability in some cases [6–10]. The use of crystalline bulking agents can solve this problem. Bulking agents are typically used to cover undesired cake appearance as “fillers” if the API dosage is low and they can also help to adjust tonicity [11–13]. Drying of crystalline bulking agents is not limited by T_g' , but by their eutectic melting temperature (T_e) which is markedly higher [14]. Since the crystalline excipients do not provide stabilization of the API like the amorphous cryo- and lyoprotectants, low concentrations are preferred. Unfortunately, the crystallisation is affected by the other formulation components such as the sugars used as cryo- and lyoprotectant, buffer components and the protein drug itself [12,15–17]. Mannitol (Man) as one of the common used bulking agents typically requires a 4/1 ratio of Man to sucrose (Suc) for complete crystallization [18,19]. Incomplete crystallization can lead to subsequent crystallization during storage which might induce instability reactions or lead to inadequate cake appearance due to collapse of the whole matrix. Highly concentrated protein formulations can facilitate incomplete crystallization despite high T_c of the formulation. Thus, the essential ratio of bulking agent to amorphous stabilizer needs to be established in order to ensure crystallinity of the bulking agent. A lower bulking agent concentration would hence be favoured in exchange for a higher stabilizer concentration without loss of cake appearance if dried above T_c in a fast freeze-drying cycle.

A few amino acids (AA) are known for their crystallization tendency upon freeze-drying. Table 6-1 gives an overview of the common AAs ordered by hydrophobicity. Their crystallization tendency upon freeze-drying was investigated in a few studies. The most comprehensive studies are based on glycine (Gly) [6,20–28]. Although it shows a higher crystallization tendency than Man [22], the essential Gly/Suc ratio to induce Gly crystallization is still approximately 5/2 [20]. Recently, a variety of AAs was compared to Suc regarding their potential to stabilize proteins [29]. Almost all AAs showed beneficial results upon two months storage of lyophilizates at 50 °C. Crystallinity of the products was not

evaluated. Arginine, glutamine, Gly and histidine showed crystallization tendency with substantial impact of the counter-ion in case of arginine combined with citric acid [30–34].

Table 6-1. Physico-chemical characteristics of AAs and Man. They are sorted by their hydrophobicity. Man was included for comparison purposes.

Amino Acid / Additive	Hydro-phobicity [35]	Sample morphology aFD of			pK _{a1} (COOH) at 25 °C [36–38]	pK _{a2} (NH ₄ ⁺) at 25 °C [36,39]	Solubility at 25 °C [g/100 g] [38,40]
		pure AA solution [41,42]	AA/Suc 2.5/47.5 solutions [8]	pI [36]			
Isoleucine	1.000	Crystalline	Crystalline	6.05	2.32	9.76	4.12
Phenylalanine	0.951	Crystalline	Amorphous	5.49	2.16	9.18	2.97
Valine	0.923	Crystalline	-	6.00	2.29	9.74	8.86
Leucine	0.918	Crystalline	Crystalline	6.01	2.33	9.74	2.19
Methionine	0.811	Crystalline	Crystalline	5.74	2.13	9.28	3.38
Alanine	0.806	Crystalline	-	6.11	2.35	9.87	16.51
Glycine	0.770	Crystalline	Amorphous	6.06	2.35	9.78	24.99
Cysteine	0.721	Crystalline	-	5.05	1.92	10.78	-
Proline	0.678	Crystalline	-	6.30	2.95	10.65	162.3
Threonine	0.634	Crystalline	-	5.60	2.09	9.10	-
Serine	0.601	Crystalline	-	5.68	2.19	9.21	5.02
Histidine	0.548	Tg = 37 °C	Amorphous	7.60	1.80	9.33	4.29
Glutamic acid	0.458	-	-	3.15	2.10	9.47	0.84
Glutamine	0.430	-	-	5.65	2.17	9.13	-
Aspartic acid	0.417	-	-	2.85	1.99	9.90	0.50
Lysine	0.263	Tg = 68 °C	-	9.60	2.16	9.78	-
Arginine	0.000	Tg = 42 °C	Amorphous	10.76	1.82	8.99	-
Mannitol	-	Crystalline	-	-	13.5	-	21.6

AA – Amino acid, aFD – after freeze-drying.

Phenylalanine is a promising candidate. Vacuum-drying time could be accelerated if Phe was included into Suc/rhG-CSF formulations due to Phe crystallization, without losing protein stability [43]. Phe, leucine (Leu), isoleucine (Ile) and methionine (Met) combined with trehalose and sucrose showed crystalline structures after “aggressive” freeze-drying [8]. A low AA/stabilizer ratio of only 2.5/47.5 was sufficient to detect crystallization peaks via XRPD. An acceptable macroscopic appearance and considerably lower residual moisture levels compared to other AAs were found. Consequently, in the present study, Phe, Leu, Ile and Met were evaluated as potential crystalline bulking agents that could be used at much lower concentrations compared to the typical bulking agents Man and Gly. Additionally, the crystalline AA scaffolds should be mechanically stable enough to enable fast drying at high T_p above T_c of the amorphous phase. The cycle may require optimization including a potential annealing step to foster crystallization in terms of best balance between fast process and satisfying AA crystallization [24,44,45].

One of the drawbacks of the AAs with a higher crystallization tendency is their poor solubility in water due to their mainly hydrophobic character (Table 6-1). Their use in high concentrations is hence additionally limited. Furthermore, AAs can react sensitively on changes of the pH environment because of their dipolar character. Consequently, also the effect of pH on the bulking agent properties of the AAs was to be evaluated.

For this study, three AA/Suc ratios with increasing AA content were investigated: 2.5/47.5, 5/45 and 10/40 with Phe, Ile, Leu, and Met. The aim of this study was to establish alternative bulking agents that (1) crystallize in low bulking agent to Suc ratio and (2) crystallize at fast freeze-drying cycle conditions above the formulations' Tg'. It was further focused on the impact of pH, annealing step, chamber pressure and protein concentration on AA crystallization and other cake characteristics as macroscopic appearance, glass transition temperature (Tg) or reconstitution time.

2. Materials and Methods

2.1. Materials

Stock solutions of L-glycine (m/V) (VWR International, Ismaning, Germany), L-isoleucine (m/V) (Sigma-Aldrich Chemie GmbH, Steinheim, Germany), L-leucine (m/V) (Sigma-Aldrich Chemie GmbH), L-methionine (m/V) (Sigma-Aldrich Chemie GmbH), L-phenylalanine (m/V) (Sigma-Aldrich Chemie GmbH), D-mannitol (m/V) (VWR International), Poloxamer 188 (m/m) (Kolliphor® P188, BASF AG, Ludwigshafen am Rhein, Germany), polysorbate 20 (m/m) (Tween® 20, VWR International), polysorbate 80 (m/m) (Tween® 80, VWR International), and sucrose (m/V) (Sigma-Aldrich Chemie GmbH) were prepared in highly purified water (HPW) or in 10 mM L-histidine (Sigma-Aldrich Chemie GmbH) buffer pH 6.0 if protein was included in the formulation. The pH of aqueous solutions without histidine was adjusted with sodium hydroxide or hydrochloric acid. Different bulking agent/sucrose (AA/Suc or Man/Suc) weight ratios were investigated: 2.5/47.5, 5/45 and 10/40 [mg/mL]. Bulking agents were amino acids or mannitol. The formulations were filtered with 0.2 µm polyethersulfone membrane syringe filters (VWR International GmbH) prior to use.

A monoclonal IgG₁ antibody (MW ~ 150 kDa, $\epsilon = 1.49 \text{ mL mg}^{-1} \text{ cm}^{-1}$, referred to as mAb) served as model protein. A 81 mg/mL (for 5/45 AA/Suc formulations) or 94 mg/mL (for 10/40 AA/Suc formulations) mAb stock solution in 10 mM L-histidine buffer pH 6.0 was prepared by tangential flow filtration in Minimate™ capsules (30 kDa Omega membrane, PALL Life Science, Port Washington, NY, USA). The protein was formulated at 2 mg/mL and 50 mg/mL.

2.2. Methods

2.2.1. Lyophilization

Lyophilization stoppers (Westar®, B2-TR coating, West Pharmaceutical Services Deutschland GmbH & Co. KG, Eschweiler, Germany) and ISO 2R Vials (Fiolax®, Schott AG, Mainz, Germany) were cleaned with HPW and dried for 8 hours at 100 °C and 40 °C, respectively. 1.2 mL sample per vial were investigated. The two outer rows of vials in the batch were not used for subsequent analysis: this is due the fact they are also heated by radiation from chamber walls, beside the shelf, and, thus, additional and uncontrolled overheating may occur. Thermocouples were placed center bottom in different vials within the freeze-dryer.

The formulations were freeze-dried according to the protocols given in Table 6-2 to Table 6-5. At first, the operating conditions were selected in such a way that the limit product temperature is trespassed in all the formulations investigated (Table 6-2; Table 6-3), and the influence of the annealing step in the freezing stage was investigated. Then, with the goal of improving cake appearance, the original cycle was modified in such a way that product temperature is lowered: chamber pressure was decreased to reach this goal, at first to 0.52 mbar (Table 6-4) and, then, to 0.4 mbar (Table 6-5). An FTS Lyostar 3 (SP Scientific, Stone Ridge, USA) and an Epsilon 2D-6 LSCplus (Martin Christ Gefriertrocknungsanlagen GmbH, Osterode am Harz, Germany) were used. The end of primary drying was controlled by comparative pressure measurement between Pirani and MKS sensor (FTS) or set manually (Christ). After secondary drying, the vials were stoppered under nitrogen atmosphere at 800 mbar, crimped with flip-off seals and stored at 2-8 °C.

Table 6-2. Freeze-drying cycle with annealing step ran on the Christ freeze-dryer (Cycle 1).

Step	Ramp [°C min ⁻¹]	Shelf temperature [°C]	Pressure [mbar]	Hold Time [min]
Freezing 1	1	-50	-	60
Annealing	1	-20	-	120
Freezing 2	1	-50	-	120
Primary Drying	1	20	2.2	420
Secondary Drying	1	40	2.2	120

Table 6-3. Freeze-drying cycle without annealing step ran on the Christ freeze-dryer (Cycle 2).

Step	Ramp [$^{\circ}\text{C min}^{-1}$]	Shelf temperature [$^{\circ}\text{C}$]	Pressure [mbar]	Hold Time [min]
Freezing	1	-50	-	120
Primary Drying	1	20	2.2	420
Secondary Drying	1	40	2.2	120

Table 6-4. Freeze-drying cycle without annealing step and at reduced chamber pressure of 0.52 mbar ran on the FTS freeze-dryer (Cycle 3).

Step	Ramp [$^{\circ}\text{C min}^{-1}$]	Shelf temperature [$^{\circ}\text{C}$]	Pressure [mbar]	Hold Time [min]
Freezing	1	-50	-	120
Primary Drying	1	20	0.52	750
Secondary Drying	1	40	0.52	120

Table 6-5. Freeze-drying cycle without annealing step and at reduced chamber pressure of 0.40 mbar ran on the Christ freeze-dryer (Cycle 4).

Step	Ramp [$^{\circ}\text{C min}^{-1}$]	Shelf temperature [$^{\circ}\text{C}$]	Pressure [mbar]	Hold Time [min]
Freezing	1	-50	-	120
Primary Drying	1	0	0.40	1200
Secondary Drying	1	40	0.40	120

2.2.2. Macroscopic Appearance

Macroscopic appearance was evaluated visually and pictures were taken with a Nikon digital camera D5300 (Nikon GmbH, Düsseldorf, Germany) in a black photobox.

2.2.3. Digital Microscopy

Digital microscopy was performed with the digital microscope Keyence VHX-500F (Keyence Corporation, Osaka, Japan). The lyophilizates were extracted from the vial without destruction of the cake. A 50-fold magnification was recorded.

2.2.4. Differential Scanning Calorimetry (DSC)

Glass transition temperatures (T_g) of the lyophilizates were determined with a Mettler Toledo DSC 821e (Mettler-Toledo GmbH, Giessen, Germany). Samples were prepared under controlled humidity conditions (< 10% r. h.). 5 to 15 mg of crushed cake were weighted into aluminum crucibles and sealed hermetically. The modulated DSC scan was conducted from 25 $^{\circ}\text{C}$ to 100 $^{\circ}\text{C}$ or 140 $^{\circ}\text{C}$ at 2 $^{\circ}\text{C}/\text{min}$ and modulated with an amplitude of $\pm 1^{\circ}\text{C}$ every 120 s. The Mettler StarE Software was used for data analysis.

Glass transition temperatures of maximally freeze-concentrated solutions (T_g') were evaluated with the same instrument and additionally with a DSC 204 Phoenix (Netzsch, Selb, Germany). 30 μL of the liquid formulations were investigated in hermetically sealed crucibles. Samples were cooled at 10 $^{\circ}\text{C}/\text{min}$ from 20 $^{\circ}\text{C}$ to -60 $^{\circ}\text{C}$ (Mettler) and -100 $^{\circ}\text{C}$ (Netzsch), respectively, and heated to 20 $^{\circ}\text{C}$ at the same rate.

2.2.5. Karl-Fischer Titration

Karl Fischer titration was used to determine the residual moisture (RM) of the freeze-dried cakes. It was performed with an Aqua 40.00 titrator (Analytik Jena AG, Halle, Germany) connected to a headspace oven set at constant temperature of 100 $^{\circ}\text{C}$. For analysis, 5 to 20 mg of crushed cake were transferred to 2 R vials under controlled humidity conditions (< 10% r. h.).

2.2.6. X-Ray Powder Diffraction (XRPD)

Crystallinity of the excipients was determined by XRPD. An XRD 3000 TT diffractometer (Rich. Seifert & Co. GmbH & Co. KG, Ahrensburg, Germany) equipped with a copper anode (40 kV, 30 mA, $\lambda = 0.154178$ nm) and a scintillation detector at 1000 V was used. The freeze-dried samples were crushed and smoothed homogeneously on copper sample holders of 0.2 mm height. Samples were analyzed in steps of 0.05 $^{\circ}$ 2- Θ for 2 s/step from 5 to 45 $^{\circ}$ 2- Θ . Reference peaks used for identification of the crystalline phases are listed in Table 6-6.

Table 6-6. Reference XRPD peaks of the excipients.

Excipient	Main peaks [$^{\circ}$ 2- θ]								References	
Sucrose	11.8	12.7	13.1	18.9	20.9	24.8	25.2		[46–48]	
Phenylalanine	hydrate	6.4	14.7	17.4	21.3				[8]	
	hydrate	6.8	10.9	15.2	17.9	21.7	24.1	26.6	27.9	[49]
	hydrate	6.4	8.4	13.8	17.4	19.3	20.7	22.4	27.5	[50]
	anhydrate	5.7			17.1		22.8	28.6	34.5	[49]
	anhydrate	5.5			16.9	17.7	22.6	28.4	34.3	[50]
Isoleucine		6.5	13.0		25.7	32.4				[51]
		6.4	12.8	19.1	25.4	32.3	38.6			[8,52]
Leucine		6.1								[8]
		6.5		19.2	24.4	30.6				[51]
		6.4	12.3	19.1	24.4	30.7				[53]
Methionine		5.8								[8]
		6.1	23.6	35.2						[51]
Mannitol	α	9.3	13.7	17.2	18.7					[54–56]
	β	10.4	14.6		18.8	20.3	23.4			
	δ	9.7				20.4	22.0	24.6	25.3	
	hemihydrate	9.6		17.9			23.1		25.7	

2.2.7. Reconstitution Time

Reconstitution times were determined by dissolving the lyophilizates with the required volume of HPW. The reconstitution volume was calculated based on formulation density and solid content. The time until complete dissolution of the cake was considered. The vials were gently rolled to ensure wetting.

2.2.8. Turbidity

Turbidity of the samples before freeze-drying and after reconstitution of the lyophilizates was measured with a NanoDrop 2000 spectrophotometer (Thermo Fisher Scientific, Waltham, MA, USA) at 350 nm. Each formulation was measured as triplicate with its corresponding placebo without protein as blank solution.

2.2.9. Light Obscuration (LO)

A PAMAS SVSS-35 particle counter with a HCB-LD-25/25 sensor (PAMAS – Partikelmess- und Analysesysteme GmbH, Rutesheim, Germany) was used to determine the number of subvisible particles before freeze-drying and after dissolution of the lyophilizates. The system

was cleaned with HPW between the analyses. The rinsing volume was 0.2 mL, followed by four measurements of 0.2 ml according to USP 788 [57]. PAMAS PMA software was used to determine the number of particles $\geq 1 \mu\text{m}$, $\geq 10 \mu\text{m}$ and $\geq 25 \mu\text{m}$ per mL.

2.2.10. High Performance Size Exclusion Chromatography (HP-SEC)

Size exclusion chromatography was performed with an Agilent 1100 series HPLC system equipped with an UV/Vis detector for detection at 280 nm (Agilent Technologies, Santa Clara, CA, USA). A TSKgel® G3000 SWXL column (dimension: 300 x 7.8 mm, TOSOH Bioscience GmbH, Stuttgart) and 100 mM sodium phosphate / 100 mM sodium sulfate buffer at pH 6.8 mobile phase with a flow rate of 0.5 mL/min was used. Prior to analysis, 50 mg/mL samples were diluted to 2 mg/mL. All samples were centrifuged (5 min, 4000 rpm, Sigma 1-15 microfuge, Sigma Laborzentrifugen GmbH, Osterode am Harz, Germany). After blank subtraction the integrated peak intensity was compared before and after freeze-drying using the ChemStation software (Agilent Technologies, Santa Clara, CA, USA). Soluble aggregates and fragments were also referred to the AUC of monomer before freeze-drying.

3. Results and Discussion

3.1. Characterization of AA - Suc Formulations

Crystalline bulking agents are desirably used in concentrations as low as possible if their only purpose is the coverage of unwanted cake appearance. At the 2.5/47.5 AA/Suc ratio crystallization of several AAs has been shown [8]. As proteins or amorphous excipients as sugars are able to suppress bulking agent crystallization and higher portions of crystalline material may also be required for mechanical cake stabilization, increased AA/Suc ratios (5/45 and 10/40 AA/Suc ratio) were also included into the study design to favour complete AA crystallization. The crystallizing AAs were selected based on literature [20,21,29,34,41,43]. Phe, Leu, Ile, Gly, and Met were investigated as potential crystallizing AAs. Man was tested at the same bulking agent/Suc ratios for comparison although a Man/Suc ratio of 4/1 is considered essential for complete Man crystallization [18,19].

3.1.1. DSC of Freeze-Concentrated AA/Suc Formulations

Formulations in the frozen state were characterized by DSC. Increasing AA/Suc ratios of Phe/Suc and Leu/Suc formulations resulted in increased Tg' values indicating that the individual Tg' value of the AA was higher than the one of pure Suc (Table 6-7). A Tg' of -10.5 °C was reported for Phe [8]. Tg' values of Leu, Ile and Met were not found in literature and could not be measured since the AAs crystallized already during cooling. Ile/Suc mixtures showed Tg' values close to that of pure Suc. Ile was either already crystalline below -33 °C or the Tg' value of pure Ile is close to the one of Suc. Gly, Met and Man were investigated at the 10/40 ratio only. Tg' values were close to the results of Suc for Man/Suc (-34.5 °C) and for Met/Suc (-33.5 °C). Tg' values of Gly/Suc were lower than pure Suc samples in accordance with a Tg' of -51.5 °C recorded to Gly/Suc 5/2 reported by [20].

Table 6-7. Tg' values of AA/Suc and Man/Suc formulations. For n≥3: mean ± SD, for n=2: mean. n. d.: not determined.

AA/Suc ratio	Tg' [°C]					
	Phe/Suc	Ile/Suc	Leu/Suc	Gly/Suc	Met/Suc	Man/Suc
0/50				-32.9 ± 0.3		
2.5/47.5	-32.0 ± 0.2	-33.3 ± 0.3	-33.1 ± 0.2	n. d.	n. d.	n. d.
5/45	-31.0 ± 0.6	-32.9 ± 0.5	-32.5 ± 0.5	n. d.	n. d.	n. d.
10/40	-29.6 ± 0.6	-33.0 ± 0.6	-28.5 ± 0.8	-37.6 ± 0.8	-33.5	-34.5 ± 0.5

Exothermic crystallization peaks were detected in the heating scans of Phe/Suc 10/40 at -18.3 ± 0.2 °C, Ile/Suc 10/40 at -14.4 ± 1.7 °C, Leu/Suc 10/40 at -20.8 ± 0.2 °C and Met/Suc 10/40 at -17.1 °C. During cooling, peaks were detected for all AAs at approximately -30 °C. Thus, DSC analysis of the liquid samples pointed at pronounced crystallization tendencies of the selected AAs but also at the potential for incomplete crystallization after freezing.

3.1.2. Screening of AAs and the Impact of Annealing on the Lyophilizates

AA/Suc formulations were freeze-dried applying a fast freeze-drying cycle with or without annealing (Table 6-2, Table 6-3).

Macroscopic and Microscopic Appearance

Phe, Ile and Leu lyophilizates showed promising macroscopic appearance at 5/45 and 10/40 AA/Suc while the 2.5/47.5 cakes were shrunken (Figure 6-1). Cakes with Leu, Ile and Met were lifted up from the bottom probably due to the high chamber pressure of 2.2 mbar resulting in fast sublimation. The microscopic structure of Phe/Suc 10/40 and Leu/Suc 10/40 lyophilizates could not be differentiated by the selected freezing protocol and homogeneous, dense cakes were detected (Figure 6-2). The two typical bulking agents Man and Gly resulted in collapsed matrices except of the annealed 10/40 Man/Suc formulation. Microscopy confirmed a slightly improved cake appearance of Man/Suc 10/40, but still, many visible larger pores were evident. The bulking agent/Suc ratio was below the crystallization threshold of Gly and Man of Man/Suc $\geq 4/1$ and Gly/Suc $\geq 2/5$ [6,20,55]. Except for the annealed 10/40 Man/Suc formulation, annealing did not improve the macroscopic and microscopic appearance of the AA/Suc cakes indicating the crystallization of the AAs without the need of an additional annealing step.

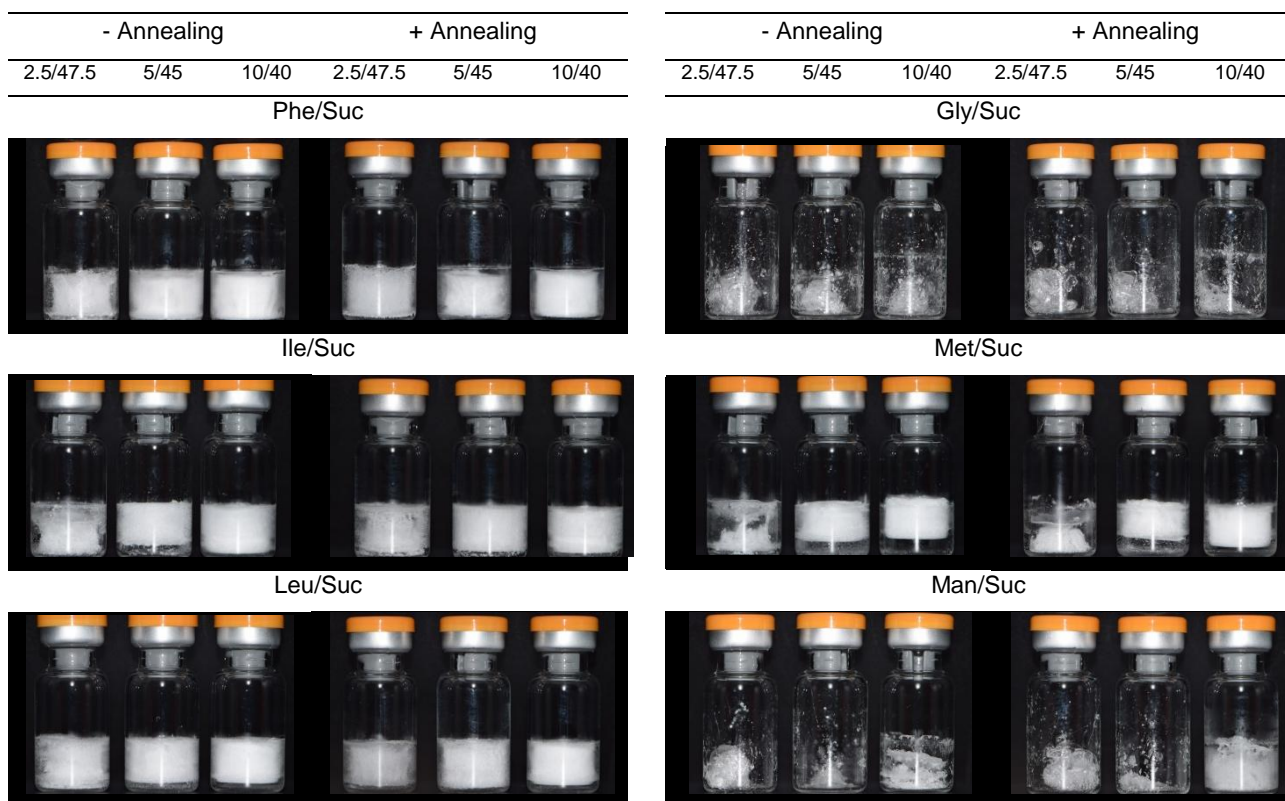


Figure 6-1. Macroscopic appearance of AA/Suc and Man/Suc lyophilizates freeze-dried with (Table 6-2) or without annealing (Table 6-3).

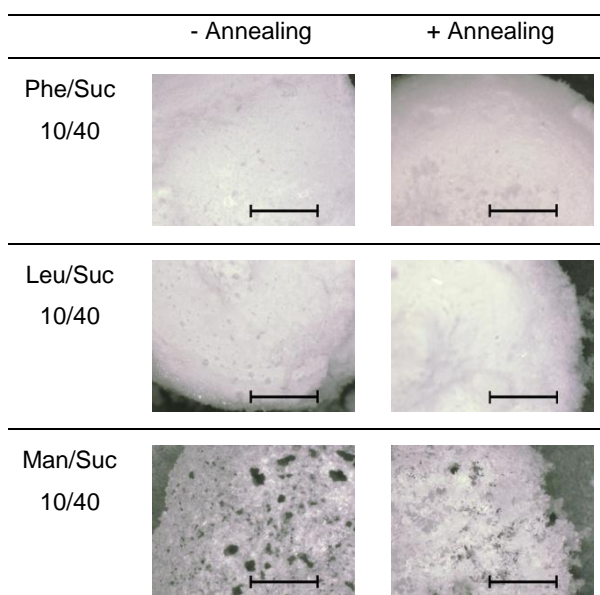


Figure 6-2. Microscopic Appearance of Phe/Suc 10/40, Leu/Suc 10/40 and Man/Suc 10/40 lyophilizates freeze-dried with (Table 6-2) and without annealing step (Table 6-3). The bar refers to a 2.0 mm length.

XRPD

AA based lyophilizates with an acceptable macroscopic appearance (Phe, Ile, Leu and Met), in our study the most important quality attribute, were further investigated by XRPD (Figure 6-3 A-D). Peaks that indicated AA crystallization were detected (Table 6-6). Man/Suc 10/40 showed crystalline Suc and Man peaks (data not shown). Independent of the annealing step

the higher the AA/Suc ratio the more pronounced was the peak pattern. Ile and Leu showed significant peaks also at the lowest AA/Suc ratio of 2.5/47.5 while detection of Phe peaks was more difficult and at 2.5/47.5 no peaks could be assigned.

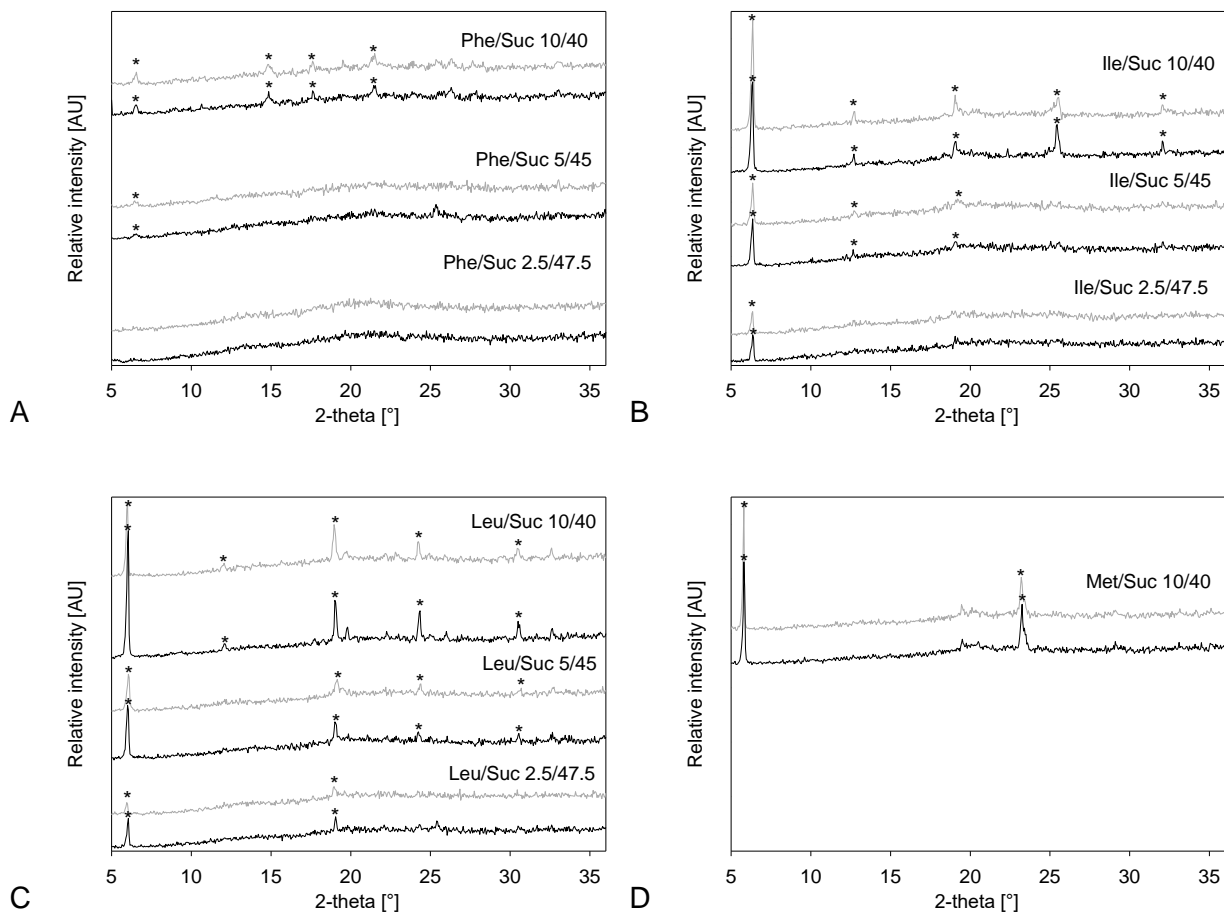


Figure 6-3. XRD diffractograms of A - Phe/Suc, B - Ile/Suc, C - Leu/Suc, D - Met/Suc lyophilizates freeze-dried with (Table 6-2, grey lines) or without annealing step (Table 6-3, black lines).

DSC of Freeze-Dried AA/Suc Systems

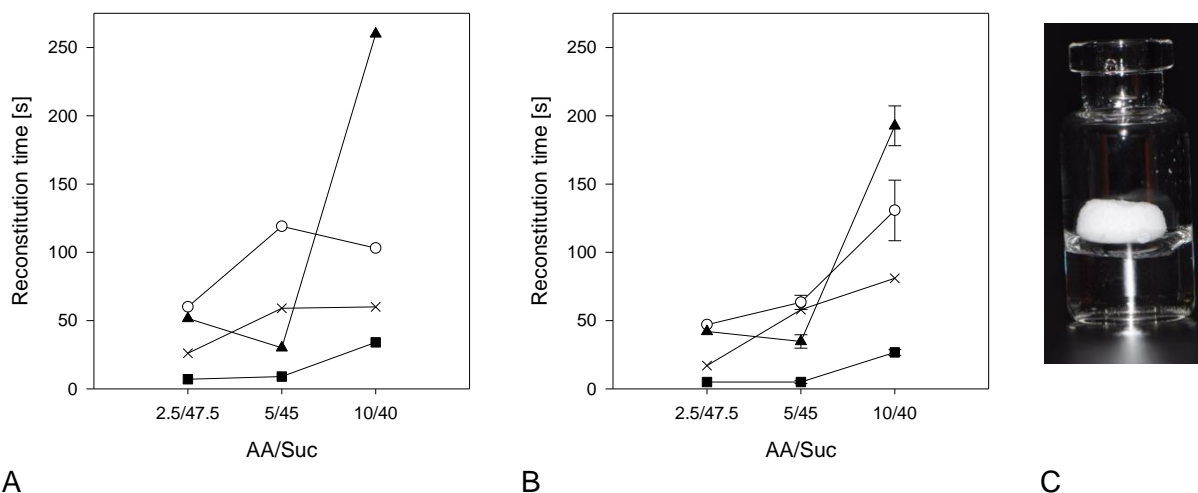
T_g values of the freeze-dried formulations were above 25 °C for all AA/Suc ratios and above 50 °C for the 10/40 AA/Suc ratio (Table 6-8). Annealing had no impact on the T_g values since the amorphous phase was not affected. Higher AA/Suc ratios showed higher T_g values compared to the 2.5/47.5 AA/Suc ratios. Microcollapse of these formulations was a possible reason for insufficient drying behaviour leading to higher RM values and hence lower T_g values (Table 6-9).

Table 6-8. Tg values of freeze-dried AA/Suc formulations. The formulations were freeze-dried with (Table 6-2, + Annealing) or without annealing step (Table 6-3, - Annealing). For n=3: mean \pm SD, for n=2: mean.

AA/Suc ratio		Tg [°C]	
		- Annealing	+ Annealing
Phe/Suc	10/40	67.4 \pm 0.6	69.7 \pm 1.1
	5/45	66.1 \pm 2.4	67.2
	2.5/47.5	58.8	62.1
Ile/Suc	10/40	54.7	54.9
	5/45	36.3 \pm 2.3	47.0
	2.5/47.5	29.7	28.2
Leu/Suc	10/40	50.5	51.4
	5/45	50.9	51.0
	2.5/47.5	38.9	43.4
Met/Suc	10/40	51.0	50.9
	5/45	55.4	55.4

Reconstitution Times

Reconstitution times are an important quality attribute of freeze-dried formulations although they are not directly coupled to API stability and a diversity of different reconstitution times has been reported [59–63]. Prolonged times can be due to the API itself, e.g. high concentrated protein formulations, or due to excipients. Approaches for improvement are addition of wetting agents, adapted freezing procedures, heated reconstitution media or reconstitution with the 2-fold volume [60–66]. The reconstitution times differed significantly (Figure 6-4 A-B) whereas Phe/Suc lyophilizates dissolved in less than one minute. Most other lyophilizates required one to two minutes increasing with higher AA portion and annealed Leu/Suc 10/40 needed about four minutes for complete reconstitution. Compromised wetting behaviour was observed for Leu and Ile lyophilizates (Figure 6-4 C). Dissolution was not hindered as long as the lyophilizate was submersed. As soon as the outer cake region dissolved and the cake became detached from the vial wall, floating occurred and reconstitution was retarded.



A **B** **C**
Figure 6-4. Reconstitution times AA/Suc formulations freeze-dried with (A, Table 6-2) or without annealing step (B, Table 6-3). Phe/Suc - black squares, Ile/Suc - white circle, Leu/Suc - black triangles and Met/Suc - black cross. For n=3: mean \pm SD, for n=2: mean. C - Leu/Suc 10/40 lyophilizate during reconstitution after loss of contact with the vial wall.

The reconstitution times were in an acceptable range of less than five minutes. Nevertheless, different approaches were tested to improve the rehydration, in particular for Leu/Suc and Ile/Suc 10/40 lyophilizates (Figure 6-5 A-D). The hydrophobic character of the selected AAs implied poor wetting and dissolution behavior of the crystalline phases. However, reconstitution of Phe lyophilizates was clearly faster than the reconstitution of Ile and Leu lyophilizates. In order to improve solubility, the reconstitution medium was adjusted to the pK_a and pK_b values of the AAs (Table 6-1). The reconstitution times of Ile/Suc 10/40 decreased at pH 2.33 and 9.75 compared to the reconstitution at pH 6.0 while the ones of Leu/Suc did not change significantly (Figure 6-5 A).

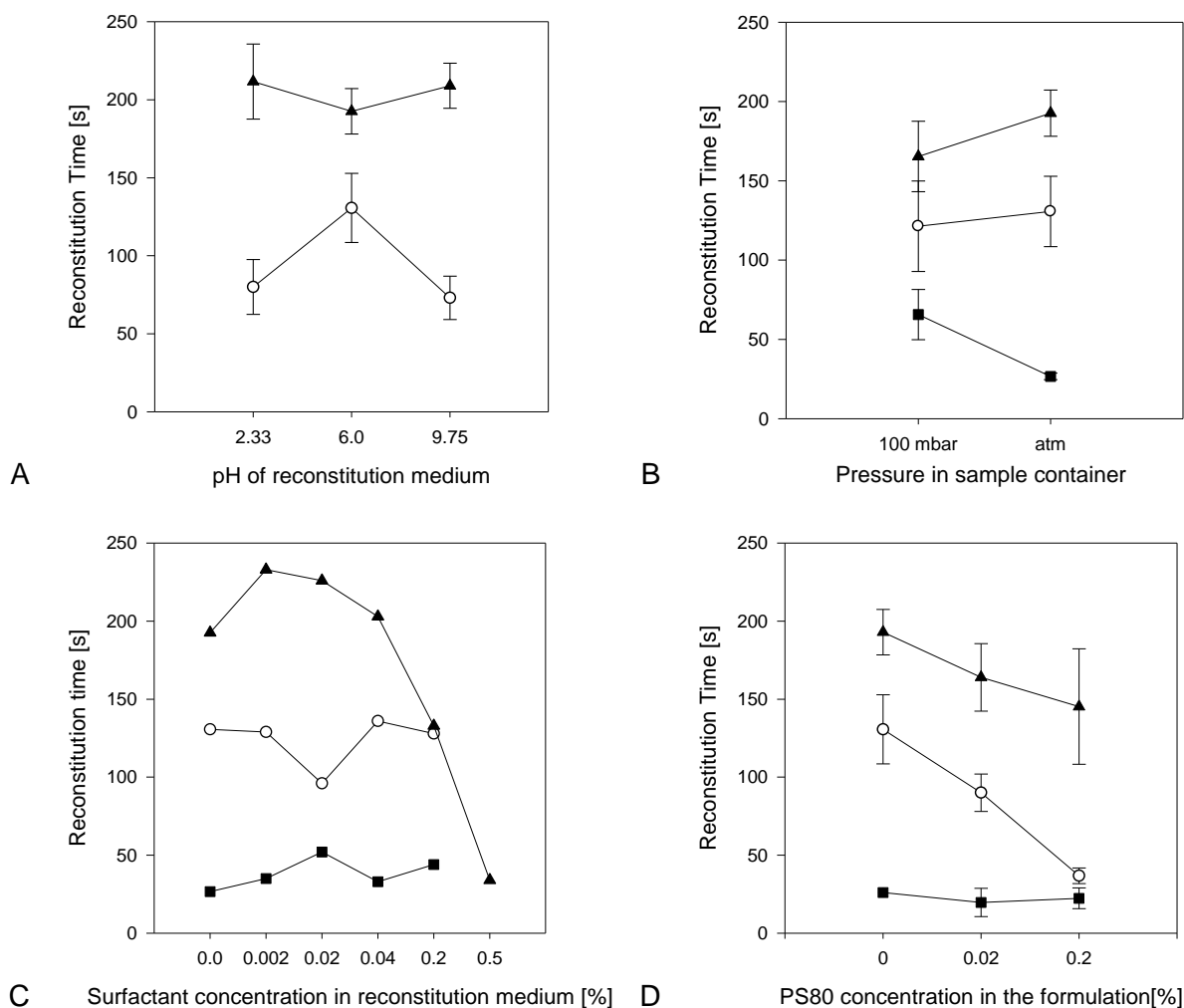


Figure 6-5. Reconstitution times of AA/Suc 10/40 lyophilizates freeze-dried without annealing step (Table 6-3). For $n \geq 3$: mean \pm SD, for $n=2$: mean. A - pH adjustment of reconstitution medium. B - Pressure adjustment within the sample container. C - Addition of surfactant to reconstitution medium. D - Addition of surfactant to the formulation. Phe/Suc 10/40 - black squares, Ile/Suc 10/40 - white circles and Leu/Suc 10/40 - black triangles.

Werk et al. reported that reconstitution times decreased if a warmed reconstitution medium was utilized [65]. However, for the AA/Suc lyophilizates, a prewarmed reconstitution medium of 40 °C resulted in the same reconstitution times as water at ambient temperature. Bhatnagar showed that vacuum within the sample container could help to improve reconstitution times if complete disintegration of the cake was caused by the incoming liquid flow [60]. Ile and Leu lyophilizates showed slightly, but not significantly faster reconstitution when the sample container was stoppered at 100 mbar after freeze-drying instead of ventilation of the vial before reconstitution (Figure 6-5 B). Since the limiting factor was the wetting of the cake and the contact with water, neither warmer HPW and pH adjustment nor vacuum could increase the contact area with the lyophilizate and hence the rate determining floating of the cake was not prevented.

Surfactants are commonly used in freeze-dried formulations to cope with the interface related stress such as at the ice-freeze concentrate interface during freezing [67–70]. Surfactants at high concentration in the reconstitution medium act as wetting agents and decrease reconstitution times [62,63]. The reconstitution times of Leu/Suc 10/40 decreased only if surfactant concentrations of 0.2% and higher were used (Figure 6-5 C). Reconstitution of the other lyophilizates was not affected by the addition of surfactant because floating of the cake could not be prevented. As an alternative, 0.02% or 0.2% polysorbate 80 in the solutions to be lyophilized were evaluated (Figure 6-5 D). Reconstitution was facilitated, in particular for the Ile/Suc 10/40 formulation. Phe/Suc 10/40 and 5/45 lyophilizates did not benefit as they dissolved already fast without surfactant. Phe/Suc 5/45 and Leu/Suc 5/45 suffered shrinkage when 0.2% PS80 was included. In addition, in combination with Ile, 0.2% PS80 induced the formation of crystalline Suc at both AA/Suc ratios. Thus, the addition of 0.2% PS80 could improve the reconstitution time but it affected other important quality attributes negatively. As a compromise, lower polysorbate concentrations were added to the formulations for the following experiments. 0.04% PS20 was chosen in order to avoid shrinkage and Suc crystallization.

Thus, the screening of the AAs demonstrated that Phe, Ile and Leu resulted in lyophilizates with appropriate physical characteristics when combined with Suc in different ratios. Higher AA/Suc ratios of 5/45 and 10/40 were superior with respect to macroscopic appearance and crystallinity compared to the 2.5/47.5 AA/Suc ratio. Annealing did not improve these characteristics. Inclusion of polysorbate into the formulations could improve the reconstitution times of the poorly wetting Ile/Suc and Leu/Suc lyophilizates. Phe/Suc lyophilizates reconstituted faster in spite of comparable hydrophobicity (Table 6-1). Higher T_g values may correlate to a different lyophilizate structure enabling better wetting and hence reconstitution.

3.1.3. Impact of pH on Physical Characteristics of AA/Suc Lyophilizates

Solubility and crystallization of the amphoteric AAs strongly depend on pH. Indeed, the macroscopic appearance of lyophilizates based on AA/Suc mixtures was affected by the formulation pH especially at lower AA/Suc ratio (Figure 8-5). In general, pH conditions from pH 5 to pH 7 resulted in better cake appearances than more extreme acidic or basic conditions. Met/Suc and Gly/Suc lyophilizates did not improve macroscopic appearance under the applied pH conditions. Within the formulations with good cake structure, the crystallization tendencies were not affected, except of Phe/Suc 10/40 which showed a different peak pattern at a formulation pH equal to the pK_a of Phe despite comparable macroscopic appearance (Figure 8-6). The peaks could be assigned to the anhydrous form of Phe, whereas the common form of crystalline Phe after freeze-drying is the monohydrate

[8]. Physical instabilities of these two Phe forms in lyophilizates have not yet been described in literature. Potentially, release of the hydrate upon storage might induce degradation reactions, however, only its formation occurred at low pH. The known Maillard reaction was also favoured at acidic pH condition [72,73] and was detected by browning of the acidic Phe/Suc formulations after few days of storage at ambient temperature. Leu/Suc 10/40 at a pH equal to pK_a did show additional peaks that could not be assigned to further typical Leu reference peaks. In contrast to Phe, no other Leu modification could be found in literature. The peaks were also not in accordance with Suc peaks. Thus, macroscopic appearance and AA crystallinity were affected only by extreme pH conditions but not in the pH region of interest. T_g values decreased at pH values equal to the pK_a , pK_b , pK_a+1 and pK_b-1 , but were stable in the pH region of pH 5 – 7. (Table 8-1). Reconstitution times were comparable over a broad pH range (pH 5 - 7) (Figure 8-7). Only Leu/Suc 10/40 showed an improved reconstitution in the extreme basic or acidic region. A formulation pH of 6.0 resulted in the best characteristics regarding appearance, crystallinity, T_g values and reconstitution times for Phe/Suc, Ile/Suc and Leu/Suc lyophilizates.

3.1.4. Impact of Lower T_p on the Quality of AA:Suc Lyophilizates

As cake shrinkage and lifted cakes were detected during the screening experiments, the freeze-drying cycle was adapted to improve macroscopic appearance without losing AA crystallinity at still short process time. First, the chamber pressure was reduced from 2.2 mbar to 0.52 mbar (Table 6-4) resulting in a reduction of T_p from $-10\text{ }^\circ\text{C}$ to $-20\text{ }^\circ\text{C}$ during primary drying. Thus, the T_p was still markedly above the T_g' of Suc. Alternatively, the chamber pressure was set to 0.40 mbar and the shelf temperature set to $0\text{ }^\circ\text{C}$ instead of $20\text{ }^\circ\text{C}$ during primary drying (Table 6-5) resulting in a T_p of $-27\text{ }^\circ\text{C}$, only slightly above T_g' .

At the reduced chamber pressures settings lifting of the lyophilizates could be prevented whereas the cake appearance was not changed (Figure 6-6). Phe/Suc 5/45 dried at 0.52 mbar and Ile/Suc 5/45 dried at 0.40 mbar formed shrunken cakes. A decreased T_p seemed to hinder the arrangement of AA crystals (Figure 6-7). However, Phe/Suc 5/45 was not collapsed at a T_p of $-27\text{ }^\circ\text{C}$ despite of an amorphous XRD pattern since the T_p was close to the T_g' of the formulation. Thus, crystallization of the AAs was not completed after the freezing step, but was favoured at increased T_p during primary drying. The crystallization tendency depended on the AA portion. Low AA/Suc ratio combined with low T_p during primary drying prevented AA crystallization.

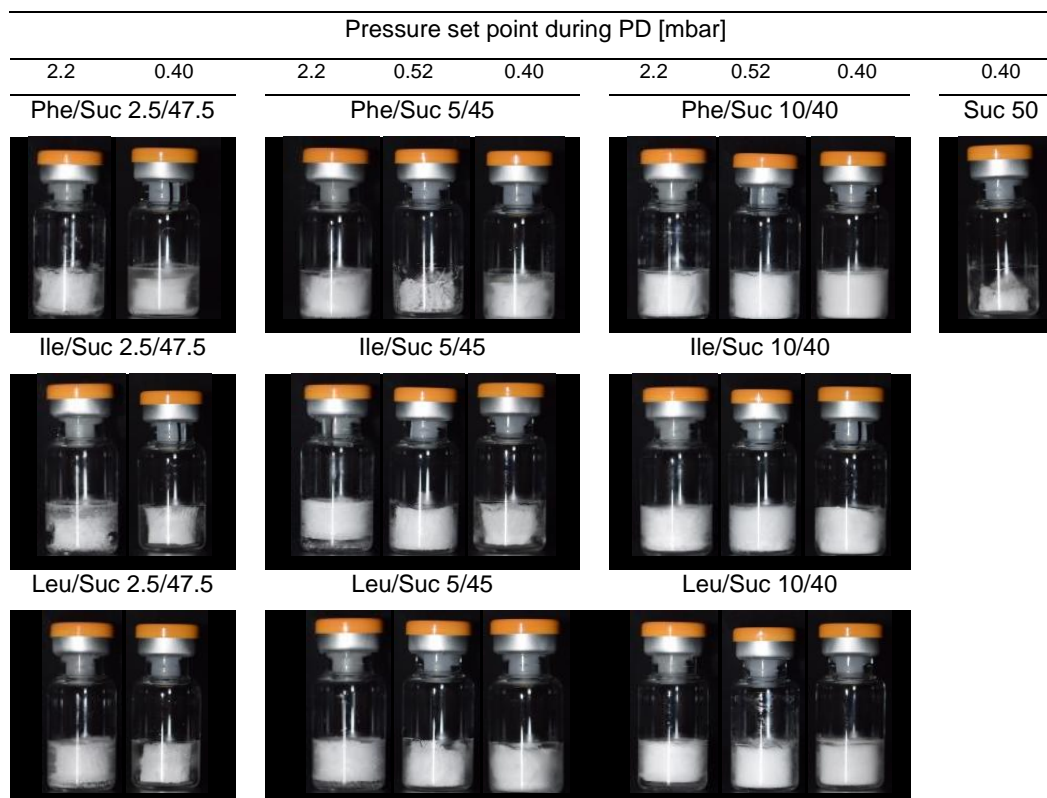


Figure 6-6. Macroscopic Appearance of AA/Suc and Suc lyophilizates dried at different chamber pressure settings (Table 6-3 - Table 6-5).

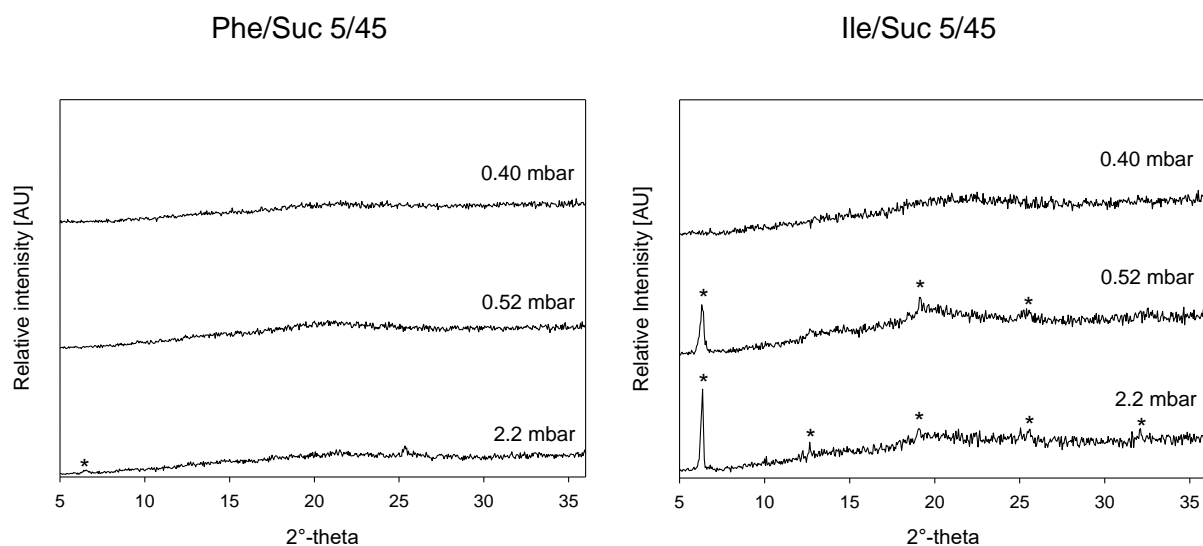


Figure 6-7. XRD diffractogram of Phe/Suc 5/45 and Ile/Suc 5/45 lyophilizates freeze-dried according to Table 6-3 – Table 6-5. The chamber pressure set points during PD are given.

T_g values correlated to the RM levels (Table 6-9). Fast freeze-drying cycle at the highest T_p of -10 °C led to the highest RM levels in Ile/Suc and Leu/Suc formulations. This cycle was implemented for Man/Suc 4/1 formulations with acceptable RM levels [74]. For Phe/Suc 10/40 RM below 0.5% resulted. For Ile/Suc and Leu/Suc freeze-drying at 0.52 mbar resulted

in lower RM levels and hence higher Tg values. The lack of crystalline bulking agent in AA/Suc 2.5/47.5 resulted in collapse and as a consequence in higher RM and lower Tg values. A chamber pressure of 0.52 mbar resulted in the most suitable RM levels of 0.1 – 0.7% leading to Tg values above 55 °C.

Table 6-9. Tg values and residual moisture levels of AA/Suc freeze-dried at different chamber pressure settings according to Table 6-3-Table 6-5. For n=3: mean \pm SD, for n=2: mean. – not determined.

AA/Suc ratio		Tg [°C]			Residual Moisture [%]		
		2.2 mbar	0.52 mbar	0.40 mbar	2.2 mbar	0.52 mbar	0.40 mbar
Phe/Suc	10/40	67.4 \pm 0.6	70.9	68.9 \pm 2.0	0.1 \pm 0.1	0.1 \pm 0.1	0.3 \pm 0.1
	5/45	66.1 \pm 2.4	39.9	62.1 \pm 2.2	0.5 \pm 0.1	0.7 \pm 1.1	1.0 \pm 0.3
	2.5/47.5	58.8	-	55.3 \pm 3.6	-	-	1.3 \pm 0.4
Ile/Suc	10/40	54.7	55.1	61.5 \pm 5.0	1.7	0.6 \pm 0.5	0.8 \pm 0.2
	5/45	36.3 \pm 2.3	56.4	52.6 \pm 2.2	2.8 \pm 0.02	0.3 \pm 0.3	1.9 \pm 0.3
	2.5/47.5	29.7	-	50.1 \pm 2.4	-	-	1.5 \pm 0.3
Leu/Suc	10/40	50.5	62.8	58.3 \pm 5.9	1.6 \pm 0.1	0.3 \pm 0.2	0.7 \pm 0.1
	5/45	50.9	55.3	65.9 \pm 2.3	2.5 \pm 0.05	0.3 \pm 0.2	0.7 \pm 0.2
	2.5/47.5	38.9	-	51.6 \pm 6.7	-	-	1.3 \pm 0.2
Suc	50	-	-	51.1 \pm 4.1	-	-	2.3 \pm 0.4

Reconstitution times were measured for these cycles as well, but did not lead to significant differences between the freeze-drying cycles.

Thus, a lower chamber pressure of 0.52 mbar leading to a Tp of -20 °C prevented lifting of the cakes and led to acceptable cake appearances, Tg values and RM levels in most formulations. AA crystallinity was detected in all AA/Suc formulations processed with this cycle except of Phe/Suc 5/45. An even lower pressure set point of 0.40 mbar resulting in a Tp of -27 °C reduced crystallinity of the AAs, higher RM levels and lower Tg values. The low 2.5/47.5 AA/Suc ratio led to crystalline AAs but the ratio of crystalline to amorphous phase was not investigated quantitatively. The macroscopic appearance was also not acceptable in the 2.5/47.5 AA/Suc ratios. As a consequence, protein runs were only performed with two AA/Suc ratios, 5/45 and 10/40, dried at 0.52 mbar.

3.2. Freeze-Drying of the Model mAb in AA/Suc Formulations

To test whether the AA/Suc formulations were able to stabilize proteins upon freeze-drying a model mAb was investigated at two different concentrations (2 mg/mL and 50 mg/mL). Phe/Suc, Ile/Suc and Leu/Suc formulations were evaluated (AA/Suc 5/45 and 10/40). 0.04% Polysorbate 20 was included in the formulations for improvement of the reconstitution times.

The resulting lyophilizates were characterized in terms of their physical properties. Furthermore, protein process stability was examined regarding aggregate formation. Freeze-drying was carried out at 0.52 mbar with a Tp of -20 °C during the 12 h primary drying step (Table 6-4).

3.2.1. Physical characterization

Lyophilizates with 50 mg/mL mAb did not suffer any cake defects independent of the chosen AA (Figure 6-8). This was due to the high total solid content of 100 mg/mL. The 10/40 AA/Suc ratio resulted in acceptable macroscopic appearance for all formulations and marked AA crystallinity. In contrast, for the 5/45 AA/Suc ratio and 2 mg/mL mAb, best cake appearance was given for Leu/Suc 5/45 followed by Ile/Suc 5/45 and Phe/Suc 5/45 which suffered shrinkage. The crystallization tendency of Phe was strongly affected by the protein while Ile and Leu crystallized at both mAb concentrations (Figure 6-9). The higher mAb concentration of 50 mg/mL suppressed Phe crystallization completely whereas Ile/Suc and Leu/Suc lyophilizates showed crystalline Ile and Leu, respectively. Thus, Ile and Leu had a stronger crystallization tendency in contrast to Phe and were less affected by crystallization suppressing excipients as protein or surfactant.

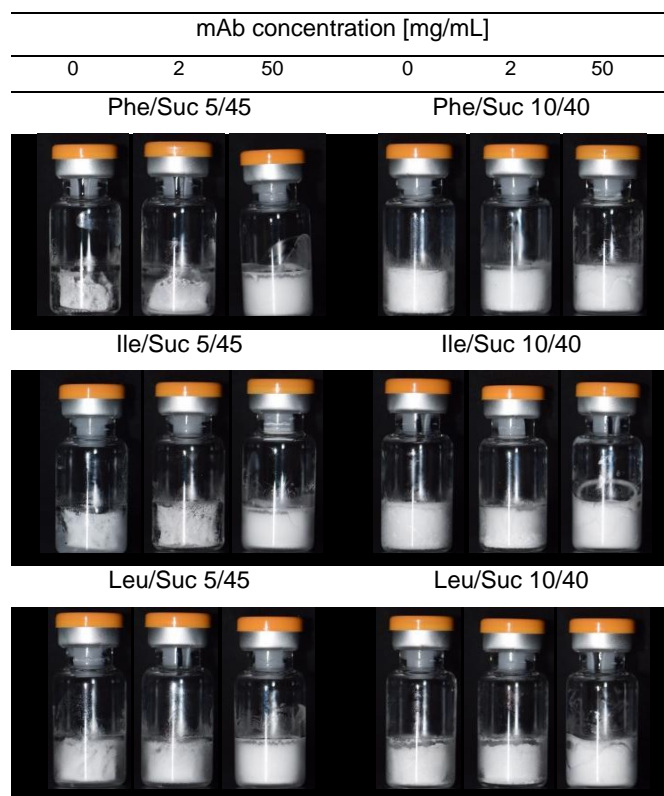


Figure 6-8. Macroscopic Appearance of AA/Suc lyophilizates at different protein concentrations (0 mg/mL, 2 mg/mL and 50 mg/mL) freeze-dried according to Table 6-4.

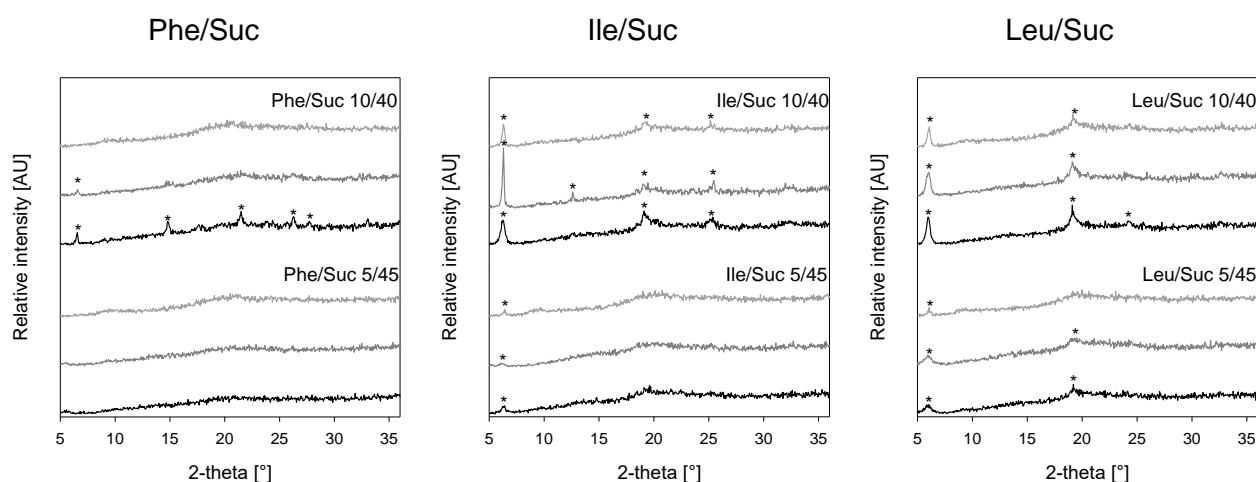


Figure 6-9. XRD diffractograms of Phe/Suc, Ile/Suc and Leu/Suc lyophilizates at different mAb concentrations (0 mg/mL – black, 2 mg/mL – grey, 50 mg/mL dark grey). * mark reference peaks according to Table 6-6.

Tg values and RM contents complemented macroscopic appearance and XRPD (Table 6-10). Inacceptable cake appearance was accompanied by high RM levels and low Tg values (Phe/Suc 5/45). The mAb concentration of 50 mg/mL led to better cake appearance, improved drying behavior and hence low RM levels and higher Tg values. Similar results were achieved by Ile/Suc and Leu/Suc in this AA/Suc ratio of 5/45. The higher AA/Suc ratio of 10/40 resulted in consistently lower residual moisture levels coupled to higher Tg values.

Table 6-10. Impact of protein concentration on Tg values and RM levels of AA/Suc lyophilizates freeze-dried according to Table 6-4. n=3: mean \pm SD, n=2: mean, -: not detected.

AA/Suc Ratio		Tg [°C]			RM [%]		
		0 mg/mL	2 mg/mL	50 mg/mL	0 mg/mL	2 mg/mL	50 mg/mL
Phe/Suc	10/40	67.4 \pm 2.8	59.0	75.0	0.1 \pm 0.1	0.1	0.1
	5/45	39.1	43.6	88.0	2.3	2.4	0.1
Ile/Suc	10/40	67.4 \pm 2.4	72.8	87.2	0.1 \pm 0.2	0.3	0.04
	5/45	57.9 \pm 4.6	52.5	-	0.7	0.7	0.1
Leu/Suc	10/40	65.1 \pm 2.2	57.0	46.3	0.2 \pm 0.2	0.1	0.0
	5/45	61.4	67.5	65.5	0.4	0.4	0.03

Reconstitution times of formulations with only 2 mg/mL protein concentration were below 30 s for AA/Suc 5/45 and below 100 s for AA/Suc 10/40 and comparable to protein free formulations independent of the AA. In contrast, 50 mg/mL protein induced a pronounced prolongation of the reconstitution as described in literature [60,62,64].

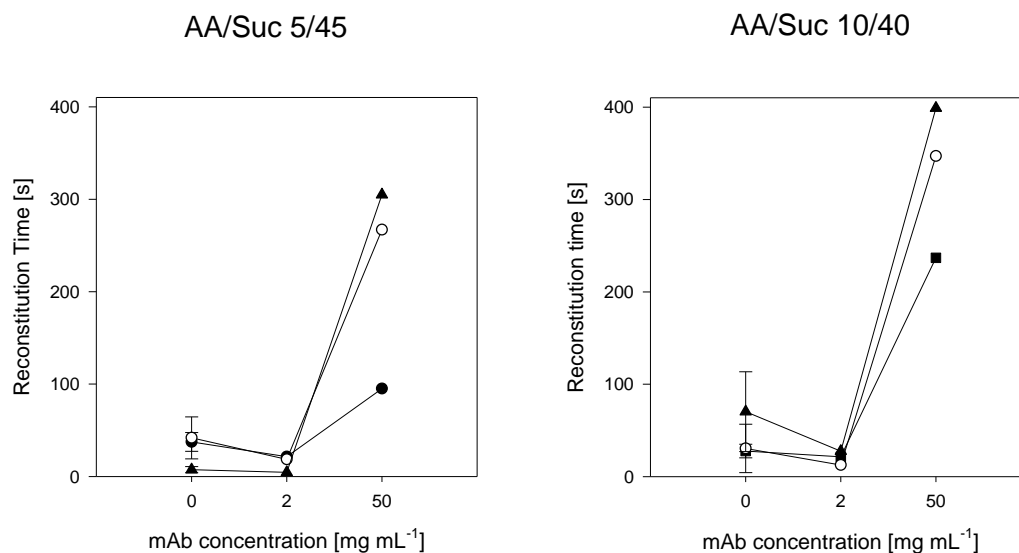


Figure 6-10. Impact of protein concentration on reconstitution times of AA/Suc 5/45 and 10/40 lyophilizates freeze-dried according to Table 6-4. Phe/Suc – black squares, Ile/Suc – white circles, Leu/Suc – black triangles.

3.2.2. Protein stability

Insoluble aggregates larger than 35 nm can be detected due to their scattering of light at 350 nm [75]. After freeze-drying and reconstitution the formulations were clear without indications of visible aggregate formation. Absorbance values before and after freeze-drying were comparably low at 0.06 AU for all formulations. Thus, no insoluble aggregates were formed during freeze-drying. Light obscuration was used to determine the amount of sub-visible particles. The particle numbers were below 25,000 particles per mL ($\geq 1 \mu\text{m}$), below 250 particles per mL ($\geq 10 \mu\text{m}$) and below 20 particles per mL ($\geq 25 \mu\text{m}$) and did not increase with freeze-drying. The amount of soluble aggregates before and after freeze-drying and reconstitution was below 1% for all samples without significant impact of freeze-drying at both protein concentrations (Figure 6-11).

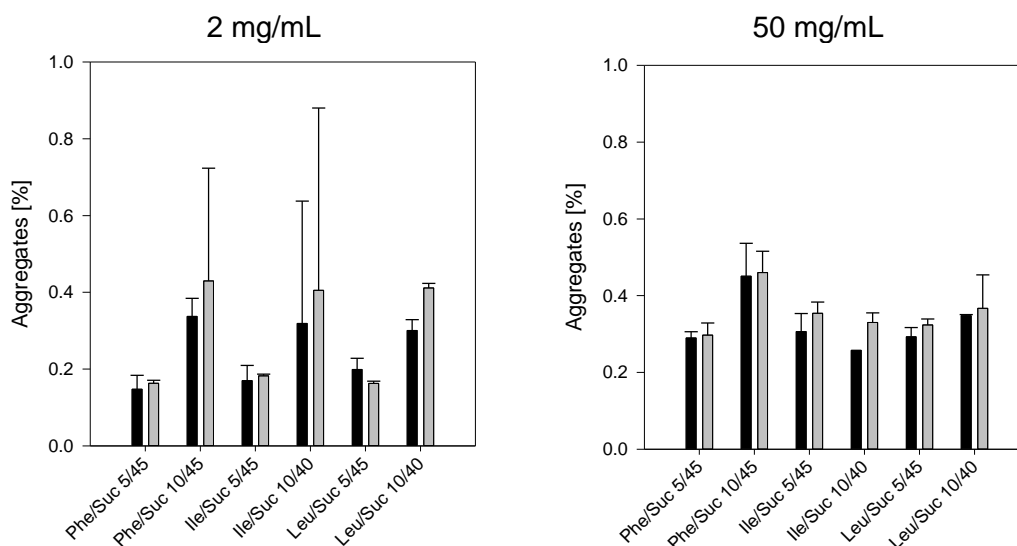


Figure 6-11. Soluble aggregates of mAb/AA/Suc formulations freeze-dried according to Table 6-4. n=3: mean \pm SD. bFD - black bars, aFD - grey bars.

Thus, the analysis of mAb process stability did not show any significant protein aggregation. As only a small amount of bulking agent was used in comparison to other common crystalline bulking agents, sufficient amorphous Suc was present. Upon storage, the high fraction of amorphous Suc should provide adequate stabilization. It has to be ensured that Suc remains amorphous upon storage and that AA crystallization, if amorphous, is avoided.

4. Conclusions

The aim of this study was to investigate several AAs as alternatives to the typical bulking agents Man and Gly which require high bulking agent/Suc ratios. Low AA/Suc ratios were freeze-dried above T_g' to enable fast freeze-drying. The amino acids Phe, Ile and Leu showed better crystallization characteristics than the typical bulking agents Man and Gly at the essential bulking agent to Suc ratio freeze-dried above T_g' . At 2.5/47.5 AA/Suc acceptable cake appearance could not be achieved despite of crystalline Ile and Leu peaks. 5/45 and 10/40 AA/Suc offered a substantially improved lower bulking agent concentration at high stabilizer content. Annealing at -20°C could not enhance crystallization in contrast to varied T_p during primary drying. Lower T_p decreased the crystallization tendencies of the AAs. Thus, fast freeze-drying at -20°C for 12 hours primary drying time rendered the best physico-chemical characteristics of the AA/Suc lyophilizates. A pH range of pH 5 to pH 7 was suitable at the tested AA/Suc ratios while extreme pH conditions induced collapse. Reconstitution times were longer in Ile and Leu lyophilizates compared to Phe and Man due to poor wettability and floating of the cakes containing the hydrophobic AAs. Including surfactants in the formulation improved the reconstitution behaviour. The protein was

protected by the high amount of sucrose. The crystallization tendency of Phe was reduced by protein in contrast to Ile and Leu.

Concluding, the three AAs Ile, Leu and Phe were found to be alternative bulking agents to Man and Gly enabling fast drying at high stabilizer content but low bulking agent concentration. In contrast to other crystallizing excipients, Ile and Leu crystallization was not suppressed by protein enabling also increased protein concentrations.

References

- [1] J. Kasper, G. Winter, W. Friess, Recent advances and further challenges in lyophilization, *Eur. J. Pharm. Biopharm.* 85 (2013) 162–169.
- [2] J. Colandene, L. Maldonado, A. Creagh, J. Vrettos, K. Goad, T. Spitznagel, Lyophilization Cycle Development for a High-Concentration Monoclonal Antibody Formulation Lacking a Crystalline Bulking Agent, *J. Pharm. Sci.* 96 (2007) 1598–1608.
- [3] R. Depaz, S. Pansare, S. M. Patel, Freeze-Drying Above the Glass Transition Temperature in Amorphous Protein Formulations While Maintaining Product Quality and Improving Process Efficiency, *J. Pharm. Sci.* 105 (2016) 40–49.
- [4] J. Liu, Physical characterization of pharmaceutical formulations in frozen and freeze-dried solid states: techniques and application in freeze-drying development., *Pharm. Dev. Technol.* 11 (2006) 3-28.
- [5] S. M. Patel, S. L. Nail, M. J. Pikal, R. Geidobler, G. Winter, A. Hawe, J. Davagnino, S. Rambhatla Gupta, Lyophilized Drug Product Cake Appearance: What Is Acceptable?, *J. Pharm. Sci.* 106 (2017) 1706–1721.
- [6] K. Chatterjee, E. Shalaev, R. Suryanarayanan, Partially Crystalline Systems in Lyophilization: II. Withstanding Collapse at High Primary Drying Temperatures and Impact on Protein Activity Recovery, *J. Pharm. Sci.* 94 (2005) 809–820.
- [7] K. Schersch, O. Betz, P. Garidel, S. Muehlau, S. Bassarab, G. Winter, Systematic Investigation of the Effect of Lyophilizate Collapse on Pharmaceutically Relevant Proteins, Part 2: Stability During Storage at Elevated Temperatures, *J. Pharm. Sci.* 101 (2012) 2288–2306.
- [8] T. Bosch, Aggressive Freeze-Drying – a fast and suitable method to stabilize biopharmaceuticals, Ludwig-Maximilians Universität München, (2014).
- [9] D. Wang, J. Hey, S. L. Nail, Effect of Collapse on the Stability of Freeze-Dried Recombinant Factor VIII and alpha-Amylase, *J. Pharm. Sci.* 93 (2004) 1253–1263.
- [10] K. Schersch, O. Betz, P. Garidel, S. Muehlau, S. Bassarab, G. Winter, Systematic investigation of the effect of lyophilizate collapse on pharmaceutically relevant proteins III: Collapse during storage at elevated temperatures, *Eur. J. Pharm. Biopharm.* 85 (2013) 240–252.
- [11] D. Fissore, Freeze Drying of Pharmaceuticals, in: J. Swarbrick (Ed.), *Encycl. Pharm. Sci. Technol.*, Fourth, Taylor & Francis, New York, (2013) 37–41.

- [12] D. Dixon, S. Tchessalov, A. Barry, N. Warne, The impact of protein concentration on mannitol and sodium chloride crystallinity and polymorphism upon lyophilization, *J. Pharm. Sci.* 98 (2009) 3419–3429.
- [13] J. F. Carpenter, B. Chang, W. Garzon-Rodriguez, T. W. Randolph, Rational Design of Stable Lyophilized Protein Formulations: Theory and Practice, in: Springer US, (2002) 109–133.
- [14] X. Tang, M. J. Pikal, Design of Freeze-Drying Processes for Pharmaceuticals: Practical Advice, *Pharm. Res.* 21 (2004) 191–200.
- [15] S. Jena, J. Horn, R. Suryanarayanan, W. Friess, A. Aksan, Effects of Excipient Interactions on the State of the Freeze-Concentrate and Protein Stability, *Pharm. Res.* 34 (2017) 462–478.
- [16] X. Liao, R. Krishnamurthy, R. Suryanarayanan, Influence of the active pharmaceutical ingredient concentration on the physical state of mannitol-implications in freeze-drying, *Pharm. Res.* 22 (2005) 1978–1985.
- [17] W. Cao, Y. Xie, S. Krishnan, H. Lin, M. Ricci, Influence of Process Conditions on the Crystallization and Transition of Metastable Mannitol Forms in Protein Formulations During Lyophilization, *Pharm. Res.* 30 (2013) 131–139.
- [18] A. Hawe, W. Friess, Physicochemical Characterization of the Freezing Behavior of Mannitol – Human Serum Albumin Formulations, *AAPS PharmSciTech.* 7 (2006) 1–9.
- [19] R. Johnson, C. Kirchhoff, H. Gaud, Mannitol-sucrose mixtures--versatile formulations for protein lyophilization., *J. Pharm. Sci.* 91 (2002) 914–922.
- [20] K. Kasraian, T. Spitznagel, J. Juneau, K. Yim, Characterization of the sucrose/glycine/water system by differential scanning calorimetry and freeze-drying microscopy., *Pharm. Dev. Technol.* 3 (1998) 233–9.
- [21] A. Pyne, R. Suryanarayanan, Phase transitions of glycine in frozen aqueous solutions and during freeze-drying, *Pharm. Res.* 18 (2001) 1448–1454.
- [22] A. Pyne, K. Chatterjee, R. Suryanarayanan, Solute Crystallization in Mannitol-Glycine Systems - Implications on Protein Stabilization in Freeze-Dried Formulations, *J. Pharm. Sci.* 92 (2003) 2272–2283.
- [23] X. Li, S. L. Nail, Kinetics of glycine crystallization during freezing of sucrose/glycine excipient systems, *J. Pharm. Sci.* 94 (2005) 625–631.

- [24] M. Akers, N. Milton, S. Byrn, S. L. Nail, Glycine Crystallization During Freezing: The Effects of Salt Form, pH, and Ionic Strength, *Pharm. Res. An. Off. J. Am. Assoc. Pharm. Sci.* 12 (1995) 1457–1461.
- [25] D. Varshney, S. Kumar, E. Y. Shalaev, P. Sundaramurthi, S. Kang, L. Gatlin, R. Suryanarayanan, Glycine Crystallization in Frozen and Freeze-dried Systems: Effect of pH and Buffer Concentration, *Pharm. Res.* 24 (2007) 593–604.
- [26] J. Meyer, R. Nayar, M. C. Manning, Impact of bulking agents on the stability of a lyophilized monoclonal antibody, *Eur. J. Pharm. Sci.* 38 (2009) 29–38.
- [27] K. Bauer, S. Suhm, A. Wöll, J. Hubbuch, Impact of additives on the formation of protein aggregates and viscosity in concentrated protein solutions, *Int. J. Pharm.* 516 (2017) 82–90.
- [28] J. F. Carpenter, M. J. Pikal, B.S. Chang, T. W. Randolph, Rational design of stable lyophilized protein formulations: Some practical advice, *Pharm. Res.* 14 (1997) 969-975.
- [29] K. Forney-Stevens, R. Bogner, M. J. Pikal, Addition of Amino Acids to Further Stabilize Lyophilized Sucrose-Based Protein Formulations: I. Screening of 15 Amino Acids in Two Model Proteins., *J. Pharm. Sci.* 105 (2016) 697–704.
- [30] K. Izutsu, S. Kadoya, C. Yomota, T. Kawanishi, E. Yonemochi, K. Terada, Freeze-drying of proteins in glass solids formed by basic amino acids and dicarboxylic acids., *Chem. Pharm. Bull.* 57 (2009) 43–48.
- [31] T. Yamaki, R. Ohdate, E. Nakadai, Y. Yoshihashi, E. Yonemochi, K. Terada, H. Moriyama, K. Izutsu, C. Yomota, H. Okuda, T. Kawanishi, Component Crystallization and Physical Collapse during Freeze-Drying of L-Arginine-Citric Acid Mixtures, *Chem. Pharm. Bull.* 60 (2012) 1176–1181.
- [32] P. Stärtzel, H. Gieseler, M. Gieseler, A. M. Abdul-Fattah, M. Adler, H. C. Mahler, P. Goldbach, Freeze Drying of L-Arginine/Sucrose-Based Protein Formulations, Part I: Influence of Formulation and Arginine Counter Ion on the Critical Formulation Temperature, Product Performance and Protein Stability, *J. Pharm. Sci.* 104 (2015) 2345–2358.

- [33] P. Stärtzel, H. Gieseler, M. Gieseler, A. M. Abdul-Fattah, M. Adler, H. C. Mahler, P. Goldbach, Freeze-Drying of L-Arginine/Sucrose-Based Protein Formulations, Part 2: Optimization of Formulation Design and Freeze-Drying Process Conditions for an L-Arginine Chloride-Based Protein Formulation System., *J. Pharm. Sci.* 104 (2015) 4241-4256.
- [34] P. Stärtzel, H. Gieseler, M. Gieseler, A. M. Abdul-Fattah, M. Adler, H. C. Mahler, P. Goldbach, Mannitol/L-Arginine-Based Formulation Systems for Freeze Drying of Protein Pharmaceuticals: Effect of the L-Arginine Counter Ion and Formulation Composition on the Formulation Properties and the Physical State of Mannitol, *J. Pharm. Sci.* 105 (2016) 3123-3135.
- [35] NCBI, Amino acid explorer part of the NCBI (National Center for Biotechnology Information) Structure Database: United States Government, (2009). https://www.ncbi.nlm.nih.gov/Class/Structure/aa/aa_explorer.cgi?display=0.
- [36] S. Bräse, J. Bülle, A. Hüttermann, *Organische und bioorganische Chemie*, Wiley-VCH-Verlag, (2008).
- [37] K. Včeláková, I. Zusková, E. Kenndler, B. Gaš, Determination of cationic mobilities and pKa values of 22 amino acids by capillary zone electrophoresis, *Electrophoresis*. 25 (2004) 309–317.
- [38] Mannitol, NLM (United States National Library of Medicines), ChemIDplus Database. (2017). <https://chem.nlm.nih.gov/chemidplus/rn/69-65-8>.
- [39] R. Weast, M. Astle, W. Beyer, *Handbook of chemistry and physics*, 72nd ed., CRC Press, Boca Raton, (1984).
- [40] H.D. Belitz, W. Grosch, *Lehrbuch der Lebensmittelchemie*, Springer Berlin Heidelberg, (2013).
- [41] M. Mattern, G. Winter, U. Kohnert, G. Lee, Formulation of proteins in vacuum-dried glasses. II. Process and storage stability in sugar-free amino acid systems., *Pharm. Dev. Technol.* 4 (1999) 199–208.
- [42] W. Kaiyaly, U. Khan, S. Mawlud, Influence of mannitol concentration on the physicochemical, mechanical and pharmaceutical properties of lyophilised mannitol, *Int. J. Pharm.* 510 (2016) 73–85.

- [43] M. Mattern, G. Winter, R. Rudolph, G. Lee, Formulation of proteins in vacuum-dried glasses. I: Improved vacuum- drying of sugars using crystallising amino acids, *Eur. J. Pharm. Biopharm.* 44 (1997) 177–185.
- [44] X. Lu, M. J. Pikal, Freeze-Drying of Mannitol–Trehalose–Sodium Chloride-Based Formulations: The Impact of Annealing on Dry Layer Resistance to Mass Transfer and Cake Structure, *Pharm. Dev. Technol.* 9 (2004) 85–95.
- [45] A. M. Abdul-Fattah, D. Kalonia, M. J. Pikal, The challenge of drying method selection for protein pharmaceuticals: Product quality implications, *J. Pharm. Sci.* 96 (2007) 1886–1916.
- [46] P. Chinachoti, M. Steinberg, Crystallinity of sucrose by X-ray diffraction as influenced by absorption versus desorption, waxy maize starch content, and water activity, *J. Food Sci.* 51 (1986) 456–459.
- [47] R. Surana, R. Suryanarayanan, Quantitation of Crystallinity in Substantially Amorphous Pharmaceuticals and Study of Crystallization Kinetics by X-Ray Powder Diffractometry, *Powder Diffr.* 15 (2000) 2–6.
- [48] H. Gloria, D. Sievert, Changes in the Physical State of Sucrose during Dark Chocolate Processing Changes in the Physical State of Sucrose during Dark Chocolate, *J. Agric. Food Chem.* 49 (2001) 2433–2436.
- [49] R. Mohan, K. Koo, C. Strege, A. Myerson, Effect of Additives on the Transformation Behavior of L -Phenylalanine in Aqueous Solution, *Ind. Engeneering Chem. Res.* 40 (2001) 6111–6117.
- [50] P. Williams, C. Hughes, A. Buanz, S. Gaisford, K. Harris, Expanding the solid-state landscape of l -phenylalanine: Discovery of polymorphism and new hydrate phases, with rationalization of hydration/dehydration processes, *J. Phys. Chem. C.* 117 (2013) 12136–12145.
- [51] S. Mallakpour, A. Abdolmaleki, S. Borandeh, Covalently functionalized graphene sheets with biocompatible natural amino acids, *Appl. Surf. Sci.* 307 (2014) 533–542.
- [52] R. Fuhrherr, Spray-dried antibody powders for pulmonary application, Ludwig-Maximilian University, München, (2005).
- [53] S. Adhikari, T. Kar, Bulk Single Crystal Growth and Characterization of l-Leucine - A Nonlinear Optical Material, *Mater. Chem. Phys.* 133 (2012) 1055–1059.

- [54] B.. Peters, L. Staels, J. Rantanen, F. Molnár, T. De Beer, V. Lehto, J. Ketolainen, Effects of cooling rate in microscale and pilot scale freeze-drying – Variations in excipient polymorphs and protein secondary structure, *Eur. J. Pharm. Sci.* 95 (2016) 72–81.
- [55] A. Hawe, W. Frieß, Impact of freezing procedure and annealing on the physico-chemical properties and the formation of mannitol hydrate in mannitol-sucrose-NaCl formulations, *Eur. J. Pharm. Biopharm.* 64 (2006) 316–325.
- [56] Y. Xie, W. Cao, S. Krishnan, H. Lin, N. Cauchon, Characterization of mannitol polymorphic forms in lyophilized protein formulations using a multivariate curve resolution (MCR)-based Raman spectroscopic method, *Pharm. Res.* 25 (2008) 2292-2301.
- [57] USP <788>, USP/NF general chapter <788> particulate matter in injections, Ed. Rockville, MD United States Pharmacopoeial Conv. (2008).
- [58] W. Wang, Lyophilization and development of solid protein pharmaceuticals, *Int. J. Pharm.* 203 (2000) 1–60.
- [59] T. Werk, J. Huwyler, M. Hafner, J. Luemkemann, H. C. Mahler, An Impedance-Based Method to Determine Reconstitution Time for Freeze-Dried Pharmaceuticals, *J. Pharm. Sci.* 104 (2015) 2948–2955.
- [60] B. Bhatnagar, Reconstitution of Highly Concentrated Lyophilized Proteins, in: *Int. Soc. Lyophilization Free.*, Havana, Cuba, (2017).
- [61] P. Hiwale, A. Amin, L. Kumar, A. Bansal, Variables Affecting Reconstitution Time of Dry Powder for Injection, *Pharm. Technol.* 37 (2008) 1–8.
- [62] W. Cao, S. Krishnan, M. Ricci, L. Shih, D. Liu, J. Gu, F. Jameel, Rational design of lyophilized high concentration protein formulations-mitigating the challenge of slow reconstitution with multidisciplinary strategies, *Eur. J. Pharm. Biopharm.* 85 (2013) 287–293.
- [63] L. Lin, R. Bunnell, Overcoming challenges in the reconstitution of a high-concentration protein drug product, *BioPharm Int.* 26 (2013) 28-39.
- [64] R. Geidobler, I. Konrad, G. Winter, Can Controlled Ice Nucleation Improve Freeze-Drying of Highly-Concentrated Protein Formulations?, *J. Pharm. Sci.* 102 (2013) 3915–3919.

- [65] T. Werk, I.S. Ludwig, H. C. Mahler, J. Luemkemann, J. Huwyler, M. Hafner, The effect of formulation, process and method variables on the reconstitution time in dual chamber syringes., *PDA J. Pharm. Sci. Technol.* 70 (2016) 508–522.
- [66] K. Beech, J. Biddlecombe, C. van der Walle, L. Stevens, S. Rigby, J. Burley, S. Allen, Insights into the influence of the cooling profile on the reconstitution times of amorphous lyophilized protein formulations, *Eur. J. Pharm. Biopharm.* 96 (2015) 247-254.
- [67] J. Schwegman, J. F. Carpenter, S. L. Nail, Evidence of partial unfolding of proteins at the ice/freeze-concentrate interface by infrared microscopy, *J. Pharm. Sci.* 98 (2009) 3239–3246.
- [68] S. Wang, G. Wu, X. Zhang, Z. Tian, N. Zhang, T. Hu, W. Dai, F. Qian, Stabilizing two IgG1 monoclonal antibodies by surfactants: Balance between aggregation prevention and structure perturbation, *Eur. J. Pharm. Biopharm.* 114 (2017) 263–277.
- [69] K. Imamura, K. Murai, T. Korehisa, N. Shimizu, R. Yamahira, T. Matsuura, H. Tada, H. Imanaka, N. Ishida, K. Nakanishi, Characteristics of sugar surfactants in stabilizing proteins during freeze-thawing and freeze-drying, *J. Pharm. Sci.* 103 (2014) 1628-1637.
- [70] S. Webb, S. Golledge, J. Cleland, J. F. Carpenter, T. W. Randolph, Surface adsorption of recombinant human interferon- γ in lyophilized and spray-lyophilized formulations, *J. Pharm. Sci.* 91 (2002) 1474–1487.
- [71] M. Mehta, S. Bhardwaj, R. Suryanarayanan, Controlling the physical form of mannitol in freeze-dried systems, *Eur. J. Pharm. Biopharm.* 85 (2013) 207–213.
- [72] M. C. Manning, D. Chou, B. Murphy, R. Payne, D. Katayama, Stability of protein pharmaceuticals: An update, *Pharm. Res.* 27 (2010) 544–575.
- [73] D. Chambré, C. Idițoiu, M.R. Szabo, The reaction conditions influence on sucrose acid hydrolysis studied by means of DSC method, *J. Therm. Anal. Calorim.* 88 (2007) 681-686.
- [74] J. Horn, J. Schanda, W. Friess, Impact of Fast and Conservative Freeze-Drying on Product Quality of Protein-Mannitol-Sucrose-Glycerol Lyophilizates, *Eur. J. Pharm. Biopharm.* 127 (2018) 342-354.
- [75] H. C. Mahler, W. Friess, U. Grauschopf, S. Kiese, Protein Aggregation: Pathways, Induction Factors and Analysis, *J. Pharm. Sci.* 98 (2009) 2909–2934.

- [76] A. M. Fathallah, M. Chiang, A. Mishra, S. Kumar, L. Xue, R. Middaugh, S. Balulyer, The Effect of Small Oligomeric Protein Aggregates on the Immunogenicity of Intravenous and Subcutaneous Administered Antibodies, *J. Pharm. Sci.* 104 (2015) 3691–3702.
- [77] Ph.Eur., 2.9.19 Particulate contamination: Sub-visible Particles, *Eur. Dir. Qual. Med.* 8 (2014) 438–441.
- [78] S. Jena, R. Suryanarayanan, A. Aksan, Mutual Influence of Mannitol and Trehalose on Crystallization Behavior in Frozen Solutions., *Pharm. Res.* 33 (2016) 1413–25.

Chapter 7

Final Summary

The present thesis focused on the reduction of the freeze-drying process time without detrimental impact on protein stability and macroscopic cake appearance. Therefore, different crystalline bulking agents were investigated: (1) the already well established mannitol (Man) to develop a fast freeze-drying cycle (**Chapter 5**) and (2) crystallizing amino acids as potential alternative bulking agents to Man (**Chapter 6**). Further aspects as the characterization of the freeze-concentrate play an important role for understanding of protein stability during freeze-drying as described in **Chapter 4**. A novel measuring device for the collapse temperature (T_c) was the focus of **Chapter 3**.

Monitoring of the freeze-drying process is an important aspect for improved process understanding. The optical fiber system (OFS) was investigated as potential detection tool for the T_c in freeze/thawing and freeze-drying studies (**Chapter 3**). OFS results were compared to the current standard measuring tools DSC and FDM. Suc, Tre and stachyose solutions as well as highly concentrated IgG₁ and lysozyme formulations were used to identify that the T_{OFS} peak during thawing was in accordance with T_c and not with T_g' . Crystallization behaviour of Man measured by OFS in vials correlated well to DSC analysis. Thus, the OFS can be used as alternative method for T_c determination or crystallization in the product container. During freeze-drying experiments collapse of 20% sucrose or stachyose solutions could be detected with the OFS but not for lower sugar concentrations. Thus, detection of T_c and crystallization in freeze/thaw and collapse of highly concentrated freeze-dry solutions can be provided by the OFS as measuring device although the sensitivity of the sensor can still be improved.

Freezing and annealing are both steps that can affect protein stability in the final lyophilisate (**Chapter 4**). Excipients, in particular, crystallizing agents, can have a major impact on unfolding and hence aggregation of the protein. This was investigated in a study with Man, trehalose (Tre) and BSA at an annealing temperature of -20 °C for 20 hours. Differential scanning calorimetry (DSC), X-ray diffraction and FTIR spectroscopy demonstrated the diverse crystallization behaviour of Man and Tre at different concentrations of BSA,

polysorbate 20 and deuterium oxide. The secondary structure of BSA was measured by IR spectroscopy in frozen solution and by circular dichroism in thawed solutions. Unfolding of BSA occurred if Tre crystallization took place. However, increased BSA content delayed and reduced both, Man and Tre crystallization. Polysorbate 20 (< 0.2% w/w) and deuterium oxide (> 5% w/w) similarly induced crystallization behaviour. The extent of excipient crystallization was directly coupled to retention of BSA in its native conformation in frozen and thawed solution. BSA unfolding could not be correlated to particle or aggregate formation. Nevertheless, the physical state of the freeze-concentrate should be studied in future at different excipient and protein concentrations.

In the subsequent part of the thesis fast freeze-drying at high product temperature (T_p) was evaluated (*process development, Chapter 5*) targeting good protein stability and elegant cake appearance at the same time (*formulation development, Chapter 5 and Chapter 6*). Fast freeze-drying is usually limited as the typical protein stabilizer sucrose (Suc) collapses at high T_p above its collapse temperature (T_c). Crystalline bulking agents can prevent macrocollapse, however, do not stabilize the proteins. Short freeze-drying cycles save time and costs. First, 4/1 Man/Suc formulations were used to develop of a fast freeze-drying cycle above T_g' of the formulation (*Chapter 5*). At a T_p of $-10\text{ }^\circ\text{C}$ during primary drying (PD) this phase was completed in only 7 hours. The T_p was only slightly below the eutectic temperature of Man preventing macrocollapse of the formulation. The cake characteristics were adequate with T_g values above $60\text{ }^\circ\text{C}$, a residual moisture level of 1%, reconstitution times about 30 seconds, crystalline δ -mannitol and elegant appearance. A lower Man/Suc ratio and hence a higher stabilizer content was prevented by incomplete Man crystallization. Protein process stability was shown using lysozyme and two monoclonal IgG₁ antibodies at two concentrations each. Characterisation of protein stability rendered low aggregation and particle levels for both, the fast and a long conservative freeze-drying process with a T_p of $-39\text{ }^\circ\text{C}$, without defects in macroscopic appearance. Thus, fast freeze-drying of 4/1 Man/Suc formulations above the T_g' at a T_p of $-10\text{ }^\circ\text{C}$ resulted in good protein process stability and appropriate cake characteristics at substantial process time reduction.

The high Man fraction was necessary to ensure crystallization, but limited Suc concentration, although more protein stabilizer could be beneficial, particularly for highly concentrated protein formulations. Crystallizing amino acids (AA) could be a promising alternative to Man enabling lower bulking agent/Suc ratios (*Chapter 6*). Glycine (Gly), phenylalanine (Phe), methionine (Met), leucine (Leu) and isoleucine (Ile) were freeze-dried at low bulking agent/Suc ratios of 2.5/47.5, 5/45 and 10/40 with the fast freeze-drying cycle and compared to Man at the same ratios. Both, Man/Suc and Gly/Suc formulations suffered macrocollapse with incomplete crystallization. Phe/Suc, Leu/Suc and Ile/Suc crystallized at 5/45 and 10/40,

but showed less pronounced crystallization in 2.5/47.5 AA/Suc ratio leading to unacceptable cake structures. Annealing did not enhance crystallization and a broad pH screen showed superior macroscopic appearance and AA crystallization at pH 5 - 7. Crystallization peaks were not suppressed by protein in Leu and Ile lyophilizates. Protein stability after freeze-drying was not affected either. Leu and Ile as bulking agents resulted in prolonged reconstitution time compared to Phe due to the insufficient wetting of these AAs and floating of the cakes. The reconstitution behaviour could be improved by addition of surfactant. The physic-chemical properties T_g , residual moisture, cake appearance and crystallinity of the lyophilizates were adequate. Additionally, process stability was shown for a monoclonal antibody. Thus, two novel bulking agents, Ile and Leu were identified which can be used at clearly lower bulking agent/Suc ratio as compared to Man enabling fast freeze-drying at T_p above T_g' .

In summary, this thesis provided several new findings regarding the freeze-drying of proteins. Bulking agents enable to dry Suc formulations at T_p above T_g' without losing cake appearance. A higher stabilizer concentration is facilitated by the crystallizing AAs Phe, Leu and Ile as bulking agents. But crystallization of Man and Tre in the freeze-concentrate affects protein stability. Furthermore, the OFS as measuring device for T_c and crystallization in the product container could be established while interpretation of the OFS signal during freeze-drying is still a challenging task.

Chapter 8

Appendix

Table of Content

1. Supplementary Material of Chapter 5	171
2. Supplementary Material of Chapter 6	173
3. Presentations and Publications Associated with this Thesis	176
3.1. Publications.....	176
3.1.1. Peer- Reviewed Research Articles	176
3.1.2. Book Chapters	176
3.2. Presentations	176
3.2.1. Oral Presentations	176
3.2.2. Poster Presentations	176

1. Supplementary Material of Chapter 5

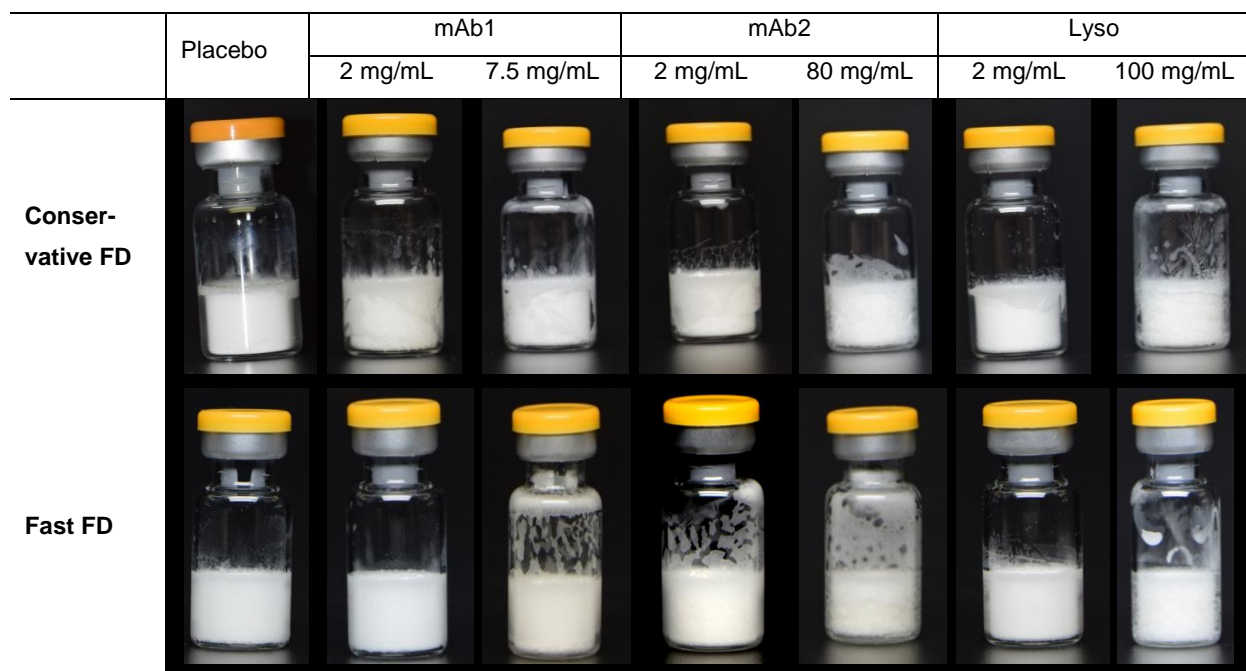


Figure 8-1. Macroscopic appearance of Protein/Man/Suc/Gly (x/40/9.5/0.5) formulations after conservative (Table 5-1, Process 1) and fast (Table 5-1, Process 8) freeze-drying.

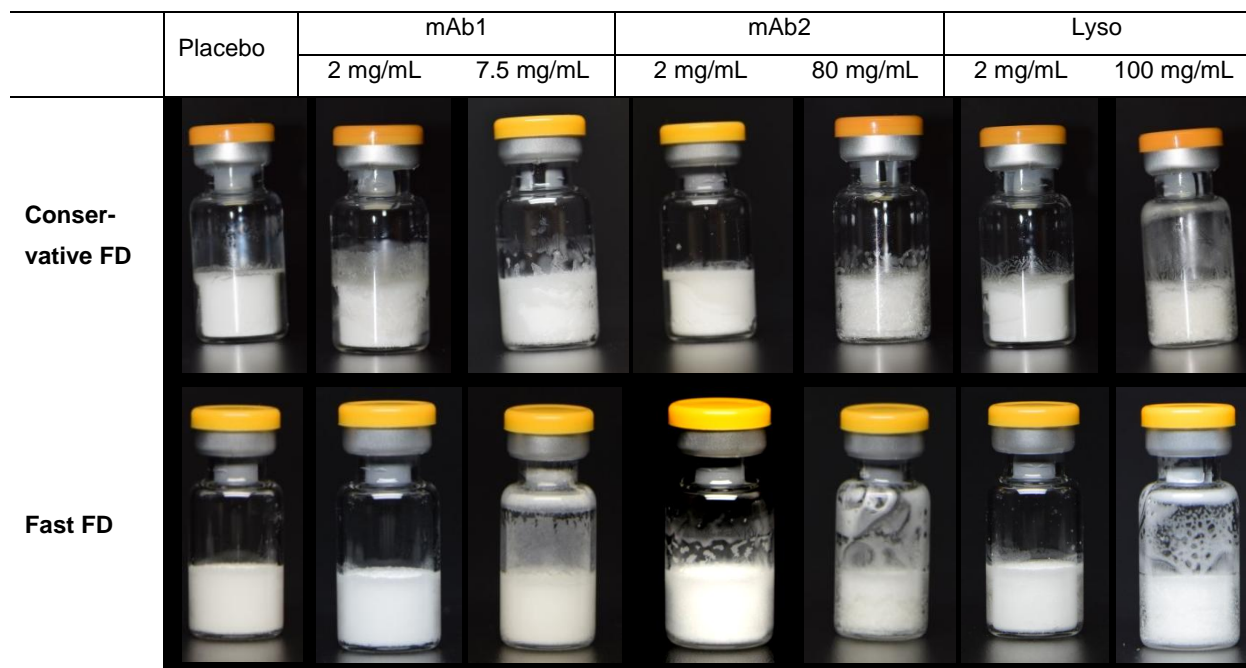


Figure 8-2. Macroscopic appearance of Protein/Man/Suc/Gly (x/40/9/1) formulations after conservative (Table 5-1, Process 1) and fast (Table 5-1, Process 8) freeze-drying.

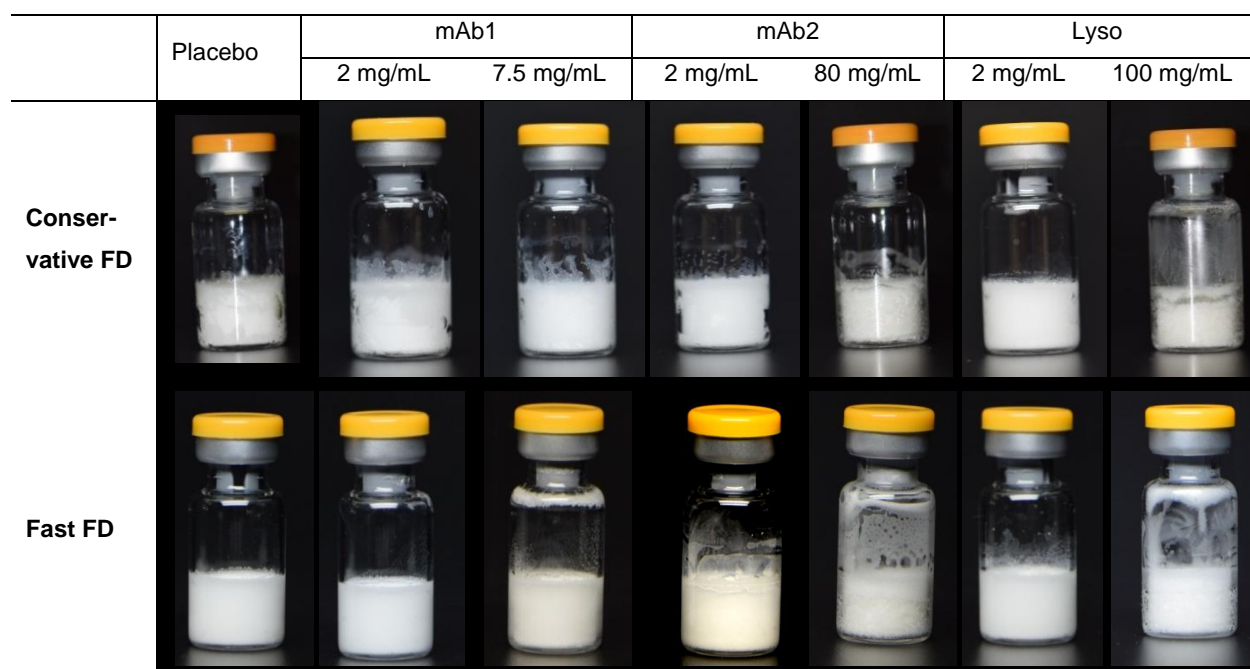


Figure 8-3. Macroscopic appearance of Protein/Man (x/40) formulations after conservative (Table 5-1, Process 1) and fast (Table5-1, Process 8) freeze-drying.

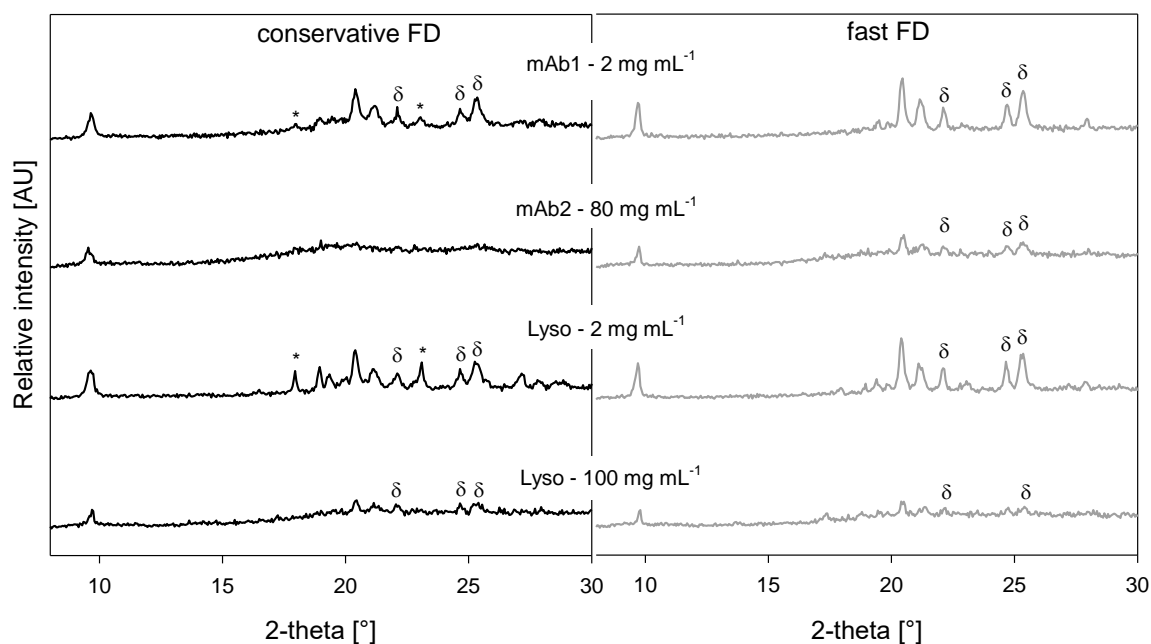


Figure 8-4. Exemplary XRD diffractograms of selected Man/Suc 40/10 formulations. Formulations freeze-dried with the conservative FD cycle are depicted in black while formulations processed with the fast FD cycle are in grey. Peaks marked with * represent peaks of mannitol-hemihydrate.

2. Supplementary Material of Chapter 6



Figure 8-5. Macroscopic Appearance of AA/Suc lyophilizates at different formulation pH freeze-dried without annealing step (Table 6-3).

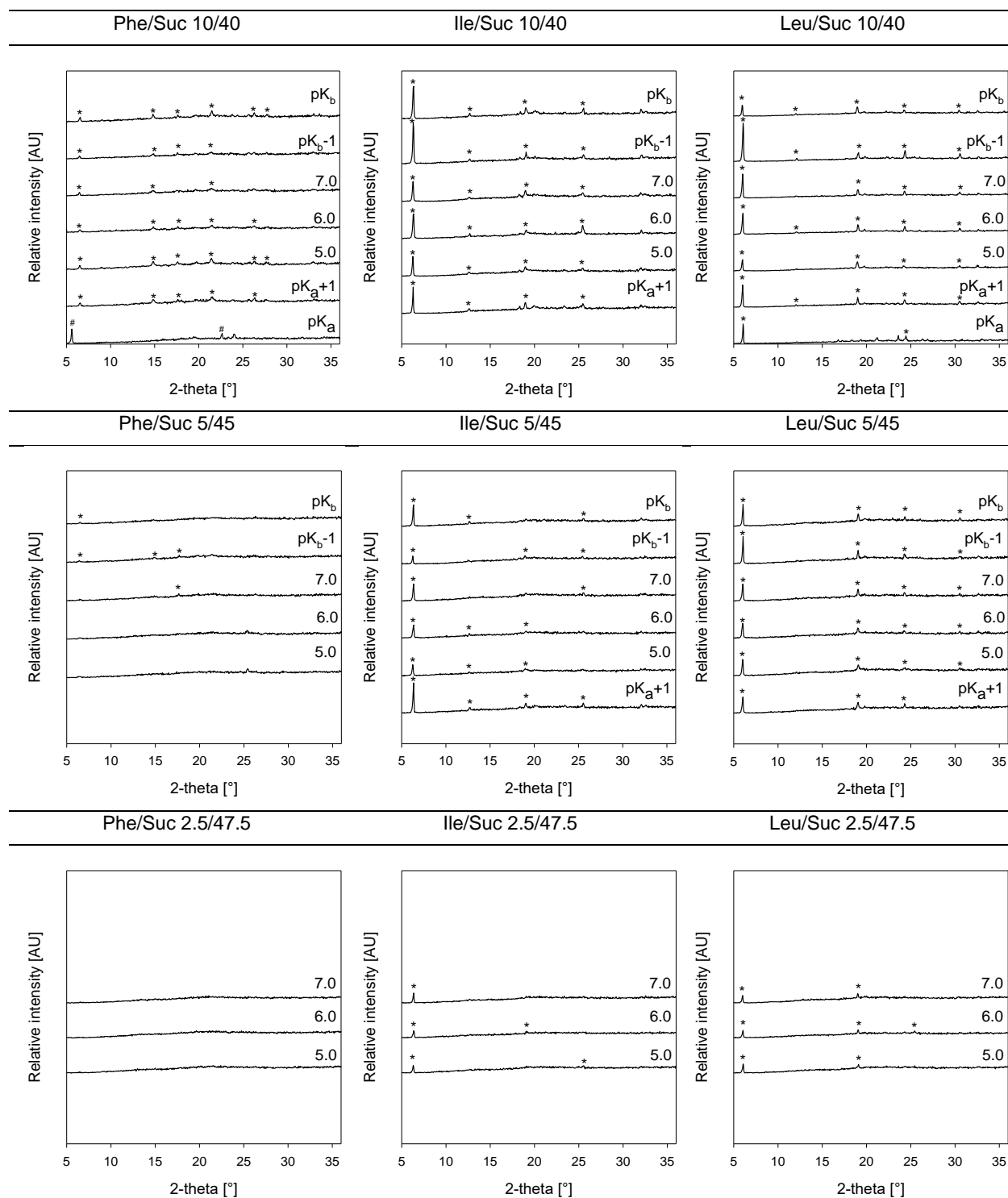


Figure 8-6. XRD diffractograms of Phe/Suc, Ile/Suc and Leu/Suc lyophilizates at different formulation pH values freeze-dried without annealing step (Table 6-3). * mark reference peaks of the AAs, # mark the anhydrous form of Phe (Table 6-6).

Table 8-1. Tg values of freeze-dried AA/Suc formulations at different formulation pH. The formulations were freeze-dried without annealing step (Table 6-3). For n=3: mean \pm SD, for n=2: mean. c. collapsed.

AA/Suc ratio		Tg [°C]						
		pH	pK _a +1	5.0	6.0	7.0	pK _b -1	pK _b
Phe/Suc	10/40		62.7	63.1	67.4 \pm 0.6	67.2	59.2	c.
	5/45		c.	67.1	66.1 \pm 2.4	67.1	67.1	c.
Ile/Suc	10/40		c.	51.2	54.7	47.1	47.3	43.3
	5/45		c.	47.6	36.3 \pm 2.3	35.7	35.9	35.3
Leu/Suc	10/40		43.0	47.4	50.5	47.4	39.9	c.
	5/45		c.	43.8	50.9	47.2	39.8	32.0

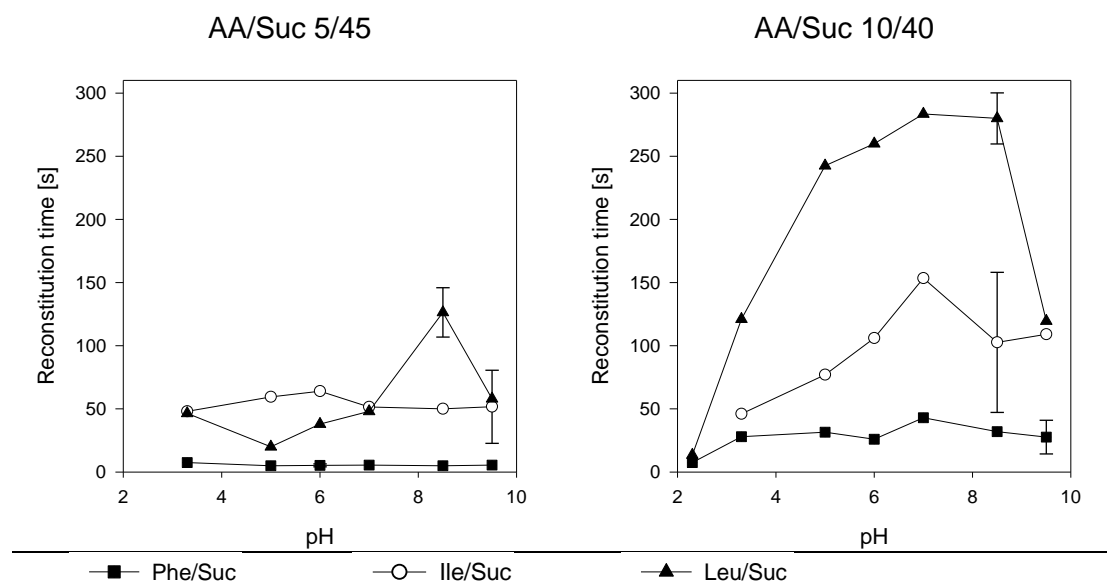


Figure 8-7. Reconstitution times of Phe/Suc (black squares), Ile/Suc (white circles) and Leu/Suc (black triangles) formulations with different formulation pH freeze-dried without annealing step (Table 6-3). For n=3: mean \pm SD, for n=2: mean.

3. Presentations and Publications Associated with this Thesis

3.1. Publications

3.1.1. Peer- Reviewed Research Articles

J.Horn, E. Tolardo, D. Fissore, W. Friess, Crystallizing Amino Acids as Bulking Agents in Freeze-Drying, *Eur. J. Pharm. Biopharm.*, submitted in March 2018.

J. Horn, J. Schanda, W. Friess, Impact of Fast and Conservative Freeze-Drying on Product Quality of Protein-Mannitol-Sucrose-Glycerol Lyophilizates, *Eur. J. Pharm. Biopharm.*, online available (2018).

J. Horn, W. Friess, Detection of Collapse and Crystallization of Saccharide, Protein, and Mannitol Formulations by Optical Fibers in Lyophilization, *Front. Chem.* 6 (2018) 1–9.

S. Jena, J. Horn, R. Suryanarayanan, W. Friess, A. Aksan, Effects of Excipient Interactions on the State of the Freeze-Concentrate and Protein Stability, *Pharm. Res.* 34 (2017) 462-478.

3.1.2. Book Chapters

Horn J., Mahler, H.-C., Friess, W., Drying for Protein formulation and its Formulation Aspects, in *Drying Technologies for Biotechnology and Pharmaceutical Applications: Current Status and Future Trends*, Ohtake, Izutsu, Lechuga-Ballesteros, Wiley & Sons, submitted 2017.

3.2. Presentations

3.2.1. Oral Presentations

J. Horn, M. Resch, W. Frieß; A Novel Tool for Online Monitoring of Tg' in Freeze-Drying, 10th World Meeting on Pharmaceutics, Biopharmaceutics and Pharmaceutical Technology, Glasgow, Scotland, April 4-7, 2016.

3.2.2. Poster Presentations

S. Jena, J. Horn, R. Suryanarayanan, W. Friess, A. Aksan; Protein Stability and Excipient Crystallization in Freeze-Dried Mannitol-Trehalose Formulations, AAPS Annual Meeting and Exposition, San Diego, California, USA; November 12-15, 2017.

S. Jena, J. Horn, R. Suryanarayanan, W. Friess, A. Aksan; Effects of Specific Interactions on Crystallinity and Protein Stability in the Frozen State, AAPS Annual Meeting and Exposition, Denver, Colorado, USA, November 13-17, 2016.

J. Horn, J. Schanda, W. Frieß; Fast Freeze-Drying above Sugars' Tg' without Loss of Cake Structure, CPPR Freeze-Drying of Pharmaceuticals and Biologicals, Breckenridge, Colorado, USA, July 12-15, 2016.

J. Horn, M. Resch, W. Frieß; The Optical Fiber System (OFS) as Novel Tool for Collapse Detection in Lyophilizates, CPPR Freeze-Drying of Pharmaceuticals and Biologicals, Breckenridge, Colorado, USA, July 12-15, 2016.

J. Horn, M. Neuhauser, C. Sönnichsen, W. Frieß; Influence of Glycerol on Lyophilized mAb Formulations, International BioAnalytical & Formulation Congress, Berlin, Germany, September 15-16, 2015.

J. Horn, W. Frieß; The Impact of Mannitol on the Glass Transition Temperatures of Sucrose - Plasticizer Lyophilizates, Freeze Drying of Pharmaceuticals & Biologicals – Short course and Conference, Garmisch-Patenkirchen, Germany, September 23-26, 2014.